



Alshehri, Feras (2017) The hydrogenation of substituted benzenes over Rh/silica. PhD thesis.

<http://theses.gla.ac.uk/8342/>

Copyright and moral rights for this work are retained by the author

A copy can be downloaded for personal non-commercial research or study, without prior permission or charge

This work cannot be reproduced or quoted extensively from without first obtaining permission in writing from the author

The content must not be changed in any way or sold commercially in any format or medium without the formal permission of the author

When referring to this work, full bibliographic details including the author, title, awarding institution and date of the thesis must be given

Enlighten:Theses
<http://theses.gla.ac.uk/>
theses@gla.ac.uk



University
of Glasgow

The Hydrogenation of Substituted Benzenes over Rh/silica

FERAS ALSHEHRI

MSc

**Submitted in fulfilment of the requirements for the
Degree of Doctor of Philosophy**

**School of Chemistry
College of Science and Engineering
University of Glasgow**

2017

*This work is dedicated to my father
I hope I've made you proud*

هذه الرسالة مهداة إلى والدي
أتمنى أن تكون فخوراً بي

Abstract

The catalytic hydrogenation of substituted benzenes to saturated cyclic products is an industrially relevant reaction. It is important in the production of fine chemicals, petroleum and in the fuel industry. It is used in the process of lowering the aromatic content in diesel fuels to follow up the up-to-date environmental legalisation. It has been widely reported that aromatic ring hydrogenation is a structure insensitive reaction, however more recent studies have suggested that structure sensitivity may indeed exist.

Therefore, the demand to perform more research on substituted benzenes to understand their behaviour during the hydrogenation has increased. Unlike most of what was found in literature, this study involved substituents which include methyl, ethyl, propyl, hydroxyl and methoxy groups. These reactions were performed at different parameters of temperatures, H₂ pressure and concentrations and over Rh/SiO₂ catalyst.

Different mechanisms were suggested for the hydrogenation of aromatic compounds. A stepwise mechanism is generally accepted to explain the reaction mechanism. This suggestion was built on the fact aromatic adsorption is zero order in aromatics which suggests a strong adsorption of the substrates. This mechanism was confirmed in this work by the observation of alkyl cyclohexenes as intermediates during the hydrogenation of alkyl benzenes.

Interesting points were observed during the hydrogenation of phenols. Firstly, cyclohexane was formed independently and directly from the original phenol. This observation was not found in most of previous studies. The other point was that phenol and anisole reacted in different ways from each other. Phenol was found to react in three independent routes, the formation of cyclohexanone, the formation of cyclohexanol and the formation of cyclohexane. Whereas, cyclohexanol was not formed directly from anisole, it was formed from cyclohexanone and after the total conversion of anisole.

Competitive hydrogenations were also executed in order to investigate the behaviour of different groups in the same reaction. The findings of these tests were different from what was observed during the solo tests. As for the hydrogenation of alkylbenzenes, a steric effect might explain the differences between these substrates. It was observed that the reaction rate decreased as the alkyl group attached to the ring increased. These findings were not the same during the competitive hydrogenation. n-Propylbenzene, which has a

larger group attached to the aromatic ring, showed higher reactivity in the presence of toluene and ethylbenzene, which suggests that the steric effect was not the only factor affecting the hydrogenation of substituted benzenes. These findings were explained by an electronic effect applied by the alkyl groups attached to the ring. The effect of these groups increases as the group size increases.

In addition to steric and electronic effects, the mode of adsorption was also suggested to affect the competitive hydrogenations of phenols. Different modes of adsorption and different medium species formed leads to different behaviour during the competitive hydrogenation.

In addition, NMR analysis was performed on selected samples from toluene and deuterated toluene reactions with deuterium and hydrogen. Toluene reaction with deuterium showed that all hydrogen atoms were replaced by deuterium at the beginning of the reaction. It was also shown from NMR results that $-CD_3$ group was contacted to the surface which confirms the ability of $-CH_3$ group to be adsorbed to the surface as well as the aromatic ring.

Table of Contents

Abstract	ii
List of figures	xi
Acknowledgment	xviii
1 Introduction	1
1.1 Aromatics hydrogenation mechanism	4
1.2 Alkylbenzenes hydrogenation	5
1.3 Phenol hydrogenation	6
1.4 Anisole hydrogenation	9
1.5 Steric and electronic effects	11
1.6 Solvent effects	13
1.7 Deuterium exchange reactions	14
2 Aims of project	15
3 Experimental	16
3.1 Catalyst characterisation	16
3.1.1 Determination of surface area	16
3.1.2 Thermo-Gravimetric Analysis	17
3.2 Instruments	17
3.2.1 Gas chromatography (GC)	17
3.2.1.1 GC reference standards	18
3.2.2 Stirred tank reactor (Buchi)	18

3.3	Performing the hydrogenation reaction	19
3.3.1	Pre-reaction procedure	19
3.3.2	Catalyst reduction and solvent degassing	19
3.3.3	Hydrogenation reaction procedure	20
3.4	Hydrogenation tests	20
3.4.1	Kinetic studies	20
3.4.1.1	Determination of rate constant (k)	21
3.4.1.2	Activation energy E_a	21
3.4.1.3	Reaction order in H_2 pressure and in substrate concentration	22
3.4.2	Competitive hydrogenations	22
3.4.3	Deuterium reactions	23
3.5	NMR spectroscopy	23
3.6	Chemicals	24
4	Results	25
4.1	Catalyst characterisation	25
4.1.1	Surface area	25
4.1.2	Thermo-gravimetric Analysis (TGA)	25
4.2	Alkyl aromatics hydrogenation	26
4.2.1	Toluene	26
4.2.1.1	Temperature variation	28
4.2.1.2	Pressure variation	31
4.2.2	Ethylbenzene	35

4.2.2.1	Temperature variation.....	35
4.2.2.2	Pressure variation.....	40
4.2.3	n-Propylbenzene.....	43
4.2.3.1	Temperature variation.....	43
4.2.3.2	Pressure variation and order of reaction in H ₂ pressure.....	45
4.2.3.3	Concentration variation and reaction order in substrate concentration ..	48
4.3	Alkyl aromatics competitive hydrogenation	50
4.3.1	Toluene.....	52
4.3.2	Ethylbenzene	52
4.3.3	n-Propylbenzene.....	52
4.4	Phenol and anisole hydrogenation.....	56
4.4.1	Phenol.....	57
4.4.1.1	Temperature variation and E _a calculation.....	57
4.4.1.2	Pressure variation and reaction order in H ₂	59
4.4.1.3	Concentration variation and order in phenol concentration.....	61
4.4.1.4	Products selectivity at different parameters.....	63
4.4.2	Anisole	64
4.4.2.1	Temperature variation and E _a calculation.....	64
4.4.2.2	Pressure variation and reaction order in H ₂	68
4.4.2.3	Concentration variation and reaction order in anisole	70
4.4.2.4	Products selectivity at different parameters.....	72
4.5	Competitive hydrogenation of phenol, anisole and toluene	73
4.5.1	Toluene.....	74

4.5.2	Phenol.....	75
4.5.3	Anisole	75
4.6	Cyclohexanone hydrogenation	79
4.6.1	Cyclohexanone hydrogenation as a single substrate	80
4.6.1.1	Activation energy.....	82
4.6.2	Cyclohexanone competitive hydrogenation.....	82
4.6.2.1	Toluene	82
4.6.2.2	Phenol	84
4.6.2.3	Anisole.....	87
4.7	Competitive hydrogenation of phenol, anisole and methoxyphenol.....	90
4.7.1	Methoxyphenol	92
4.7.2	Phenol.....	93
4.7.3	Anisole	93
4.8	Hydrogen- <i>deuterium</i> exchange reactions	95
4.8.1	NMR results	103
5	Discussion	112
5.1	Alkyl aromatics hydrogenation	112
5.1.1	Single substrate hydrogenation	112
5.1.2	Competitive hydrogenation.....	113
5.2	Phenol and anisole hydrogenation.....	115
5.2.1	Phenol hydrogenation.....	115
5.2.2	Anisole hydrogenation	118

5.2.3	Phenol, anisole and toluene competitive hydrogenation.....	121
5.3	Cyclohexanone hydrogenation	124
5.3.1	Cyclohexanone competitive hydrogenation.....	125
5.3.2	Phenol, anisole and methoxyphenol competitive hydrogenation.....	125
5.4	Deuterium Isotope studies	128
5.5	NMR isotope study.....	131
6	Conclusion	134
7	Future work	136
8	Appendix.....	137
8.1	Toluene reaction profiles using iridium catalyst	137
9	List of references.....	142

List of tables

Table 1. Composition of Pygas	2
Table 2. Effect of metal size ranging on benzene hydrogenation	3
Table 3. Hydrogenation relative rate for different alkylbenzenes [35]	5
Table 4. Rates of ketones hydrogenation	12
Table 5. Integrated forms of rate equations	21
Table 6. Reactants with their densities and number of moles	23
Table 7. Chemicals used in the project	24
Table 8. Catalyst properties.....	25
Table 9. Conversion and rate constant of toluene at different temperatures.....	29
Table 10. Data used to generate Arrhenius plot.....	30
Table 11. Conversion and rate constant of toluene at different H ₂ pressures.....	32
Table 12. Data used to determine reaction order in H ₂	33
Table 13. Conversion and rate constant of toluene at different temperatures.....	39
Table 14. Data used to generate Arrhenius plot	39
Table 15. Conversion to ethylcyclohexane at different pressures	40
Table 16. Data used to generate Arrhenius plot	45
Table 17. Conversion to propylcyclohexane at different pressures	46
Table 18. Conversion to propylcyclohexane at different concentrations.....	49
Table 19. Main findings for the hydrogenation of single alkyl benzenes (50 °C-1mL-3barg)	50
Table 20. Conversion of phenol at different temperatures.....	57

Table 21. Phenol conversion at different pressures	59
Table 22. Conversion and k values for phenol at different concentrations.....	63
Table 23. Products selectivity of phenol hydrogenation at different temperatures.....	63
Table 24. Products selectivity of phenol hydrogenation at different pressures	64
Table 25. Products selectivity of phenol hydrogenation at different concentrations	64
Table 26. Anisole hydrogenation at 50 °C.....	67
Table 27. Rate constants for anisole hydrogenation at different temperatures	67
Table 28. Products selectivity of anisole hydrogenation at different temperatures	72
Table 29. Products selectivity of anisole hydrogenation at different pressures	72
Table 30. Products selectivity of anisole hydrogenation at different concentrations	73
Table 31. Results concerning three substrates as singles.....	73
Table 32 Data used to generate Arrhenius plot.....	82
Table 33. KIE for different substrates.....	95
Table 34 NMR tests on selected samples.....	103
Table 35. Reactions rates for alkylbenzenes hydrogenation at different temperatures.....	113
Table 36 Inverse KIE for xylenes [126].....	128

List of figures

Figure 1. Stepwise hydrogenation of aromatics mechanism.....	4
Figure 2. Possible reaction routes for phenol hydrogenation,hydrogenolysis, Ni/SiO ₂ [13].	7
Figure 3. Sequential process of phenol hydrogenation under moderate conditions over Pd/Al ₂ O ₃ [61]	8
Figure 4. Modes of phenol adsorption [64].....	9
Figure 5 Possible reaction routes for the hydrogenation of anisole over Rh [71].....	10
Figure 6 Proposed anisole hydrogenation to form cyclohexanone [59, 73]	10
Figure 7. Phenol resonance structures [79].....	11
Figure 8. Benzene and toluene adsorbed species	12
Figure 9. Temperature ramp profile	17
Figure 10. Reference standards profiles.....	18
Figure 11. Stirred tank reactor	19
Figure 12. TGA profile for the catalyst.....	26
Figure 13. Toluene reaction profile at 30 °C	27
Figure 14. Toluene reaction profile at 50 °C	27
Figure 15. 0 th , 1 st and 2 nd order rate constant for toluene at 50 °C.....	28
Figure 16. Conversion of toluene at different temperatures	29
Figure 17. Toluene E _a plot	30
Figure 18. Toluene reaction profile at 2 barg H ₂ pressure	31
Figure 19. Toluene reaction profile at 5 barg H ₂ pressure	31

Figure 20. Formation of methylcyclohexane from toluene.....	32
Figure 21. Toluene reaction order in H ₂	33
Figure 22. Reaction profile for the hydrogenation of 0.5ml toluene	34
Figure 23. Reaction profile for the hydrogenation of 1.5ml toluene	34
Figure 24. Ethylbenzene reaction profile at 30 °C.....	35
Figure 25. Ethylbenzene reaction profile at 50 °C.....	36
Figure 26. Temperature effect on conversion during ethylbenzene hydrogenation.....	36
Figure 27. 0 th , 1 st and 2 nd order rate constant for ethylbenzene at 70 °C	37
Figure 28. 0 th , 1 st and 2 nd order rate constant for ethylbenzene at 50 °C	38
Figure 29. Ethylbenzene E _a plot.....	39
Figure 30. Ethylbenzene conversion to ethylcyclohexane at different pressures	40
Figure 31. Ethylbenzene reaction profile at 2 barg	41
Figure 32. Ethylbenzene reaction profile at 5 barg	41
Figure 33. Ethylbenzene reaction order in H ₂ pressure.....	42
Figure 34. Conversion of ethylbenzene at different mass per volume.....	42
Figure 35. n-propylbenzene hydrogenation profile at 35 °C	43
Figure 36. n-propylbenzene hydrogenation profile at 60 °C	44
Figure 37. Temperature effect on n-propylbenzene hydrogenation.....	44
Figure 38. n-propylbenzene E _a plot.....	45
Figure 39. n-Propylbenzene reaction profile at 2 barg.....	46
Figure 40. n-Propylbenzene reaction profile at 5 barg.....	46

Figure 41. H ₂ pressure effect on n-propylbenzene hydrogenation.....	47
Figure 42. n-Propylbenzene reaction order in H ₂ pressure	47
Figure 43. Reaction profile for hydrogenation of 0.5 ml n-propylbenzene	48
Figure 44. Reaction profile for hydrogenation of 1.5 ml n-propylbenzene	48
Figure 45. Concentration effect on n-propylbenzene hydrogenation.....	49
Figure 46. Reaction order in n-propylbenzene concentration	50
Figure 47. Conversion of three alkylbenzenes as single substrates	51
Figure 48. Conversion of three alkylbenzenes as a 1:1:1 mixture	51
Figure 49. Toluene reaction profiles a) single substrate b) with ethylbenzenes, c) with n-propylbenzene and d) in mixture of three	53
Figure 50. Ethylbenzene reaction profiles a) single substrate b) with toluene, c) with n-propylbenzene and d) in mixture of three	54
Figure 51. n-Propylbenzene reaction profiles a) single substrate b) with toluene, c) with ethylbenzenes and d) in mixture of three	55
Figure 52. Competitive hydrogenation of alkylbenzenes	56
Figure 53. Phenol reaction profile at 30 °C	58
Figure 54. Phenol reaction profile at 70 °C	58
Figure 55. Phenol E _a plot	59
Figure 56. Phenol reaction profile at 2 barg.....	60
Figure 57. Phenol reaction profile at 5 barg.....	60
Figure 58. Phenol reaction order in H ₂	61
Figure 59. Phenol reaction profile at 0.5 mL	62

Figure 60. Phenol reaction profile at 1.5 mL	62
Figure 61. Anisole reaction profile at 30 °C	65
Figure 62. Anisole reaction profile at 70 °C	65
Figure 63. Anisole hydrogenation products profile at different temperatures	66
Figure 64. Anisole E _a Plot.....	68
Figure. 65 Anisole hydrogenation products profile at different pressures.....	68
Figure 66. Anisole reaction profile at 2 barg	69
Figure 67. Anisole reaction profile at 2 barg	69
Figure 68. Anisole reaction order in H ₂	70
Figure 69. Anisole hydrogenation products profile at different concentrations	70
Figure 70. Anisole reaction profile at 1.5 mL.....	71
Figure 71. Anisole reaction profile at 0.5 mL.....	71
Figure 72. Single substrates conversion.....	74
Figure 73. Mixture of three substrates conversion at a 1:1:1 ratio.....	74
Figure 74. Toluene reaction profiles a) single substrate, b) with phenol, c) with anisole and d) in mixture of three.....	76
Figure 75. Phenol reaction profiles a) single substrate, b) with anisole, c) with toluene and d) in mixture of three.....	77
Figure 76. Anisole reaction profiles a) single substrate, b) with phenol, c) with toluene and d) in mixture of three.....	78
Figure 77. Competitive hydrogenation of toluene, phenol and anisole	79
Figure 78. Cyclohexane reaction profile at 30 °C.....	80

Figure 79. Cyclohexane reaction profile at 70 °C.....	81
Figure 80. Temperature effect on cyclohexanone hydrogenation.....	81
Figure 81. Cyclohexanone E _a plot.....	82
Figure 82. a) Toluene as single substrate and b) with cyclohexanone.....	83
Figure 83. Phenol and cyclohexane comparison in single reaction and after mixed with cyclohexanone.....	84
Figure 84. Cyclohexanol concentration from phenol in single reaction and after mixed with cyclohexanone.....	85
Figure 85. Phenol and cyclohexanone reaction profiles as single substrates a) and b) respectively c) phenol with cyclohexanone	86
Figure 86. Anisole, methoxycyclohexane and cyclohexane comparison in single reaction and after mixed with cyclohexanone.....	87
Figure 87. Cyclohexanol concentration from anisole in single reaction and after mixed with cyclohexanone.....	88
Figure 88. Anisole and cyclohexanone reaction profiles as single substrates a) and b) respectively c) anisole with cyclohexanone	89
Figure 89. Methoxyphenol reaction profile	90
Figure 90. Single substrates conversion.....	91
Figure 91. Mixture of three substrates conversion.....	91
Figure 92. Conversion of anisole and methoxyphenol in the complete hydrogenation....	92
Figure 93. Competitive hydrogenation of methoxyphenol, phenol and anisole	94
Figure 94. Toluene hydrogenation with a) H ₂ and b) D ₂	96
Figure 95. Ethylbenzene hydrogenation a) H ₂ and b) D ₂	97
Figure 96. n-Propylbenzene hydrogenation a) H ₂ and b) D ₂	98

Figure 97. 4-Methoxyphenol hydrogenation a) H ₂ and b) D ₂	99
Figure 98. Phenol hydrogenation with a) H ₂ and b) D ₂	100
Figure 99. Anisole hydrogenation with a) H ₂ and b) D ₂	101
Figure 100. Reaction profiles for a) toluene + H ₂ , b) toluene d8 + H ₂ , c) toluene + D ₂ and d) toluene d8+ D ₂	102
Figure 101. Sample 1, ¹ H NMR spectrum	104
Figure 102. Sample 1, ² H NMR spectrum	105
Figure 103. Sample 2, ² H NMR spectrum	106
Figure 104. Sample 2, ¹ H NMR spectrum	107
Figure 105. Sample 3, ² H NMR spectrum	108
Figure 106. Sample 4, ² H NMR spectrum	109
Figure 107. Sample 4, ¹ H NMR spectrum	110
Figure 108. Sample 5, ² H NMR spectrum	111
Figure 109. Competitive hydrogenation of alkylbenzenes	114
Figure 110. Sequential process of phenol hydrogenation under moderate conditions (Pd/Al ₂ O ₃) [60]	116
Figure 111. Phenol reaction profile under 5 barg H ₂ pressure.....	117
Figure 112. Phenol hydrogenation over Rh/SiO ₂	117
Figure 113. Anisole hydrogenation over Rh/SiO ₂ (except for the 30 °C test).....	119
Figure 114. Anisole reaction profile at 50 °C	120
Figure 115. Cyclohexane yield from phenol and anisole hydrogenation.....	121
Figure 116 Competitive hydrogenation of toluene, phenol and anisole	122

Figure 117. Single substrates conversion.....	123
Figure 118. Mixture of three substrates conversion.....	124
Figure 119. Cyclohexane reaction profile at 70 °C.....	125
Figure 120. Phenate and 4-methoxyphenate	126
Figure 121. Single substrates conversion.....	126
Figure 122. Mixture of three substrates conversion.....	127
Figure 123. Anisole hydrogenation and deuteration reaction profiles.....	129
Figure 124. ² H NMR results for toluene + D ₂ (top) and toluene d ₈ sample (bottom).....	131
Figure 125. Reaction profiles for a) toluene + H ₂ , b) toluene d ₈ + H ₂ , c) toluene + D ₂ and d) toluene d ₈ + D ₂	132
Figure 126. Toluene-40 °C-1mL-3b	137
Figure 127. Toluene-50 °C-1mL-3b	137
Figure 128. Toluene-60 °C-1mL-3b	138
Figure 129. Toluene-70 °C-1mL-3b	138
Figure 130. Toluene-60 °C-1mL-2b	139
Figure 131. Toluene-60 °C-1mL-4b	139
Figure 132. Toluene-60 °C-1mL-5b	140
Figure 133. Toluene-60 °C-0.5 mL-3b	140
Figure 134. Toluene-60 °C-0.75 mL-3b	141
Figure 135. Toluene-60 °C- 1.5 mL-3b	141

Acknowledgment

First of all, **Praise be to God** almighty for providing me courage and strength to complete this work.

I am sincerely grateful to my supervisor, Professor David Jackson, for his guidance, support and patience over the years. For being there when needed. This work would not be completed without his help and advice. Thank you for everything.

I'm also thankful to all my friends in catalysis group, 'some have gone and some remain'. I wish you all the best.

A big thank you for all of my friends who helped and supported me during my stay in Glasgow since 2010. Thank you all for all the good times we had outside the university labs.

I would like to thank King Abdul-Aziz City for Science and Technology (KACST) and also Saudi Cultural Bureau in London.

Author declaration

I declare that this thesis, submitted for the degree of Doctor of Philosophy, is the result of my own work except where due reference is made to other authors. It has not been submitted for any other degree at the University of Glasgow or any other university.

1 Introduction

Hydrogenation technology in chemicals production is ubiquitous. It has often been considered mature technology with little scope for new developments: an area that is not fashionable. However, this belies the difficulties that are still extant in hydrogenation. Selectivity, as in the ability to hydrogenate a given functionality in the presence of another or to saturate to a given degree, is a key parameter that has not been brought under scientific control. Catalytic hydrogenation reactions can be defined as the addition of hydrogen to unsaturated multiple bonds after modifying these bonds by adsorption on to a catalyst under selected reaction conditions. It is an essential method that is widely carried out in industrial applications as well as in research labs [1]. It is used in a wide range of applications from bulk chemicals to high value products such as pharmaceuticals, flavours and fragrances and fine chemicals [1]. Heterogeneous catalysts are widely used in the field of hydrogenation due to several factors, for example catalyst stability and product separation [1]. Catalysts such as Raney Ni catalyst, supported metals (Ni and Cu) and supported noble metals (Pd, Pt, Ru and Rh) are all commonly used for hydrogenation [2].

In 1901, Sabatier, and his co-worker Senderence, reported the first catalytic hydrogenation of benzene. They 'attacked' the benzene ring with hydrogen at atmospheric pressure and temperatures between 70 and 200 °C over a nickel catalyst and succeeded in converting it to cyclohexane [3]. For his work in catalytic hydrogenation Sabatier won the Nobel Prize in 1912 [4]. This was the first example of hydrogenation of an aromatic ring. Nowadays aromatic hydrogenation is a major industrial process with around 4.6 Mt of benzene hydrogenated to cyclohexane each year.

An aromatic ring is more difficult to hydrogenate than unsaturated aliphatic compounds because of the stability of the ring, which is formed by resonance energy [5, 6]. The double bonds in alkenes for example are localised π -electrons. In contrast, π - electrons in the aromatics are delocalised forming a shell over and below the aromatic ring. Therefore, extra energy is needed to overcome the stability that shell confers and this is known as the resonance energy.

Aromatic hydrogenation can be performed by using homogenous catalysts [7-10], but the vast majority of research uses heterogeneous catalyst as stated earlier [1, 11]. It can be performed in the gas phase [12-14] as well as in the liquid phase. Several supported metals

have been used as aromatic hydrogenation catalysts including noble metals such as Pt, Pd, Rh, Ru and Ir, non-precious metals such as Ni and Co have also been used [11, 15, 16].

Selectivity to intermediates during the hydrogenation of aromatics is an interesting area because of their importance [12]. It is difficult to prepare alkylcyclohexenes, for example, selectively from their aromatic parent. Selectivity to alkylcyclohexenes can be achieved by adding a catalyst modifier [12, 17] or by modifying the preparation method of the catalyst [18]. It can be seen from the articles cited that Ru is the catalyst used for the partial hydrogenation of aromatics [19]. The Japanese company Asahi Chemical Industry developed a ruthenium catalyst that was used with zinc as a co-catalyst [20]. They found that the presence of the zinc enhanced the ability to hydrogenate benzene selectively to cyclohexene with 60% yield. The role of zinc can be in preventing cyclohexene from being re-adsorbed on the surface by blocking the active sites and/or by stabilising cyclohexene to prevent further hydrogenation to cyclohexane [19, 20].

The catalytic hydrogenation of substituted benzenes to saturated cyclic products is an important reaction. It is used in lowering the aromatic content in diesel fuels for environmental reasons [21]. Much of the aromatic content in fuels comes from pyrolysis gasoline (Pygas), which is a by-product of high temperature naphtha cracking to produce ethylene and propylene [22]. It is a mixture rich in unsaturated hydrocarbons and contains considerable amounts of aromatics, normally 40-80% (benzene, toluene and xylene), together with paraffins, olefins and diolefins. The composition depends on the feedstock and operating conditions and hence varies from plant to plant. A typical Pygas composition is given in Table 1 [23].

Table 1. Composition of Pygas

Components	Weight percent (wt %)
Benzene, toluene and xylenes	50
Olefins and dienes	25
Styrene and other aromatics	15
Paraffins and naphthenics	10

With an aromatic content of around 65 wt % [22] Pygas is used nowadays as gasoline blend due to its high octane number. However with new legislation mandating reduction in

the aromatic content in gasoline [24] it becomes obligatory to investigate the behaviour of aromatic hydrogenation especially as a mixture (competitive hydrogenation).

Substituted benzenes hydrogenation is also an essential method to obtain corresponding cyclohexanes. It is worth pointing out that substituted cyclohexanes can be also synthesised by the modification of cyclohexane, however is a difficult method when compared with aromatic ring reduction [25, 26]. Alongside the importance of the hydrogenation of substituted benzenes in production of fine chemicals, petroleum and fuel industry and the carry forward of the up-to-date environmental legalisation, the structure sensitivity of this reaction has gained more attention recently. In some literature it has been suggested that the hydrogenation of the aromatic ring is structure insensitive [27, 28], and hence the reaction can be used as a characterisation tool, however other research shows structure sensitivity. The following table shows some results which were obtained from benzene hydrogenation over different metals [29].

Table 2. Effect of metal size ranging on benzene hydrogenation

Catalyst	Size Range (nm)	Findings
Ni/SiO ₂	0.5 – 5	Maximum at 1.3 nm
Ru/SiO ₂	0.7 – 9.5	Maximum at 3.5 nm
Rh/Al ₂ O ₃	10 – 150	TOF constant
Pd/Al ₂ O ₃	10 – 150	TOF constant
Ir/ γ Al ₂ O ₃	0.5 – 3.3	TOF increased
Pt/SiO ₂	4.5 - 64	TOF increased

Structure sensitivity of benzene hydrogenation over Pt/Al₂O₃ catalysts was identified by Flores et al. [30]. They found that the structure sensitivity was affected by the temperature that was used to reduce the catalyst. Structure sensitivity was observed when temperatures between 100 - 300 °C were applied as reduction temperatures and with reduction temperatures over 400 °C the system was structure insensitive. Moreover, when Molina and Poncelet [31] used Ni/Al₂O₃ for benzene hydrogenation they found that for particles <4 nm the reaction was structure sensitive and was insensitive for larger particles.

It was reported that the metal particle size has an obvious effect on the hydrogenation of aromatic rings. Graydon and Langan [32] used a Rh catalyst supported on silica for the hydrogenation of benzene. They stated that Rh particles with size less than 1.2 nm had a very low activity, whereas 1.4 nm particles showed higher activity for the aromatic ring hydrogenation. More recent work, which also showed structure sensitivity by Jackson et al.

[33] used Rh/SiO₂ catalyst for the hydrogenation of para-substituted anilines. They stated that the catalyst showed an antipathetic particle size effect. The same conclusion was also found when Jackson et al. [34] used the same catalyst for the hydrogenation of para-toluidine. They investigated Rh with particle sizes between 1.2 – 3.5 nm and found that the turnover frequency (TOF) increased when larger crystallite size was used. They concluded that the ring hydrogenation takes place on terrace face surface atoms. Therefore it should be expected that the hydrogenation of an aromatic ring will be structure sensitive, and in general will favour larger metal crystallites.

1.1 Aromatics hydrogenation mechanism

In general, aromatic hydrogenation is zero order in substrate and positive first order in hydrogen pressure [35], reflecting a strong adsorption of the aromatic species and a weak adsorption of hydrogen. Despite the extensive research on the hydrogenation of aromatics, there is no clear agreement on the mechanism of reaction [36]. There are a few mechanisms that have been suggested for hydrogenation of the mono aromatic ring. One of the mechanisms suggested was the stepwise mechanism [5, 12, 21, 37], and in a more recent work by Ali [38] this mechanism was also suggested for aromatics hydrogenation. This mechanism involves the formation of cyclohexadiene, which is an unstable and highly active intermediate that is directly converted to the cycloalkane or cycloalkene in other cases [39].

Figure 1 shows the stepwise mechanism for the hydrogenation of benzene. Firstly, 1,3-cyclohexadiene is formed. This intermediate is a very active species which is hydrogenated to cyclohexene. Cyclohexene is then further hydrogenated to form cyclohexane [40, 41].

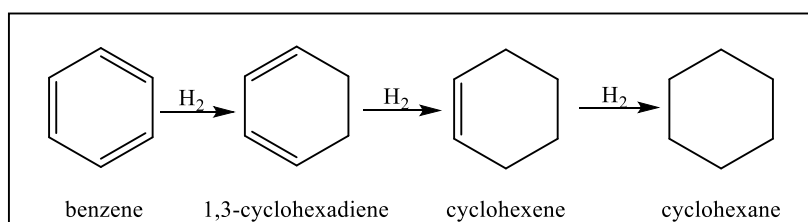


Figure 1. Stepwise hydrogenation of aromatics mechanism

Another mechanism was suggested for aromatic hydrogenation, which does not include the formation of cyclohexadiene [42, 43]. This mechanism can be explained briefly as that the adsorbed aromatic substrate forms a complex with both catalyst and hydrogen, which is then isomerised to cyclohexane without forming cyclohexadiene.

1.2 Alkylbenzenes hydrogenation

The hydrogenation of all alkylbenzenes is affected by the length and position of substituent on the benzene ring. The rate of hydrogenation decreases as the length of the substituent increases as shown in Table 3 [35]. For xylenes the *para*- position was found to be the most active [44]. This effect can be considered to be a steric effect where the benzene ring might be prevented from being adsorbed to the surface of the catalyst and/or hydrogen might be prevented from being attached to the ring [35].

Rahman and Vannice [45, 46] studied the hydrogenation of benzene, toluene, and xylenes. They used palladium as a catalyst over different supports Al_2O_3 , SiO_2 and TiO_2 . To study the effect of different supports that have varying in acidity on the catalytic hydrogenation of benzene, toluene and xylene. They found that all reactions were zero order in aromatics concentration and first order hydrogen pressure. They also concluded that the use of such acidic supports had increased the hydrogenation rate.

Table 3. Hydrogenation relative rate for different alkylbenzenes [35]

Substrate	Hydrogenation relative rate
Benzene	100
Toluene	62
Ethylbenzene	45
n-propylbenzene	41
Butylbenzene	38

Toppineen et al. [44] investigated the hydrogenation of five aromatics (di- and tri-substituted alkyl benzenes, xylenes, trimethylbenzene, and 4-isopropyltoluene) over $\text{Ni}/\text{Al}_2\text{O}_3$. They concluded that the reaction rate is affected by the number, length and position of the substituent. The hydrogenation rate increased as the number of substituent decreased (trimethylbenzene < xylenes < toluene < benzene). Also, the reaction rate increased as the length of substituent decreased (n-propylbenzene < ethylbenzene < toluene < benzene), while the *para* position found to be the most reactive.

Vannice and Lin investigated the hydrogenation of benzene and toluene over Pt [47-49]. They executed several reactions to study the effect of different supports ($\text{Al}_2\text{O}_3.\text{SiO}_2$, Al_2O_3 , SiO_2 and TiO_2) on the hydrogenation. They found that the activity of hydrogenation was increased when an acidic support was used ($\text{Al}_2\text{O}_3.\text{SiO}_2$). They suggested that the acidic supports had additional active sites, which increased the adsorption of benzene.

They also reported a low reaction order (nearly zero order on substrate and between 0.7 – 1 on hydrogen). They also noticed that benzene hydrogenation was deactivated more than toluene.

1.3 Phenol hydrogenation

Catalytic hydrogenation of alkylphenols is an important source for alkylcyclohexanone and alkylcyclohexanol [50]. The selectivity towards these products can be controlled by varying catalyst, support and reaction parameters [50, 51]. It is an important process from an environmental point of view. These oxygen containing aromatics are passed over catalysts to remove oxygen (hydrodeoxygenation, HDO) which is a catalyst poisoning factor in the catalytic hydrotreating process [52]. In addition to the importance of products produced from the hydrogenation of alkylphenols, there is the hydrogenation of phenol, which produces cyclohexanone as an intermediate and cyclohexanol [51].

Phenol hydrogenation mainly produces cyclohexanone and cyclohexanol. Cyclohexanone is an important intermediate in the industry of nylon and polyamide resins [53]. Whereas cyclohexanol is used widely in fine chemistry and perfume industry [50]. Other products are also mentioned in the literature such as benzene and cyclohexane [54-58]. The formation of the latter two products is related to the type of catalyst and solvent [55]. It is worth mentioning that in some studies [54, 55] benzene was used as a solvent and the formation of cyclohexane from benzene was taken into consideration. The argument there was that phenol hydrogenation will be ‘predominant’.

Kluson and Cerveny investigated the effect of substituting groups on the hydrogenation of the aromatic ring. They tested phenol, benzaldehyde and anisole on Ru/activated charcoal. They found that both phenol and anisole were hydrogenated to the corresponding cyclohexane. On the other hand, the carbonyl group on benzaldehyde was hydrogenated preferably, which proved that the reaction is affected by the type of substituent [59].

Giraldo et al. [55] investigated the vapour phase hydrogenation of phenol, after dissolving it in different solvents, over Rh/SiO₂ catalyst. They used cyclohexane, benzene, toluene, and ethanol as solvents for phenol. They concluded the following points:

- Higher phenol conversion was achieved when cyclohexane was used.
- Cyclohexanone selectivity was not affected by the nature of solvent when cyclohexane, benzene or toluene was used.

- Phenol conversion decreased when ethanol was used.

They also suggested that alcohols were not preferred for the hydrogenation of phenol. Their argument was based on the possibility of phenol alkylation to produce alkyl phenols.

Shin and Keane [13] prepared Ni / silica catalysts with different metal loading in order to find the effect of these catalysts on conversion and selectivity. They showed possible reaction routes and products that were expected from the hydrogenation of phenol using a nickel catalyst as shown in Figure 2.

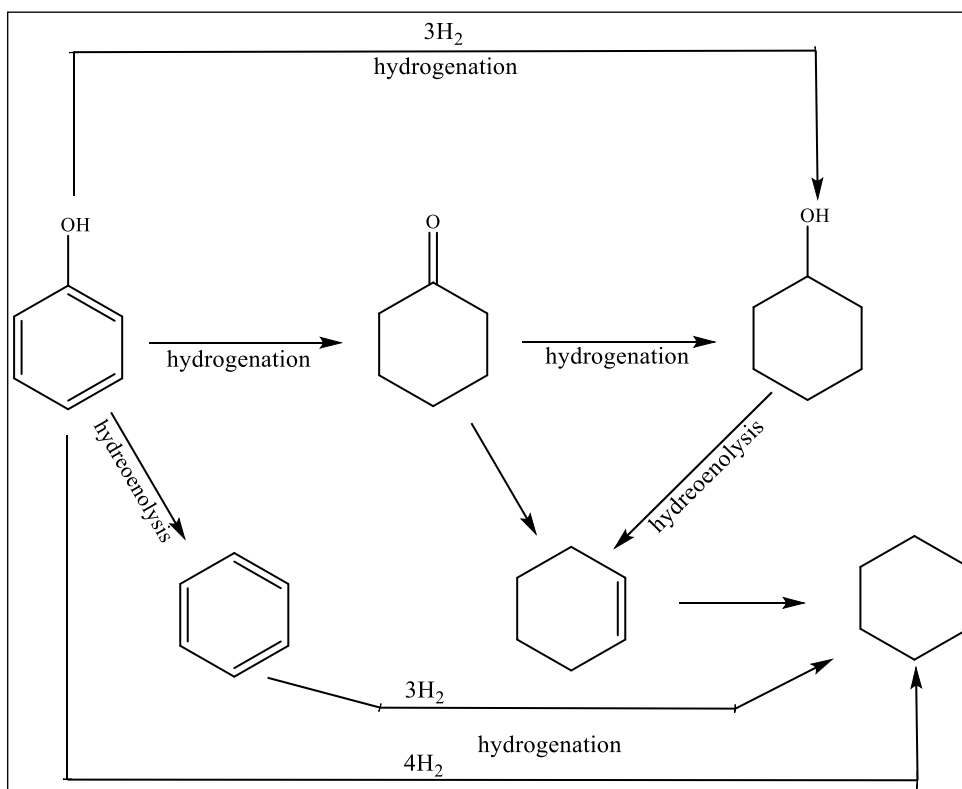


Figure 2. Possible reaction routes for phenol hydrogenation, hydrodeoxygenation, Ni/SiO₂ [13]

There is a general agreement that phenol hydrogenation proceeds in a sequential process if performed under moderate conditions as shown in Figure 3 [60].

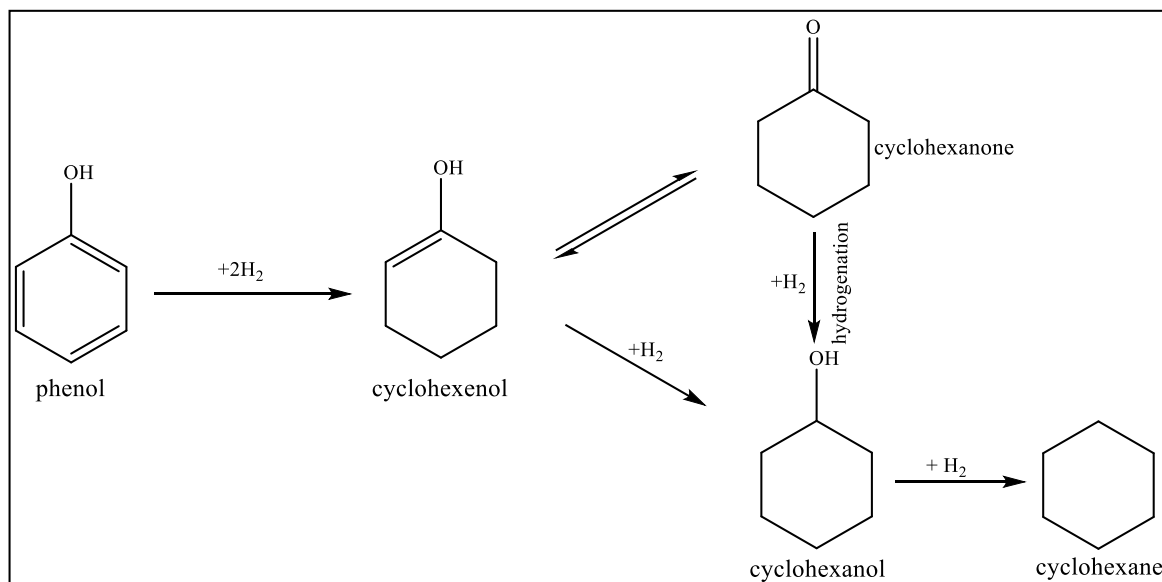


Figure 3. Sequential process of phenol hydrogenation under moderate conditions over Pd/Al₂O₃ [61]

The sequential process can follow a hydrogenolysis route or a hydrogenation route. The hydrogenolysis route, shown in Figure 2 involves the formation of benzene after the cleavage of the OH group. Benzene is then hydrogenated to cyclohexane. The hydrogenation route (Figure 3) follows the formation of an intermediate, cyclohexenol, which can be isomerised to form cyclohexanone that can subsequently be hydrogenated to form cyclohexanol, which can also be produced directly from the hydrogenation of the intermediate (cyclohexenol). Cyclohexane then might be formed from the hydrogenolysis of cyclohexanol.

There are some factors that might affect the selectivity to cyclohexanone or cyclohexanol during phenol hydrogenation such as the strength of phenol adsorption [57, 62, 63] or the form of phenol adsorption on the support [54, 64, 65].

To summarise the idea, phenol can be adsorbed on a support in two different modes (Figure 4) depending on the type of support. On acidic supports, such as silica-alumina, a coplanar adsorbed state is formed leading to a strong adsorption, which is responsible for the formation of cyclohexanol and cyclohexane [64]. The other model has nonplanar adsorption, which is formed on basic or neutral sites such as silica. This form has a weaker interaction between the benzene ring and the surface, which tends to produce cyclohexanone selectively [66].

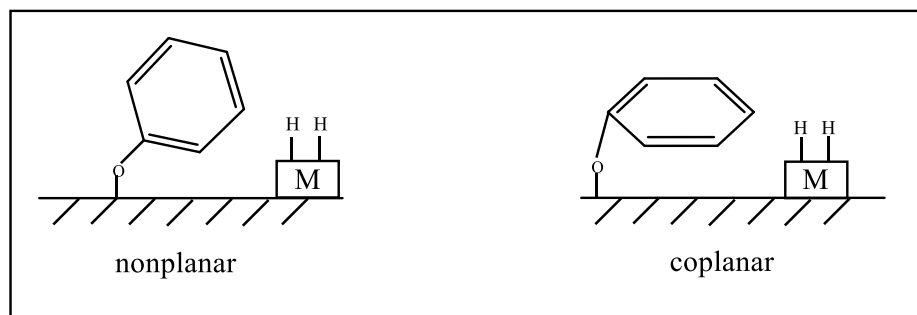


Figure 4. Modes of phenol adsorption [64]

In addition, the position and numbers of substituent location on the benzene ring might also have an effect on the selectivity. indeed selectivity to cyclohexanone has been shown to increase when the number of substituents increased or when a substituent is located in the *o*-position [50]. This was explained by the steric effect performed by the substituent groups which might inhibit complete hydrogenation to cyclohexanol. This behaviour also explains the selectivity to cyclohexanone when an alkyl group is located in the *ortho* position, which is close to the hydroxyl group position which might result in steric hindrance.

1.4 Anisole hydrogenation

Anisole hydrogenation has been studied in different systems and different catalysis in the literature [67-72]. Most of these studies used anisole as one of different substituted benzenes for comparison reasons. Only a few researches involve the mechanism and kinetic studies for anisole. In most anisole hydrogenations, methoxycyclohexane is the major product with selectivity ranging from 70% to 100% depending on catalyst, solvent and parameters applied [68]. Other products that have been cited include cyclohexanone, cyclohexanol and cyclohexane. Mevellec et al. [69], for example, studied the hydrogenation of different aromatic compounds over colloidal rhodium suspension. SiO₂-Rh⁰ nanoparticles. They found that anisole was selectively hydrogenated to methoxycyclohexane at 20 °C and 1 atm H₂ pressure. In another study, Fang et al. [70] used a poly vinyl pyrrolidone-Ru catalyst system to study the hydrogenation of aromatics, olefins and carbonyl containing compounds. They found that anisole was hydrogenated to 70% methoxycyclohexane, 16% cyclohexane and 14% cyclohexanol. They used decane as a solvent at 80 °C under 4 MPa H₂ pressure. Cyclohexanone was also reported in other researches. Denicourt-Nowicki et al. [71] used bipyridienes to stabilise Rh NPs during the hydrogenation of anisole. They produced 77% methoxycyclohexane and 23% cyclohexanone with 100% anisole conversion.

A general reaction scheme can be suggested from the hydrogenation of anisole as shown in Figure 5. It involves two routes, one is the formation of the corresponding cyclic form, methoxycyclohexane. The second route is the formation of cyclohexanone and/or cyclohexanol.

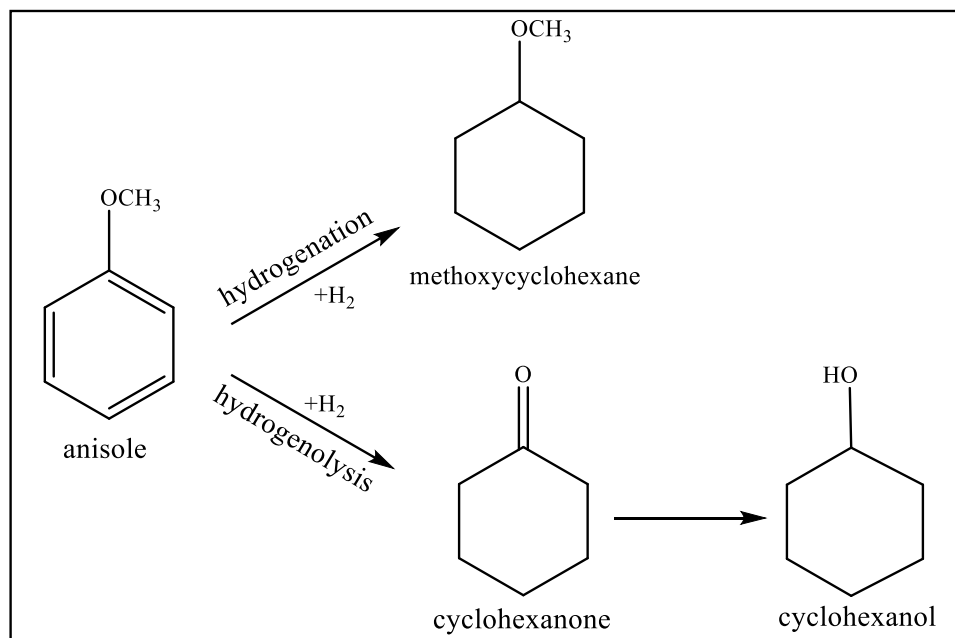


Figure 5 Possible reaction routes for the hydrogenation of anisole over Rh [71]

Cyclohexanone was suggested to form via the formation of an intermediate, methoxycyclohexene as shown in Figure 6 [73, 74]. This intermediate was detected by Widegren and Finke [73] with 2 – 8% selectivity. The hydrogenation reaction was performed at temperatures ranged from 20 – 80, hydrogen pressure was 2– 3 barg, propylene carbonate was used as a solvent and polyoxoanion-stabilized Rh(0) nanocluster as the catalyst.

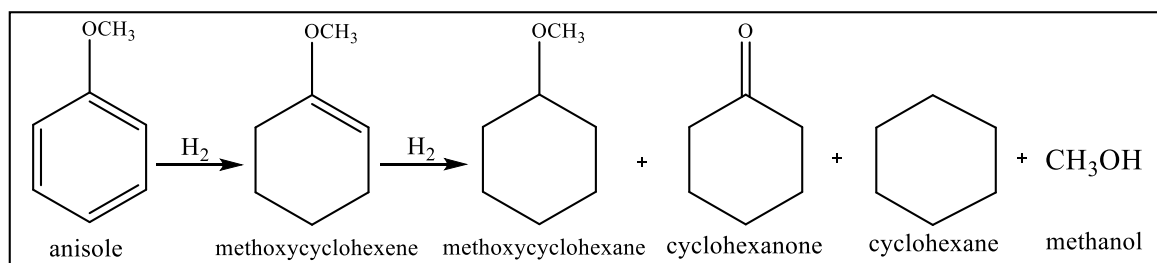


Figure 6 Proposed anisole hydrogenation to form cyclohexanone [59, 73]

1.5 Steric and electronic effects

Steric and electronic factors can have a considerable effect on the hydrogenation of substituted benzenes [21, 75]. As stated earlier, in alkylbenzene hydrogenation the rate of hydrogenation decreases as the length of substituents increases, as linear chains attached to the ring can inhibit benzene adsorption on the surface or they might prevent hydrogen from reaching to the benzene ring [35].

In addition, electronic properties of groups attached to the benzene ring can affect the activity of the hydrogenation reaction. It was stated that a benzene ring with electron donor groups such as alkyl groups, hydroxyl and methoxy groups showed faster hydrogenation rates than aromatics attached to withdrawing groups such as halogens [76, 77]. Electron donor groups have the ability to donate electrons to the aromatic ring and this behaviour will increase the electron density on the ring, which may increase the reactivity of the aromatic ring [78]. Alkyl groups increase electron density by an inductive effect, while other donating groups such as hydroxyl and methoxy increase the electron density by a resonance donating effect, which is generated from the lone pairs [79]. Hydroxyl group resonance with the ring in phenol is shown in Figure 7 as an example.

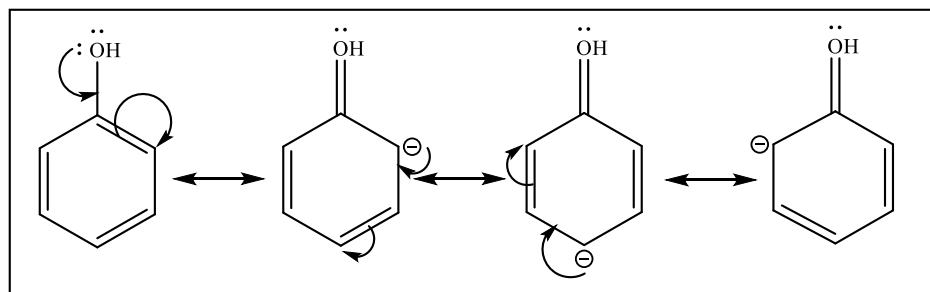


Figure 7. Phenol resonance structures [79]

Vetere et al. [80] studied substituent effects on the hydrogenation of ketones over Pt-based catalysts. In their study they used, acetophenone, 2-methyl acetophenone, 4-methoxy acetophenone and 4-chloroacetophenone as substrates. All four substrates were hydrogenated to their corresponding aromatic alcohol at the same reaction conditions; 80 °C and 1 MPa H₂ pressure. Their findings are summarised in Table 4 at 50% conversion.

Table 4. Rates of ketones hydrogenation

Substrate	Rate ($\mu\text{mol g}^{-1}\text{s}^{-1}$)
Acetophenone	156
2-methyl acetophenone	102
4-methoxy acetophenone	215
4-choloroacetophenone	69

They attributed rate variations to electronic and steric effects applied by the type and location of substituents on the aromatic ring. When comparing methoxy and methyl groups, which are donating groups, with the chloro group, which is a withdrawing group, it was found that the latter has lower rate than the others. Also when comparing between the positions of methyl group and the methoxy group they concluded that the rate was higher when substituent is far from carbonyl group (para position).

In general, aromatics are adsorbed parallel to the catalyst surface. Studies on a range of different metals agreed with that suggestion. For example, Ihm and White [81] studied the phenol reaction over Pt and they found that the benzene ring was adsorbed parallel to the surface. Tan et al. [82] reported that anisole was adsorbed while the benzene ring was also parallel to Pt surface. Nevertheless, some molecules showed different behaviour in special cases. Quiroz et al. [83] studied the electrocatalytic hydrogenation of m-xylene over Pt and they suggested that an 'edgewise' adsorption might be favoured over parallel, when the surface is highly covered with aromatic substrates or hydrogen.

Generally, benzene adsorbed on metals via π -complexes [47, 84, 85] and this behaviour is not the same when the benzene ring is attached to a substituent. Early work by Webb and Orozco [86], they investigated the hydrogenation of benzene and toluene over Pd and Pt catalysts using alumina and silica as supports. They suggested that toluene was adsorbed via the methyl group which produce a species as shown in Figure 8.

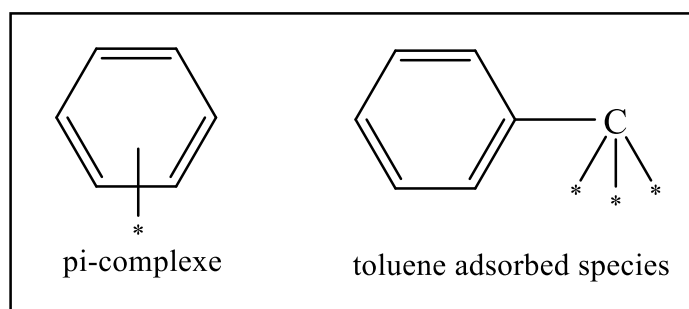


Figure 8. Benzene and toluene adsorbed species

Rahaman and Vannice [45] studied the hydrogenation of xylenes over Pd. They found that the rate of hydrogenation increased in the order o - < m - < p -xylene where m -xylene hydrogenated 4-6 times faster than o -xylene. This behaviour was attributed to the position of the methyl groups, which in p -xylene, which has the highest rate, are at opposite ends of benzene ring facilitating hydrogen attack. These findings were in agreement with Keane [87], who studied the hydrogenation of xylenes over Ni/SiO₂. The corresponding dimethylcyclohexanes were the only products in the form of *cis* and *trans* mixtures. The difference between hydrogenation rates in Ni catalyst were very close with slight increase in the order o - < m - < p -xylene. Both of these studies [45, 87] suggested a steric effect rather than an electronic one. This might be because the xylenes have the same number of methyl groups but in different positions.

1.6 Solvent effects

A solvent in the liquid phase hydrogenation might have different functions such as dissolving solid substrates or products, or, given that hydrogenation reactions are exothermic, using a solvent might help control the heat generated, or by washing the catalyst surface free of by-products that form during hydrogenation [88, 89]. It was found in number of researches that isopropanol (IPA) is a suitable reaction media in the liquid phase hydrogenation of aromatics [25, 26, 90]. Wang, et al. [26] for example, investigated different solvents such as methanol, ethanol, IPA and n-hexane on phenol hydrogenation and they found that IPA and n-hexane provided yields up to 95%.

For toluene hydrogenation, the solvent effect was investigated by Barthe, et al. [91]. They used water, hexane and dichloromethane as solvents during the hydrogenation of toluene over Rh/silica. They found that hexane showed higher activity, where 100% conversion was achieved after 0.9 h. On the other hand, when dichloromethane was used as a solvent only ~30% conversion was achieved after 5.5 h. They suggested that hexane was a better medium because it might facilitate toluene diffusion to the catalyst.

Chatterjee and co-workers [92] studied the hydrogenation of phenol over supported Pd at 50 °C. They investigated the effect of the presence of solvent, which was supercritical CO₂, and without the solvent during phenol hydrogenation. They found that cyclohexanone was formed in the presence of supercritical CO₂, whereas cyclohexanol and cyclohexanone were formed in the absence of the solvent. This behaviour was attributed to the effect of solvent on catalyst surface polarity which in turn changes the phenol adsorption behaviour. Also Michio and Shigeo [93] examined the effect of different

solvents on the hydrogenation of phenol over Pd/C. They found that the rate was decreased as the polarity of the solvent increased, which might affect the adsorption of phenol.

1.7 Deuterium exchange reactions

Deuterium exchange reactions are interesting processes used in different ways, such as the preparation of labelled substrates, which can be used as standards, or in research that involves mechanistic studies [94, 95], by comparing the difference between rate constant of hydrogen and deuterium kinetic isotope effect (KIE) [96]. Studies on isotope effects on the catalytic hydrogenation of aromatics are rare. Meerten et al. [97] studied the hydrogenation and deuteration of benzene over Pt/Al₂O₃ and Ni/SiO₂ catalysts. Only a slight isotopic effect was found when Ni was used as the catalyst and no explanation was given for this behaviour. They also examined the rate of exchange reactions between benzene with D₂ and deuterated benzene with H₂, where the former was much faster.

Due to the difference in mass between them, isotope exchange between hydrogen and deuterium has a significant effect on reaction rates and bond strengths. There are two possible effects in these types of reactions, normal and inverse KIE. The normal isotope effect, which is more common, is when the reaction in hydrogen is faster than the deuterium reaction ($k_H/k_D > 1$). In other words, C-H bonds are broken down more easily when compared to C-D bonds where the latter needs higher energy to be broken [98]. A normal isotope effect was found in this work for phenol and anisole only. The second type is the inverse isotope effect ($k_H/k_D < 1$) as was found for the three alkylbenzenes in addition to methoxyphenol.

2 Aims of project

The aim of this project was to study the hydrogenation of five different substituted benzenes over an iridium catalyst and potential compare it to a rhodium catalyst and hence increase our understanding of these poorly researched systems. Rh was already known for its activity at aromatic hydrogenation but even this area had not been extensively studied. When Ir was tested (see appendix) it was found to have a very low activity and it was decided to concentrate the project on rhodium, which was much more active. It was stated in the introduction section that the acidity of support might have an effect on the hydrogenation of aromatic species, therefore silica was used as a support rather than alumina to minimise any such effects. The catalyst chosen for the study was a 2.5% Rh/SiO₂

The substrates under study included methyl, ethyl, n-propyl, hydroxyl and methoxy substituted benzene. The study was performed under a range of different reaction parameters including temperature, hydrogen pressure and substrate concentrations to examine reaction kinetics, activation energy and order of reactions. Moreover, this project aimed to investigate the competitive hydrogenation of selected substrates to allow comparison with solo tests. Finally studies involving deuterium and deuterated substrates were examined to help delineate reaction mechanisms.

Substrates under study are known as

- . Toluene
- . Ethylbenzene
- . n-propylbenzene
- . Phenol
- . Anisole

3 Experimental

This chapter will include all instruments, tests and chemicals related to this work.

3.1 Catalyst characterisation

A Johnson Matthey 2.5% Rh/SiO₂ catalyst, M01080, which was prepared by an incipient-wetness method was used throughout this research. A surface area determination Brunauer–Emmett–Teller (BET) and a thermo-gravimetric analysis (TGA) were performed on the catalyst.

3.1.1 Determination of surface area

The surface area of the catalyst was determined by a Micromeritics Gemini III 2375 Surface Area Analyser. About 0.05 g of the catalyst was introduced to the device and was degassed overnight. N₂ gas was used for degassing at flow rate of 30 ml.min⁻¹ and the temperature applied was 110 °C.

The BET equation can be represented in the following form

$$P / [V (P_o - P)] = 1 / V_m C + [(C-1) P] / V_m C P_o$$

P = Equilibrium pressure of adsorbate gas

P_o = Saturated pressure of adsorbate gas

V = Volume of adsorbed gas

V_m = Volume of monolayer adsorbed gas

C = BET constant

$$C = e^{(q_1 - q_L)/RT}$$

q₁ = Heat of adsorption on the first layer

q_L = Heat of liquefaction on second and higher layers

$$R = 8.314 \text{ Jk}^{-1}\text{mol}^{-1}$$

A plot of P/[V(P_o-P)] against P/P_o should give a straight line where

$$\text{Slope (S)} = C-1/V_m C$$

$$\text{Intercept (I)} = 1/V_m C$$

V_m can be calculated according to

$$V_m = 1/(S + I)$$

The total surface area (S_{total}) can be calculated using the following formula

$$S_{\text{total}} = V_m N_s/M_v$$

Where M_v is the molar volume of adsorbed gas (N₂)

N_A = Avogadro's number

s = cross-sectional area of the adsorbed gas

Specific surface area (S_{specific}) can be calculated according to the following formula

$$S_{\text{specific}} = S_{\text{total}} / m$$

m = Catalyst mass in grams

3.1.2 Thermo-Gravimetric Analysis

The catalyst was analysed by a combined TGA/DSC SDT Q600 thermal analyser which was attached to an ESS mass spectrometer. Analysis carried out under 100 mlmin^{-1} flow of 2% O_2/Ar . The temperature was raised to $1000 \text{ }^\circ\text{C}$ in the rate of $10 \text{ }^\circ\text{Cmin}^{-1}$.

3.2 Instruments

3.2.1 Gas chromatography (GC)

A Focus GC with a flame ionised detector (FID) was used to analyse all reference substrates and samples obtained from reactions. An HP 1701 column was installed in the GC. It was 30 meters long and the diameter was 0.25 mm. Injector temperature was $230 \text{ }^\circ\text{C}$ and the detector temperature was $300 \text{ }^\circ\text{C}$. Figure 9 shows the column heating profile.

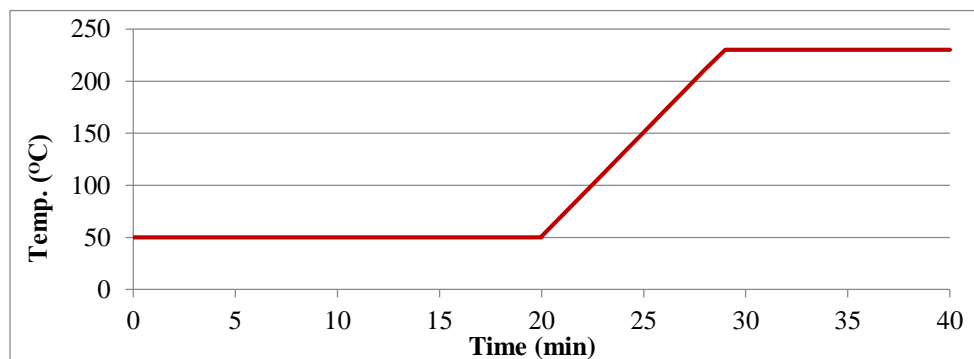


Figure 9. Temperature ramp profile

3.2.1.1 GC reference standards

Reference standards for all substrates, their corresponding cyclo products and other expected products were prepared in different concentrations and were analysed by the GC. Figure 10 shows some of the linear plots. Resulting beak areas were plotted against reference concentrations. The linear equations obtained were used to calculate concentrations of reaction products.

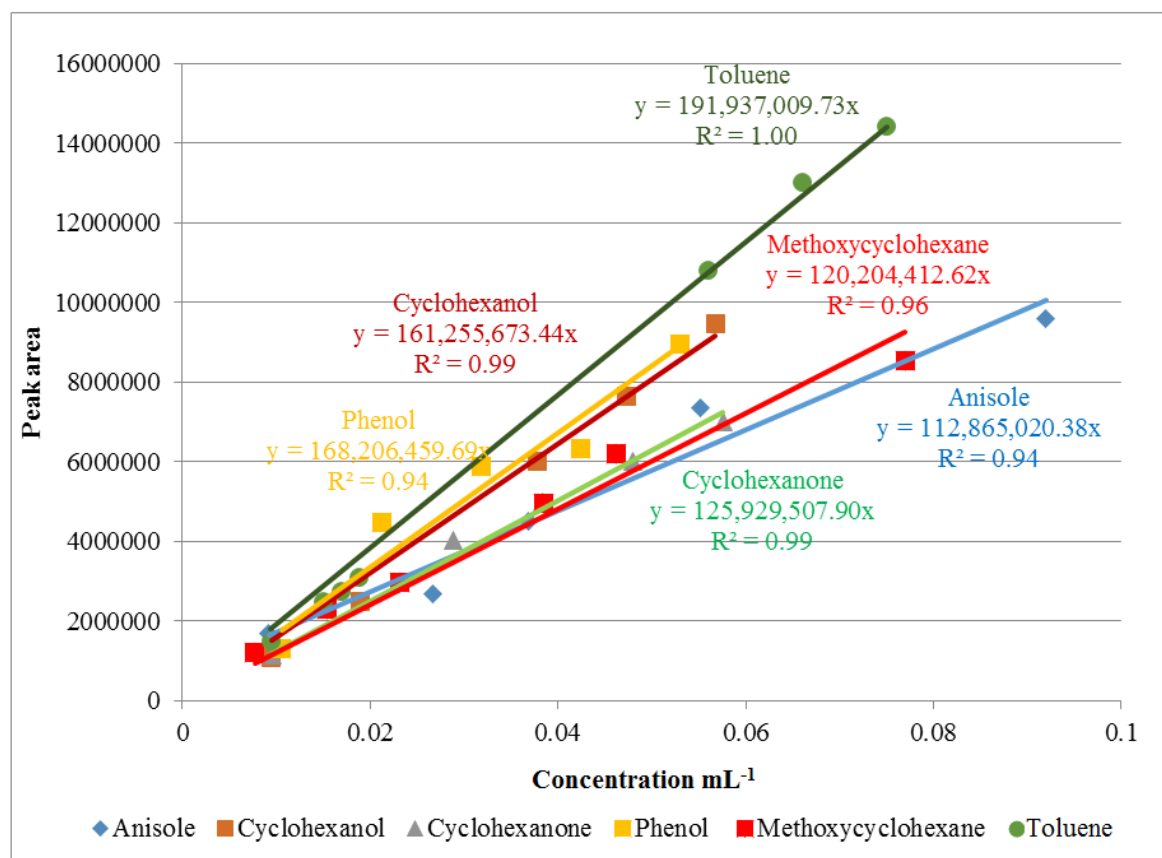


Figure 10. Reference standards profiles

3.2.2 Stirred tank reactor (Buchi)

This reactor was used to perform all the hydrogenation reactions. Reactions were carried out in a glass vessel surrounded by an oil heating jacket as shown in Figure 11. Oil temperature and circulation was controlled by Julabo system. The vessel was connected to a Pt100 thermocouple to measure the temperature in the vessel.

It was also equipped with a mechanical stirrer (Buchi 300) to control the rotation rate. The gas flow and pressure was controlled by (Pressflow gas controller .bpc. 1202).

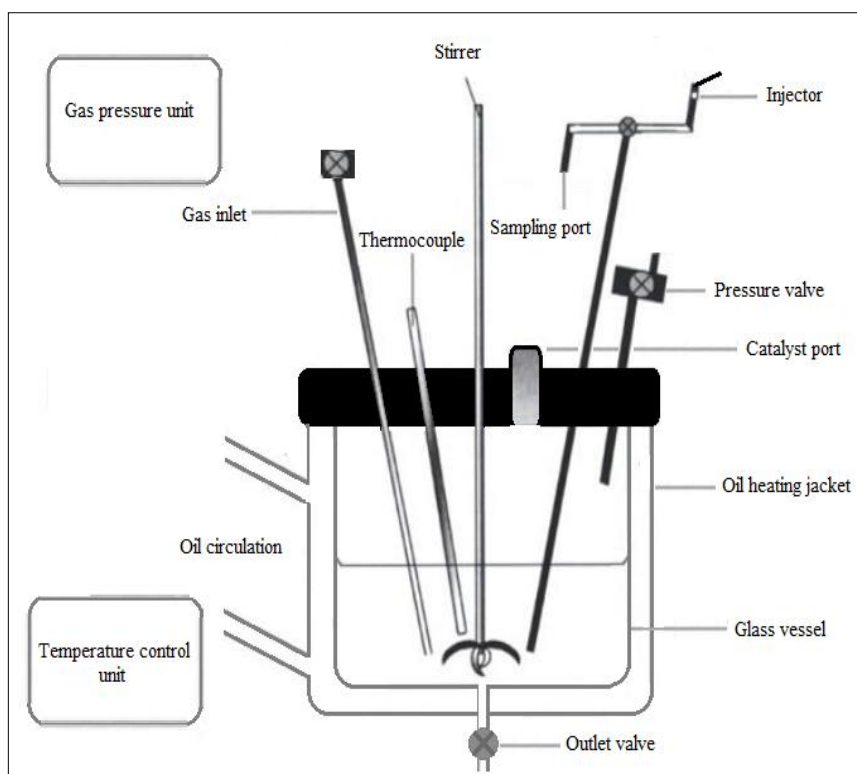


Figure 11. Stirred tank reactor

3.3 Performing the hydrogenation reaction

3.3.1 Pre-reaction procedure

The catalyst weight was 0.1 g for all reactions. Also IPA (isopropyl alcohol) was used as a solvent. The total volume was 330 ml. When a liquid substrate was tested, 320 mL was introduced to the reactor with catalyst and 10 ml was degassed before each reaction. In the case of solid substrate, 310 ml was introduced to the vessel, 10ml for degassing and 10 mL to dissolve the substrate. The amount of substrates used in all reactions was 1 mL unless otherwise indicated. Toluene = 0.0094 mole, ethylbenzene = 0.0082 mole, n-propylbenzene = 0.0072 mole, phenol = 0.0106, anisole = 0.0092 mole and methoxyphenol = 0.008 mole.

3.3.2 Catalyst reduction and solvent degassing

Reduction of the Rh/SiO₂ catalyst was performed in situ at 70 °C and under 0.5 barg hydrogen pressure before all reactions. This procedure was executed to increase the catalyst activity by reaching the metallic state of the catalyst. The reduction was carried out by adding 0.1 g of the catalyst to the vessel with 300 mL of the solvent. Afterwards, the system was heated to 70 °C and the stirrer was set to 300 rpm. After reaching 70 °C, 0.5 barg H₂ pressure was applied to the system for 30 min. After that, H₂ pressure was stopped.

Then, the system was set for the desired temperature preparing to start the hydrogenation reaction.

Whilst the catalyst was reduced, 10 mL of solvent was degassed for 30 min under a flow of nitrogen. This is to remove any gases, such as oxygen, which might affect the reaction. The degassed solvent was used to wash any substrate that might be remaining after it was introduced to the reactor vessel.

3.3.3 Hydrogenation reaction procedure

After the reduction of the catalyst, the system was set to desired temperature and pressure. The substrate was introduced to the reactor followed by the degassed solvent. They were injected to the vessel via the injection port. After that the stirrer was switched on to 1000 rpm. At about the same time, hydrogen was introduced to the vessel by starting the gas pressure unit. Next, the stirrer speed was reduced to 0 rpm and the first sample was collected via the sampling port. After that the stirrer speed was reset to 1000 rpm and after 5 minutes the second sample was collected in the same procedure.

For each reaction, 19 samples were collected during 3 h. In addition to the first sample, 6 samples were taken in the first 30 min, 6 samples for the following 60 minutes and finally 6 samples for the last 90 min.

After collecting the last sample, the gas pumping was stopped, the pressure valve was released and the stirrer speed was set to 300 rpm. Also, the oil bath heating unit was stopped. After releasing the pressure trapped in the vessel, the catalyst port was opened and the remaining substances (solvent, substrates and catalyst) in the glass vessel were drained by opening the outlet valve.

3.4 Hydrogenation tests

The hydrogenation tests include kinetic studies, competitive hydrogenations and deuterium reactions.

3.4.1 Kinetic studies

In these tests all substrates namely; toluene, ethylbenzene, n-propylbenzene, phenol and anisole were tested under different reaction parameters. The temperature range studied was 30 – 70 °C, H₂ pressure was varied between 2 and 5 barg and the volume of the substrates was examined between 0.5 – 1.5 ml. Results were used to calculate activation energies and to determine order of reactions

3.4.1.1 Determination of rate constant (k)

The rate constant was examined for each reaction. As the order of the reaction was unknown the equations for 0th, 1st and 2nd order were used to generate formulas that were used to plot linear equations as follows

For the reaction $A + B \rightarrow C + D$, rate can be given by

$$\text{Rate} = k [A]^x[B]^y \quad (1)$$

where [A] and [B] are concentrations, x and y are reaction orders in A and B respectively and k is the rate constant. Overall reaction order will be the sum of x and y.

$$\text{For zero order reaction Rate} = k \quad (2)$$

$$\text{For 1}^{\text{st}} \text{ order reaction rate} = k [A] \quad (3)$$

$$\text{For 2}^{\text{nd}} \text{ order reaction rate} = k [A]^2 \text{ or rate} = k [A][B] \quad (4)$$

These equations can be integrated to form a linear equation in the general formula

$y = mx + c$ as shown in Table 5 The units for k were found by using basic equation for each order. For example, zero order reaction

Rate = k, rate is usually in ms^{-1} therefore the unit for k in zero order reaction will be m s^{-1} .

Table 5. Integrated forms of rate equations

Order	Integrated form	Graph	k units
0	$(A_0 - A_t) = -kt$	$(A_0 - A_t)$ vs t	m s^{-1}
1	$\ln (A_0 / A_t) = -kt$	$\ln (A_0 / A_t)$ vs t	s^{-1}
2	$(A_0 - A_t) / (A_0 A_t) = kt$	$(A_0 - A_t) / (A_0 A_t)$ vs t	$\text{s}^{-1}\text{m}^{-1}$

3.4.1.2 Activation energy E_a

As stated earlier, the hydrogenation reactions of toluene at different temperatures are zero order reactions. Knowing that, the activation energy can then be determined using the Arrhenius equation. This equation represents the dependence of rate constant on temperature.

$$k = Ae^{-E_a/RT} \quad \text{Arrhenius equation} \quad (5)$$

k = rate constant A = pre-exponential factor E_a = activation energy

R = gas constant ($8.314 \text{ Jk}^{-1}\text{mol}^{-1}$) T = temperature in kelvin ($0^\circ\text{C} = 273 \text{ K}$)

From the data obtained from temperature variation reactions, an apparent activation energy can be calculated by using the integrated form of Arrhenius equation. This form can be obtained by taking the natural log for both sides of Arrhenius equation which will give:

$$\ln(k) = (-E_a/R)(1/T) + \ln(A) \quad (6)$$

$$y = mx + c$$

This equation represents a linear equation when plotting $\ln(k)$ vs. $(1/T)$. The gradient of the straight line generated gives $-E_a/R$

$$E_a = -mR \quad (7)$$

3.4.1.3 Reaction order in H₂ pressure and in substrate concentration

From the results obtained from pressure variation reactions; it was possible to determine order of reaction in H₂. It was determined by using the rate of reaction formula

$$r = k [A]^x (P)^y \quad (8)$$

by taking the natural log of equation (8) sides we get

$$\ln r = \ln k + x \ln [A] + y \ln (P) \quad (9)$$

when concentration of [A] held constant then the equation is simplified to $y = m x + c$ form. And when plotting $\ln(r)$ vs. $\ln(P)$ a straight line will be generated and m is the order of reaction.

3.4.2 Competitive hydrogenations

In this test groups of three different substrates were hydrogenated as mixtures to investigate the effect of different functional groups on the catalytic hydrogenation of the benzene ring in a competitive environment. The groups were the alkyl benzenes, toluene, ethylbenzene and n-propylbenzene, investigating the length of the alkyl chain. The second group was toluene, phenol and anisole, comparing the effect of a methyl group compared to a hydroxyl group, while the third group was phenol, anisole and 4-methoxyphenol, which examines the effect of hydroxyl compared to methoxy. In each group two substrates were tested as mixture and then the three substrates were mixed to be tested. For example, the three alkyl benzenes were tested in the following way

Toluene + ethylbenzene

Toluene + n-propylbenzene

Ethylbenzene + n-propylbenzene

Toluene + ethylbenzene + n-propylbenzene

Reaction parameters for the competitive hydrogenation reactions were 50 °C, 3 barg and 1ml of the substrate. Reactants and their number of moles in 1 ml are listed in the flowing table:

Table 6. Reactants with their densities and number of moles

Reactant	Density (gmL⁻¹)	N (mol)
Toluene	0.867	0.0094
Ethylbenzene	0.867	0.0082
n-propylbenzene	0.862	0.0072
Phenol	1.071	0.0106
Anisole	0.995	0.0092
4-Methoxyphenol	1.55	0.008

3.4.3 Deuterium reactions

In this reaction, deuterium was used instead of hydrogen for testing its effect on the catalytic reaction and to compare the results with the results obtained from the hydrogenation tests. Also in this test the reaction parameters were set at 50 °C, 3 barg and 1mL of the substrate.

Extra tests were performed on toluene, a) toluene hydrogenation under hydrogen pressure. This reaction was compared with b) toluene-d₈ + H₂, c) toluene + D₂ and d) toluene-d₈ + D₂.

3.5 NMR spectroscopy

NMR spectroscopy was used to analyse some samples that were taken from toluene + D₂. ¹H NMR analyses were conducted on a Bruker Avance 400 spectrometer. The ²H NMR were performed on a Bruker 500 Ultra Shield-NMR system using a custom pulse and acquisition AU-programme provided by the Bruker company using the Deuterium-lock channel as the data channel. These measurements were kindly performed by Dr. David Adam at the University of Glasgow.

3.6 Chemicals

All materials were used as received with no further purification.

Table 7. Chemicals used in the project

Chemical	Supplier	Purity
Hydrogen (g)	BOC	99.99%
Rh/SiO ₂ (s)	Johnson Matthey	-
Anisole (s)	Sigma Aldrich	99%
Methoxycyclohexane(l)	TCI	≥ 98%
Phenol (s)	Sigma Aldrich	≥ 99%
Cyclohexanol (l)	Sigma Aldrich	99%
Cyclohexanone (l)	Sigma Aldrich	99%
Toluene (l)	Fisher Scientific	99%
Methylcyclohexane (l)	Sigma Aldrich	≥ 99%
1-methylcyclohexene (l)	Sigma Aldrich	97%
n-propylbenzene (l)	Sigma Aldrich	98%
Propylcyclohexane (l)	Sigma Aldrich	99%
Ethylbenzene (l)	Sigma Aldrich	≥ 99.5%
Ethylcyclohexane (l)	Sigma Aldrich	≥ 99%
Isopropyl alcohol (l)	Sigma Aldrich	99.5%
4-methoxyphenol(s)	Sigma Aldrich	99%

4 Results

This chapter will include results that were obtained from the different tests and analyses that were performed during this project. Firstly, results related to catalyst characterisation will be shown. Then, the findings obtained from direct hydrogenations for single substrates will be illustrated. These findings will include kinetic results that were determined after applying different reaction parameters (temperature, pressure and concentration). The kinetic results will include activation energies and order of reactions. After that, the competitive hydrogenation results will be shown. Finally, the results obtained from hydrogen-deuterium exchange reactions will be included in this chapter.

4.1 Catalyst characterisation

4.1.1 Surface area

The catalyst was prepared and characterise by Johnson Matthey. Surface area of the catalyst was determined via a BET isotherm. Results showed that the surface area of the catalyst was $265 \text{ m}^2 \text{ g}^{-1}$. Table 8 summarises the catalyst properties.

Table 8. Catalyst properties

Surface area	Pore volume	Pore diameter	Rh loading	Rh dispersion
$265 \text{ (m}^2 \text{ g}^{-1}\text{)}$	$1.06 \text{ (mL g}^{-1}\text{)}$	13 (nm)	2.5%	43%

4.1.2 Thermo-gravimetric Analysis (TGA)

Catalyst was examined in 5% H_2/N_2 . Figure 3 shows that there is about 1% weight loss at around $100 \text{ }^\circ\text{C}$. This loss can be explained by the evaporation of physisorbed water from the catalyst. It is also shown that about 2% of weight was lost between $300 - 600 \text{ }^\circ\text{C}$. This lose can be attributed to the CO_2 adsorbed by the catalyst from the atmosphere.

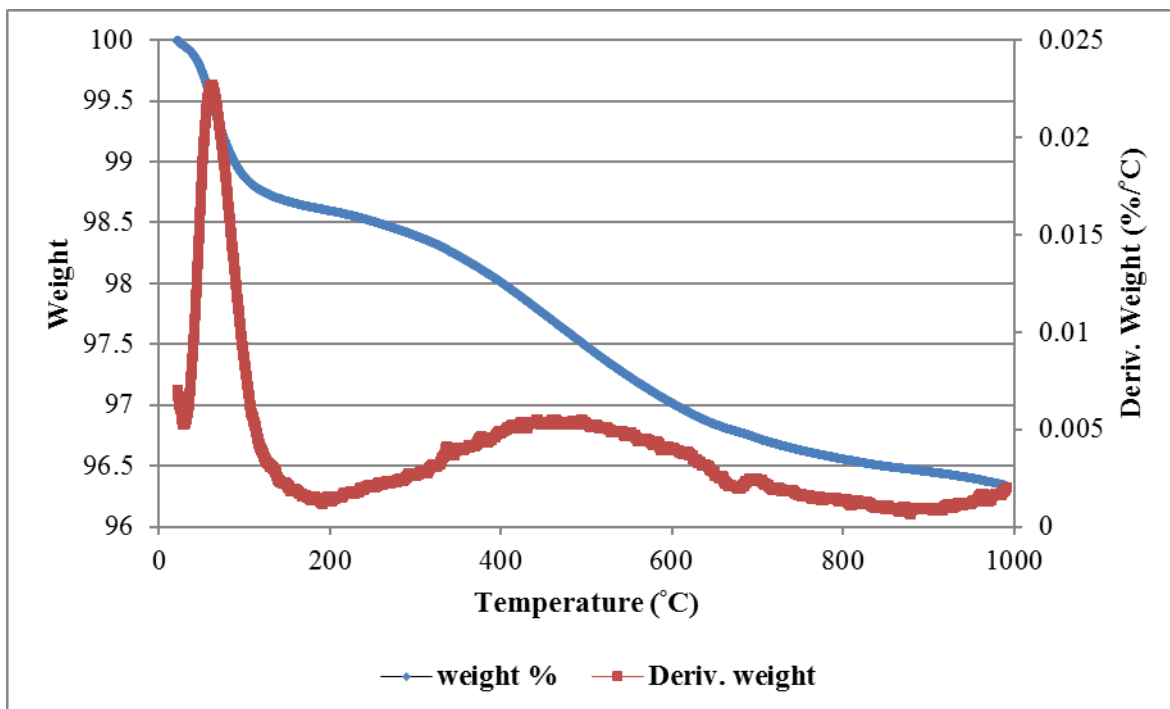


Figure 12. TGA profile for the catalyst

4.2 Alkyl aromatics hydrogenation

In this section, the results obtained from the direct hydrogenation of toluene, ethylbenzene and n-propylbenzene will be presented. This will include temperature, pressure and concentration variations. The results obtained from the variation of these parameters will be used to determine activation energies, order of reaction in both hydrogen pressure and substrate concentration. These findings will be followed by the competitive hydrogenation of the three substrates.

4.2.1 Toluene

Figure 13 shows the reaction profile for toluene at 30 °C. It shows a decrease in reactant (toluene) concentration and an increase in product (methylcyclohexane) formation. It also shows the formation of 1-methylcyclohexene but in very low concentration. Figure 14 shows the reaction profile at 50 °C. It is clear from Figure 14 that the formation of methylcyclohexane has increased as well as the concentration of 1-methylcyclohexene. Indeed as the temperature applied was increased both the conversion and product concentration increased.

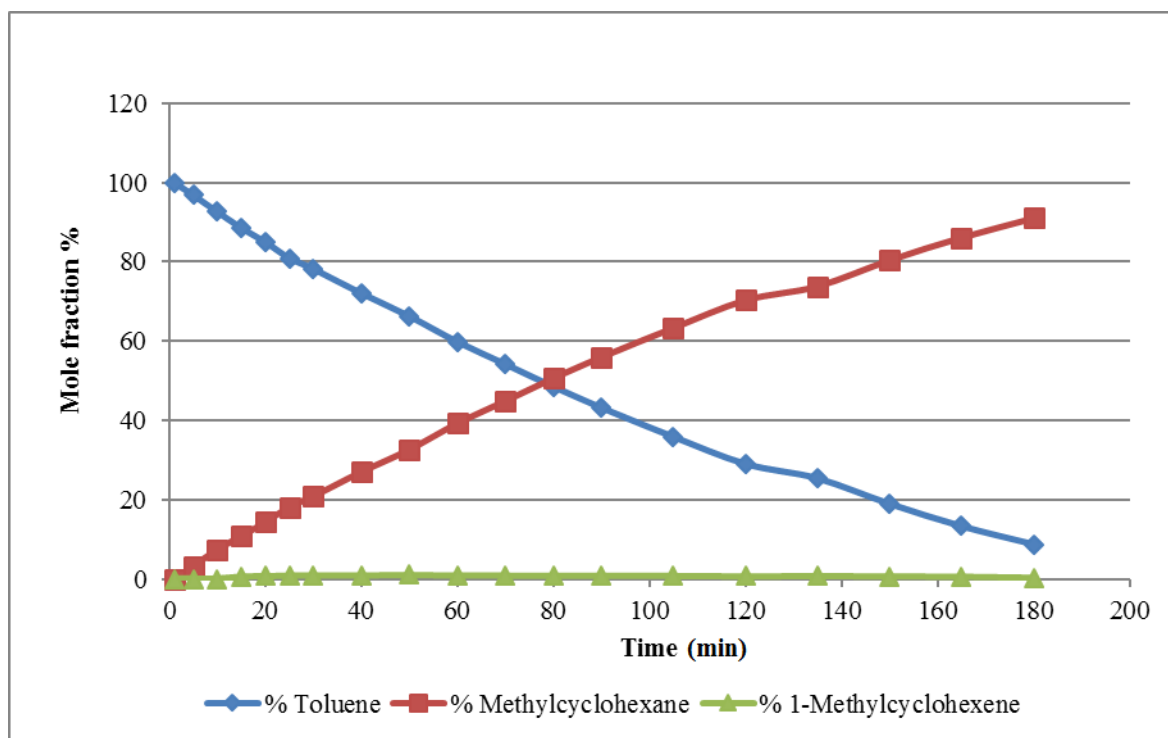


Figure 13. Toluene reaction profile at 30 °C

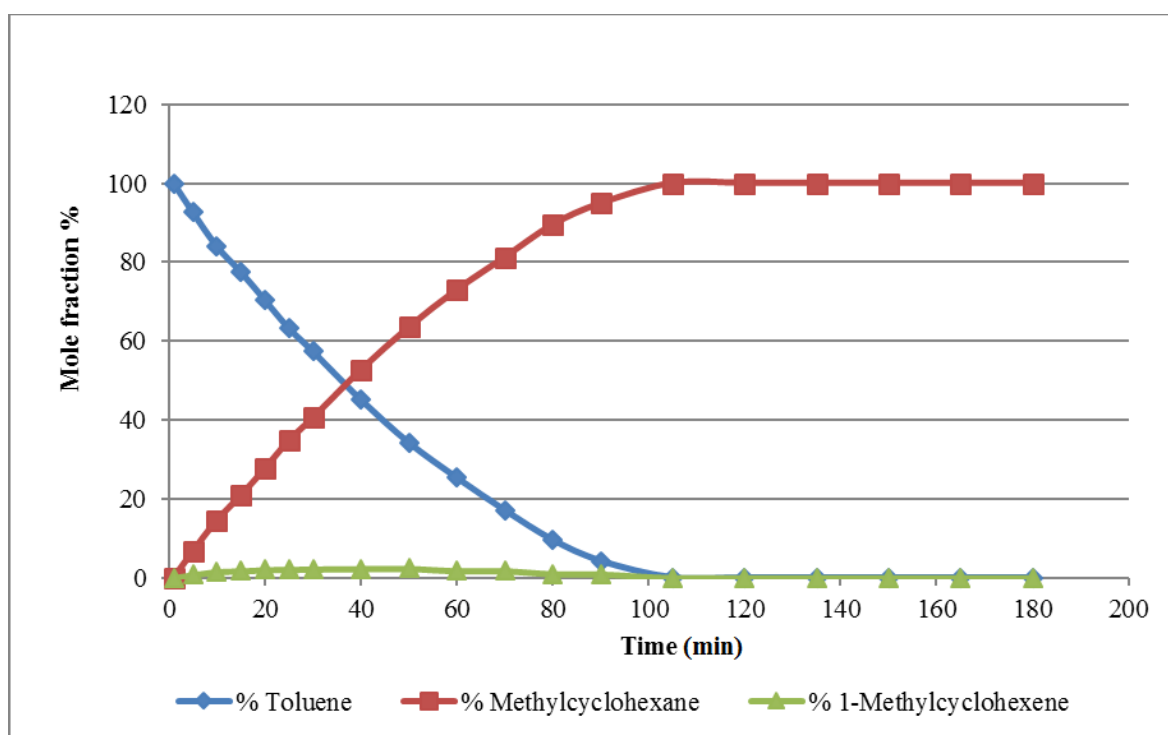


Figure 14. Toluene reaction profile at 50 °C

As explained earlier in section 3.4.1, the best plot was used for the determination of k . As shown on Figure 15, the 0th order rate constant plot has a slightly better fit than the others. Therefore for the hydrogenation reaction of toluene zero order reaction kinetics were used to analyse the data.

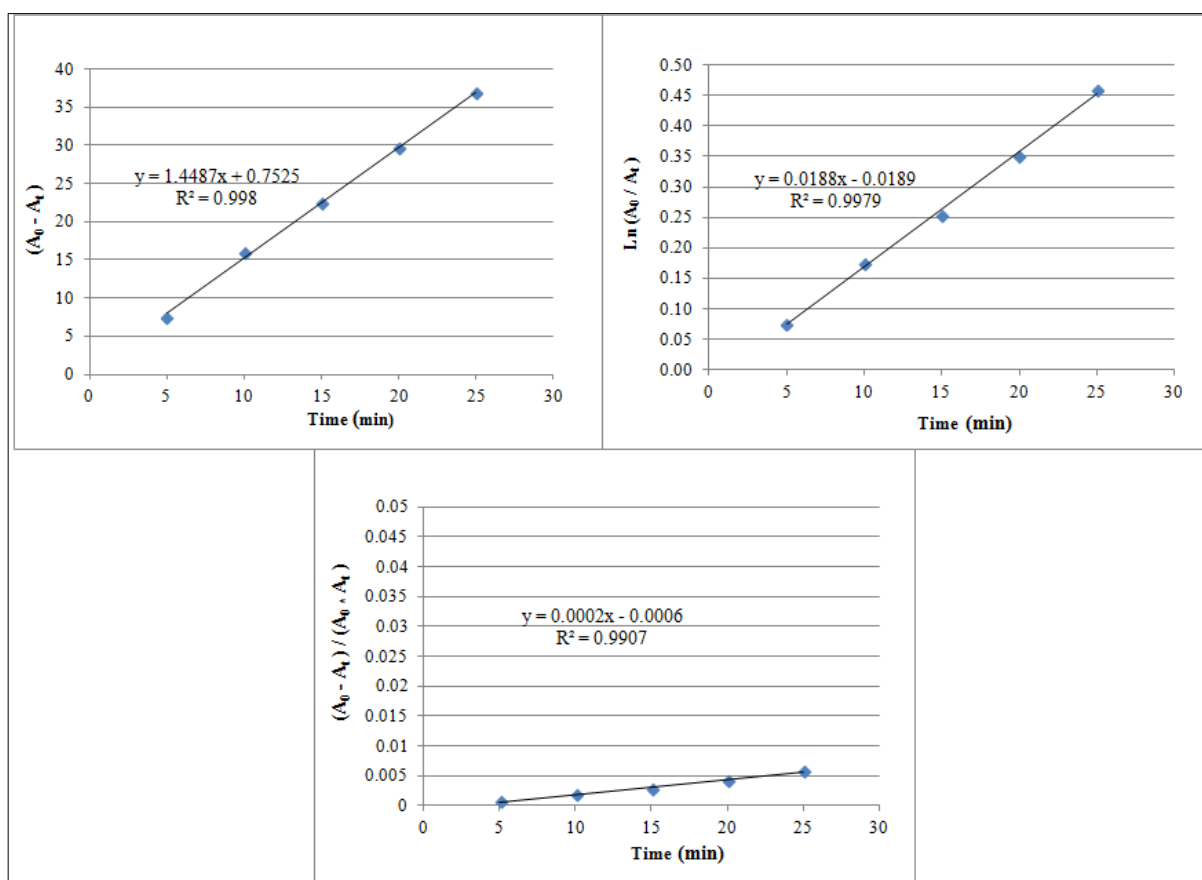


Figure 15. 0th, 1st and 2nd order rate constant for toluene at 50 °C

At each temperature a similar analysis was performed and the rate constant determined after identifying the best fit reaction order. In all cases 0th order integrated formula

$$[A_0] - [A_t] = -k.t \quad (10)$$

was the best fit and hence the zero order rate constants were used to calculate the activation energy.

4.2.1.1 Temperature variation

In this series of reactions, the hydrogenation temperatures were set to 30, 40, 50, 60 and 70 °C. The volume of substrates (1 mL) and reaction pressure (3 barg) were kept constant.

Figure 16 shows the conversion of toluene at different temperatures. The rate of formation of methylcyclohexane increased as the temperature increased. As can be seen in there is a noticeable increase in k values as the temperature increased. It takes 30 min to convert

20% of toluene at 30 °C while, it takes only 10 min to convert the same concentration at 70 °C as shown on Table 9.

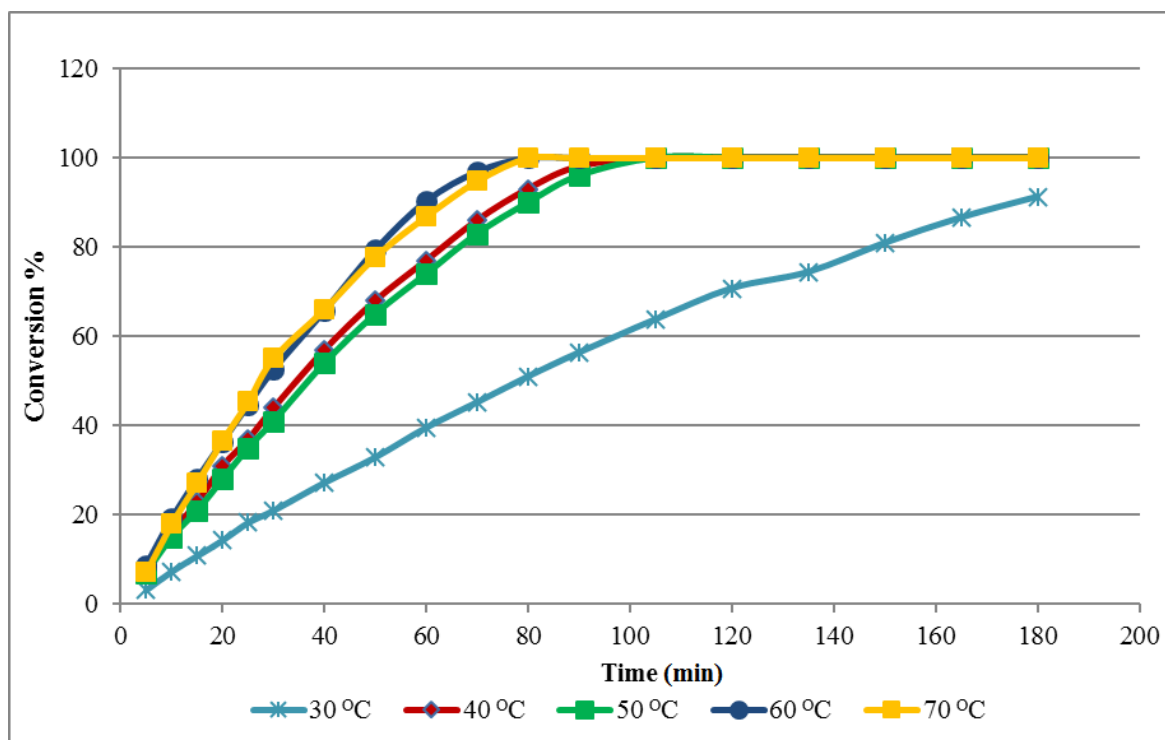


Figure 16. Conversion of toluene at different temperatures

Table 9. Conversion and rate constant of toluene at different temperatures

Temperature (°C)	30	40	50	60	70
Conv. after 180 min %	91	100	100	100	100
Time to 20% conv. (min)	30	15	15	10	10
Rate constant. k (ms ⁻¹)	0.788	1.4849	1.4487	1.8017	1.9357

4.2.1.1.1 Activation energy E_a

As stated earlier, the hydrogenation reactions of toluene at different temperatures are zero order reactions. Knowing that, the activation energy can then be determined using the Arrhenius equation (see section 3.4.1).

$$\ln(k) = (-E_a/R)(1/T) + \ln(A) \quad (6)$$

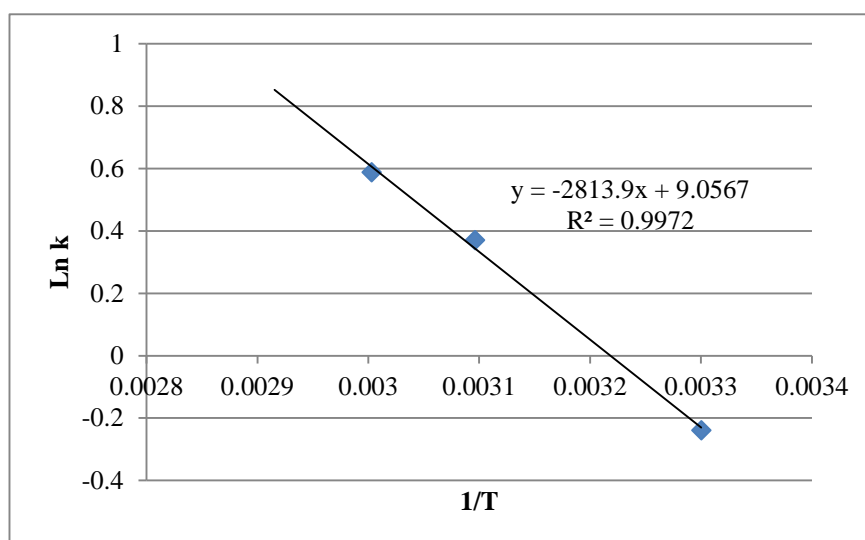
$$y = mx + c$$

This equation represents a linear equation when plotting $\ln(k)$ vs. $(1/T)$. The gradient of the straight line generated gives $-E_a/R$

$$E_a = -mR \quad (7)$$

Table 10. Data used to generate Arrhenius plot

T (k)	k (ms ⁻¹)	1/T	Ln k
303	0.788	0.0033	-0.23826
323	1.4487	0.003096	0.370667
333	1.8017	0.003003	0.588731

Figure 17. Toluene E_a plot

From equation (7) and Figure 17, the activation energy can be calculated as follows

$$E_a = (2813.9 \times 8.314) / 1000$$

$$E_a = 23 \text{ kJmol}^{-1}$$

4.2.1.2 Pressure variation

Different H₂ pressures were applied on toluene hydrogenation to investigate their effect on the reaction and also to find the reaction order in hydrogen. Pressure applied was 2, 3, 4 and 5 barg.

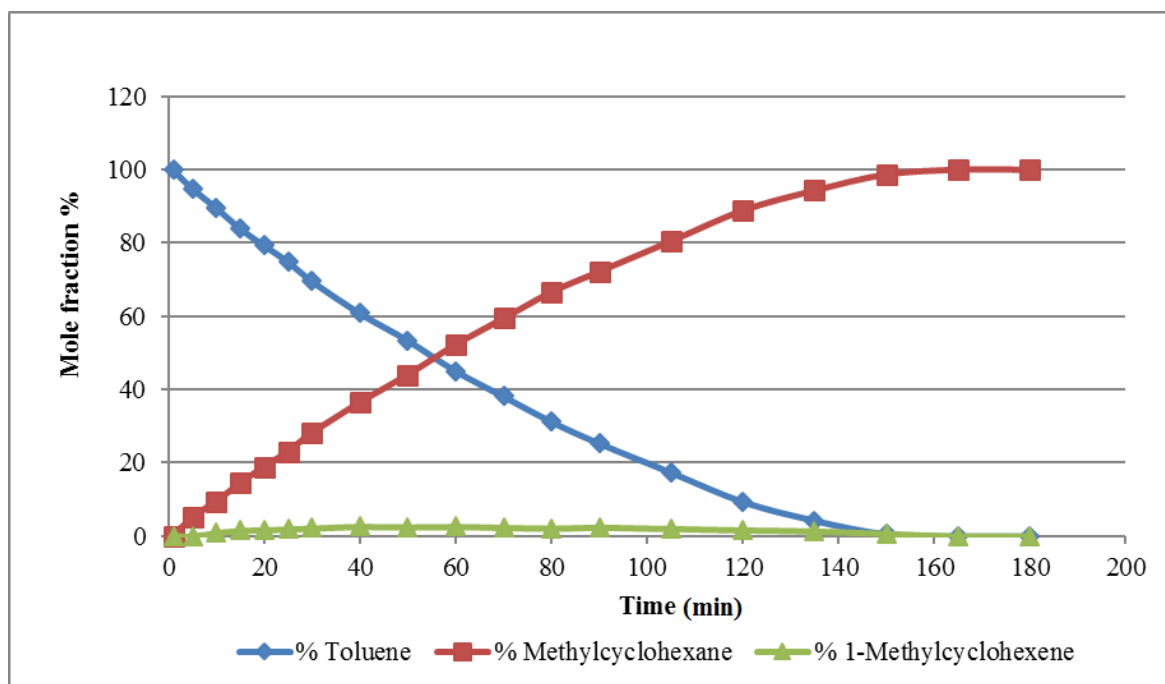


Figure 18. Toluene reaction profile at 2 barg H₂ pressure

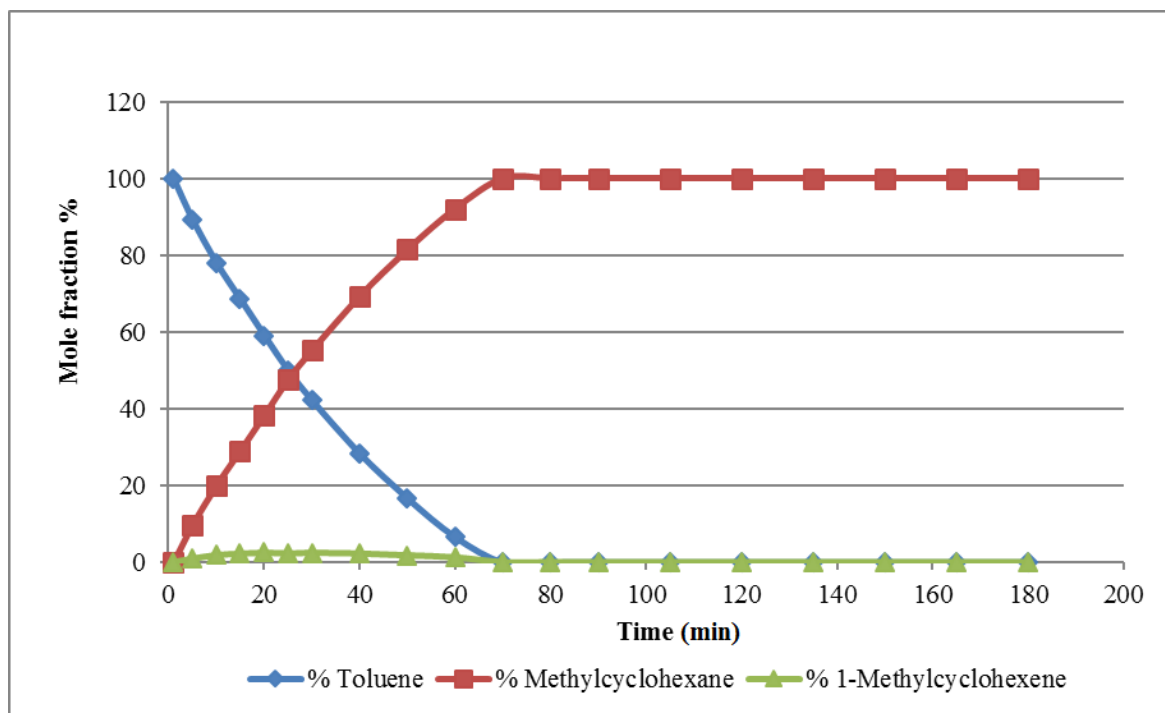


Figure 19. Toluene reaction profile at 5 barg H₂ pressure

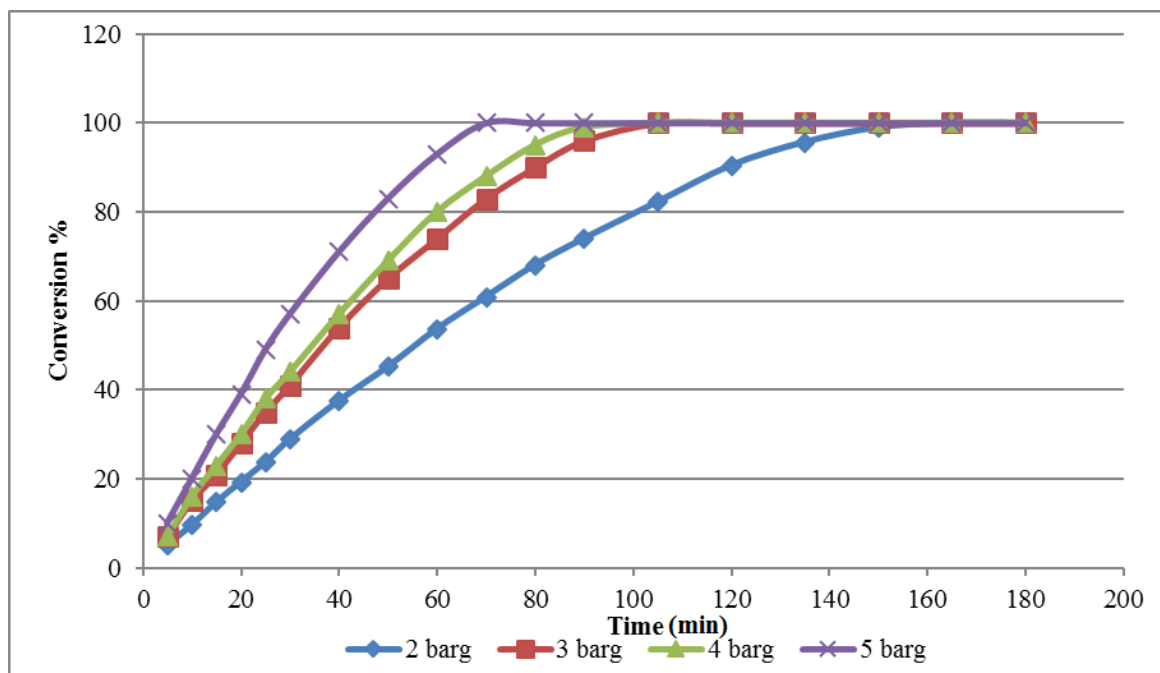


Figure 20. Formation of methylcyclohexane from toluene

Figure 20 shows the effect of hydrogen pressure applied on toluene hydrogenation. The conversion to methylcyclohexane increased as H_2 pressure applied increased. Table 11 presents the rate constant as well as the rate of reaction. It is clear that k values increased as the pressure applied increased. In addition, the formation of methylcyclohexene did not exceed 3% under all pressures as shown in Figure 18 and Figure 19.

Table 11. Conversion and rate constant of toluene at different H_2 pressures

H_2 pressure (barg)	2	3	4	5
Time to 20% conv. (min)	20	15	13	10
Rate constant. k (ms^{-1})	1.0019	1.4487	1.5296	1.9464
Rate ($\mu molL^{-1}min^{-1}$)	152	358	357	535

4.2.1.2.1 Reaction order in H_2 pressure

Form the results obtained from pressure variation reactions; it was possible to determine order of reaction in H_2 . It was determined as explained in section 3.4.1. When plotting $\ln(r)$ vs. $\ln(P)$ a straight line will be generated and m is the order of reaction. This is explained in Figure 21.

Table 12. Data used to determine reaction order in H₂

H ₂ pressure	r (ms ⁻¹)	ln H ₂	ln r
2	0.000152	0.6931	-8.7903572
3	0.000358	1.0986	-7.9351471
5	0.000535	1.6094	-7.5331412

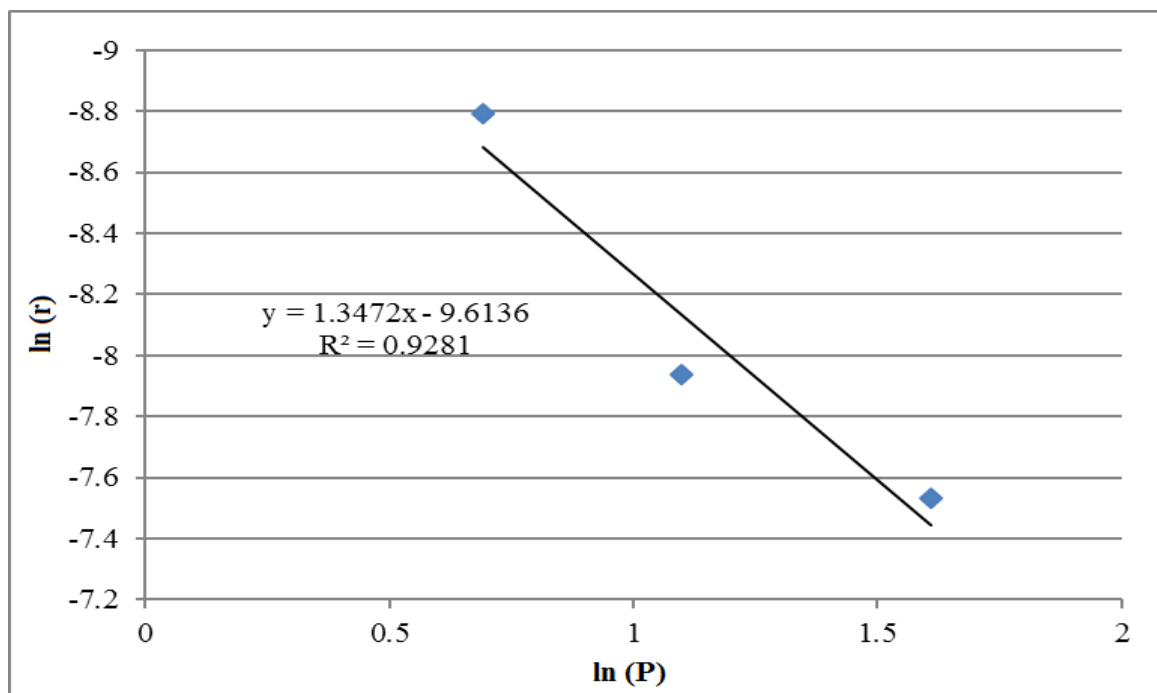
Figure 21. Toluene reaction order in H₂

Figure 21, the gradient is 1.3 therefore toluene reaction is approximately 1st order in hydrogen.

4.2.1.2.2 Reaction order in concentration

In this set of reactions, the volume of toluene was changed in 4 reactions. 0.5, 0.75, 1 and 1.5 mL of toluene was used in these reactions. The results generated from these tests were used to find the order of reaction in toluene concentration.

Figure 22 and Figure 23 show the reaction profiles of 0.5 ml and 1.5 ml of toluene respectively. It is clear that the conversion was faster when lower concentration of substrate was used.

To find the order of reaction in toluene the rate of reaction was calculated for the first 3 samples; after 5, 10 and 15 min.

The average of the rate of reactions was $4.6 \times 10^{-4} \text{ molg}^{-1}\text{min}^{-1}$ and the standard deviation was $8.7 \times 10^{-5} \text{ molg}^{-1}\text{min}^{-1}$. Hence the reaction order is approximately zero order in toluene concentration.

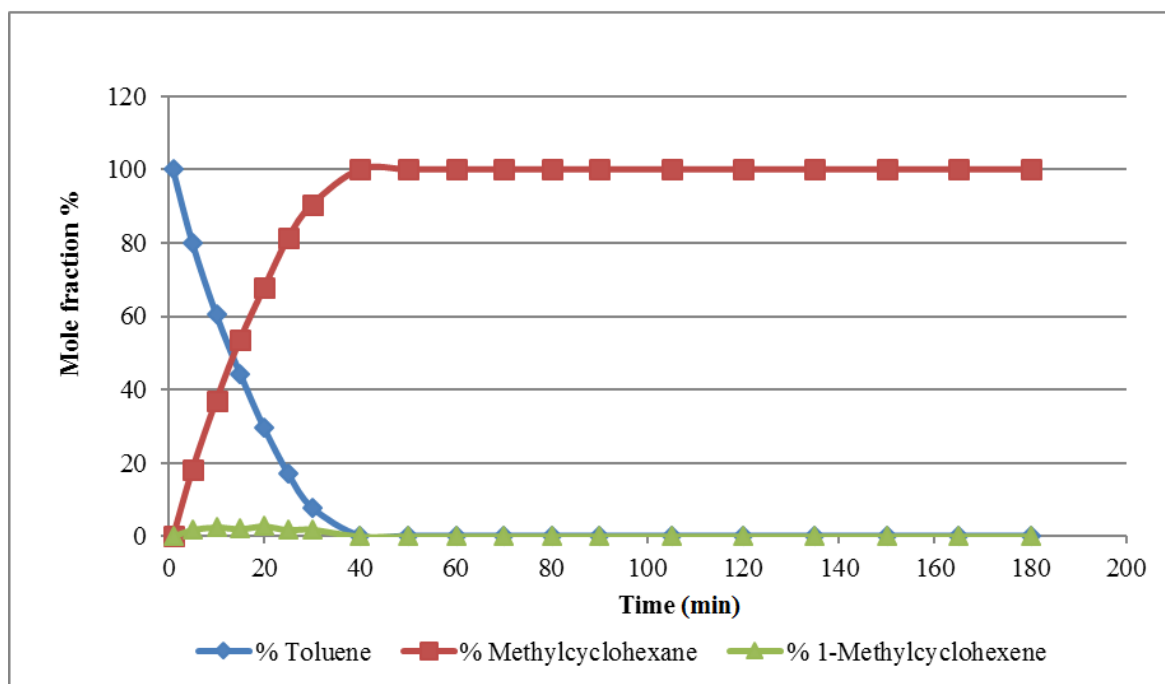


Figure 22. Reaction profile for the hydrogenation of 0.5ml toluene

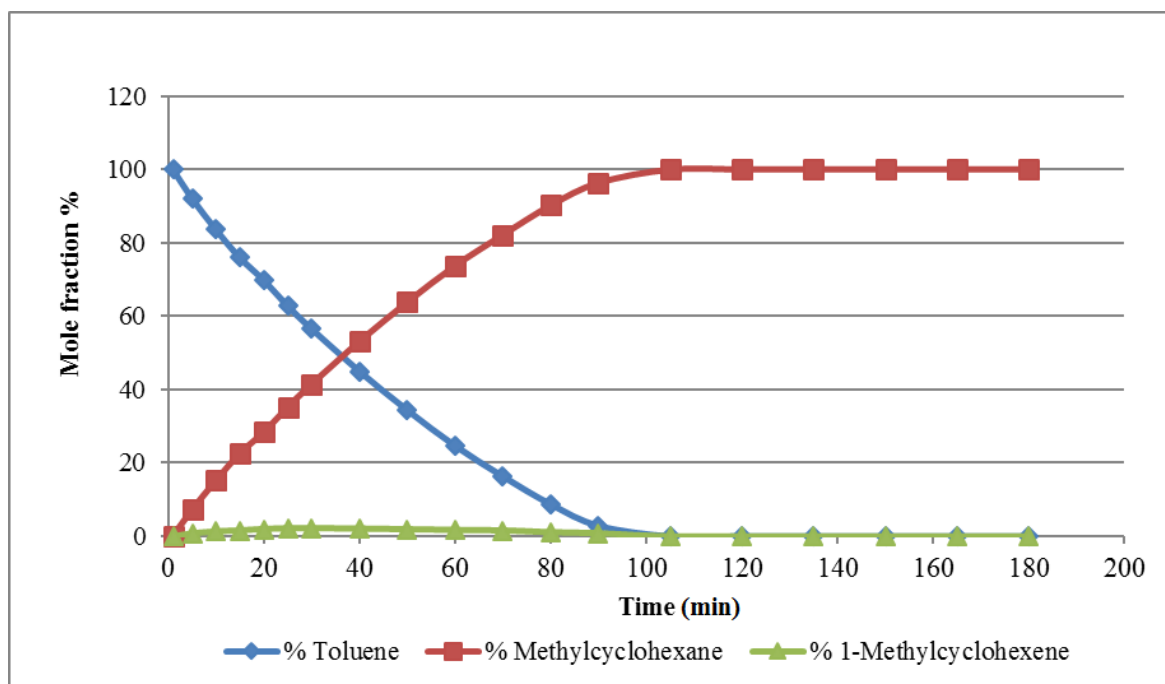


Figure 23. Reaction profile for the hydrogenation of 1.5ml toluene

4.2.2 Ethylbenzene

Ethylbenzene was tested using the same procedure as toluene. Temperature, H₂ pressure and substrate concentration were varied and the results obtained were used to calculate and identify a rate constant, activation energy and order of reaction.

4.2.2.1 Temperature variation

The reaction profiles of ethylbenzene hydrogenation at 30 and 50 °C are shown on Figure 24 and Figure 25 respectively. The formation of ethylcyclohexane, which is the direct corresponding alicyclic form of ethylbenzene, increased as the temperature increased. Also the formation of ethylcyclohexene was observed but in very low concentrations (<3%).

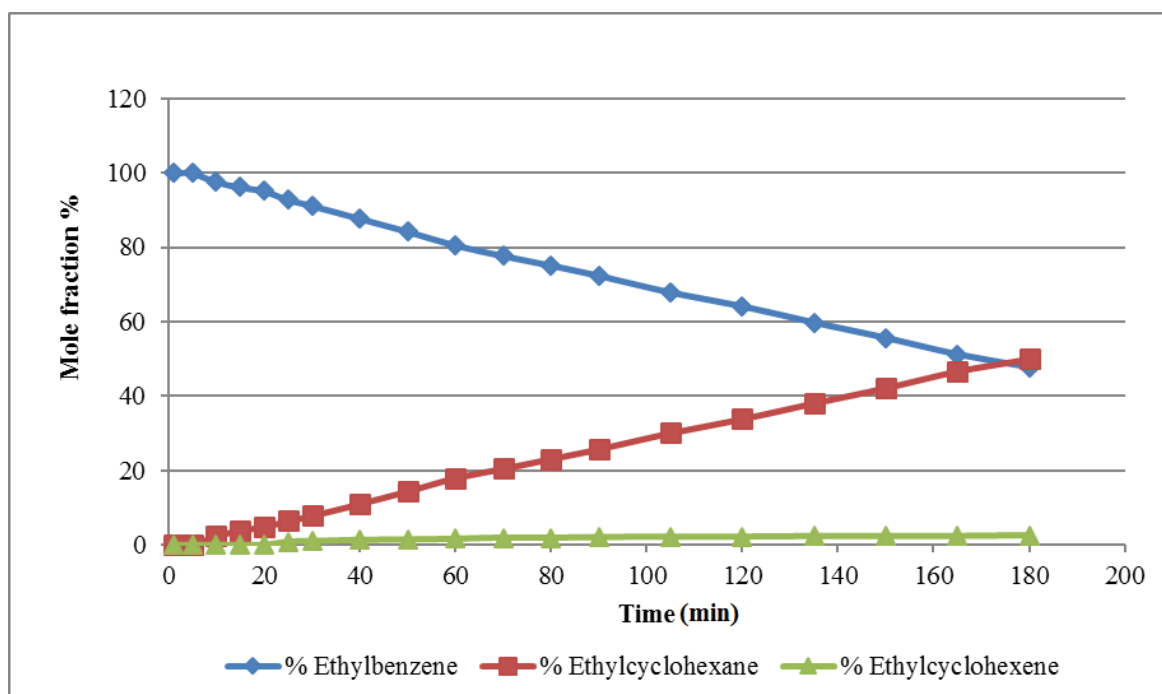


Figure 24. Ethylbenzene reaction profile at 30 °C

Figure 26 shows the effect of varying temperature on conversion during ethylbenzene hydrogenation. Temperatures of 30, 40, 50, 60 and 70 °C were applied to the reaction. Hydrogen pressure and ethylbenzene concentration were kept constant at 3 barg and 1 mL respectively. The formation of ethylcyclohexane increased as the temperature increased. In addition, ethylcyclohexene formation was observed and the maximum value was 5% at 70 °C.

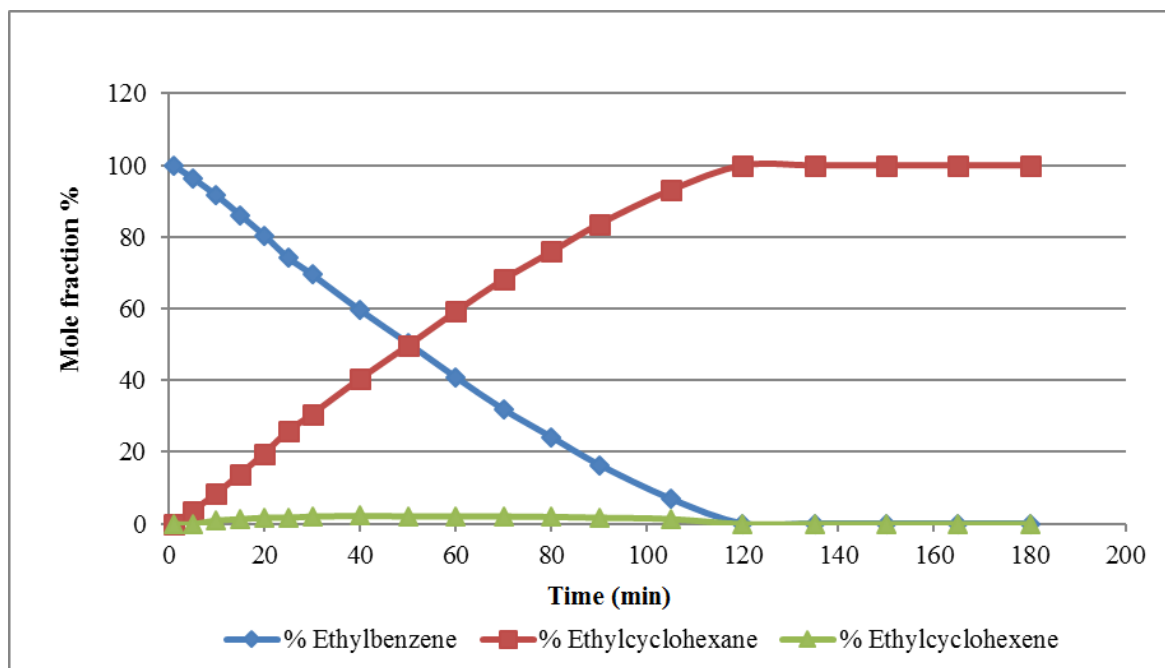


Figure 25. Ethylbenzene reaction profile at 50 °C

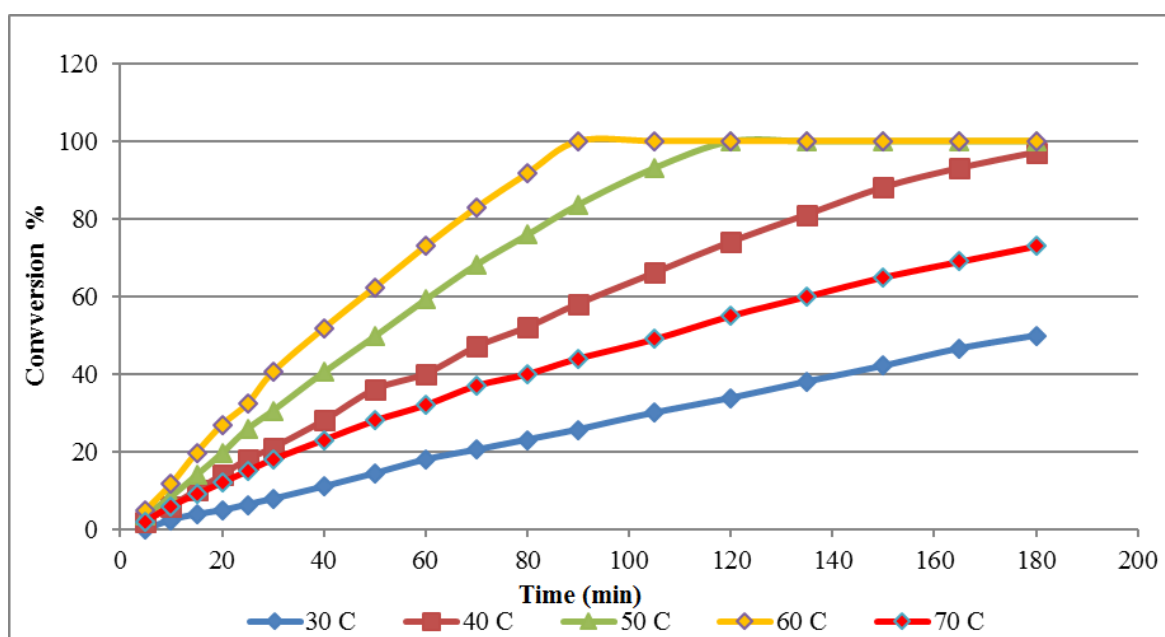
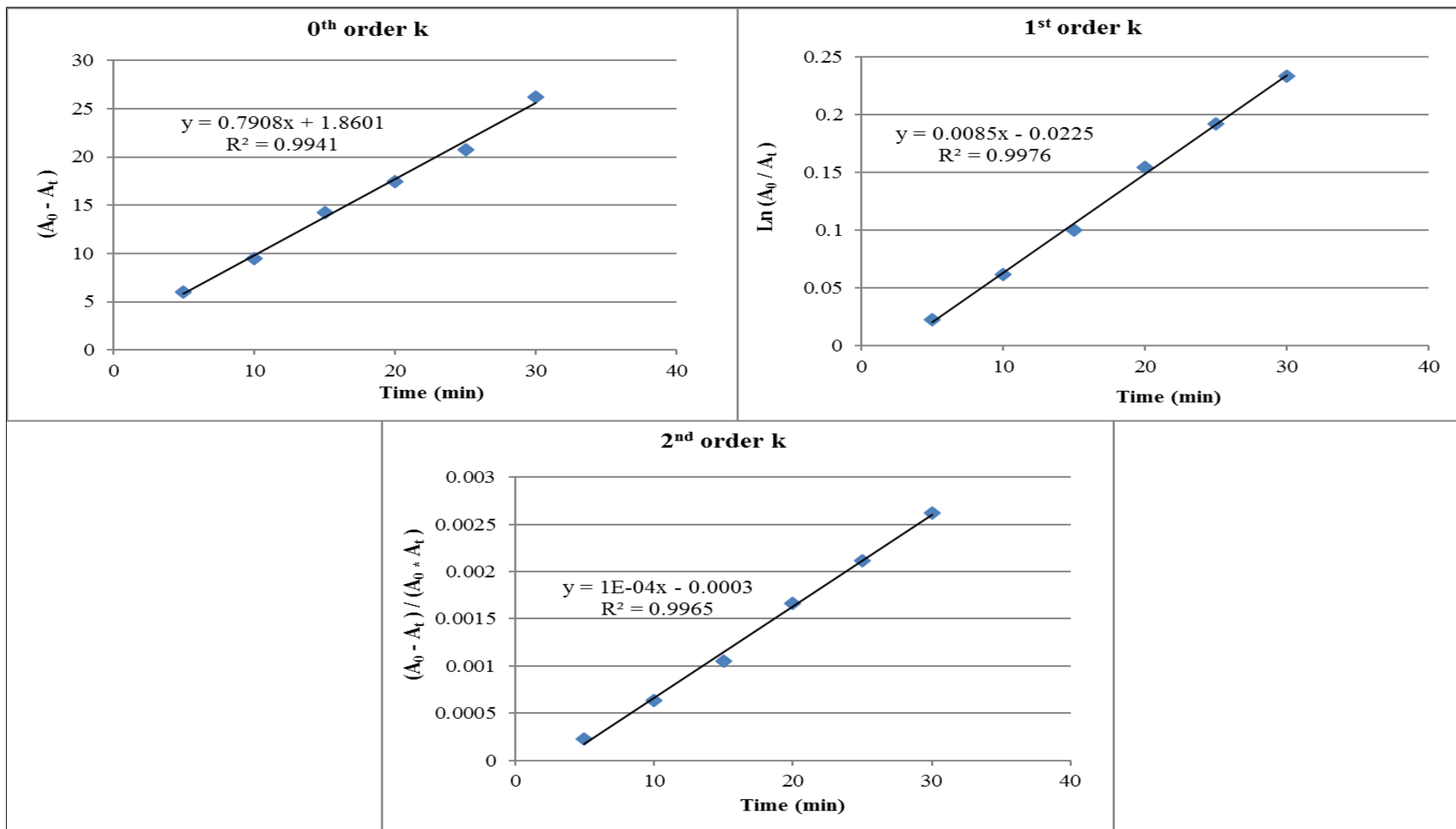
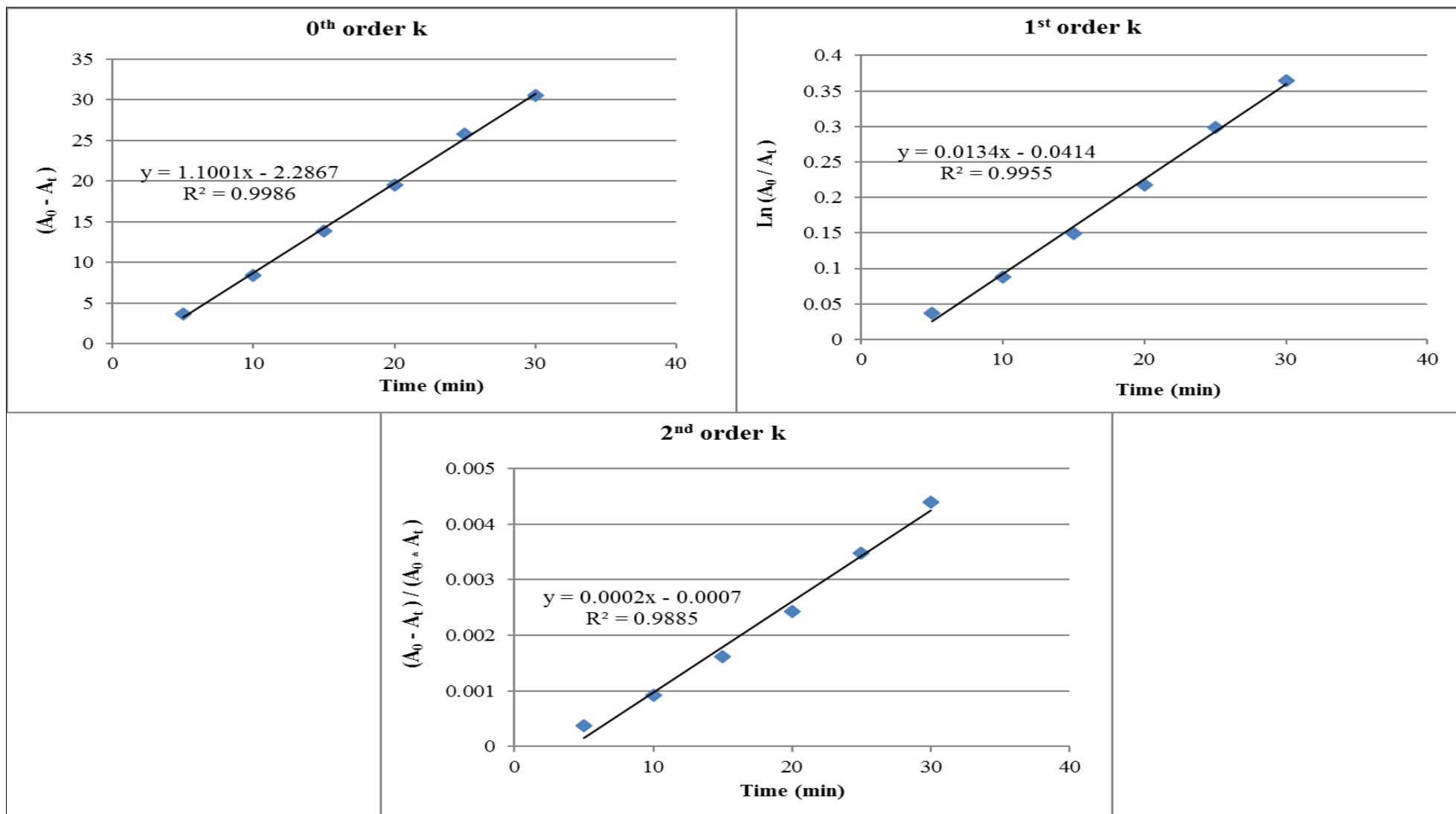


Figure 26. Temperature effect on conversion during ethylbenzene hydrogenation

The conversion has increased from 50% at 30 °C to 100% after 180 min at 50 and 60 °C. However, conversion has decreased to about 70% at 70 °C. Figure 27 shows that the reaction order has moved slightly from zero order to first order. Similar to other reactions at lower temperatures, the rate constant represents a better fit for zero order. For example, the rate constant for ethylbenzene at 50 °C provided a better fit for a zero order as shown on Figure 28.

Figure 27. 0th, 1st and 2nd order rate constant for ethylbenzene at 70 °C

Figure 28. 0th, 1st and 2nd order rate constant for ethylbenzene at 50 °C

In Table 13 the results obtained from temperature variation on ethylbenzene hydrogenation are reported.

Table 13. Conversion and rate constant of toluene at different temperatures

Temperature (°C)	30	40	50	60	70
Conv. after 180 min (%)	50	97	100	100	73
Time to 20% conv. (min)	70	30	20	15	30
Rate constant k (ms ⁻¹)	0.3244	0.8684	1.1001	1.477	0.7741

4.2.2.1.1 Activation energy

Activation energy for ethylbenzene reaction was calculated as shown in Table 10 and Figure 17.

Table 14. Data used to generate Arrhenius plot

T	K (ms ⁻¹)	1/T	Ln k
303	0.3244	0.0033	-1.12578
313	0.8684	0.003195	-0.1411
323	1.1001	0.003096	0.095401
333	1.477	0.003003	0.390013

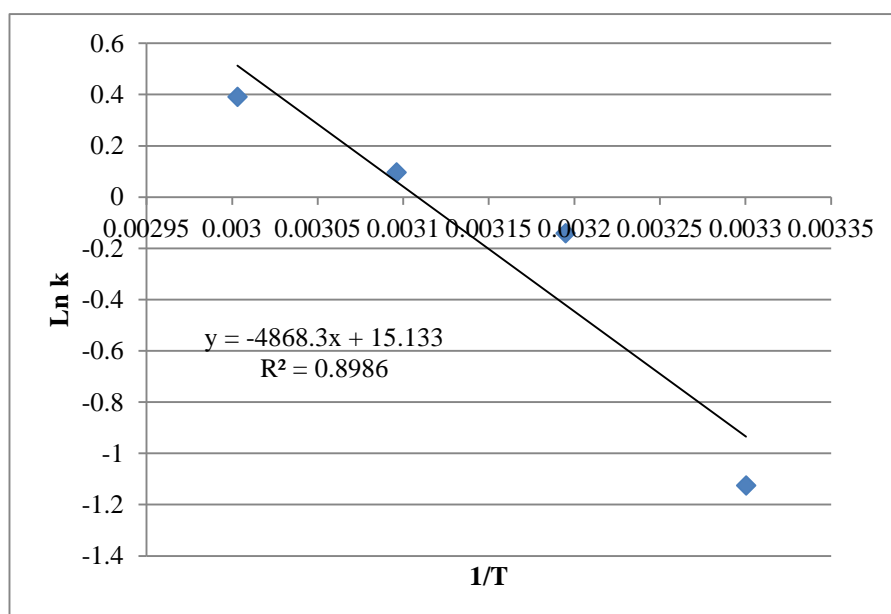


Figure 29. Ethylbenzene E_a plot

From equation (7)

$$E_a = -mR$$

$$E_a = - (-4868.3 \times 8.314) / 1000$$

$$E_a = 40.5 \text{ kJmol}^{-1}$$

4.2.2.2 Pressure variation

As described for toluene, ethylbenzene was hydrogenated under 2, 3, 4 and 5 barg hydrogen. shows the effect of hydrogen pressure applied on ethylbenzene hydrogenation. The conversion to ethylcyclohexane increased as H₂ pressure applied increased.

Table 15 presents rate constant for 0th order reaction as well as the rate of reaction. In addition, the formation of ethylcyclohexene did not exceed 3% under all pressures as shown in Figure 31 and Figure 32.

Table 15. Conversion to ethylcyclohexane at different pressures

H ₂ pressure (barg)	2	3	4	5
Time to 20% conv. (min)	20	15	13	10
Rate constant. k (ms ⁻¹)	1.0508	1.4487	1.5296	1.9464
Rate (μmolL ⁻¹ min ⁻¹)	198	241	470	481

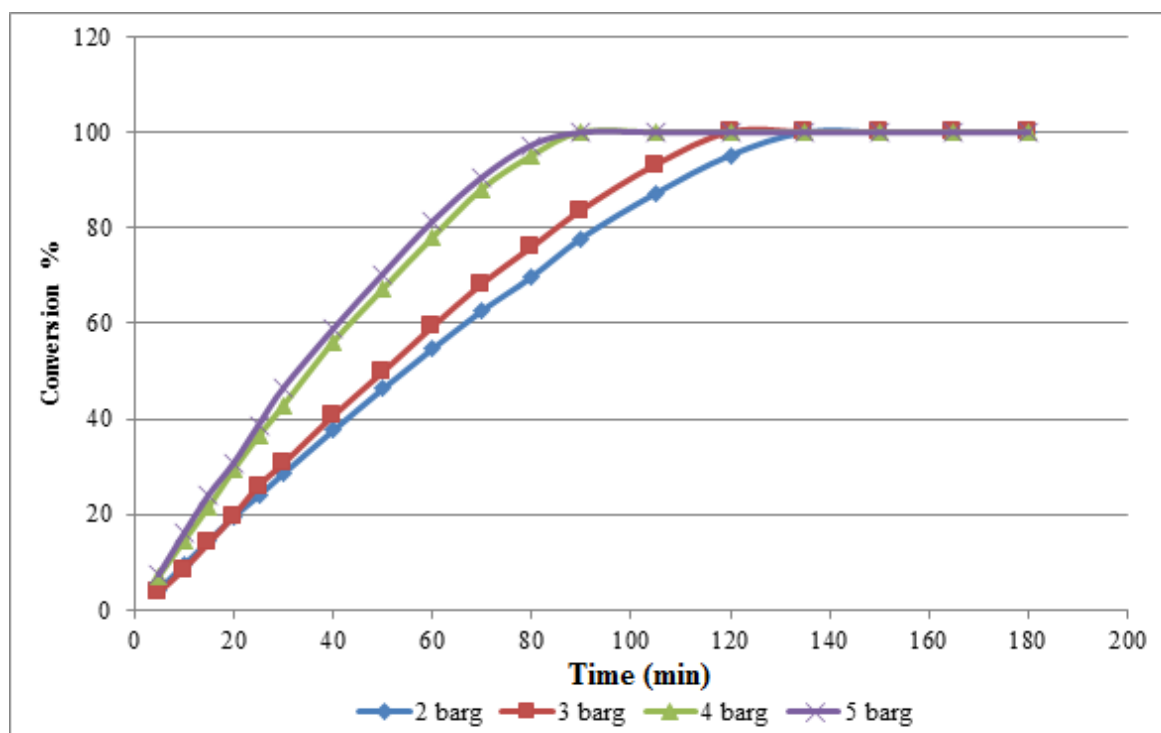


Figure 30. Ethylbenzene conversion to ethylcyclohexane at different pressures

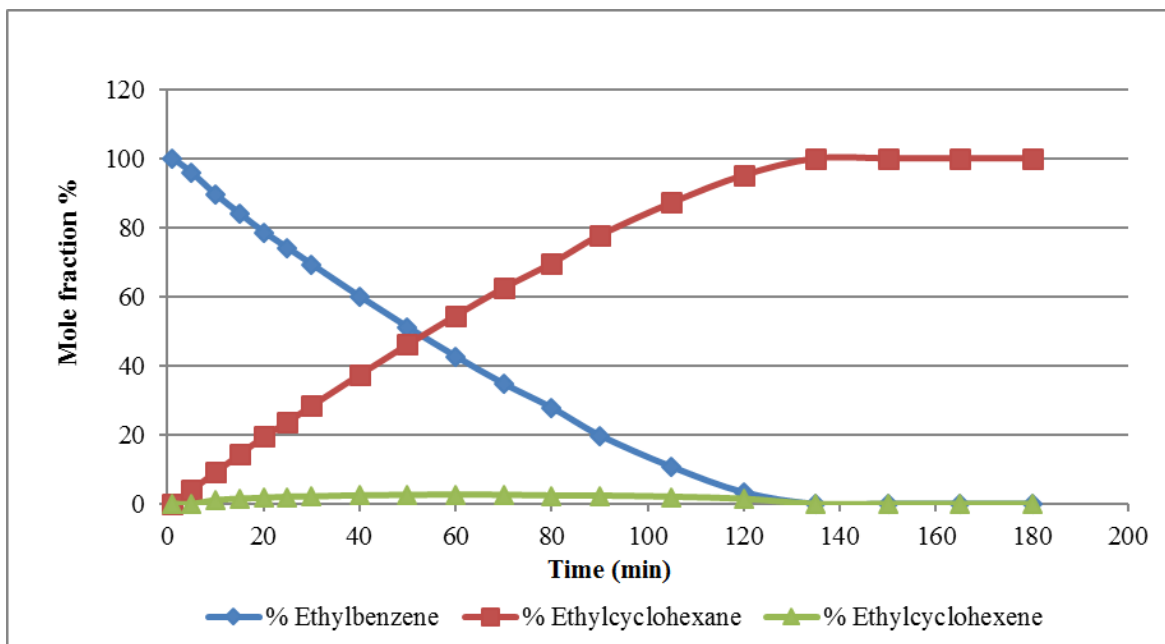


Figure 31. Ethylbenzene reaction profile at 2 barg

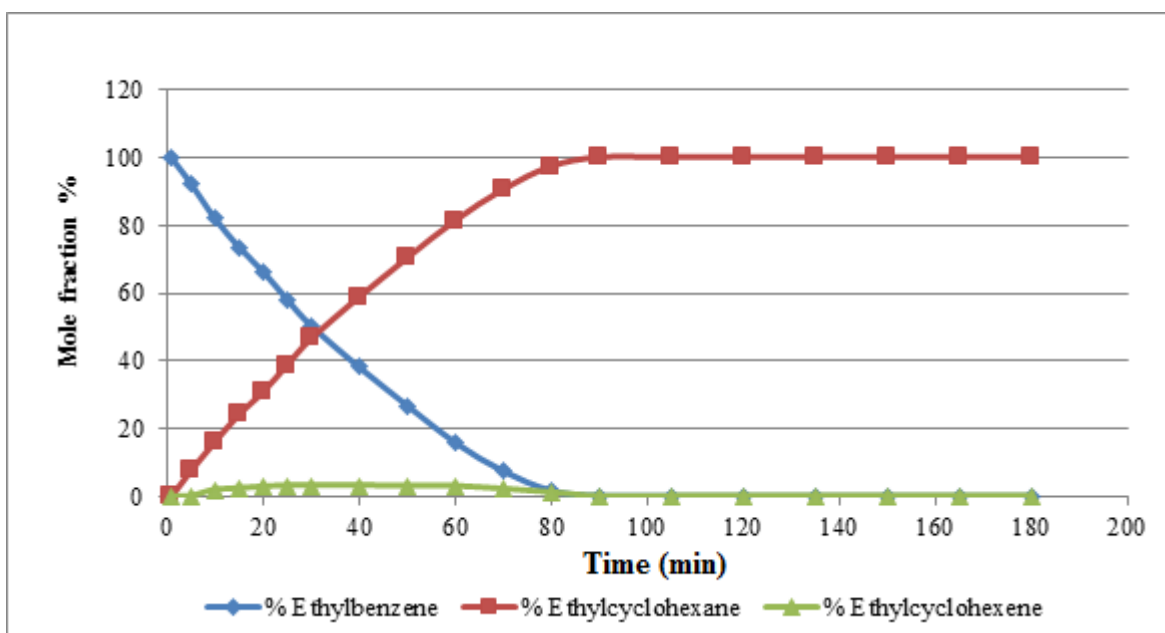


Figure 32. Ethylbenzene reaction profile at 5 barg

4.2.2.2.1 Order of reaction in H₂ pressure

The order of reaction was determined as shown in Figure 21 and Table 12 for toluene. From equation (9)

$$\ln r = \ln k + x \ln [A] + y \ln (P) \quad (9)$$

$$y = m x + c$$

and by plotting $\ln(r)$ vs. $\ln(P)$ a straight line will be generated and m is the order of reaction. As seen in Figure 33 the order of ethylbenzene reaction in H₂ pressure is 1.

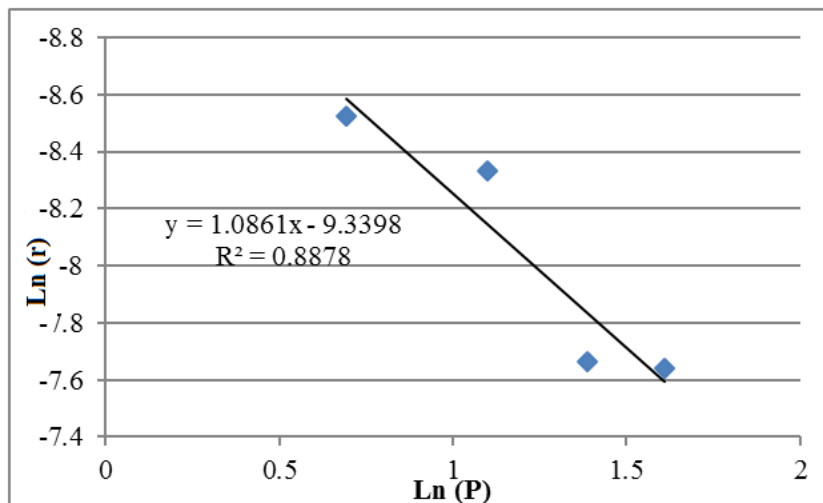


Figure 33. Ethylbenzene reaction order in H₂ pressure

4.2.2.2.2 Order of reaction in ethylbenzene concentration

The order of reaction in ethylbenzene was verified by the same method used for toluene. The rate of reaction was calculated for the first three samples; after 5, 10 and 15 min for each concentration. Then the average of rates was taken and it was $3.1 \times 10^{-4} \text{ mol g}^{-1} \text{ min}^{-1}$ and the standard deviation was $8.3 \times 10^{-5} \text{ mol g}^{-1} \text{ min}^{-1}$. This indicates a zero order in ethylbenzene concentration. Figure 34. shows the effect of concentration variation on the hydrogenation of ethylbenzene. It shows that the rate of reaction increased as the concentration decreased. In addition, the formation of ethylcyclohexene was less than 4%.

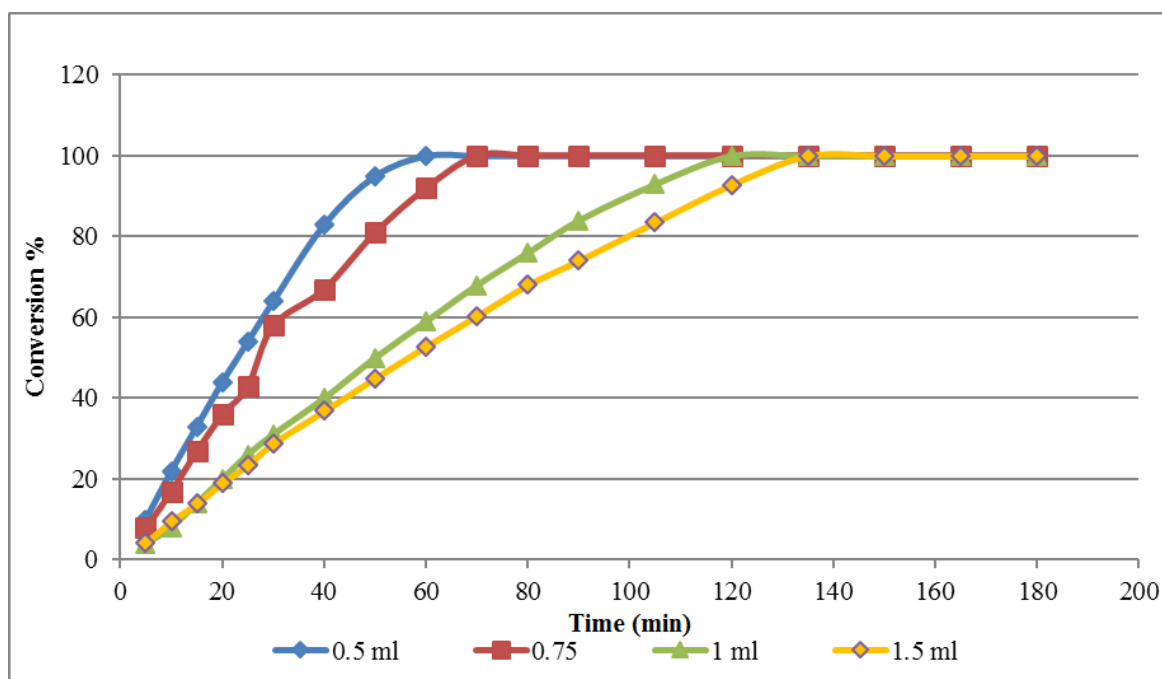


Figure 34. Conversion of ethylbenzene at different mass per volume

4.2.3 n-Propylbenzene

n-Propylbenzene was tested in a similar manner to toluene and ethylbenzene. These tests were used to identify rates constant, activation energy and order of reaction in hydrogen pressure and in n-propylbenzene concentration.

4.2.3.1 Temperature variation

n-Propylbenzene was hydrogenated at 5 different temperatures, 30, 40, 50, 60 and 70 °C. At 30 and 70 °C no products were detected. Therefore a reaction at 35 °C was performed to help to find the activation energy. Figure 35 and Figure 36 show n-propylbenzene reaction profiles at different temperatures. The formation of propylcyclohexane has increased as the temperature increased as shown on Figure 37. The formation of propylcyclohexene was lower than 3% at all temperatures.

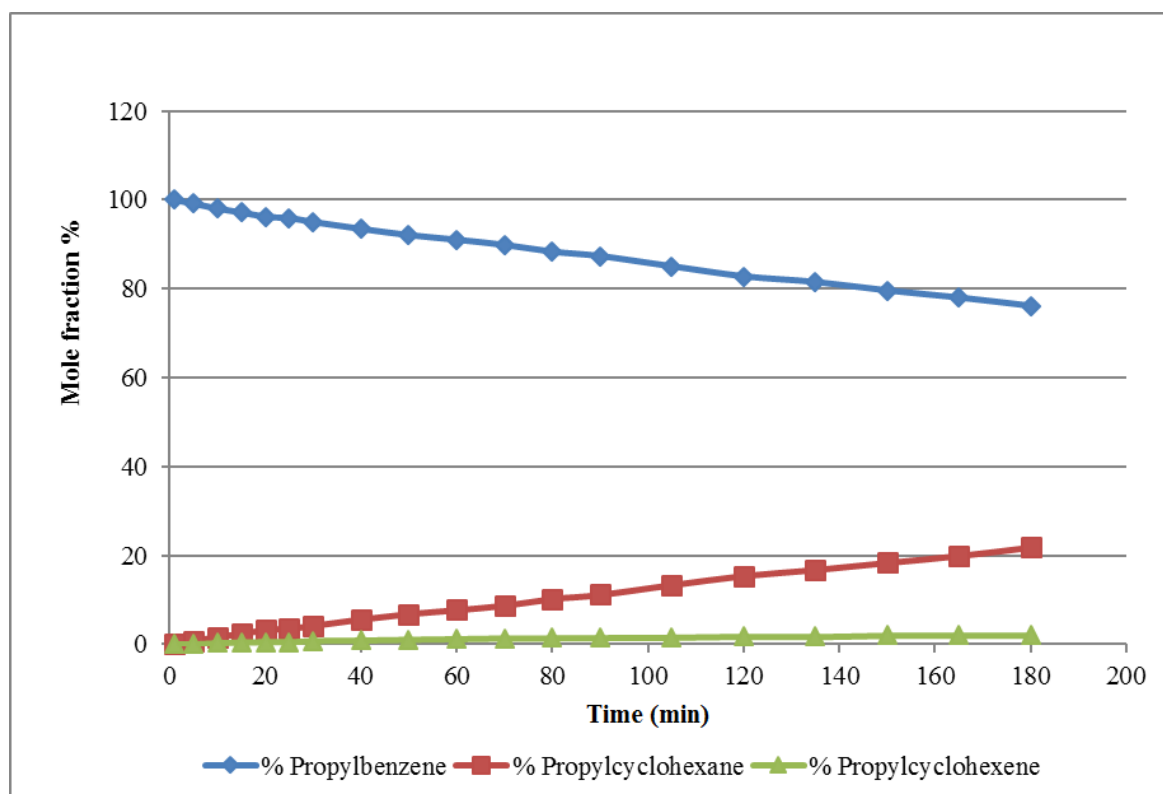


Figure 35. n-propylbenzene hydrogenation profile at 35 °C

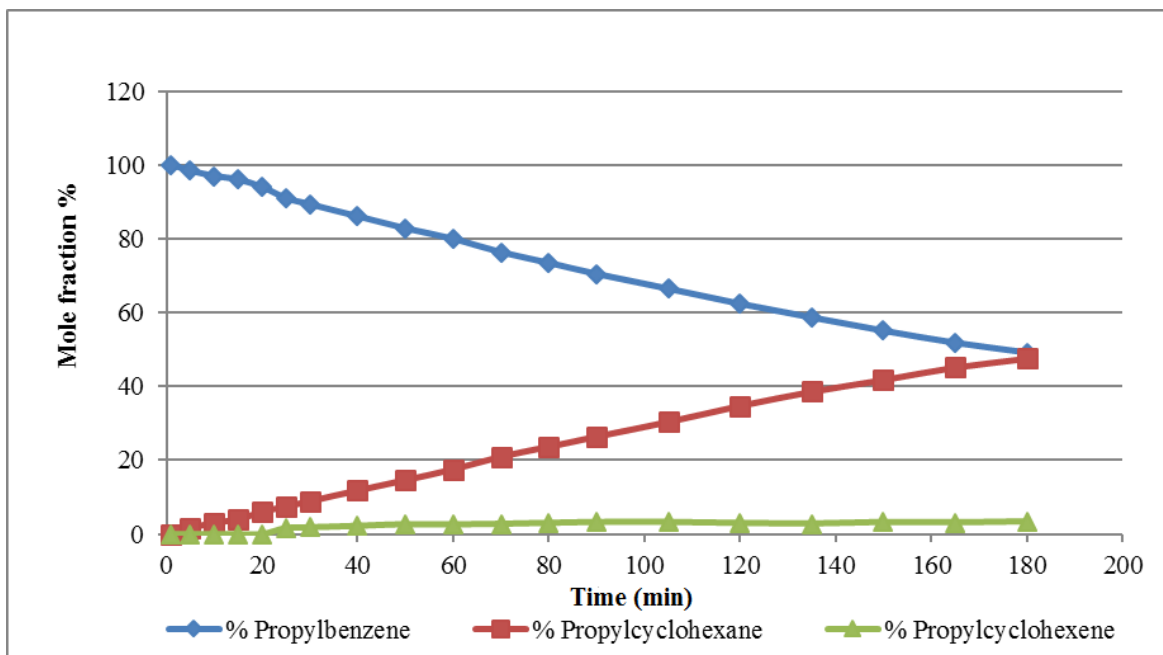


Figure 36. n-propylbenzene hydrogenation profile at 60 °C

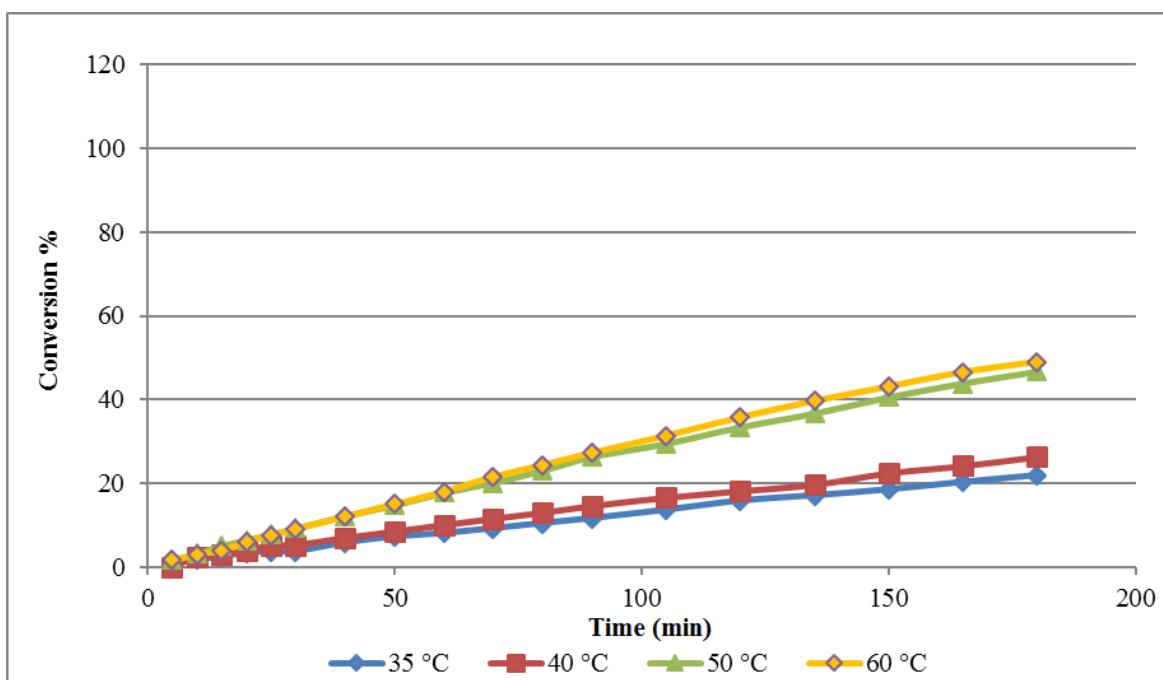


Figure 37. Temperature effect on n-propylbenzene hydrogenation

4.2.3.1.1 Rate constant and activation energy

An apparent activation energy was calculated as shown in Table 10 and Figure 17. Rate constant of zero order reactions were plotted against $1/T$ in Kelvin and a straight line was generated where

$$\ln(k) = (-E_a/R) \cdot (1/T) + \ln(A) \quad (6)$$

$$y = mx + c$$

$$E_a = -mR \quad (7)$$

From Figure 38, activation energy can be calculated in the following method

From equation (7)

$$E_a = -mR \quad (7)$$

$$E_a = -(-6011.8 \times 8.314) / 1000$$

$$E_a = 49.98 \text{ kJmol}^{-1}$$

Table 16. Data used to generate Arrhenius plot

T	k (ms ⁻¹)	1/T	Ln k
308	0.1299	0.003247	-2.04099
313	0.1601	0.003195	-1.83196
323	0.3154	0.003096	-1.15391

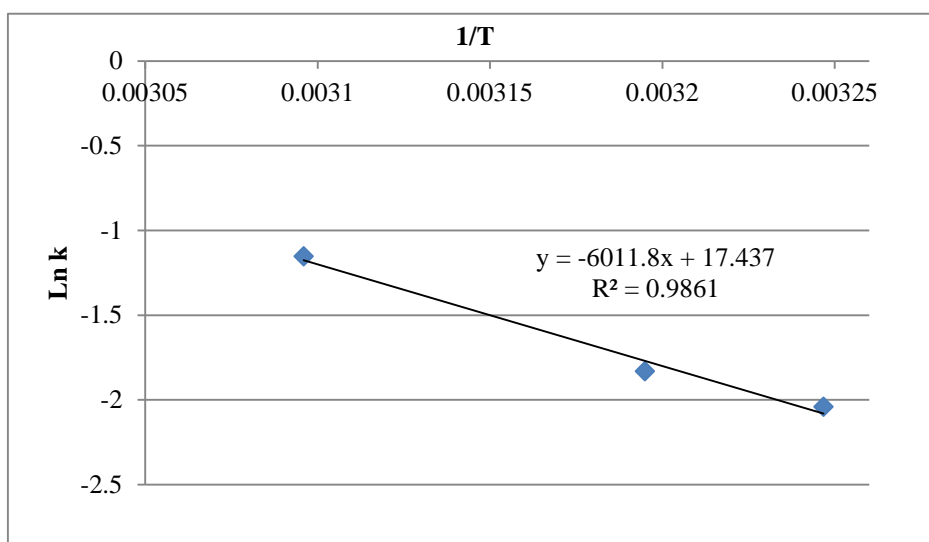


Figure 38. n-propylbenzene E_a plot

4.2.3.2 Pressure variation and order of reaction in H₂ pressure

n-propylbenzene was tested under different hydrogen pressures while temperature and concentration were kept constant at 50 °C and 1mL n-propylbenzene. The pressure was varied from 2 – 5 barg. Table 17 shows the conversion to propylcyclohexane at different pressures. Conversion has increased from 30% at 2 barg to 60% at 5 barg after 180 min. Propylcyclohexene formation was observed but in low concentration, <3%. Figure 39 and Figure 40 show reaction profiles for n-propylbenzene at 2 and 5 barg, respectively. The effect of different hydrogen pressures applied is shown on Figure 41. The formation of propylcyclohexane increased as the pressure applied increased.

Table 17. Conversion to propylcyclohexane at different pressures

H ₂ pressure (barg)	2	3	4	5
Conv. after 180 min	30	45	49	62
Time to 20% conv. (min)	120	60	60	40
Rate constant k (ms ⁻¹)	0.1573	0.2935	0.2848	0.3653
Rate (μmolL ⁻¹ min ⁻¹)	35	76	71	86

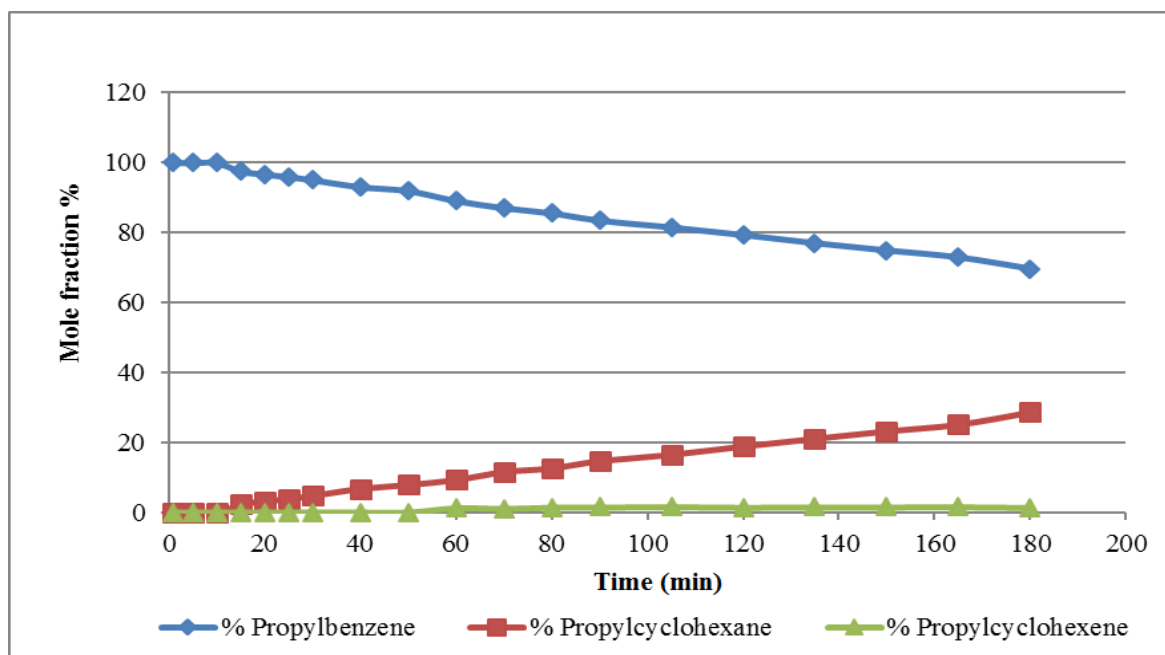


Figure 39. n-Propylbenzene reaction profile at 2 barg

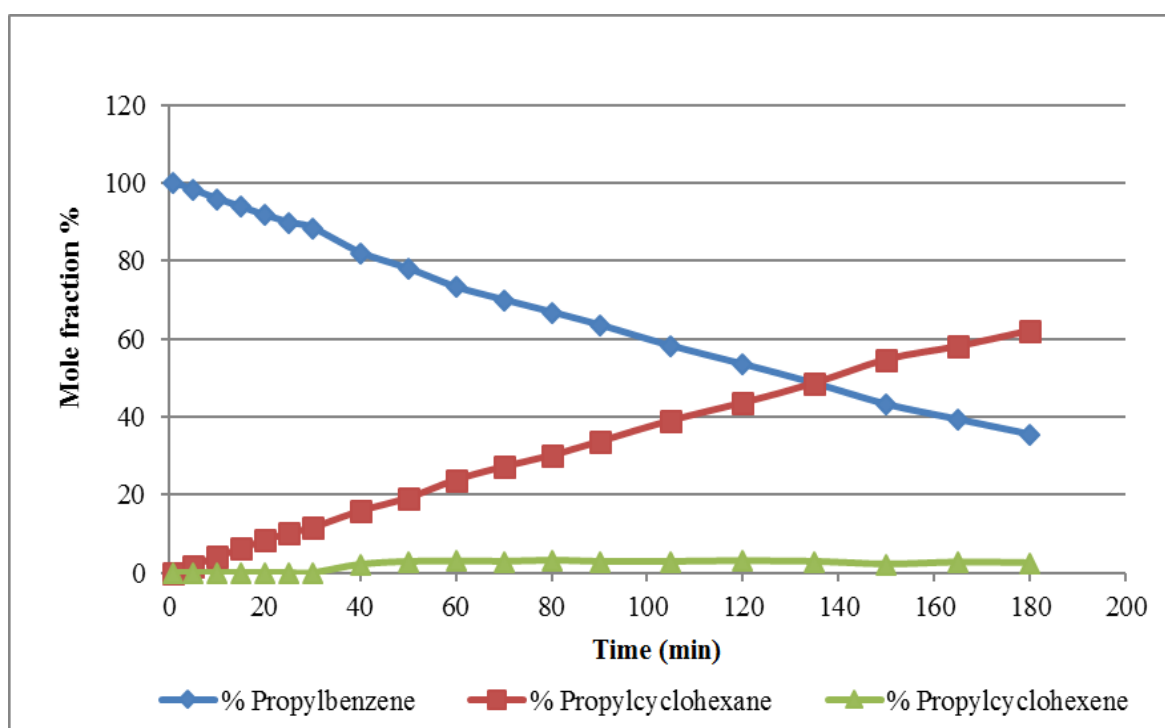


Figure 40. n-Propylbenzene reaction profile at 5 barg

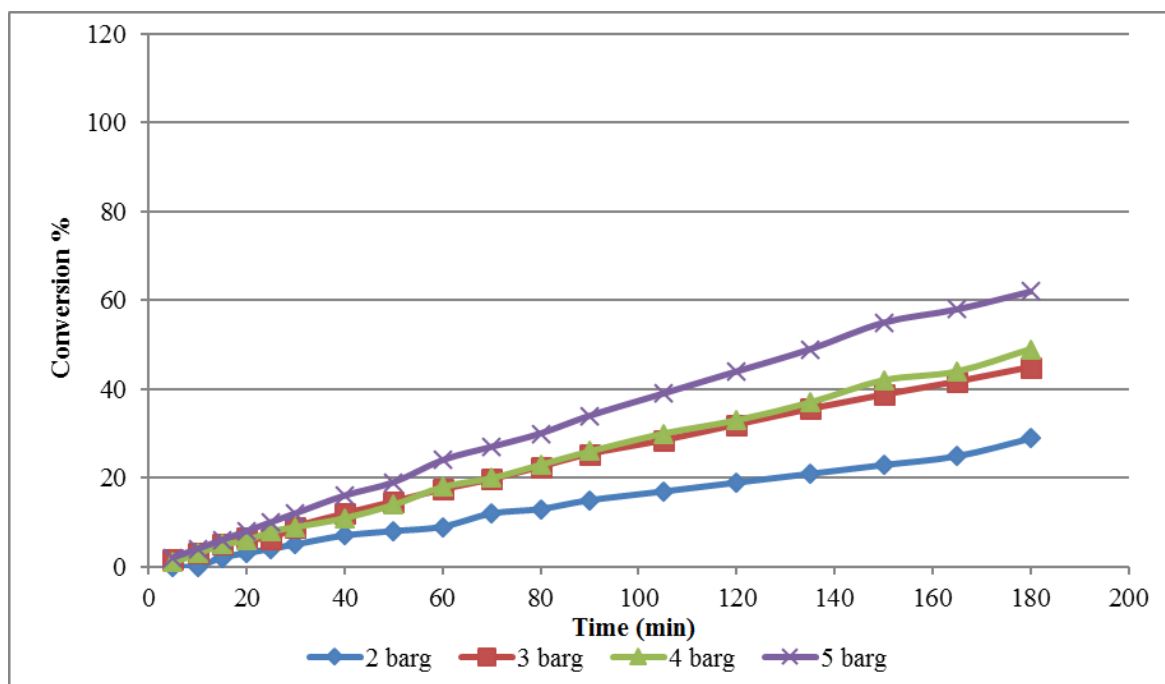


Figure 41. H₂ pressure effect on n-propylbenzene hydrogenation

The order of reaction in H₂ pressure was determined as explained in in Figure 21 and Table 12 for toluene. Form equation (9)

$$\ln r = \ln k + x \ln [A] + y \ln (P) \quad (9)$$

$$y = m x + c$$

When plotting Ln(r) vs. Ln(P) a straight line will be generated and m will be the order of the reaction. From Figure 42, it is clear that n-propylbenzene hydrogenation in H₂ pressure is 1st order reaction.

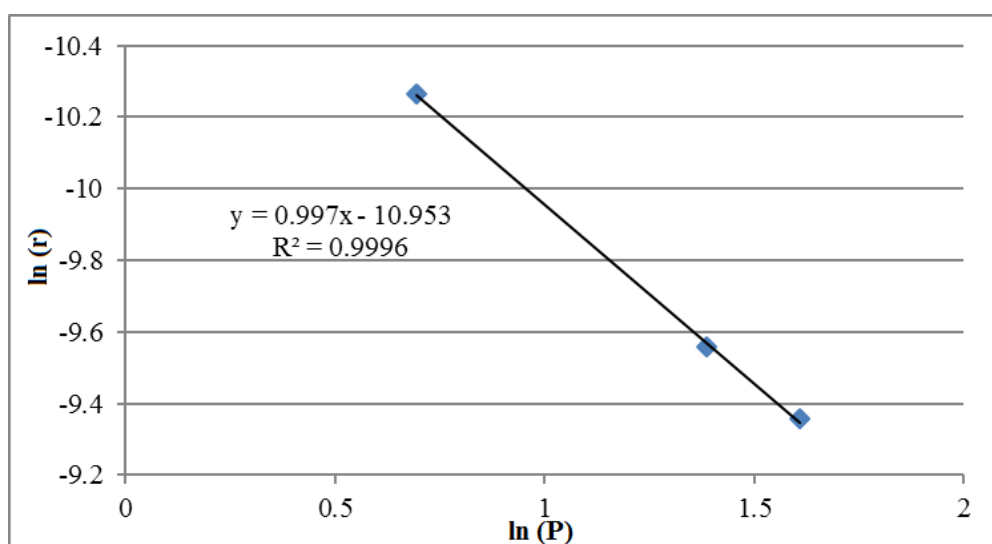


Figure 42. n-Propylbenzene reaction order in H₂ pressure

4.2.3.3 Concentration variation and reaction order in substrate concentration

In these set of reactions, the concentration of n-propylbenzene was varied to examine the effect of variation on hydrogenation and also to find reaction order in n-propylbenzene concentration. The volumes used were 0.5, 0.75, 1, and 1.5 ml of n-propylbenzene. Figure 43 and Figure 44 show two reaction profiles of n-propylbenzene at 0.5 and 1.5 mL, respectively.

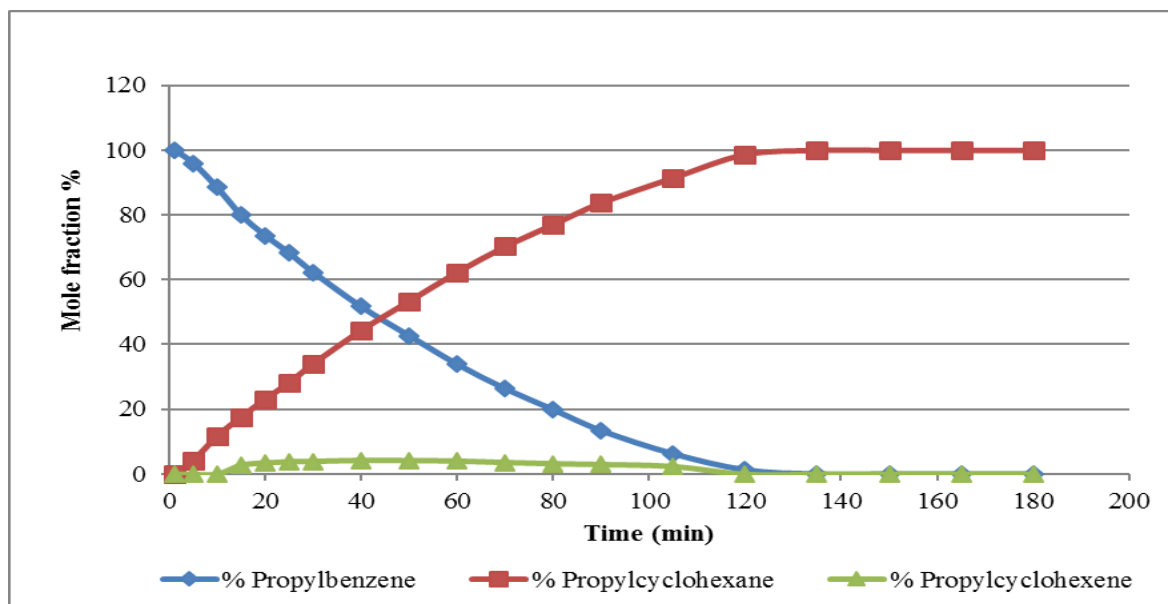


Figure 43. Reaction profile for hydrogenation of 0.5 ml n-propylbenzene

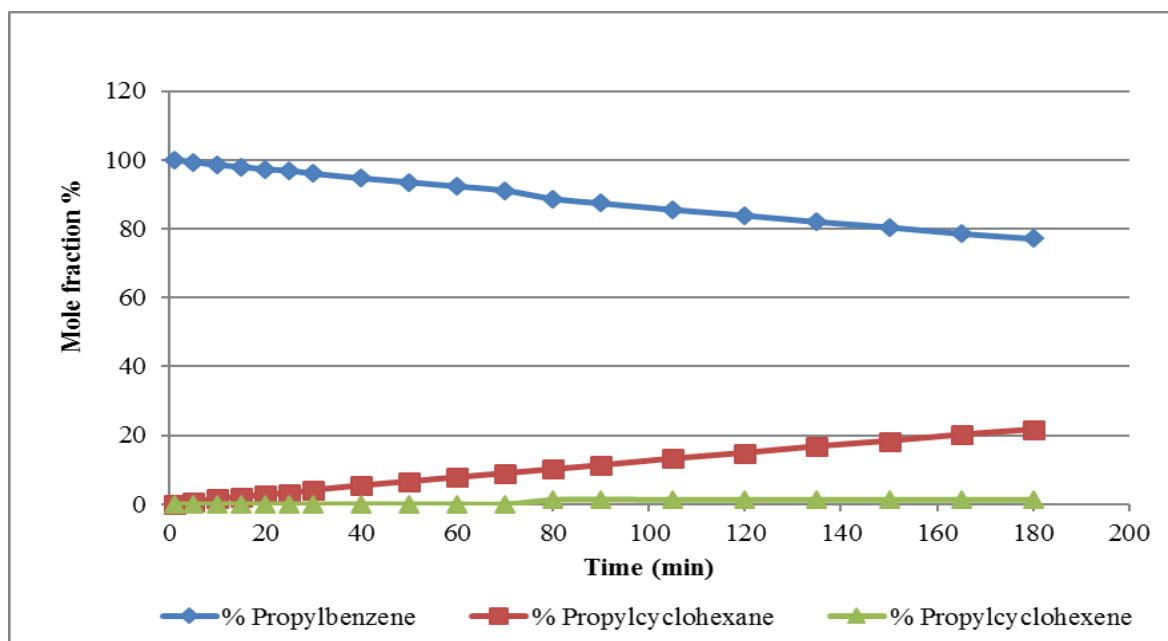


Figure 44. Reaction profile for hydrogenation of 1.5 ml n-propylbenzene

The formation of propylcyclohexane has decreased as the volume increased. About 4% of propylcyclohexene was detected during these set of reactions. shows the conversion to propylcyclohexane at different concentration. The results obtained from each reaction were summarised in Table 18. These results include zero order rate constant, total conversion after 180 min and the rate of the reactions. Conversion to propylcyclohexane has decreased from 100% at 0.5 mL to 20% when 1.5 mL of n-propylbenzene was used.

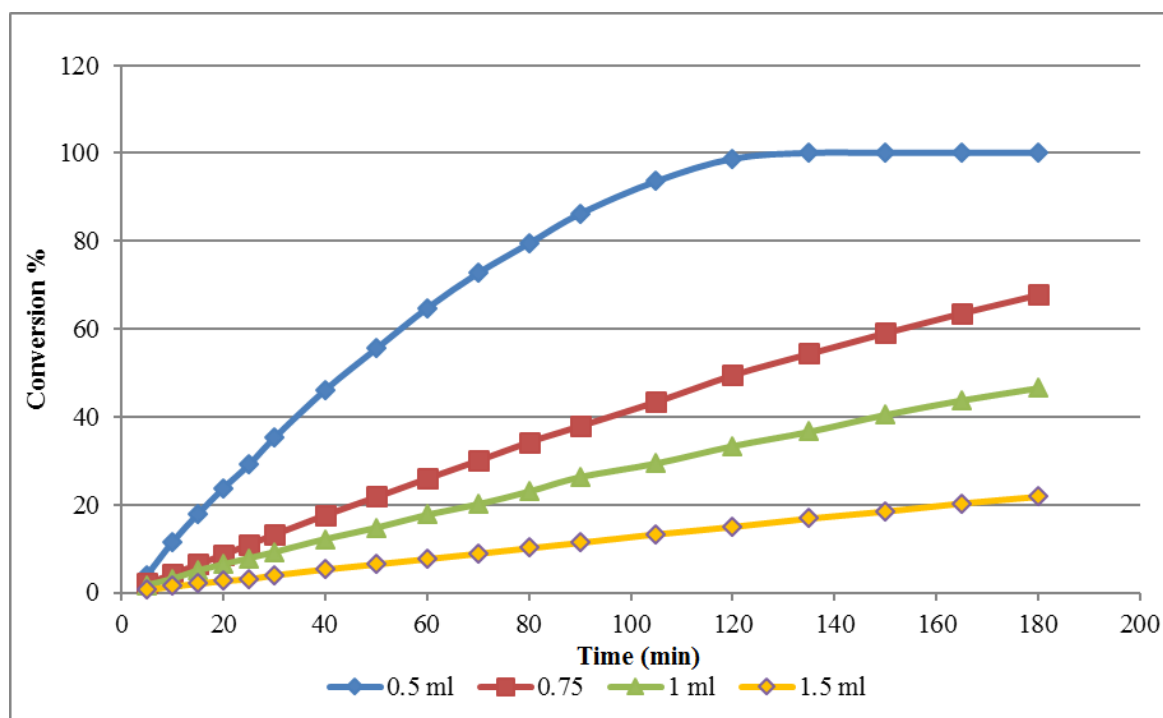


Figure 45. Concentration effect on n-propylbenzene hydrogenation

Table 18. Conversion to propylcyclohexane at different concentrations

Volume (mL)	0.5	0.75	1	1.5
Conv. after 180 min	100	66	45	22
Time to 20% conv. (min)	15	50	60	165
Rate constant. k (ms^{-1})	1.4057	0.5344	0.2935	0.1238
Rate ($\mu\text{mol.L}^{-1}\text{min}^{-1}$)	112	76	76	44

The order of reaction in n-propylbenzene concentration was determined by using equation

$$(9) \ln r = \ln k + x \ln [A] + y \ln (P) \quad (9)$$

$$y = m x + c$$

When plotting $\ln(r)$ vs. $\ln[A]$ a straight line will be generated and m will be the order of the reaction. As shown in Figure 46 the reaction in n-propylbenzene concentration is negative 1st order reaction.

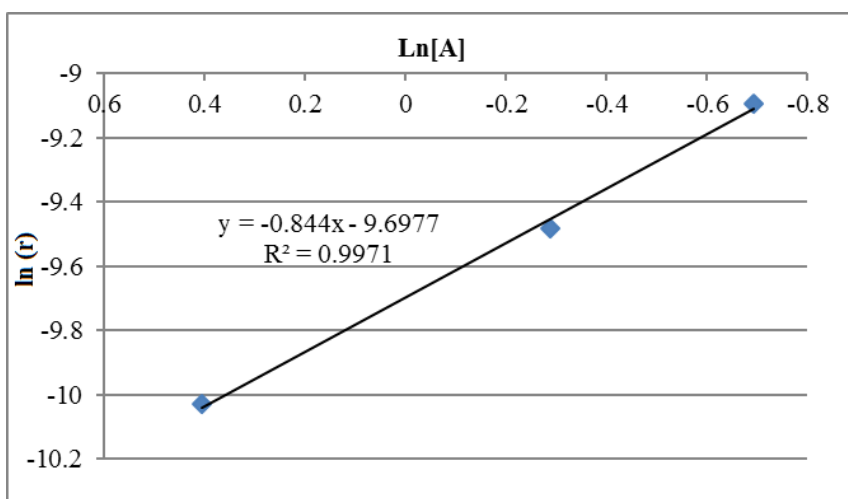


Figure 46. Reaction order in n-propylbenzene concentration

4.3 Alkyl aromatics competitive hydrogenation

In the previous section, results obtained from tests performed on the individual alkyl aromatics were reported. In this section the reactions of three alkyl benzenes as groups of two and as a group of three reactants in the same time will be presented. The effect of these substrates on each other will be tested to give a better understanding on their behaviour during a competitive hydrogenation. Firstly, main results from previous tests will be summarised. As shown in Table 19, n-propylbenzene has the highest activation energy which means that it reacts slower than toluene and ethylbenzene. In addition, order of reaction in n-propylbenzene concentration is negative 1st order.

Table 19. Main findings for the hydrogenation of single alkyl benzenes (50 °C-1mL-3barg)

Substrate	Toluene	Ethylbenzene	n-Propylbenzene
E_a (kJmol ⁻¹)	23	40.5	49.98
Conversion % (180 min)	100	100	45
Rate constant (ms ⁻¹)	1.4487	1.1001	0.2935
Order in H ₂ pressure	1	1	1
Order in substrate	0	0	-1

It is also shown in Table 19 that the rate constant of propylbenzene is significantly lower than the others. Toluene rate constant for example is almost 6 times higher which indicates a very slow reaction for n-propylbenzene.

Figure 47 and Figure 48 show the change in conversion after performing the competitive hydrogenation of three alkylbenzenes at the same time. The conversion of n-propylbenzene increased from 45% to 55% in the presence of toluene and ethylbenzene.

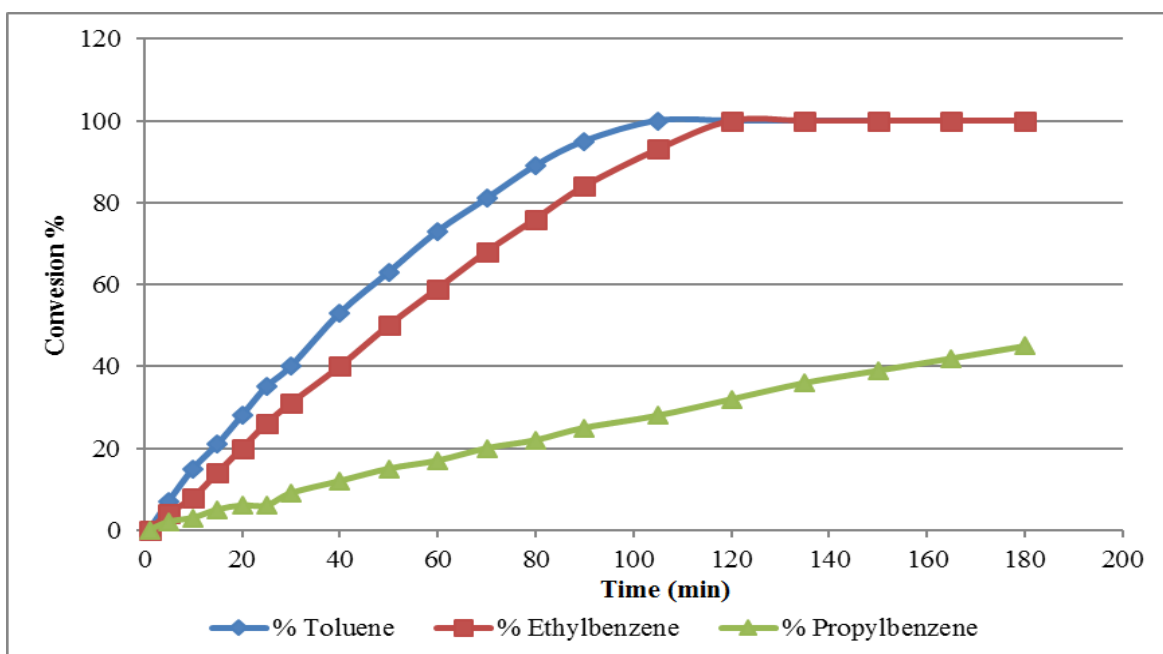


Figure 47. Conversion of three alkylbenzenes as single substrates

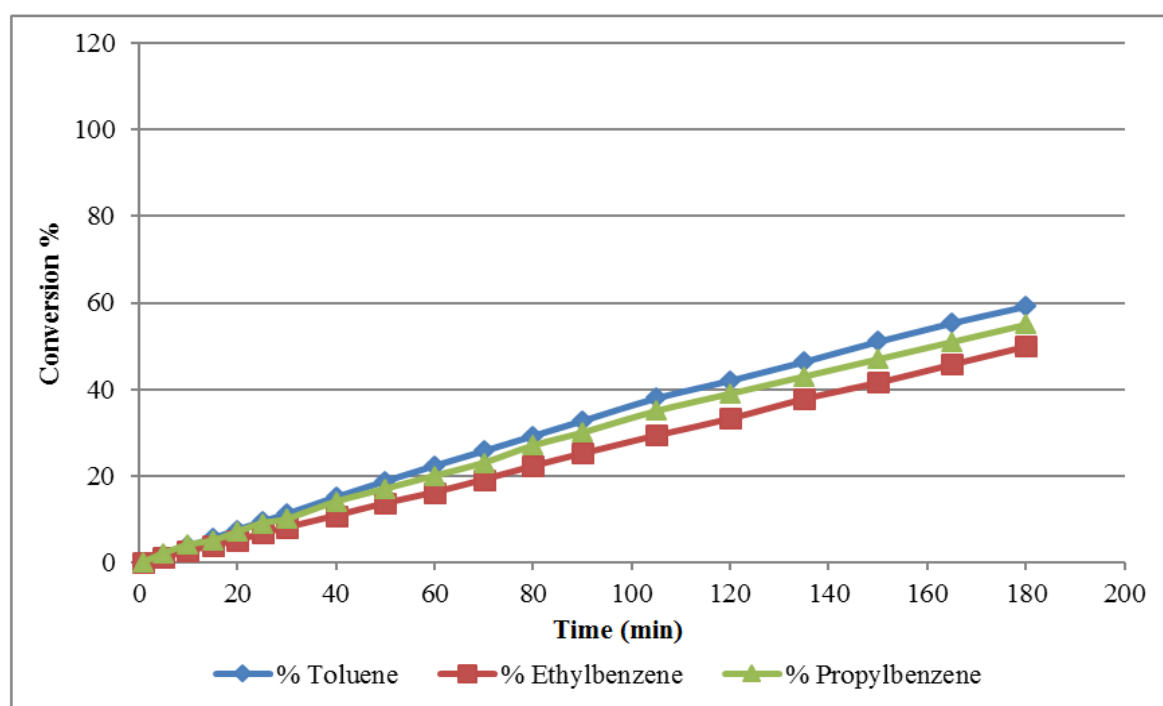


Figure 48. Conversion of three alkylbenzenes as a 1:1:1 mixture

4.3.1 Toluene

The four reaction profiles in show the hydrogenation of toluene as a single substrate (top left) and in the presence of the other alkylbenzenes. The reaction profile shows that toluene was not significantly affected by the presence of ethylbenzene, whereas it was significantly affected when reacted in the presence of n-propylbenzene and when all three reactants were hydrogenated in a mixture. Conversion to methylcyclohexane decreased from 100%, when toluene was hydrogenated as a single substrate at 105 min, to 60% conversion in the presence of n-propylbenzene and to ~40% in the mixture.

4.3.2 Ethylbenzene

The rate of ethylbenzene hydrogenation increased slightly in the presence of toluene. On the other hand, conversion decreased significantly in the mixture as well as in the presence of n-propylbenzene as shown in . Conversion to ethylcyclohexane decreased from 100% as a single substrate after 120 min. to about 30% in the mixture and to 50% in the presence of n-propylbenzene.

4.3.3 n-Propylbenzene

As shown in , n-propylbenzene reacts very slowly as a single substrate. However when mixed with toluene or ethylbenzene, the n-propylbenzene hydrogenation reaction unexpectedly increased. The rate of reaction was also increased slightly when all three alkylbenzenes were in the mixture. Conversion to propylcyclohexane increased from 45% to about 85% in the presence of toluene and to 75% in the presence of ethylbenzene.

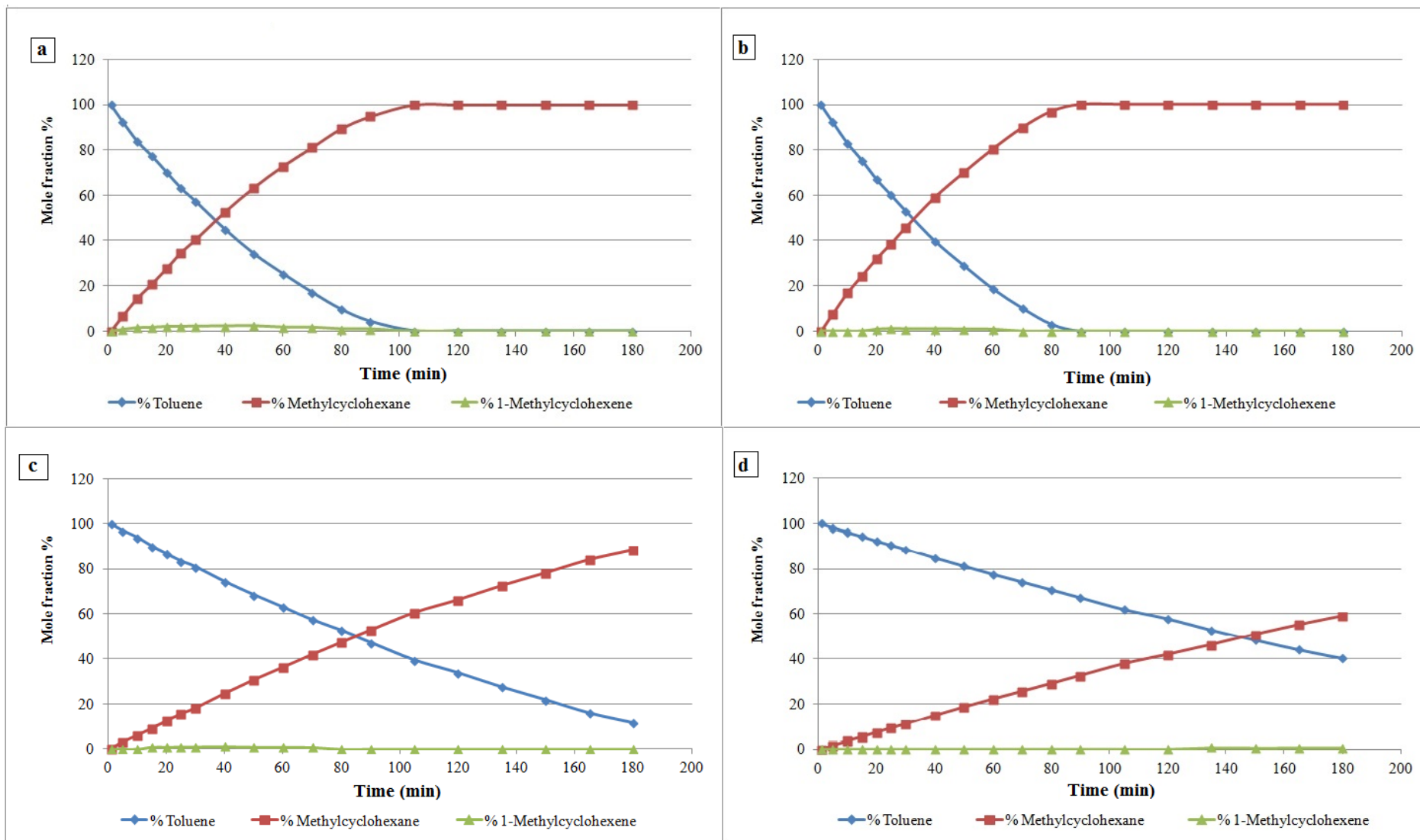


Figure 49. Toluene reaction profiles a) single substrate b) with ethylbenzenes, c) with n-propylbenzene and d) in mixture of three

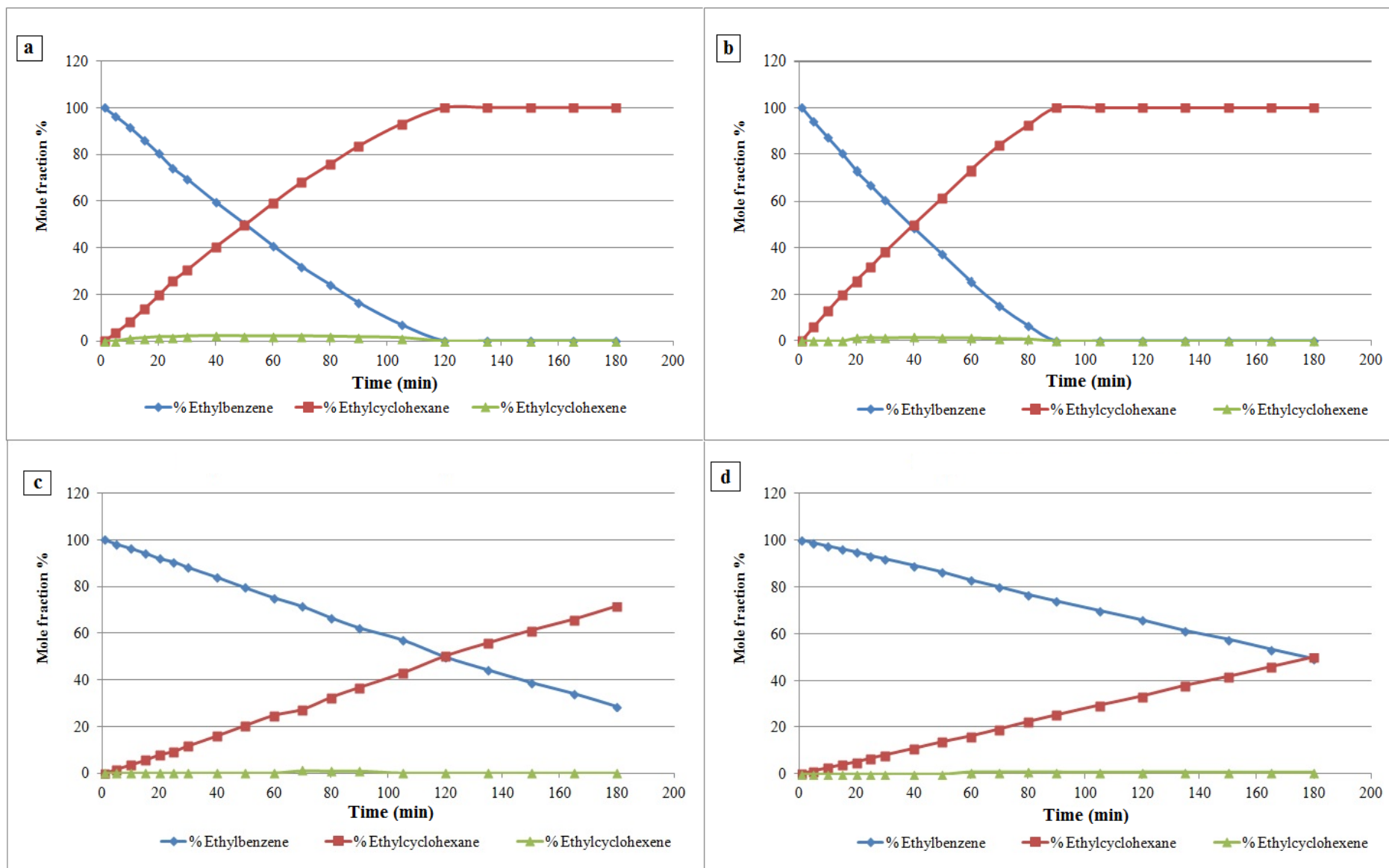


Figure 50. Ethylbenzene reaction profiles a) single substrate b) with toluene, c) with n-propylbenzene and d) in mixture of three

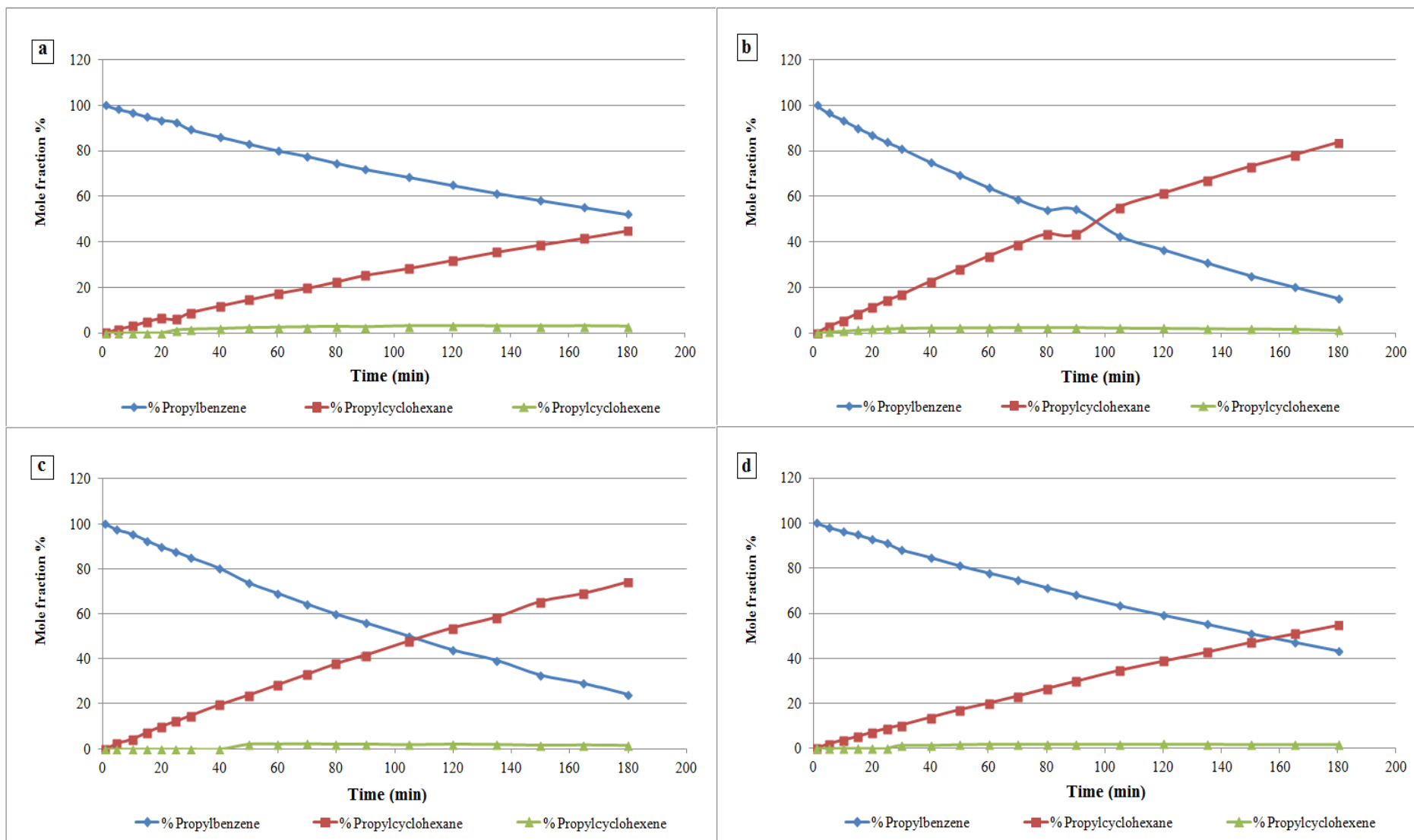


Figure 51. n-Propylbenzene reaction profiles a) single substrate b) with toluene, c) with ethylbenzenes and d) in mixture of three

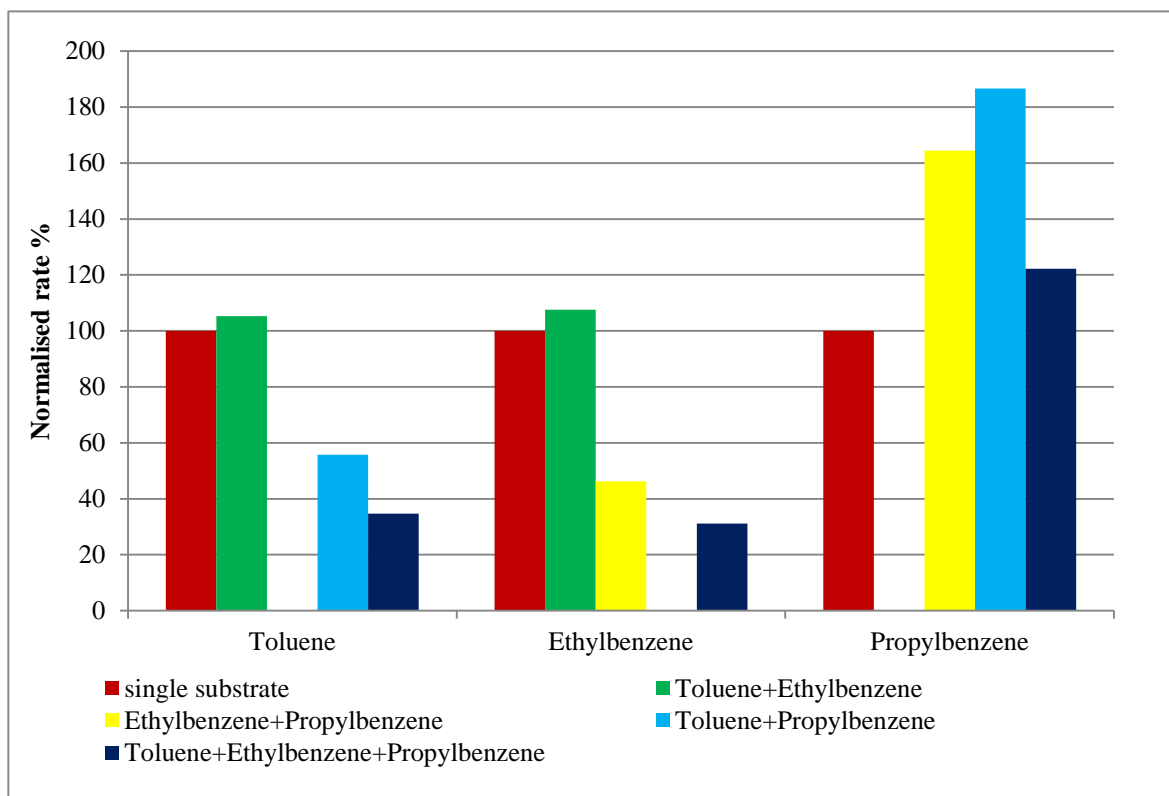


Figure 52. Competitive hydrogenation of alkylbenzenes

Figure 52 summarises the results obtained from alkylbenzenes competitive hydrogenation. These columns were divided into three groups each group starts with a red column. The red columns represent the single substrates which were set to 100 and the others were normalised against them to allow comparison with other results.

The green columns represent toluene and ethylbenzene mixture. As shown in Figure 52, toluene hydrogenation was not affected by the presence of ethylbenzene and vice versa. It also shows that both toluene and ethylbenzene were inhibited by the presence of n-propylbenzene, whereas n-propylbenzene hydrogenation was enhanced significantly by the presence of the other substrates.

4.4 Phenol and anisole hydrogenation

This section will examine the hydrogenation reactions of phenol and anisole as single substrates and the results obtained from these reactions will be reported. Results will include activation energies, rate constants and reaction order in H_2 and in substrate concentration. After that, the competitive hydrogenation of phenol and anisole with toluene will be reported.

4.4.1 Phenol

In the hydrogenation of phenol, similar tests were performed as were reported for alkylbenzenes hydrogenation. Variations of temperature, pressure and substrate concentration were applied in order to examine the effect of changing these parameters on hydrogenation behaviour. The products from each reaction were cyclohexanone, cyclohexanol and cyclohexane. In addition, the results were used to identify activation energy, rate constants and order of reaction in hydrogen pressure and in substrate concentration.

4.4.1.1 Temperature variation and E_a calculation

The conversion of phenol has increased as the temperature increased. Conversion moved from about 80% at 30 °C to 100% at 60 and 70 °C after 180 min of reaction. Table 20 shows, in addition to the conversion, the first order rate constant which increased as the temperature increased.

Figure 53 and Figure 54 show reaction profiles for phenol at 30 and 70 °C respectively. As conversion of phenol increased the formation of products has also increased. Cyclohexanol concentration for example has increased from 30% at 30 °C to about 40% at 70 °C after 180 min.

Table 20. Conversion of phenol at different temperatures

Temperature °C	30	40	50	60	70
Con. after 180 min. %	83	92	99	100	100
Time to 20% conv. (min)	25	20	15	15	10
Rate constant k (ms^{-1})	0.5594	0.6781	0.9986	1.2362	1.3625

The formation of cyclohexanone increased with time and then started to decrease as phenol was completely consumed as shown in Figure 53. In addition, formation of cyclohexane was observed as the reaction started.

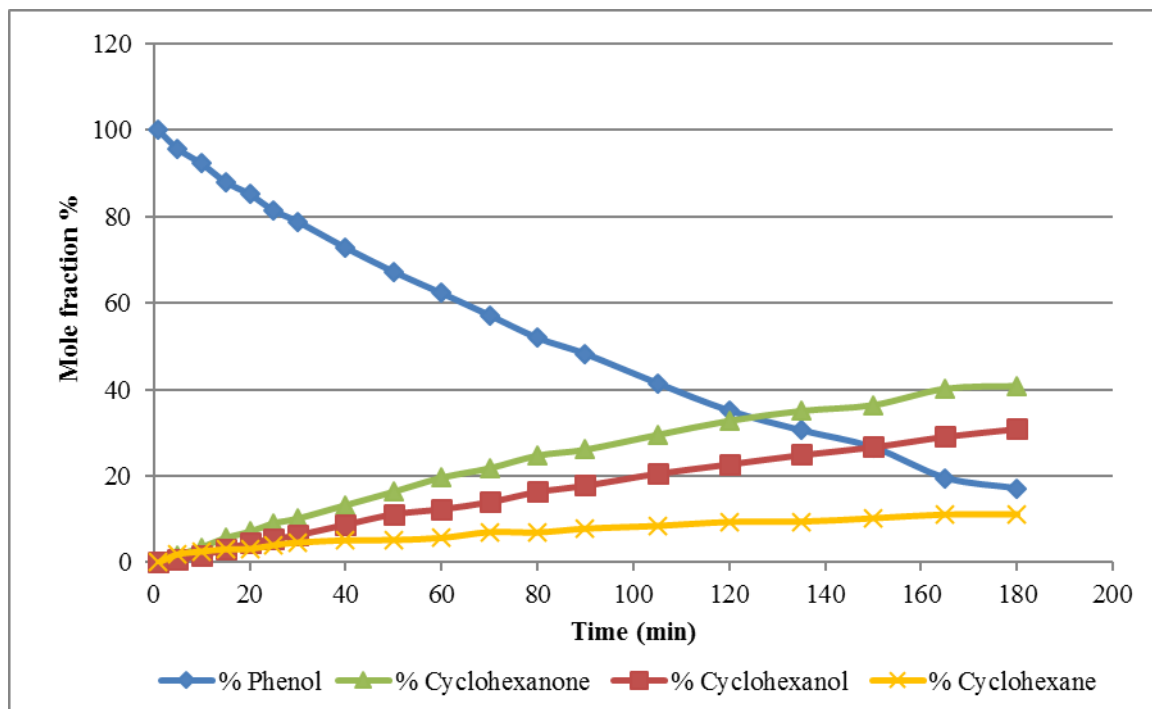


Figure 53. Phenol reaction profile at 30 °C

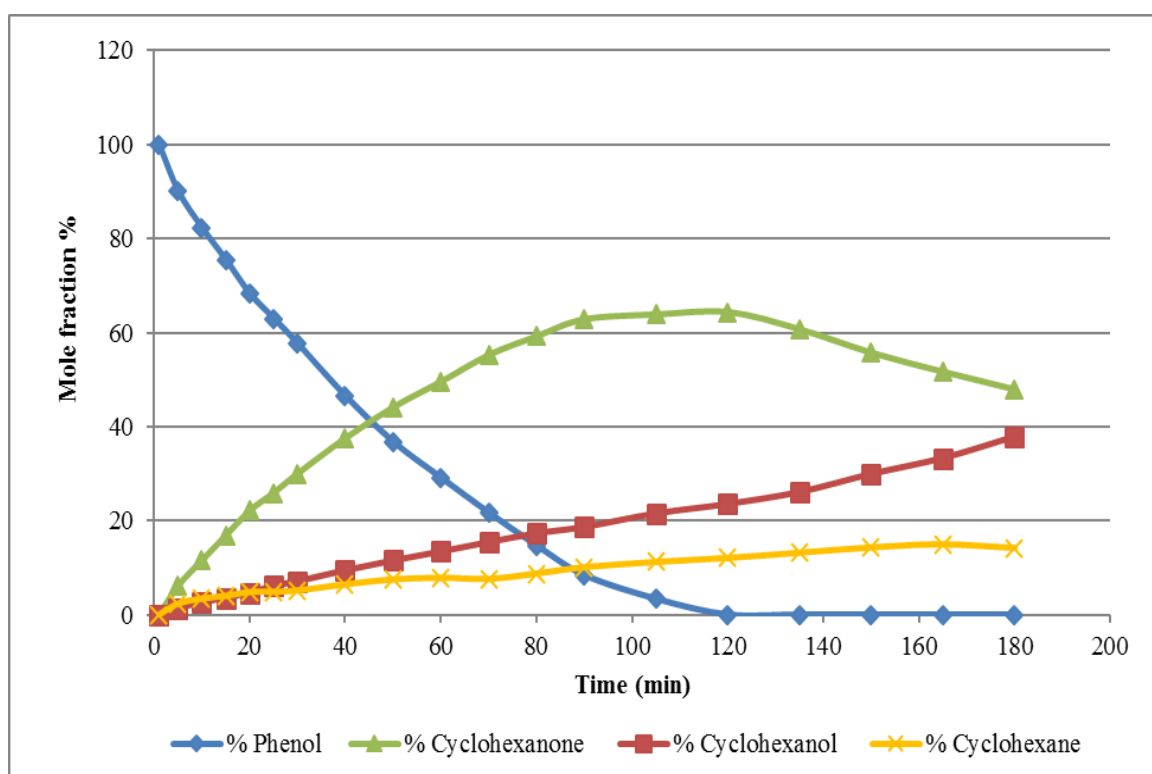


Figure 54. Phenol reaction profile at 70 °C

After finding the rate constants, activation energy can be calculated as explained earlier for alkylbenzenes.

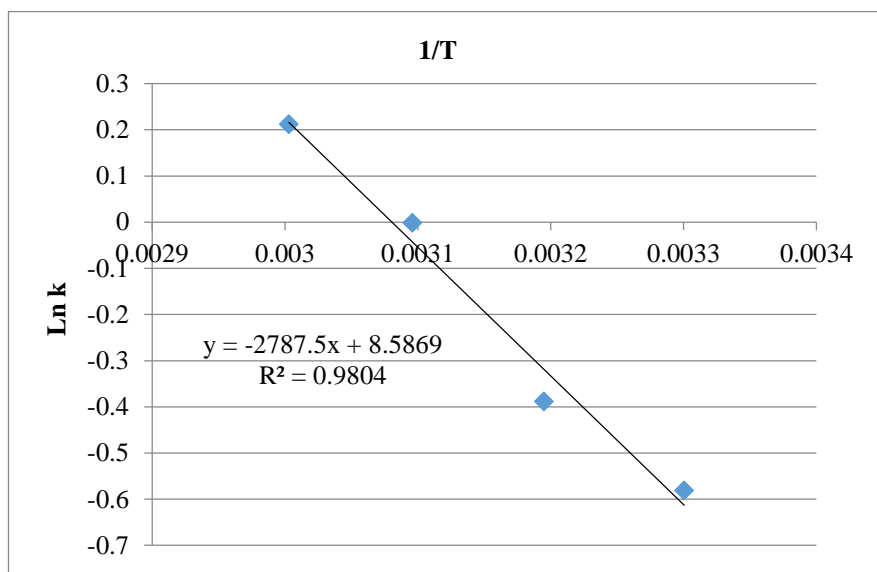


Figure 55. Phenol E_a plot

$$E_a = -mR \quad (7)$$

$$E_a = -(-2787.5 \times 8.314) / 1000$$

$$E_a = 23.17 \text{ kJmol}^{-1}$$

4.4.1.2 Pressure variation and reaction order in H_2

Pressure was varied from 2-5 barg while temperature and substrate concentration were kept constant. The results obtained were used to identify reaction order in hydrogen. Table 21 show the main findings obtained from pressure variation reactions. The rate constant increased as the pressure increased.

Table 21. Phenol conversion at different pressures

H_2 pressure (barg)	2	3	4	5
Conv. after 180 min	100	99	100	100
Time to 20% conv (min)	15	15	10	8
Rate constant k (ms^{-1})	0.7903	0.9986	1.4072	1.9333
Rate ($\mu\text{molL}^{-1}\text{min}^{-1}$)	136	153	210	357

During this set of reactions, phenol was completely converted to products. Conversion to cyclohexanol increased from 30% at 2 barg to 70% at 5 barg as shown in Figure 56 and Figure 57 respectively.

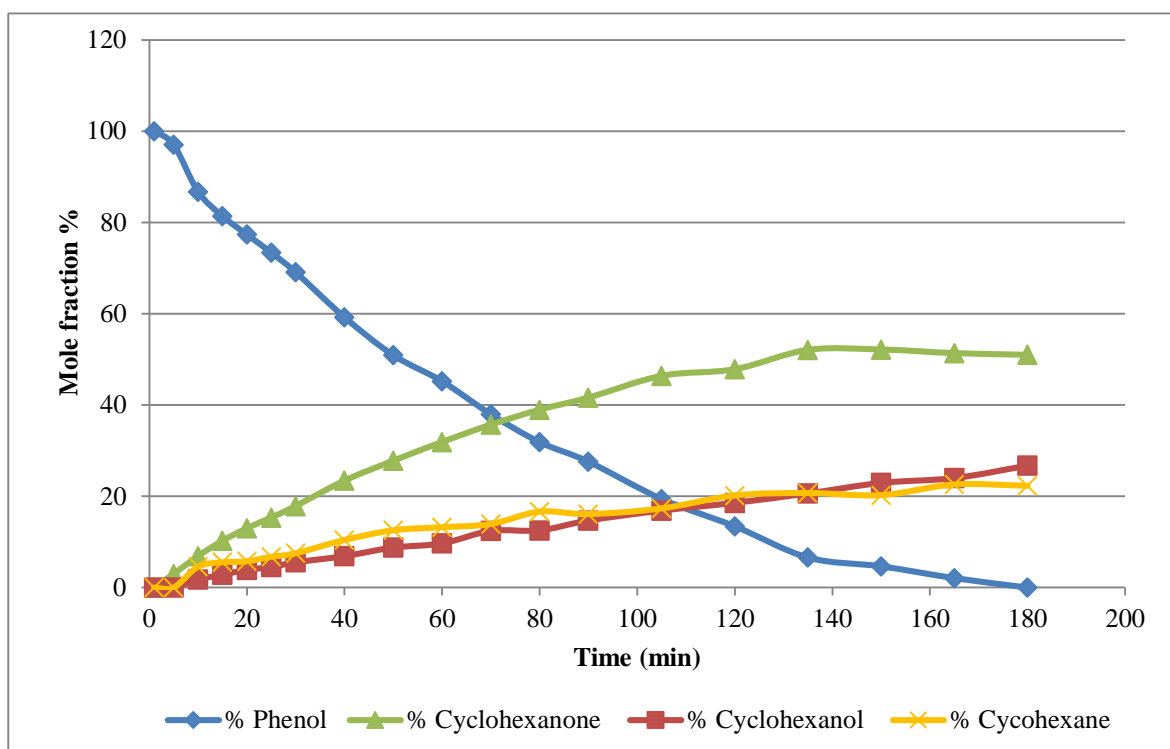


Figure 56. Phenol reaction profile at 2 barg

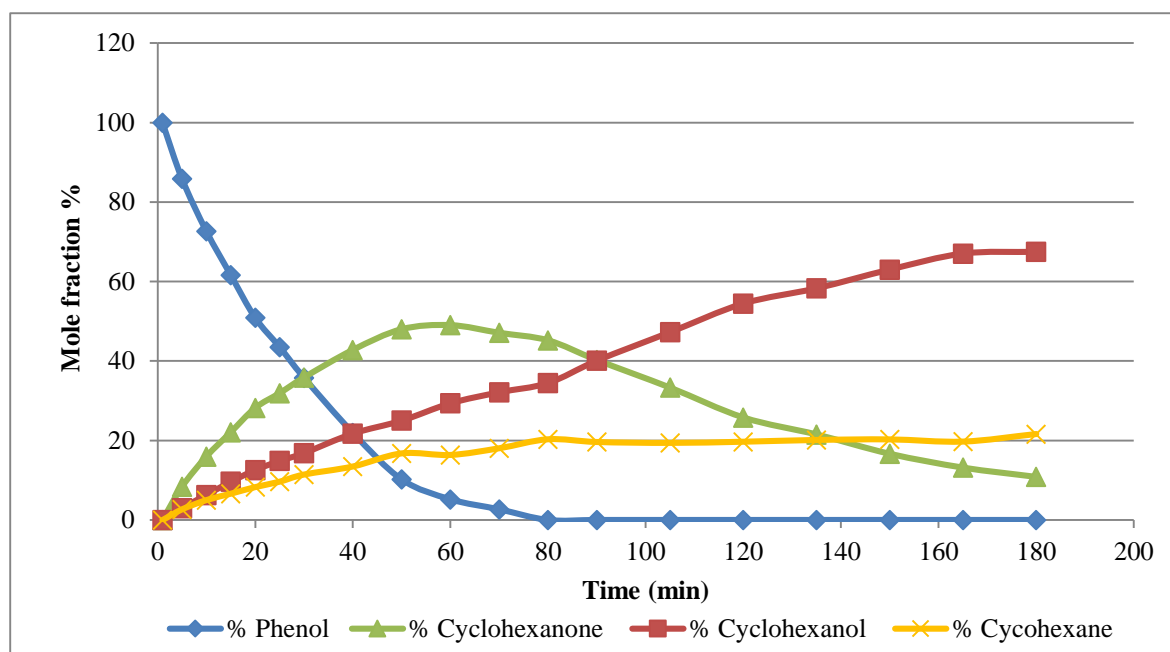


Figure 57. Phenol reaction profile at 5 barg

It is clear from Figure 57 that cyclohexanone was an intermediate formed by hydrogenation of phenol but was subsequently hydrogenated to cyclohexanol. It increased as phenol concentration decreased but then started to decrease when phenol was totally

consumed. Finally, conversion to cyclohexane decreased slightly from 25% to 20% as the pressure increased. It decreased from 25% at 2 barg to 20% at 5 barg.

Reaction order in hydrogen pressure was determined as explained earlier for alkylbenzenes. From Figure 58, phenol hydrogenation reaction in H₂ pressure is nearly first order reaction.

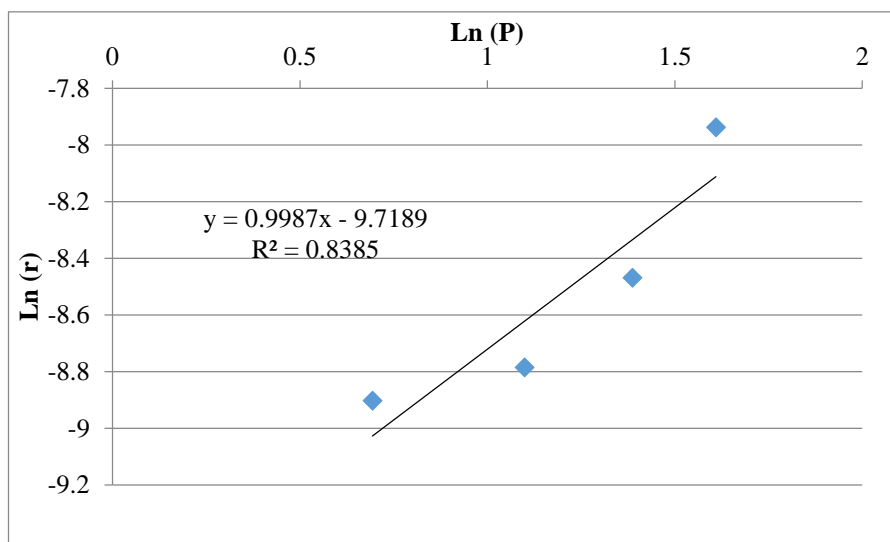


Figure 58. Phenol reaction order in H₂

4.4.1.3 Concentration variation and order in phenol concentration

In these four reactions, the concentration of phenol was varied while temperature and H₂ pressure were kept constant. Conversion of phenol decreased as the concentration increased. It decreased from 100% at 0.5 and 0.75 mL to 75% at 1.5 mL of phenol as shown in Figure 59 and Figure 60 respectively. At 0.5 ml phenol concentration, conversion to cyclohexanol was about 70% and it decreased as the concentration increased. It was only 25% at 1.5 mL. Conversion to cyclohexanone reached 50% during 0.5 and 0.75 mL reactions and it decreased as the concentration increased. Conversion to cyclohexane was ranging from 25% to 20%.

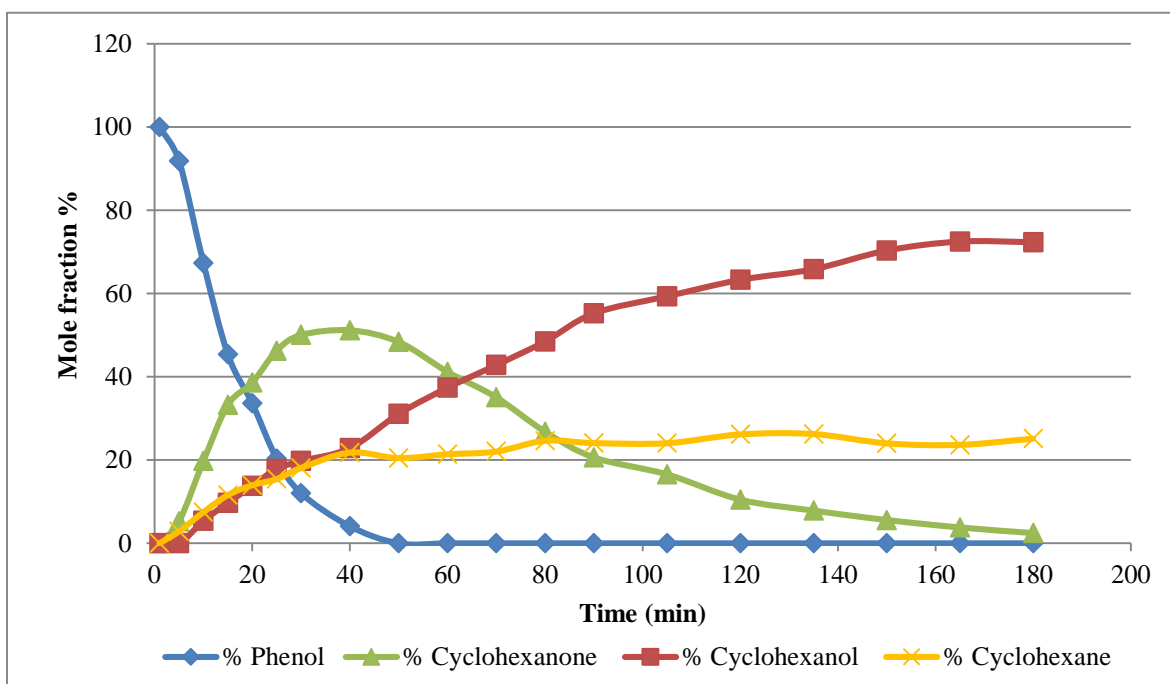


Figure 59. Phenol reaction profile at 0.5 mL

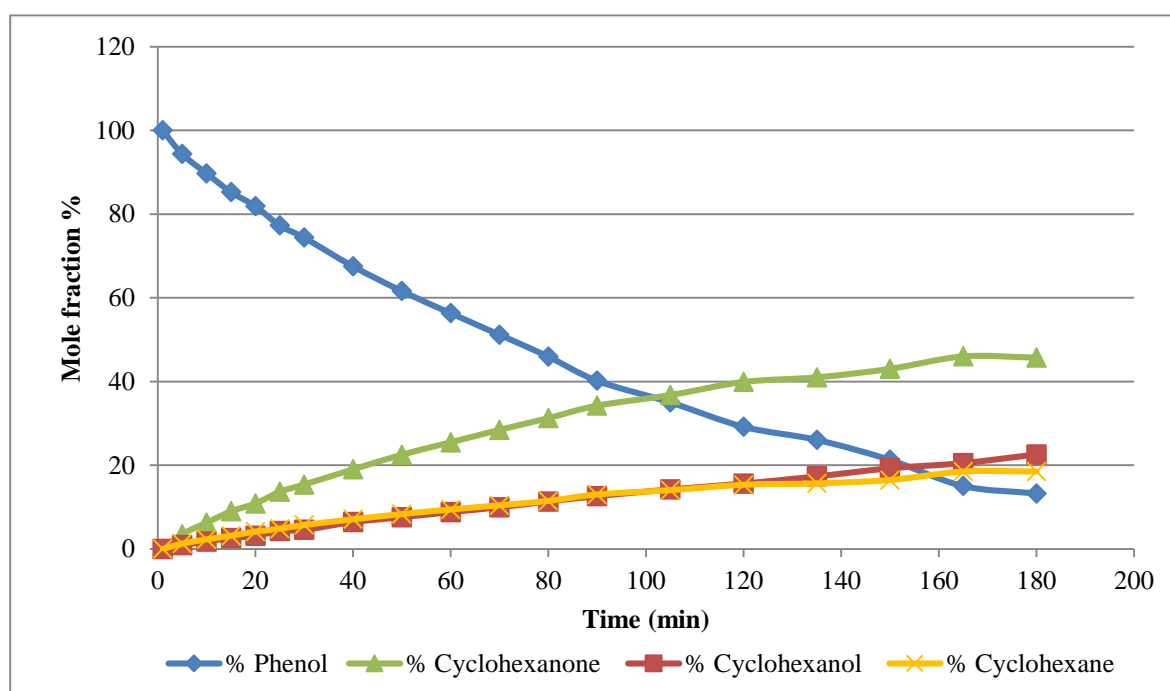


Figure 60. Phenol reaction profile at 1.5 mL

Reaction order in phenol was verified in the same method used for toluene and ethylbenzene reactions order in substrate. The rate of reaction was calculated for the first three samples; after 5, 10 and 15 min for cyclohexanone formation. Then the average of rates was taken and it was $2.1 \times 10^{-4} \text{ mol g}^{-1} \text{ min}^{-1}$ and the standard deviation was $5.2 \times 10^{-5} \text{ mol g}^{-1} \text{ min}^{-1}$. This indicates a zero order in phenol concentration.

Table 22 shows phenol conversion and rate constant values at different phenol concentrations.

Table 22. Conversion and k values for phenol at different concentrations

Volume (mL)	0.5	0.75	1	1.5
Conv. after 180 min	100	100	99	75
Time to 20% conv. (min)	7	8	15	25
Rate constant k (ms ⁻¹)	2.5382	2.0829	0.9111	0.6015
Rate (μmolL ⁻¹ min ⁻¹)	181	266	153	200

4.4.1.4 Products selectivity at different parameters

As stated earlier, cyclohexane, cyclohexanone and cyclohexanol were the only products observed in the phenol hydrogenation at different temperatures, H₂ pressures and at different phenol concentrations. The selectivity of these products differs from one parameter to another as shown on Table 23. It is worth mentioning that these selectivities were taken at 80% phenol conversion.

Table 23. Products selectivity of phenol hydrogenation at different temperatures

Temperature °C	% Cyclohexanone	% Cyclohexanol	% Cyclohexane
30	50	36	11
40	54	28	17
50	55	24	21
60	64	23	14
70	71	19	10

When temperature applied was varied, selectivity to cyclohexane and cyclohexanol decreased as the temperature increased. Selectivity to cyclohexanone increased as the temperature increased.

When pressure applied was varied, a slight decrease was observed in cyclohexanone and cyclohexane selectivities as the pressure increased, while cyclohexanol selectivity increased as the pressure applied increased, Table 24.

Table 24. Products selectivity of phenol hydrogenation at different pressures

Pressure (barg)	% Cyclohexanone	% Cyclohexanol	% Cyclohexane
2	58	21	21
3	55	24	21
4	55	25	20
5	55	28	17

Regarding phenol concentration variation, cyclohexanol and cyclohexane showed a minor increase in selectivity as the concentration increased. Cyclohexanone selectivity was decreased by increasing phenol concentration as shown in Table 25.

Table 25. Products selectivity of phenol hydrogenation at different concentrations

Conc. (mass per vol.)	% Cyclohexanone	% Cyclohexanol	% Cyclohexane
0.5	58	23	19
0.75	58	23	19
1	55	24	21
1.5	55	24	21

4.4.2 Anisole

Anisole was tested in the same way as phenol and the alkylbenzenes. Temperature, hydrogen pressure and anisole concentration were varied to examine their effect on the hydrogenation behaviour of anisole. The results obtained were used to calculate activation energy, rate constants and to determine reaction order in H_2 and in substrate concentration. The products from the hydrogenation were methoxycyclohexane, which is the corresponding cyclic form of anisole, cyclohexanone, cyclohexanol and cyclohexane. Cyclohexanol was not observed in the 30 °C reaction.

4.4.2.1 Temperature variation and E_a calculation

Rate of reaction increased as the temperature increased. Anisole was completely hydrogenated after 40 min at 30 °C and it was hydrogenated after 15 min at 70 °C. Products that were produced from this reaction were methoxycyclohexane, cyclohexanone, cyclohexanol and cyclohexane. Methoxycyclohexane formation decreased as the temperature increased. It decreased from about 80% at 30 °C to around 50% at 70 °C as shown in Figure 61 and Figure 62 respectively. Cyclohexanone was observed in low

concentration at lower temperatures and started to increase as the temperature increased. For cyclohexanol, which was not observed at 30 °C, it increased as the temperature increased. Finally, conversion to cyclohexane increased from about 20% to about 35% as the temperature increased from 30 °C to 70 °C.

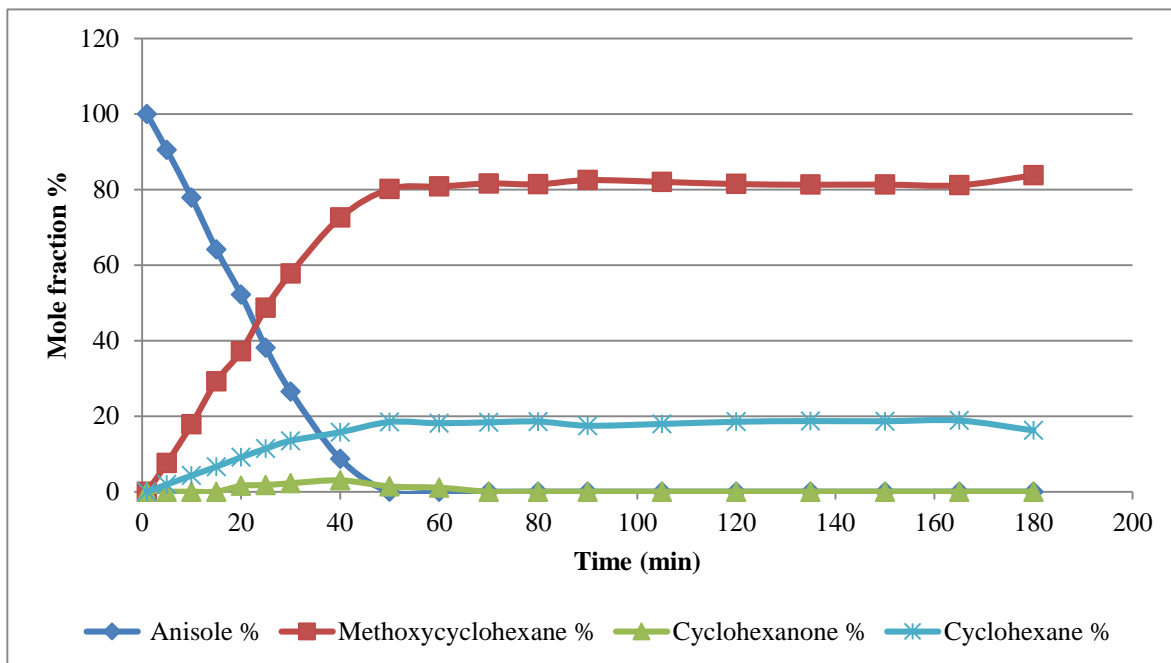


Figure 61. Anisole reaction profile at 30 °C

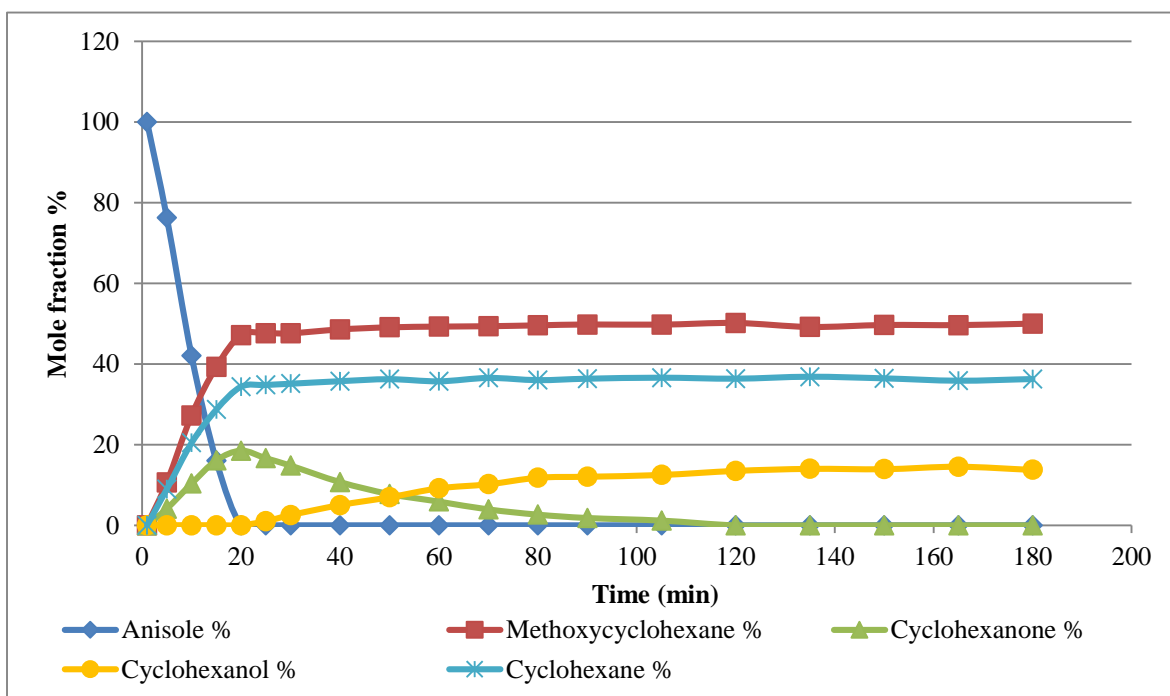


Figure 62. Anisole reaction profile at 70 °C

Products formed by the hydrogenation of anisole at different temperatures are shown in Figure 63. All values were taken at 100% anisole conversion. The 50 °C test was illustrated as an example as shown in Table 26.

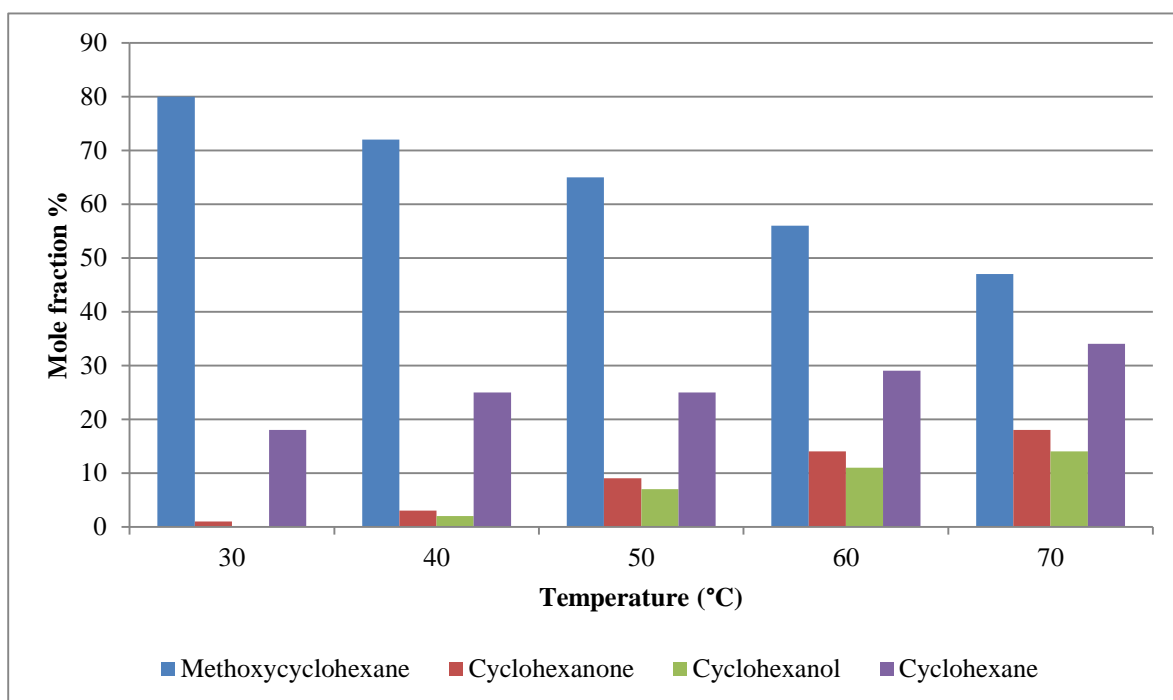


Figure 63. Anisole hydrogenation products profile at different temperatures

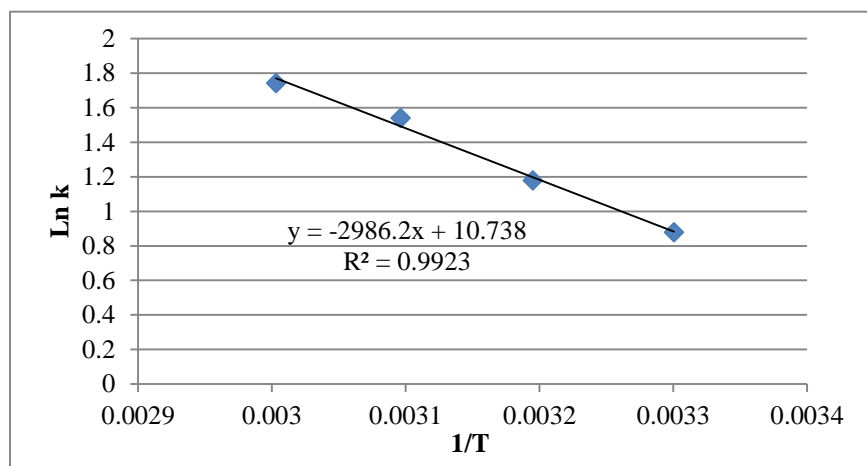
Table 26. Anisole hydrogenation at 50 °C

Time (min)	Anisole %	Methoxycyclohexane %	Cyclohexanone %	Cyclohexanol %	Cyclohexane %
1	100	0	0	0	0
5	77	14	3	0	6
10	51	30	6	0	12
15	29	45	9	0	18
20	8	59	10	0	24
25	0	65	9	0	25
30	0	66	8	1	26
40	0	66	5	2	26
50	0	67	4	4	26
60	0	67	3	5	25
70	0	67	2	6	25
80	0	67	1	6	26
90	0	67	0	6	27
105	0	67	0	6	27
120	0	67	0	6	27
135	0	67	0	7	26
150	0	67	0	7	26
165	0	67	0	7	26
180	0	67	0	7	26

Rate constants for these reactions were calculated from a zero order reaction plots as explained earlier for toluene hydrogenation. Rate constant values are shown in Table 27. Temperatures from 30 – 60 °C were used to find the activation energy.

Table 27. Rate constants for anisole hydrogenation at different temperatures

Temperature °C	30	40	50	60	70
Rate constant k (ms ⁻¹)	2.407	3.2522	4.6678	5.7146	5.5954

Figure 64. Anisole E_a Plot

Activation energy for anisole was determined by using data from Figure 64 and as explained earlier for the other substrates.

$$E_a = -mR \quad (7)$$

$$E_a = -(-2986.2 \times 8.314) / 1000$$

$$E_a = 24.8 \text{ kJmol}^{-1}$$

4.4.2.2 Pressure variation and reaction order in H_2

Results obtained from these series of reactions showed no big changes in products concentrations. Methoxycyclohexane varied between 65 to 70%, cyclohexanone was less than 10%, cyclohexanol was less than 5% and cyclohexane decreased from 30% at 2 barg pressure to 25% at 5 barg as shown in Figure. 65.

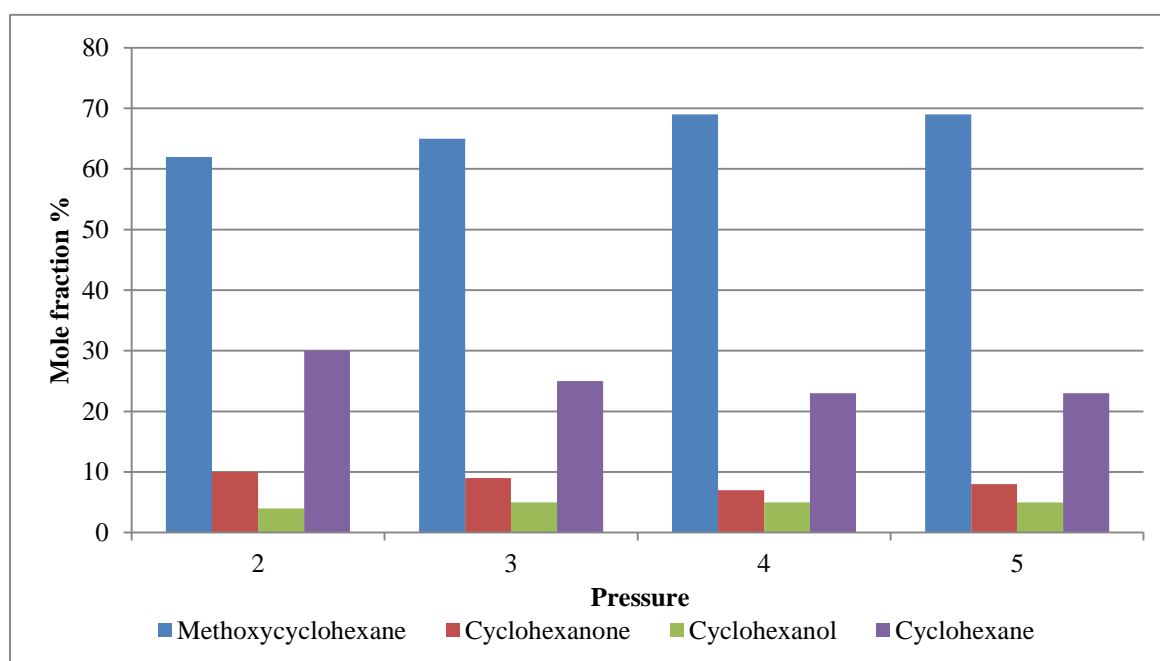


Figure. 65 Anisole hydrogenation products profile at different pressures

Figure 66 and Figure 67 show the reaction profiles for anisole at 2 barg and 4 barg respectively. The rate of reaction has increased as the pressure applied increased.

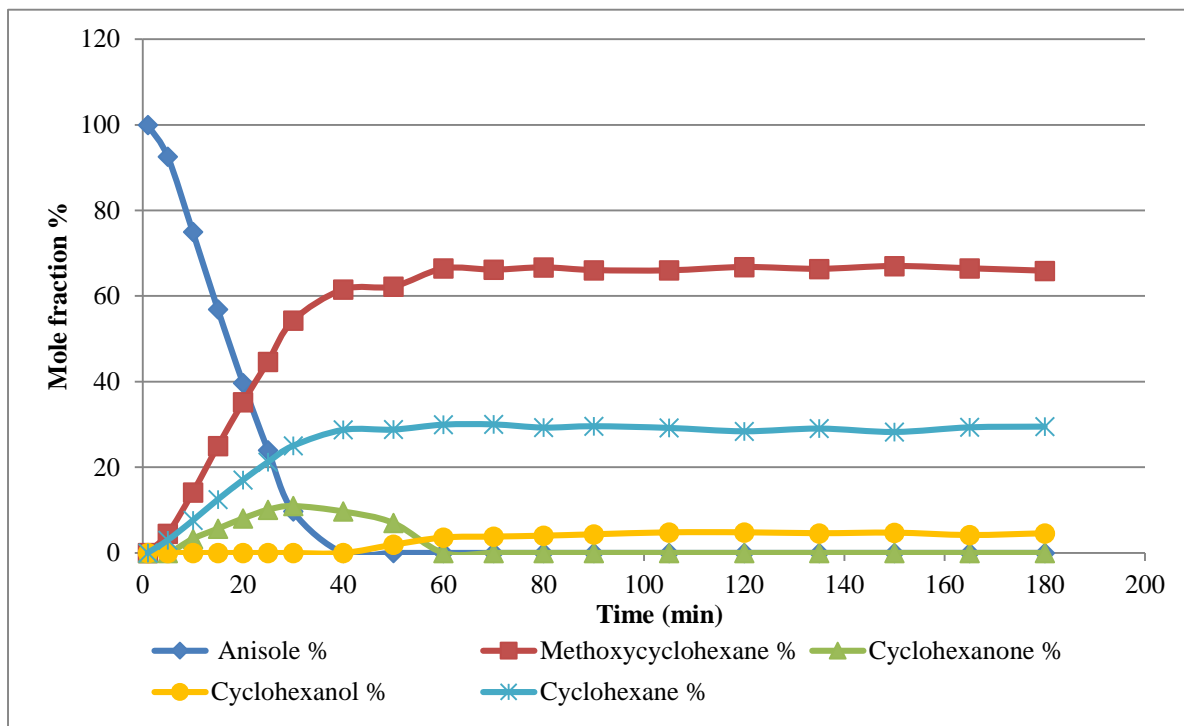


Figure 66. Anisole reaction profile at 2 barg

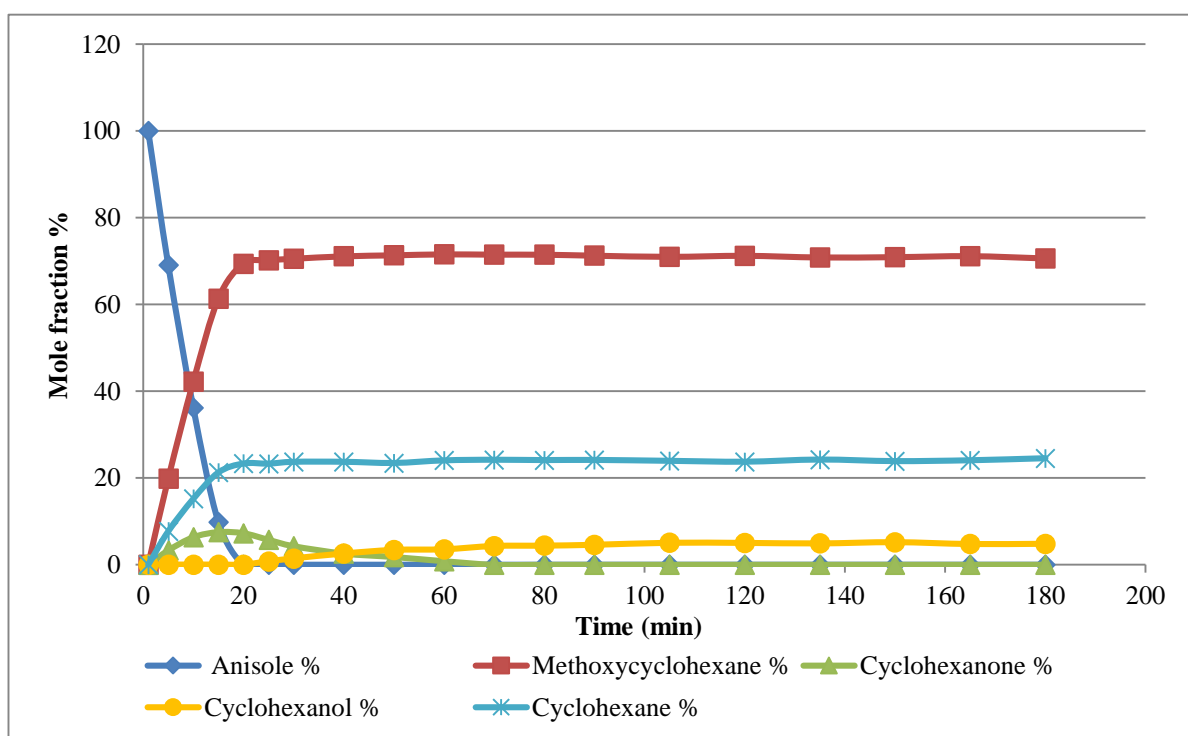


Figure 67. Anisole reaction profile at 4 barg

Reaction order was determined as explained earlier. From Figure 68, the reaction is nearly 1st order in H₂.

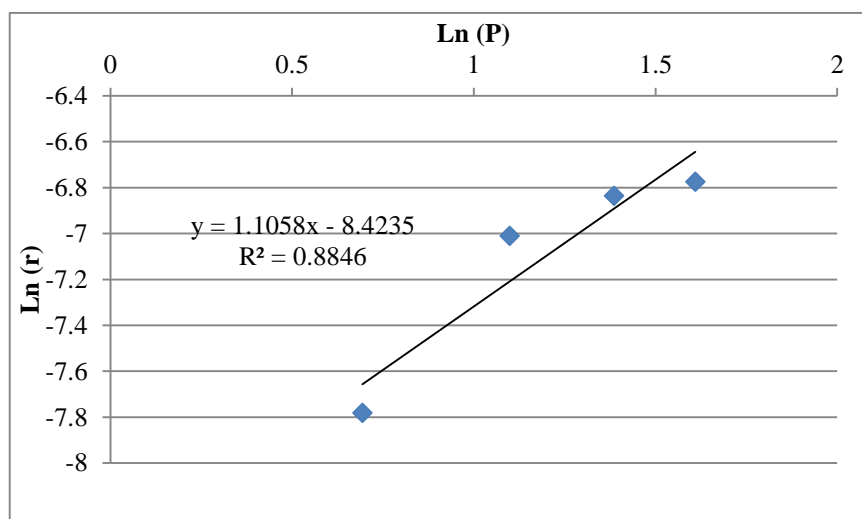


Figure 68. Anisole reaction order in H₂

4.4.2.3 Concentration variation and reaction order in anisole

The rate of reaction decreased as the concentration increased. Methoxycyclohexane increased slightly as the concentration increased. Cyclohexanone and cyclohexanol also showed a slight increase as the concentration increased. Cyclohexane showed a minor decrease as concentration increased. Results obtained from concentration variation are shown in Figure 69.

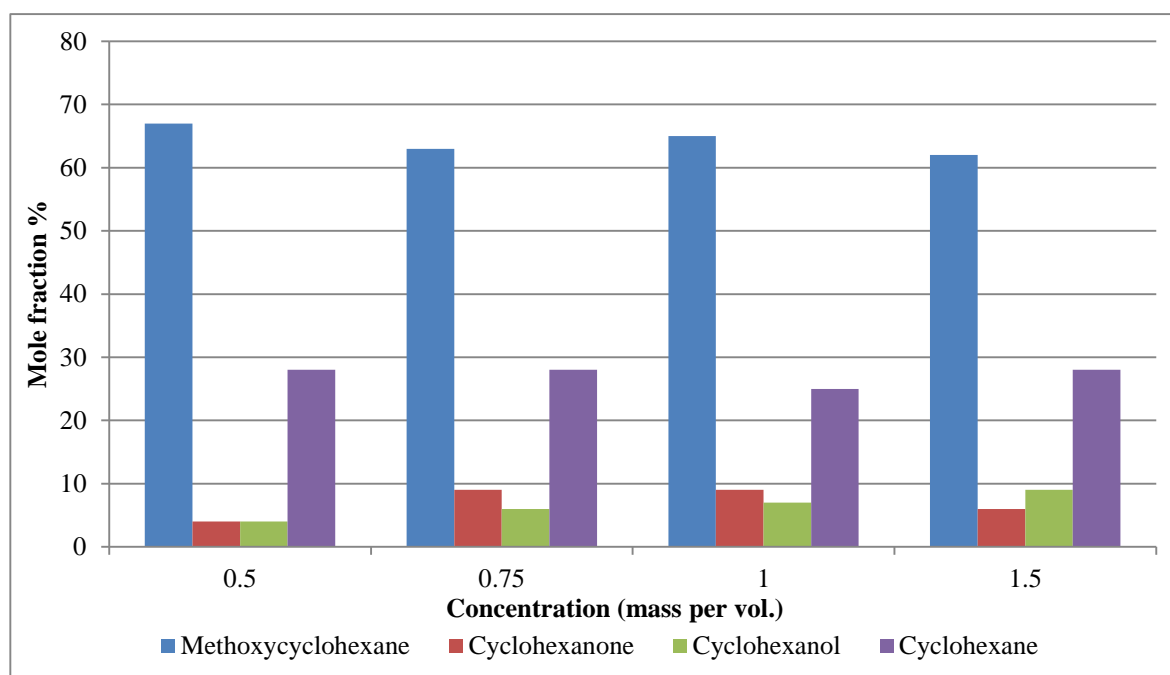


Figure 69. Anisole hydrogenation products profile at different concentrations

Figure 70 and Figure 71 show reaction profiles for anisole hydrogenation at 0.5 and 1.5 mL of anisole. Rate of reaction was faster when 0.5 mL of anisole was used.

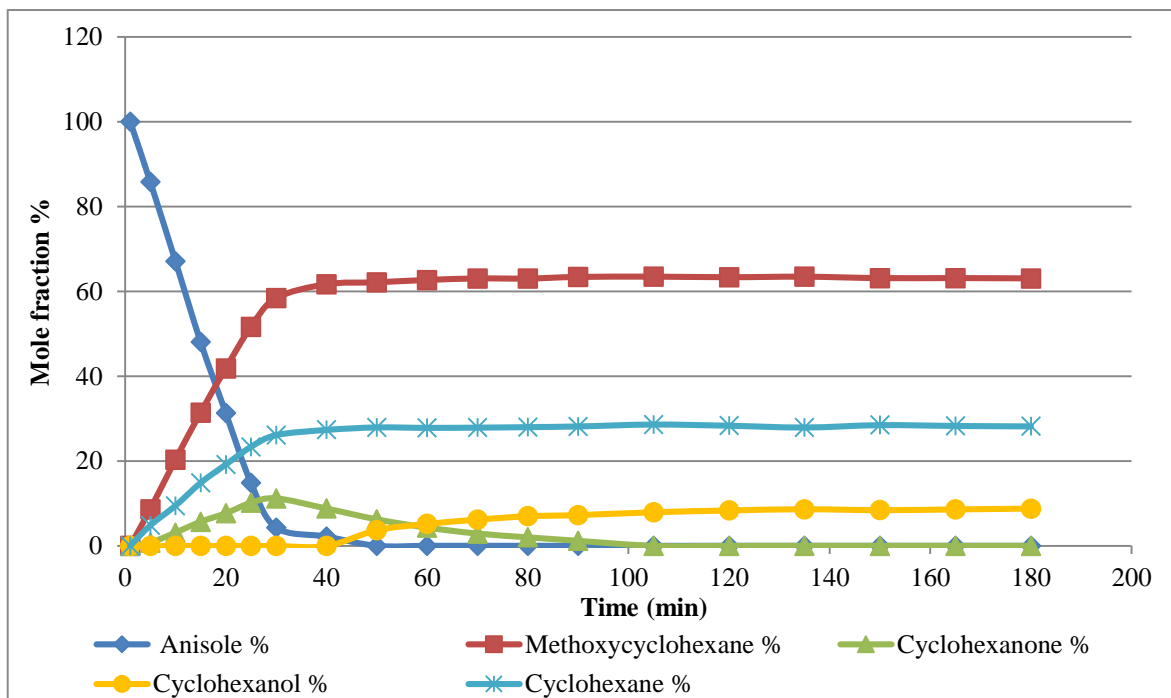


Figure 70. Anisole reaction profile at 1.5 mL

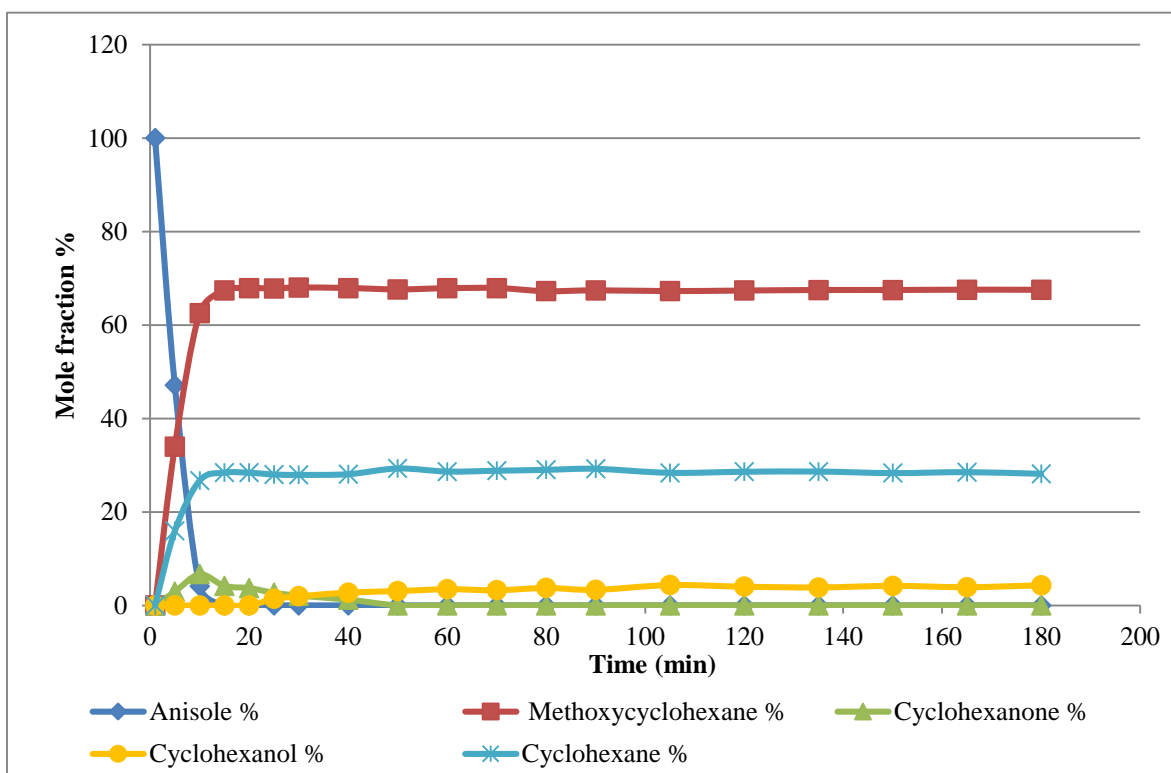


Figure 71. Anisole reaction profile at 0.5 mL

Reaction order in anisole was determined as explained earlier for phenol reaction order in substrate. The rate of reaction was calculated for the first three samples; after 5, 10 and 15 min for methoxycyclohexane formation. Then the average of rates was taken and it was $6.4 \times 10^{-4} \text{ mol g}^{-1} \text{ min}^{-1}$ and the standard deviation was $3.5 \times 10^{-4} \text{ mol g}^{-1} \text{ min}^{-1}$. This indicates a zero order in anisole concentration.

4.4.2.4 Products selectivity at different parameters

The principal product produced from anisole hydrogenation was methoxycyclohexane; in addition, cyclohexane, cyclohexanone and cyclohexanol were also formed. Selectivity to each product varied as hydrogenation parameters varied. Selectivity was taken at 100% anisole conversion except for cyclohexanol. It was measured as anisole and cyclohexanone were completely consumed, as the formation of cyclohexanol is related to the disappearance of anisole and cyclohexanone.

When the temperature applied to anisole hydrogenation was increased, selectivity of methoxycyclohexane decreased, while selectivity of the other products i.e. cyclohexane and cyclohexanone and cyclohexanol increased as temperature increased, Table 28.

Table 28. Products selectivity of anisole hydrogenation at different temperatures

Temp. (°C)	% Methoxycyclohexane	% Cyclohexanone	% Cyclohexanol	% Cyclohexane
30	80	1	0	18
40	72	3	2	25
50	65	9	7	25
60	56	14	11	29
70	47	18	14	34

Table 29. Products selectivity of anisole hydrogenation at different pressures

Pressure (barg)	% Methoxycyclohexane	% Cyclohexanone	% Cyclohexanol	% Cyclohexane
2	62	10	5	29
3	65	9	7	25
4	69	7	5	23
5	69	8	7	23

As pressure increased, selectivity for methoxycyclohexane has increased. Selectivity of cyclohexanone and cyclohexane was decreased as the pressure applied increased, Table 29.

When anisole concentration was increased selectivities of methoxycyclohexane and cyclohexane decreased. The selectivity of cyclohexanone and cyclohexanol was increased as anisole concentration increased as shown in Table 30.

Table 30. Products selectivity of anisole hydrogenation at different concentrations

Conc. (mass per vol.)	% Methoxycyclohexane	% Cyclohexanone	% Cyclohexanol	% Cyclohexane
0.5	68	7	4	29
0.75	66	8	6	27
1	65	9	7	25
1.5	63	10	9	26

4.5 Competitive hydrogenation of phenol, anisole and toluene

In this section the reactions of three substituted benzenes, toluene, phenol and anisole, as groups of two and as a group of three reactants in the same time will be presented. Firstly, main results from previous tests will be summarised. As shown in Table 31 the activation energies of three substrates are almost identical. In addition, order of reaction in hydrogen and in substrate concentration are the same.

Table 31. Results concerning three substrates as singles

Substrates	Toluene	Phenol	Anisole
E_a (kJmol ⁻¹)	23	23	25
Rate constant (ms ⁻¹)	1.4487	0.9986	4.6678
Order in H ₂ pressure	1	1	1
Order in substrate	0	0	0

Figure 72 and Figure 73 show the change in conversion after performing the competitive hydrogenation of the 3 substrates at the same time. The conversion decreased from 100% as single substrates to 60% of toluene and to about 70% for phenol and anisole.

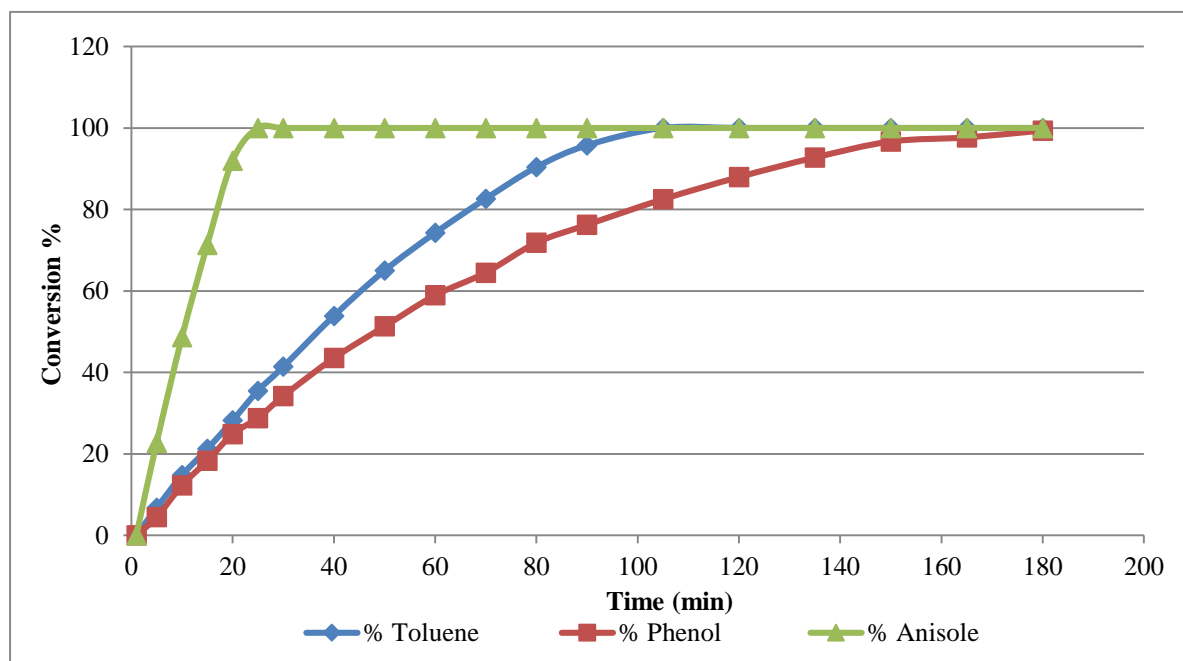


Figure 72. Single substrates conversion

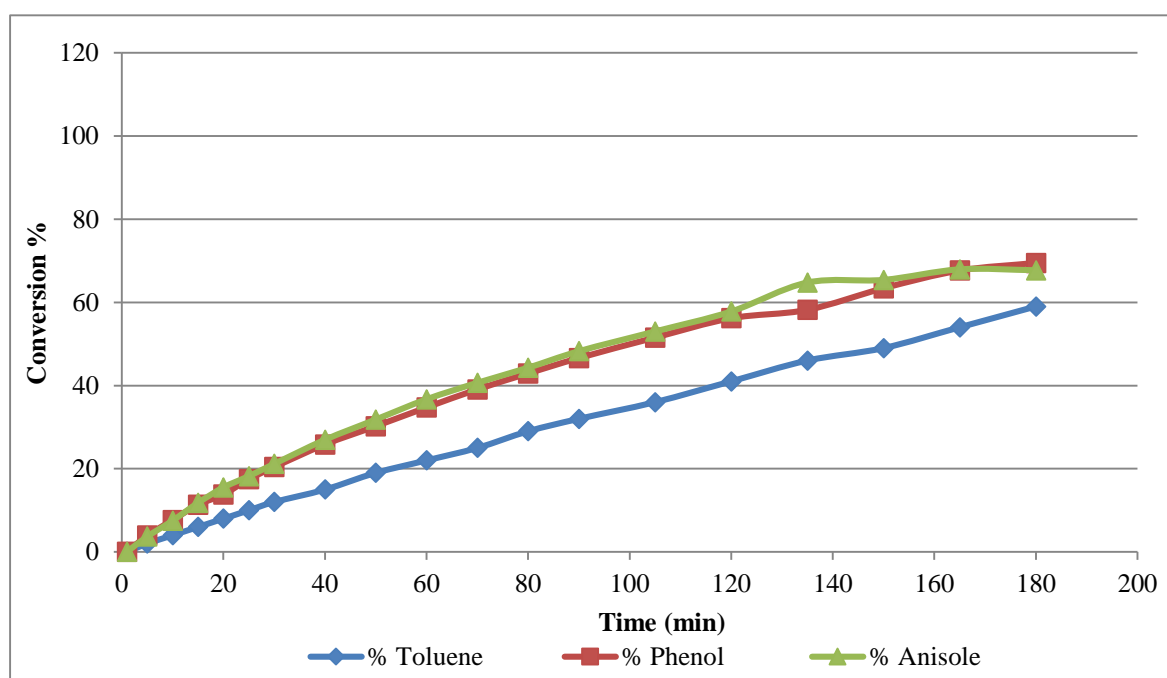


Figure 73. Mixture of three substrates conversion at a 1:1:1 ratio

4.5.1 Toluene

Figure 74 represent four reactions of toluene. These four reaction profiles show the way that toluene reacted as a single substrate, on the top left, and in the presence of phenol and anisole. In the presence of anisole toluene reaction rate increased slightly. It was affected considerably by phenol and in the mixture of the three substrates. In presence of phenol, the rate of reaction was much slower and conversion decreased from 100% to about 60%. The same behaviour was observed during the hydrogenation of the three substrates.

4.5.2 Phenol

The process of phenol hydrogenation was affected in the presence of toluene and/or anisole as shown in Figure 75. Hydrogenation of phenol as a single substrate produces cyclohexanone, cyclohexanol and cyclohexane. However, conversion to cyclohexanol was not observed when phenol was mixed with anisole and in the mixture of three substrates. Rate of reaction decreased in all competitive reactions. The conversion of phenol decreased to around 80% in the presence of toluene or anisole and decreased to about 70% in the mixture of three substrates.

4.5.3 Anisole

In anisole hydrogenation, Figure 76, as a single substrate the reaction precedes in three paths. One is hydrogenation to the corresponding cyclic form methoxycyclohexane. The second was the formation of cyclohexanone and cyclohexanol, while the third was the formation of cyclohexane. Anisole was affected slightly by the presence of toluene. The rate of reaction was decreased. The total conversion of anisole was completed after about 25 minutes as a single substrate and it was completed after about 70 min when mixed with toluene. In the presence of phenol, anisole conversion decreased to around 80% and cyclohexanol was not observed. As a mixture of three substrates, conversion of anisole also decreased to around 70% and cyclohexanol was not observed. In both reactions the formation of methoxycyclohexane decreased from about 65% as a single substrate to around 25% in the presence of phenol and in the mixture of three substrates. Another point to consider in the anisole hydrogenation as a single substrate or in the presence of toluene is that the formation of cyclohexanol starts only after total conversion of anisole. Anisole was not completely consumed in the presence of toluene or in the mixture of three substrates and cyclohexanol was not detected in both reactions.

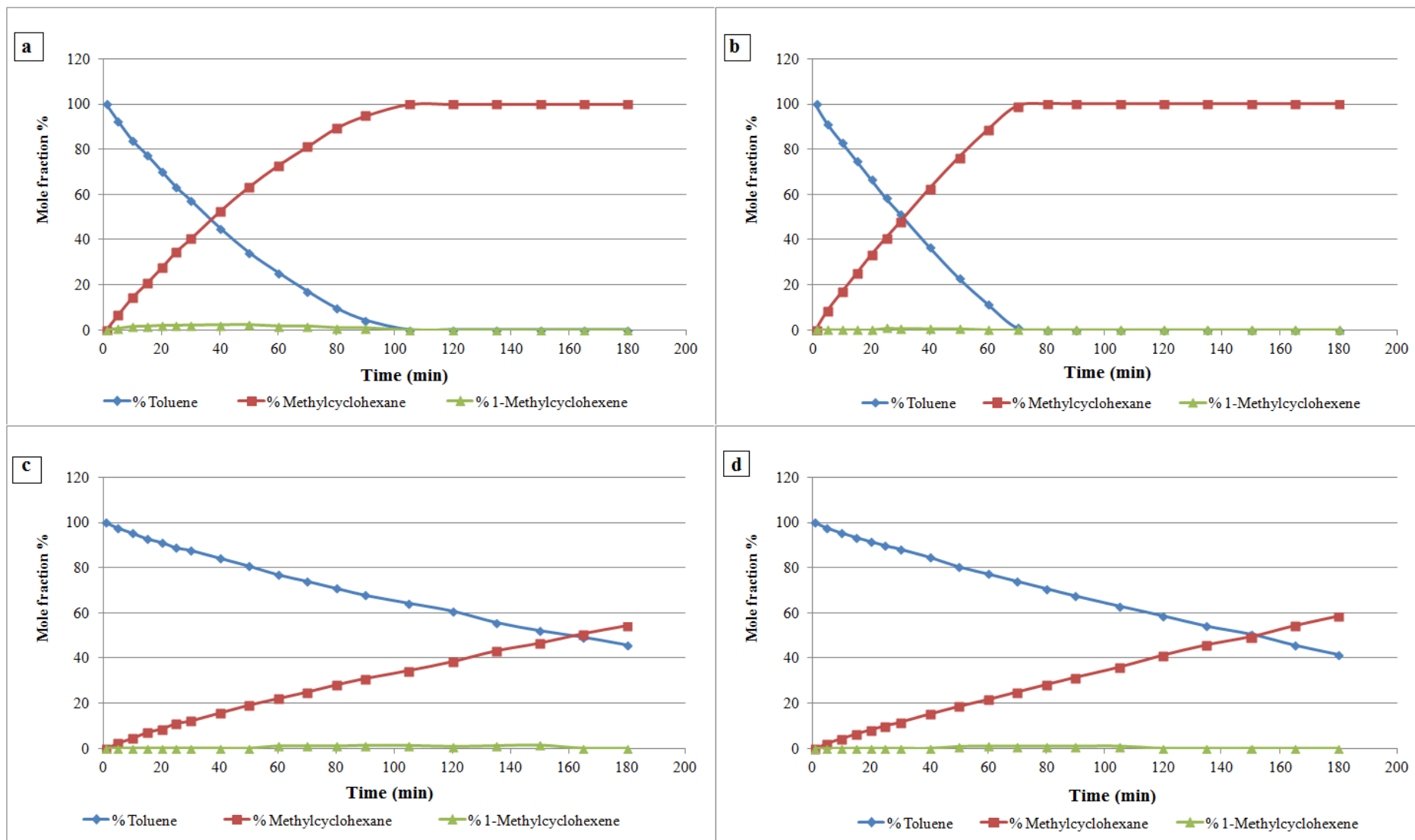


Figure 74. Toluene reaction profiles a) single substrate, b) with phenol, c) with anisole and d) in mixture of three

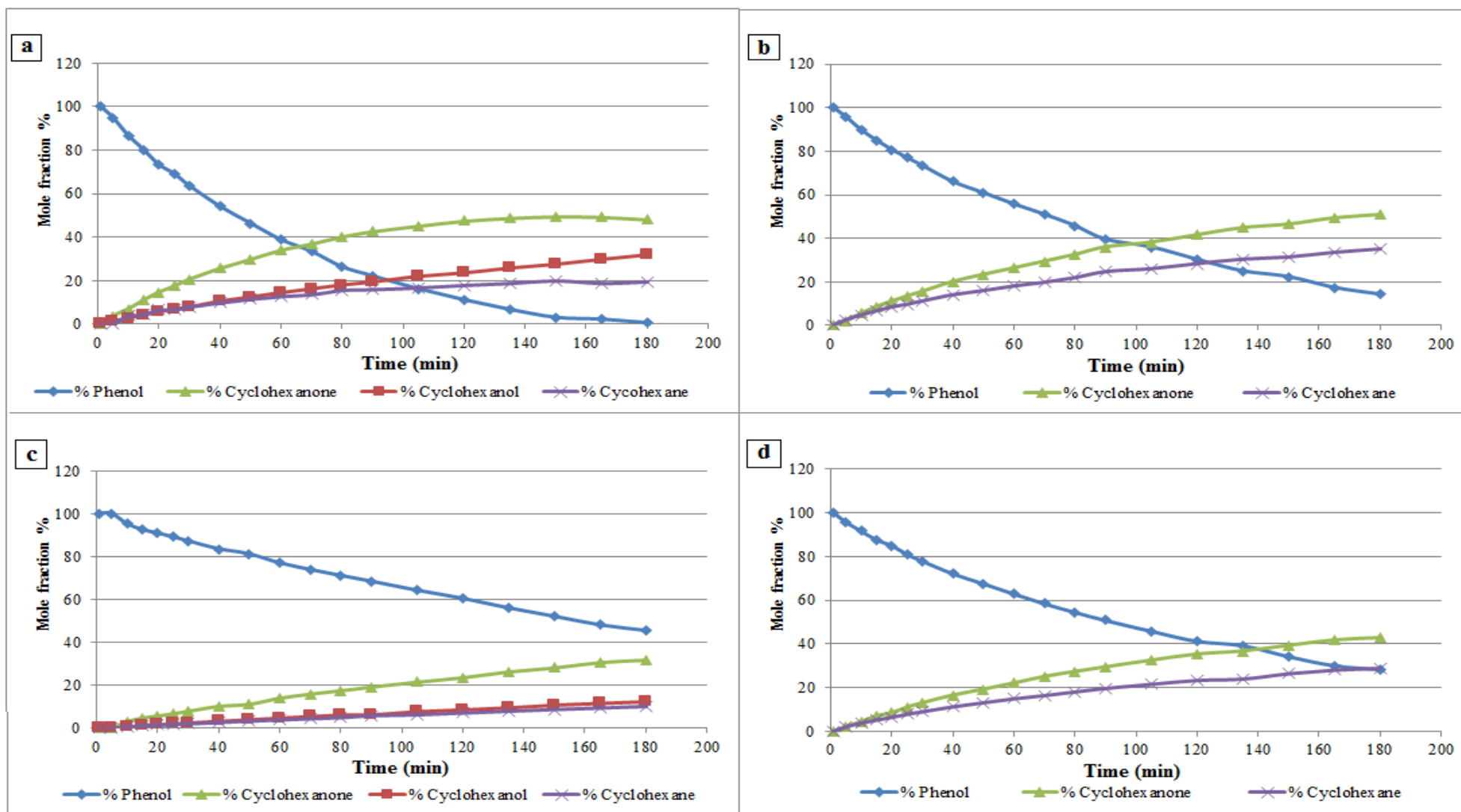


Figure 75. Phenol reaction profiles a) single substrate, b) with anisole, c) with toluene and d) in mixture of three

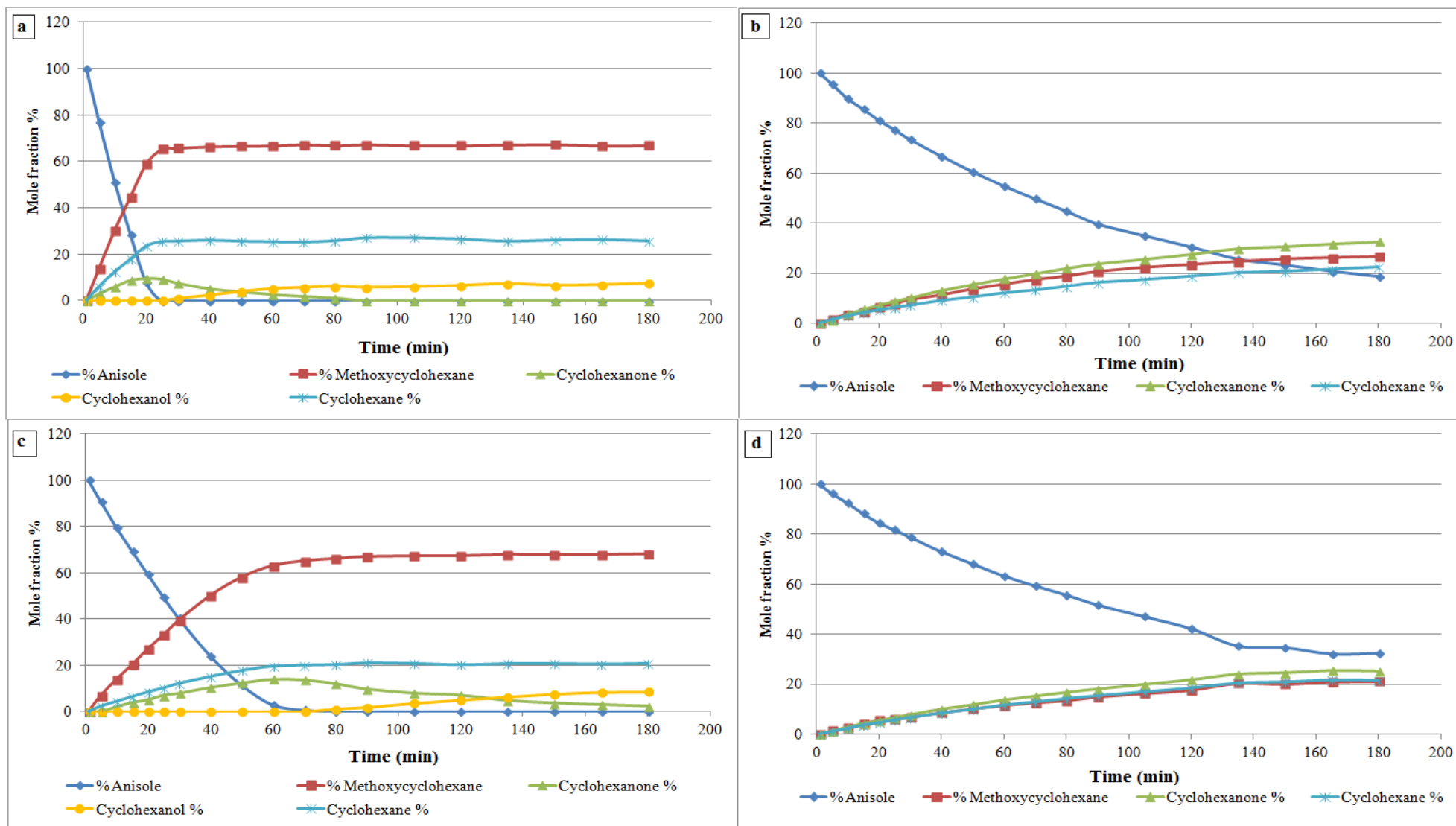


Figure 76. Anisole reaction profiles a) single substrate, b) with phenol, c) with toluene and d) in mixture of three

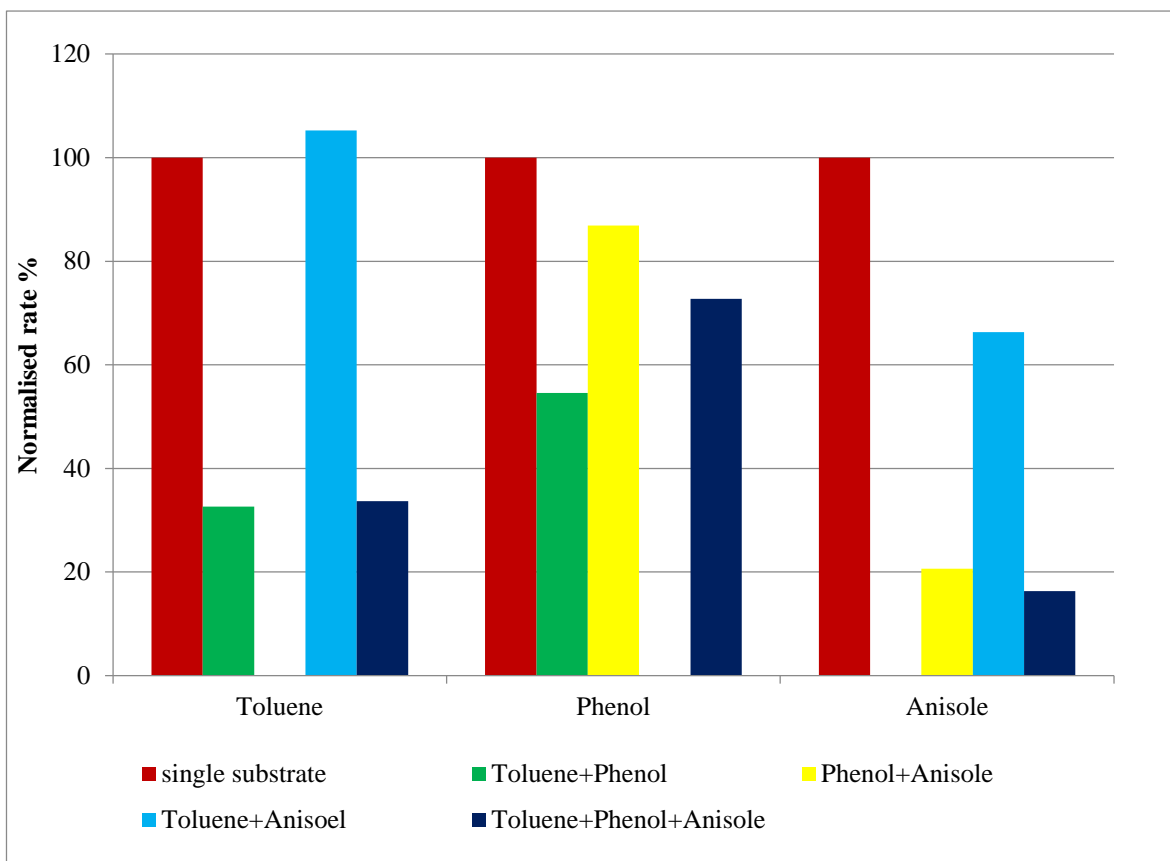


Figure 77. Competitive hydrogenation of toluene, phenol and anisole

Results from competitive hydrogenation of toluene, phenol, anisole are summarised in Figure 77. These columns were divided into three groups each group starts with a red column. The red columns represent the single substrates which were set to a 100 and the others were normalised against them to allow comparison with other results. Taking into consideration that toluene results were compared after 90 min of reaction and anisole results were compared after 20 min of reaction.

Toluene rate decreased to about 30%, in the presence of phenol and also in the mixture of three substrates. Phenol was the least affected substrates in the competitive hydrogenation. Anisole was affected significantly especially when mixed with phenol and also in the mixture of three substrates.

4.6 Cyclohexanone hydrogenation

The hydrogenation of cyclohexanone was investigated to give an indication of the behaviour of this intermediate during the hydrogenation of phenol, anisole and methoxyphenol. In addition, cyclohexanone was tested in the presence of toluene, phenol and anisole.

4.6.1 Cyclohexanone hydrogenation as a single substrate

In this set of reactions, cyclohexanone was hydrogenated at different temperatures, 30, 40, 50, 60 and 70 °C. The remaining parameters were held constant at 3 barg and 1 mL cyclohexanone concentration. Figure 78 and Figure 79 show the reaction profiles of cyclohexanone hydrogenation at 30 and 70 °C respectively. Conversion increased from 50% at 50 min at 30 °C to 50% at 25 min at 70 °C.

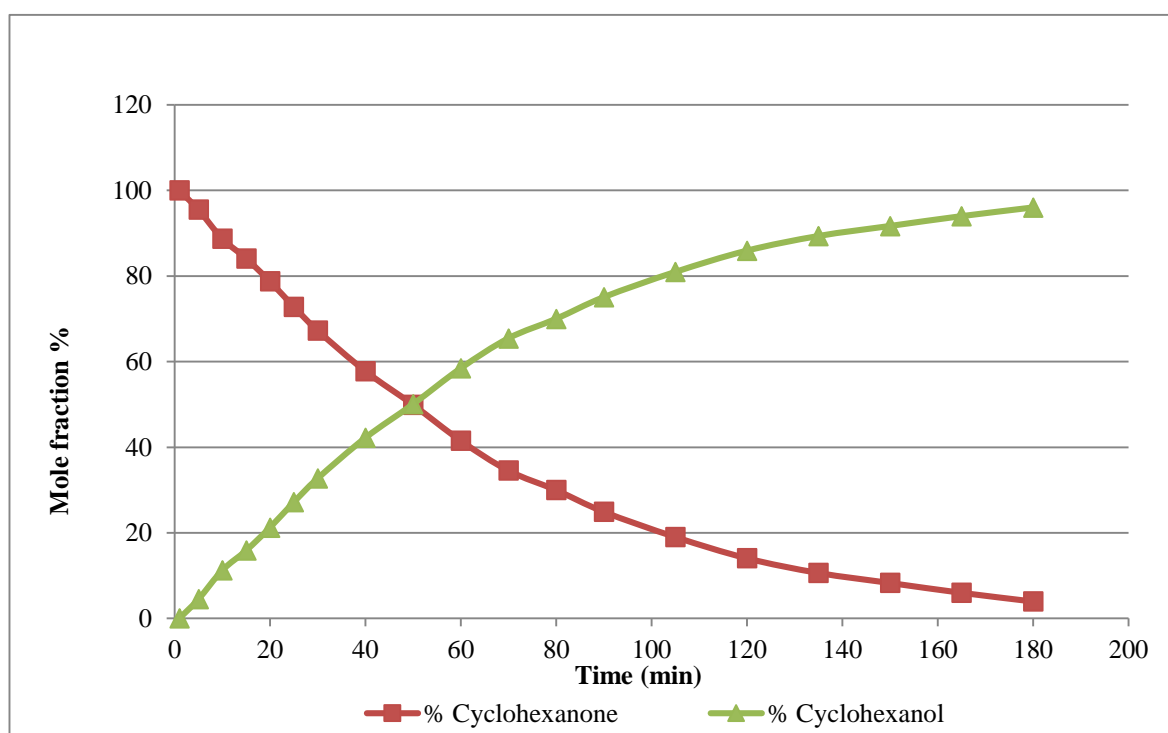


Figure 78. Cyclohexane reaction profile at 30 °C

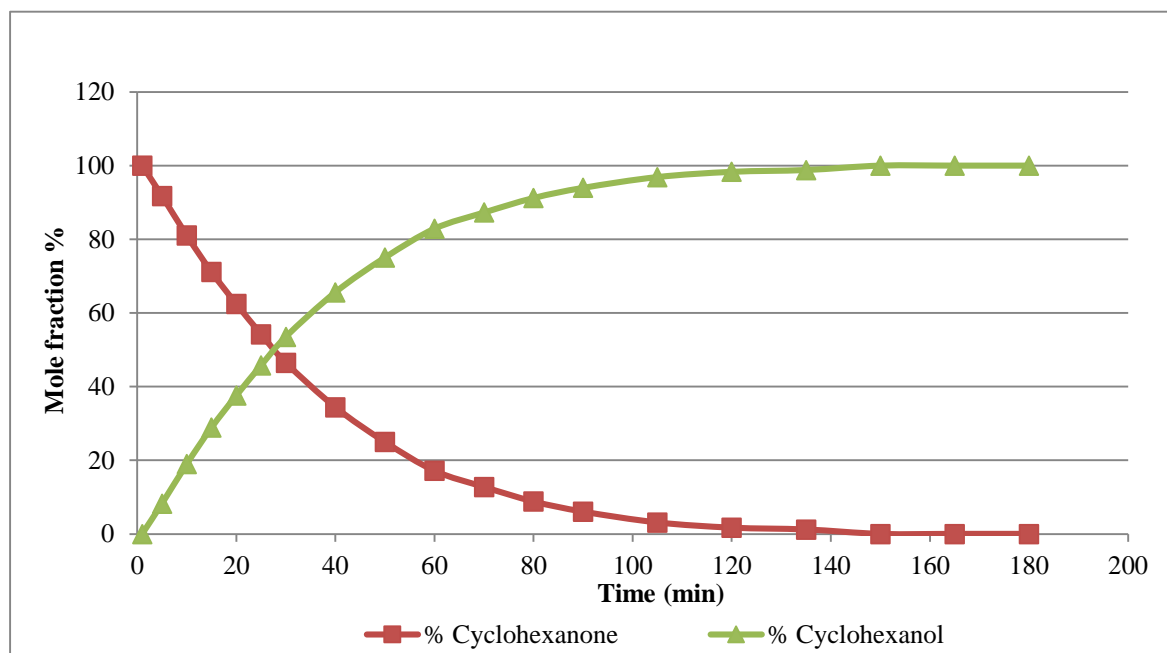


Figure 79. Cyclohexane reaction profile at 70 °C

Figure 80 shows the effect of temperature variation on cyclohexanone. There was a slight increase in conversion as the temperature increased from 30 to 50 °C. There no obvious change in conversion at temperatures higher than 50 °C. An important point to consider in these tests is that cyclohexane was not detected at most of the 5 different reaction temperatures applied. Even at 70 °C it was less than 3% yield.

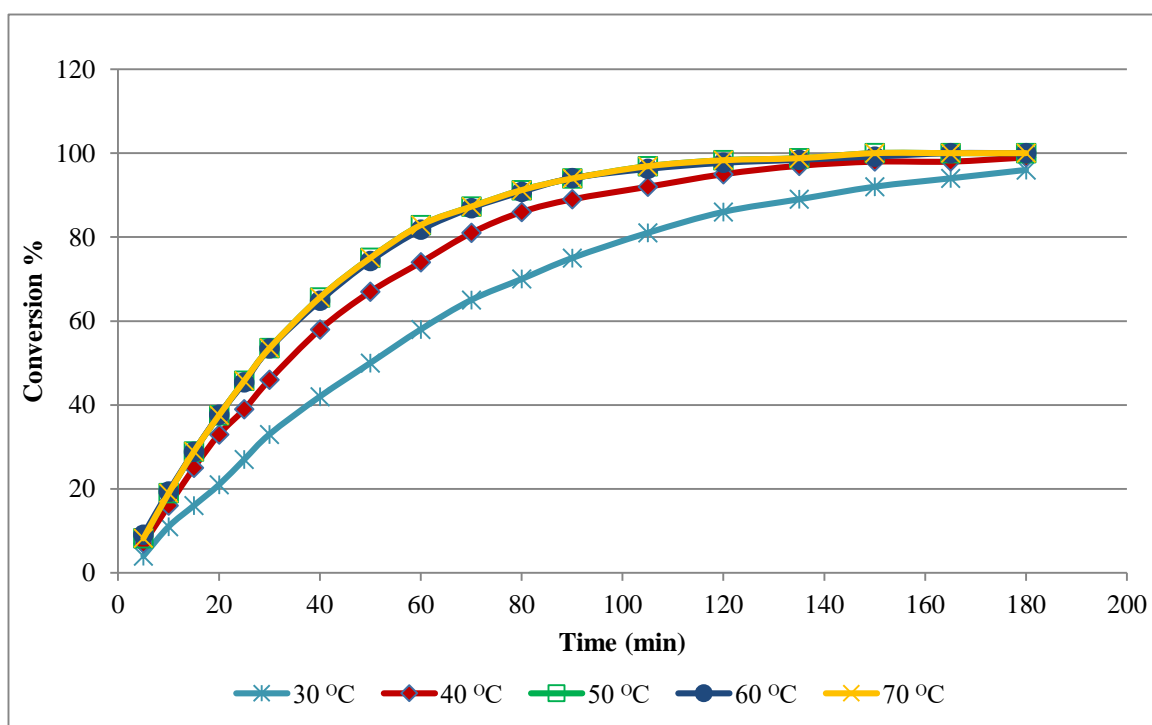


Figure 80. Temperature effect on cyclohexanone hydrogenation

4.6.1.1 Activation energy

An apparent activation energy was calculated as shown earlier for the other substrates.

$$E_a = -mR \quad (7)$$

$$E_a = -(-3299.2 \times 8.314) / 1000$$

$$E_a = 27.4 \text{ kJ.mol}^{-1}$$

Table 32 Data used to generate Arrhenius plot

T (k)	k (ms ⁻¹)	1/T	Ln k
303	0.0143	0.00330	-4.2475
313	0.0225	0.003195	-3.79424
323	0.0280	0.003096	-3.57555

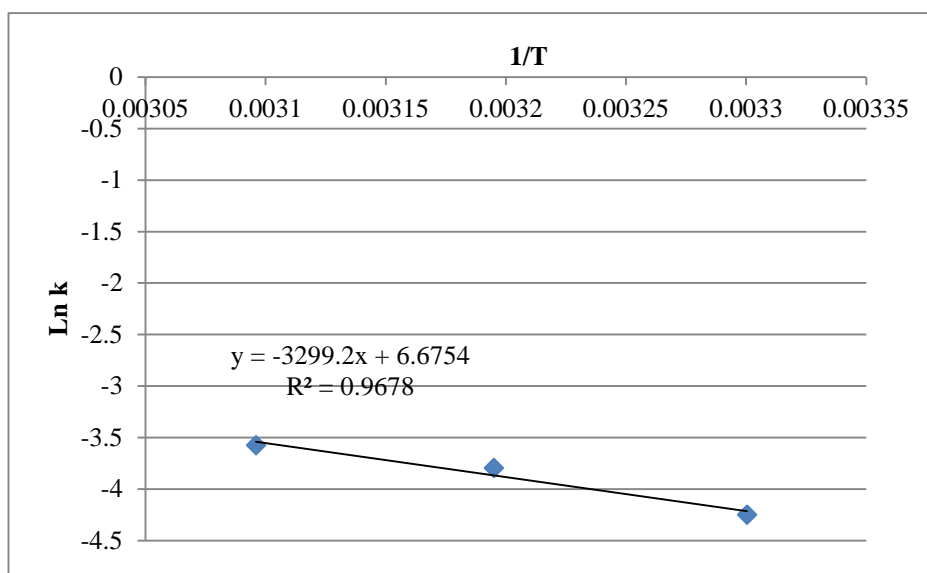


Figure 81. Cyclohexanone E_a plot

4.6.2 Cyclohexanone competitive hydrogenation

In this test, cyclohexanone was tested in the presence of toluene, phenol and anisole. The hydrogenation reaction was performed at 50 °C, 3 barg H₂ pressure and 1 ml of each substrate.

4.6.2.1 Toluene

The rate of toluene hydrogenation was enhanced by the presence of cyclohexanone. On the contrary, the presence of toluene inhibited cyclohexanone hydrogenation as shown in Figure

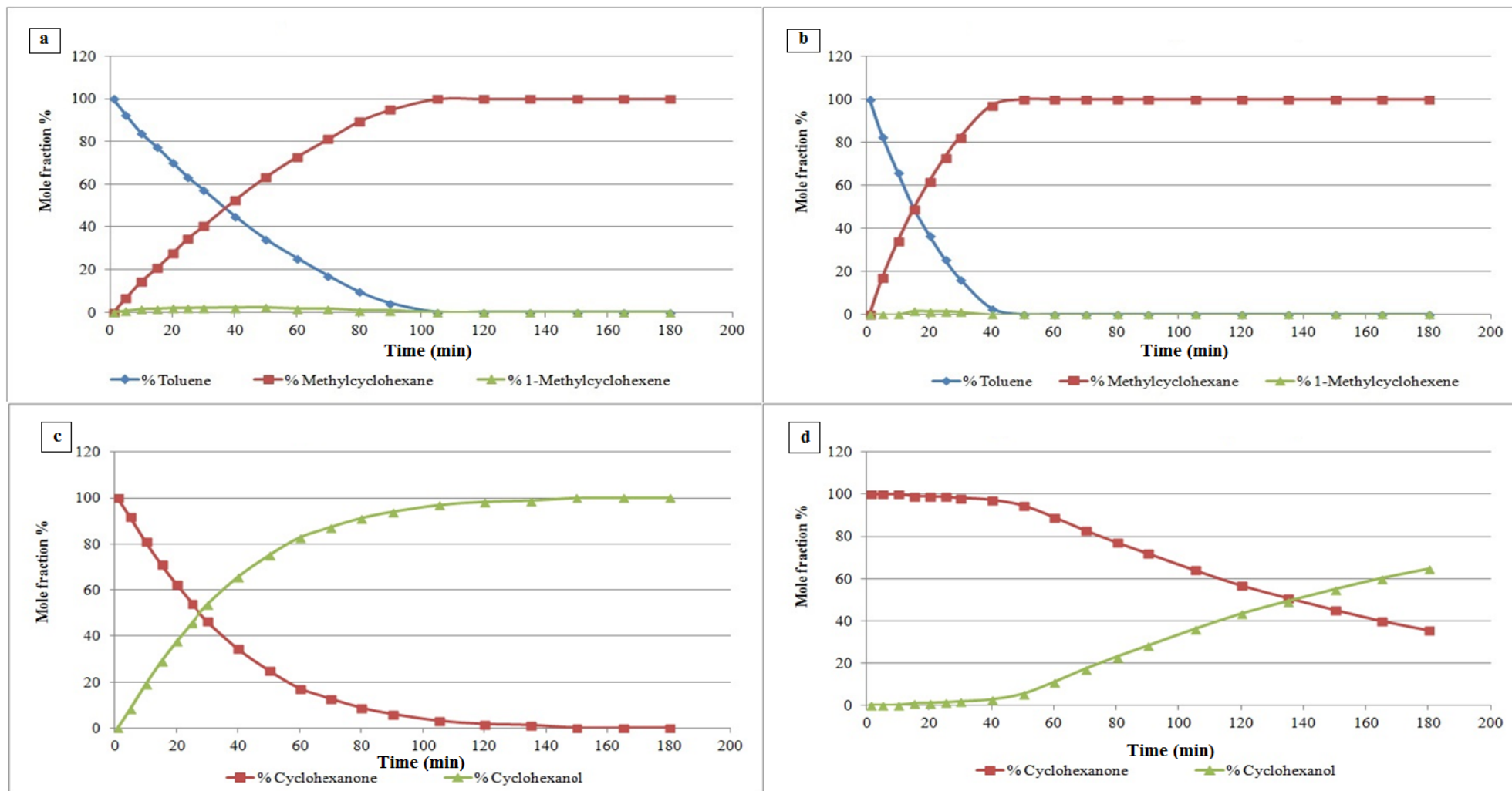


Figure 82. a) Toluene as single substrate and b) with cyclohexanone

c) Cyclohexanone as single substrate and d) with toluene

4.6.2.2 Phenol

Cyclohexanone is a direct product from the hydrogenation of phenol therefore it was difficult to make comparison between single reactions and competitive ones. Hence, conversion of phenol and cyclohexane selectivity were compared separately. Concentration of cyclohexanol was compared in a different graph.

As shown in Figure 83, phenol hydrogenation was enhanced in the presence of cyclohexanone. As a single substrate it was totally consumed after 180 minutes and in the presence of cyclohexanone a 100% phenol conversion was achieved after 120 min. Cyclohexane selectivity was slightly affected by the presence of cyclohexanone.

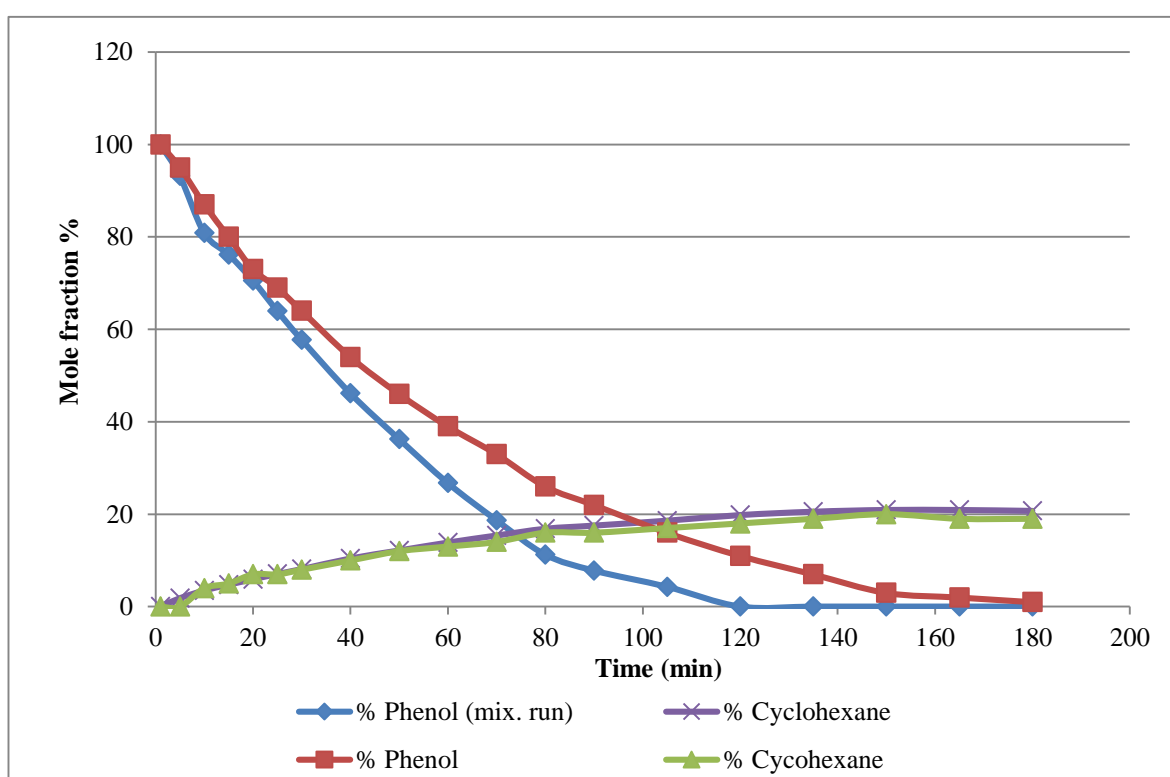


Figure 83. Phenol and cyclohexane comparison in single reaction and after mixed with cyclohexanone

Regarding cyclohexanol concentration, it was increased to more than double in the presence of cyclohexanone as shown in Figure 84.

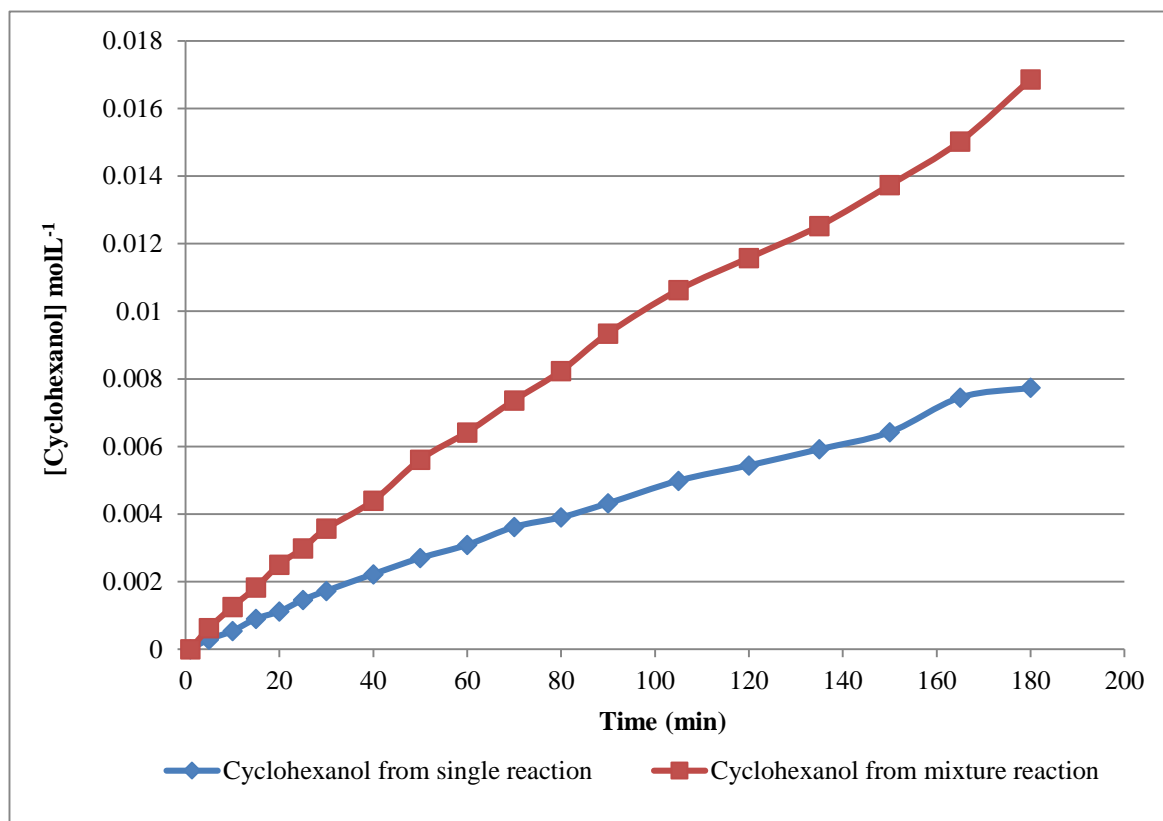


Figure 84. Cyclohexanol concentration from phenol in single reaction and after mixed with cyclohexanone

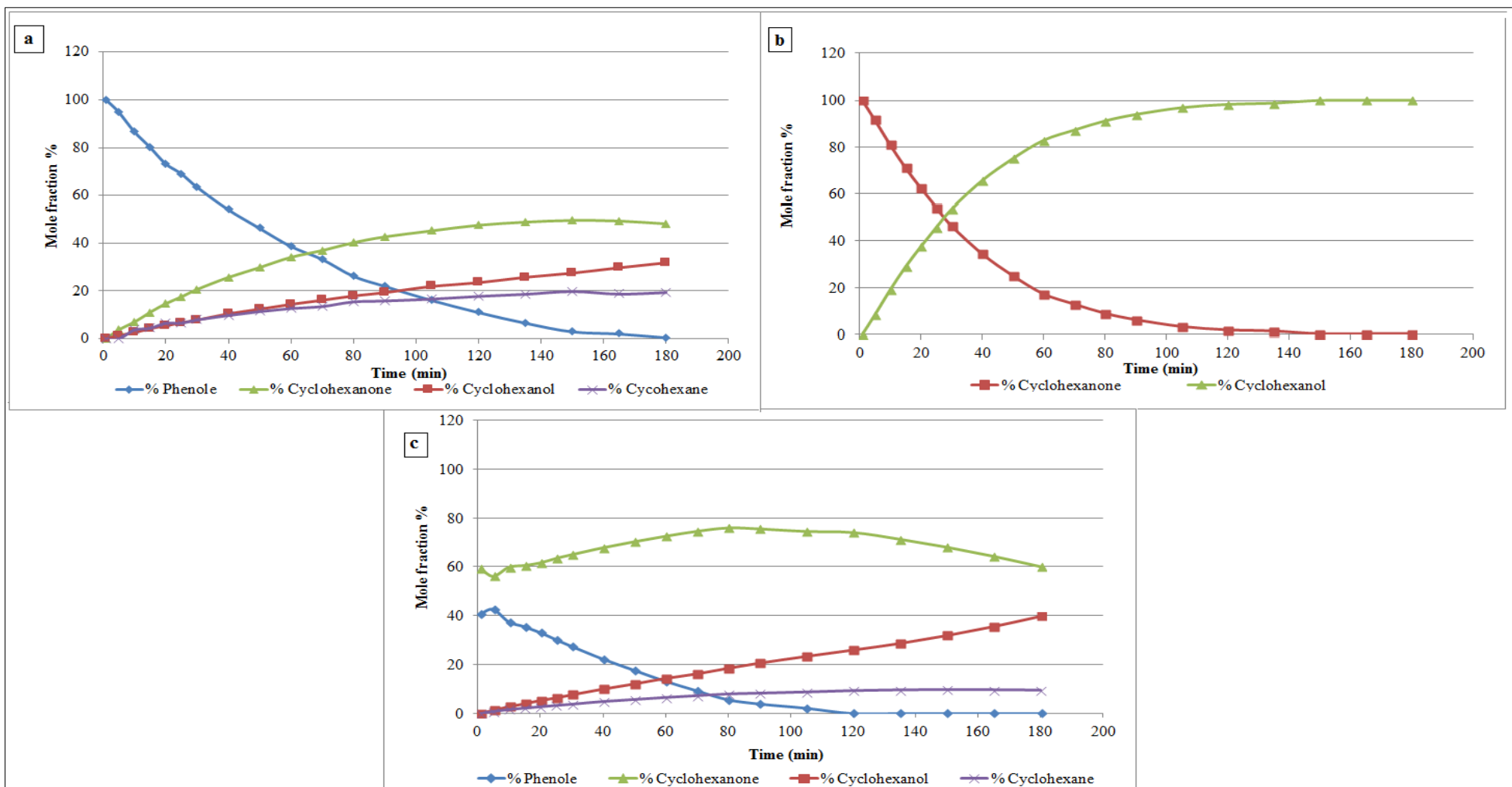


Figure 85. Phenol and cyclohexanone reaction profiles as single substrates a) and b) respectively c) phenol with cyclohexanone

4.6.2.3 Anisole

In this section results were examined as explained in the competitive hydrogenation of phenol with cyclohexanone. Anisole conversion and the selectivity of methoxycyclohexane and cyclohexane were compared separately. The concentration of cyclohexanol was examined in different graph.

As shown in Figure 86, anisole conversion was not affected by the presence of cyclohexanone. There was a slight decrease in cyclohexane formation in the presence of cyclohexanone. In contrast, the formation of methoxycyclohexane increased in the presence of cyclohexanone from about 70% to 85% after 180 min of the reaction.

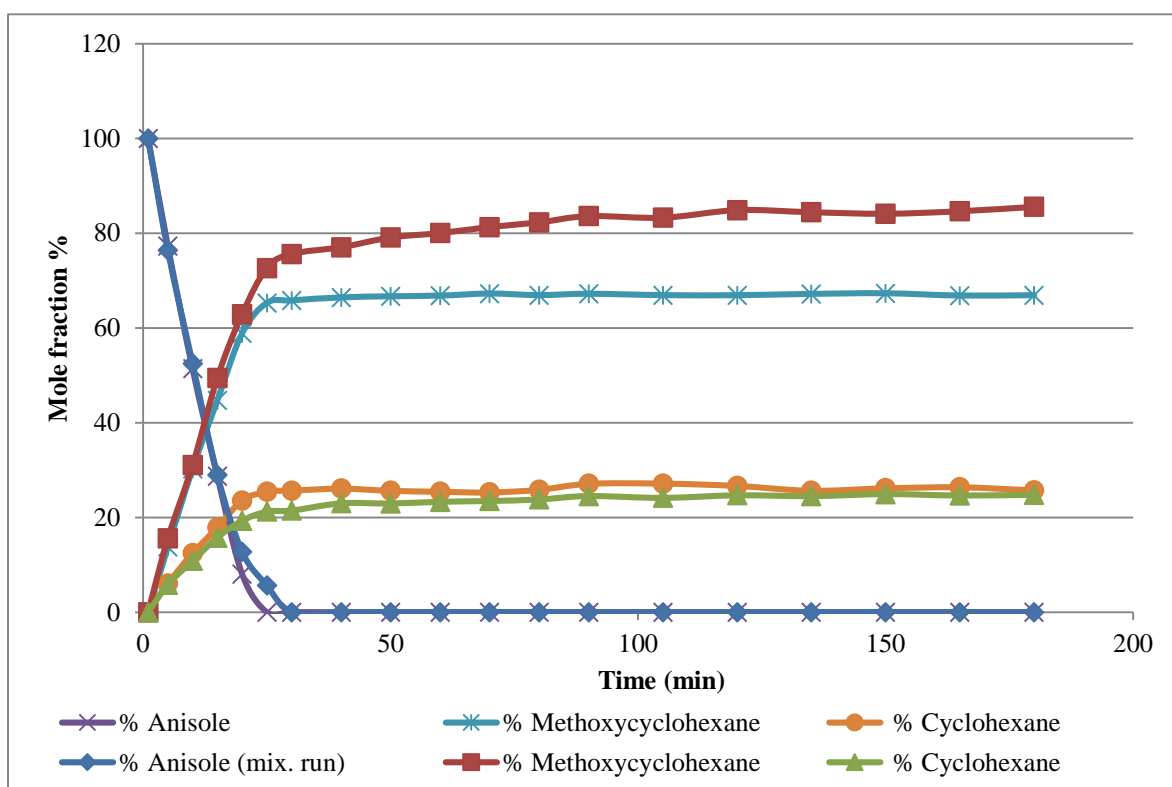


Figure 86. Anisole, methoxycyclohexane and cyclohexane comparison in single reaction and after mixed with cyclohexanone

Cyclohexanol was formed after the total consumption of anisole. Cyclohexanol concentration increased almost to double in the presence of cyclohexanone as shown in Figure 87.

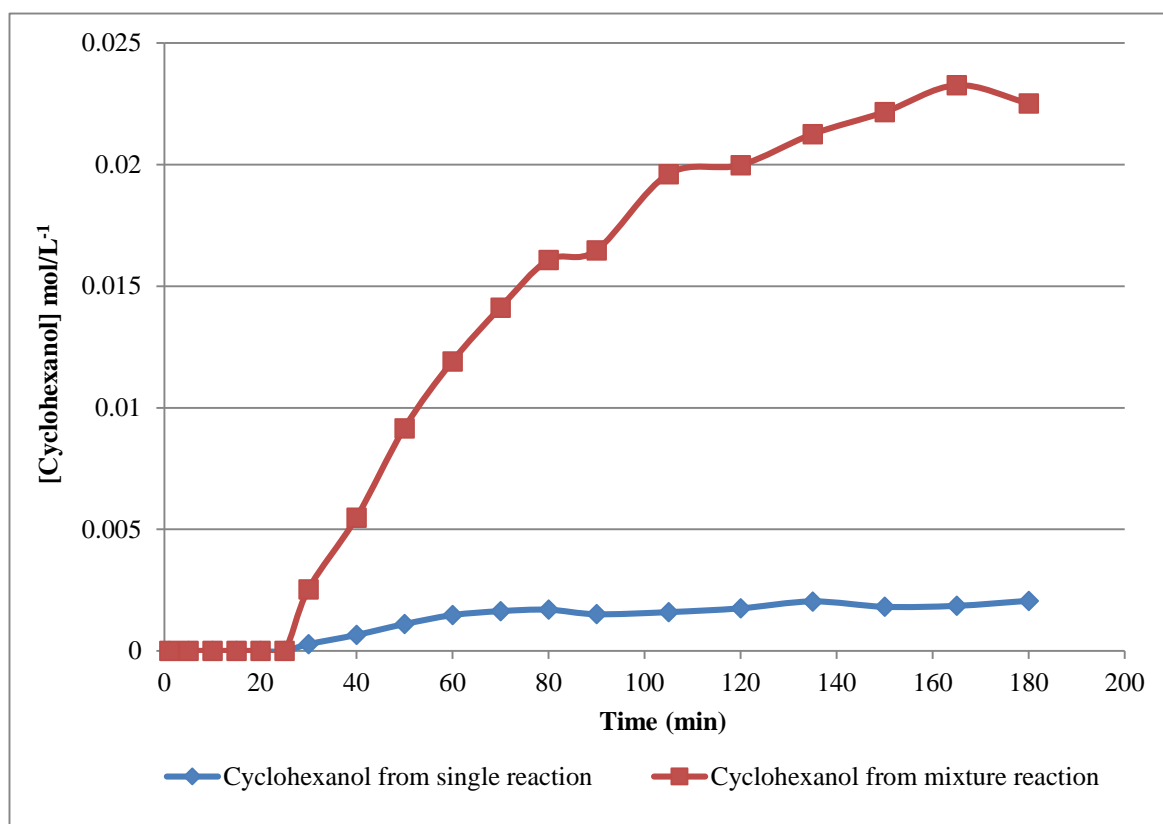


Figure 87. Cyclohexanol concentration from anisole in single reaction and after mixed with cyclohexanone

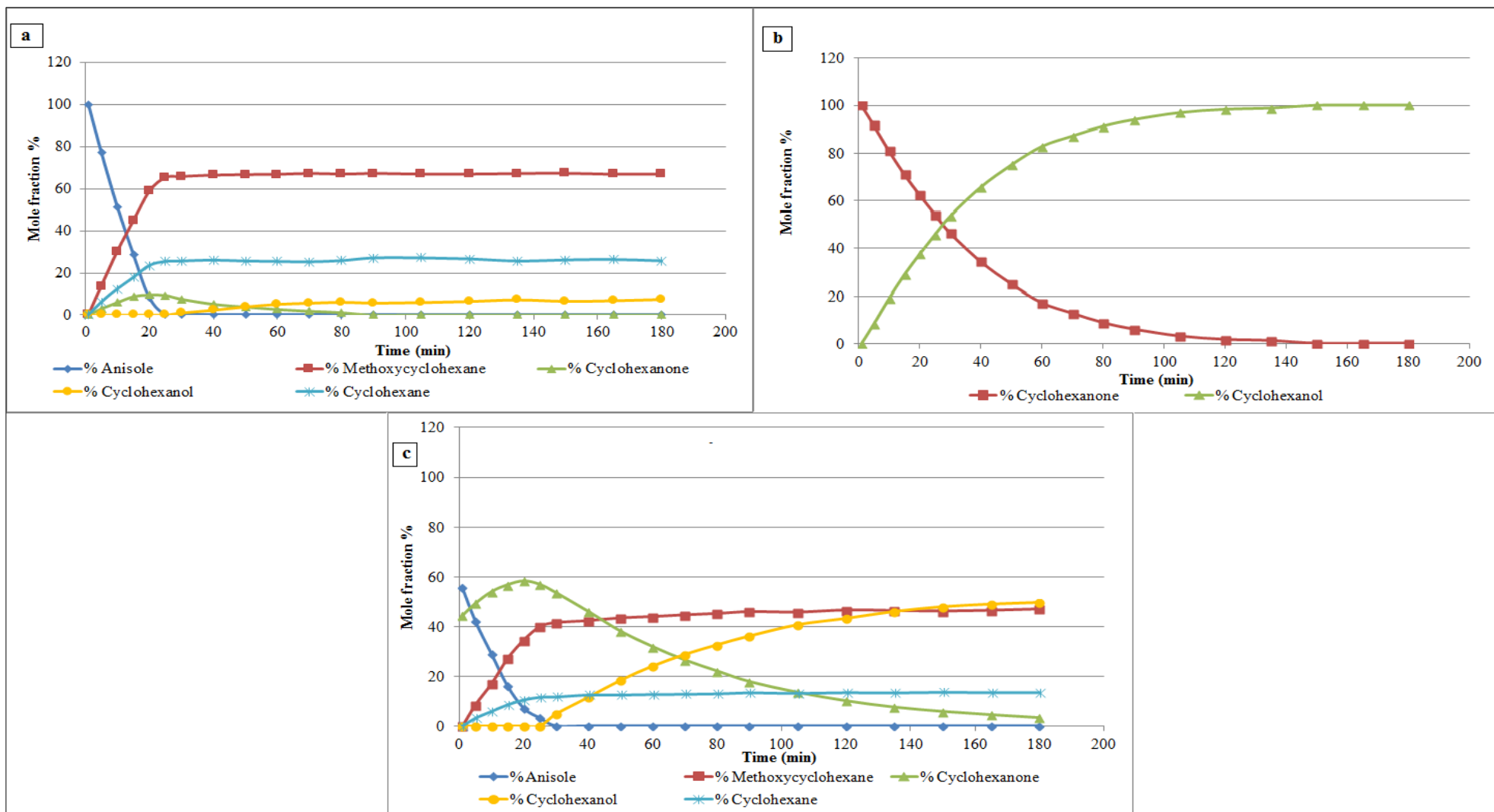


Figure 88. Anisole and cyclohexanone reaction profiles as single substrates a) and b) respectively c) anisole with cyclohexanone

4.7 Competitive hydrogenation of phenol, anisole and methoxyphenol

Another three substrates were tested as mixtures of two and as a mixture of three at the same time. These substrates were phenol, anisole and 4-methoxyphenol. Firstly, the hydrogenation of methoxyphenol as a single substrate will be shown followed by the competitive hydrogenation with phenol and/or anisole.

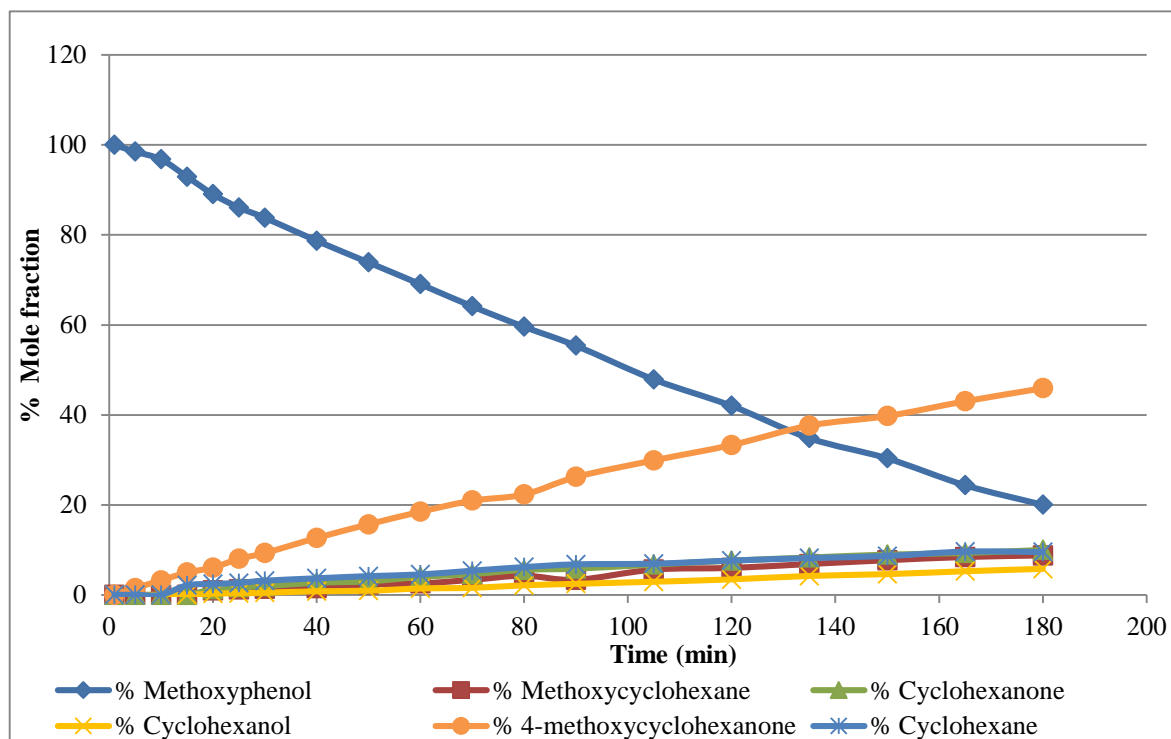


Figure 89. Methoxyphenol reaction profile

Rate of methoxyphenol reaction was relatively slow. The conversion was 80%. Five different products were observed from the hydrogenation of methoxyphenol as a single substrate as shown in Figure 89. They were 4-methoxycyclohexanone, methoxycyclohexane, cyclohexanone, cyclohexanol and cyclohexane. Concentration of 4-methoxyxycylhexanone was about 45% whereas the other products concentrations were less than 10%.

Figure 90 and Figure 91 show the different between conversions for the three substrates as singles and in the competitive hydrogenation respectively. Conversion of the three substrates were decreased where anisole and methoxyphenol were significantly affected. Conversion of anisole decreased from 100% to 60% and methoxyphenol from 80% to about 30% in the competitive hydrogenation. On the hand phenol conversion was slightly affected, it decreased from 100% to about 75%.

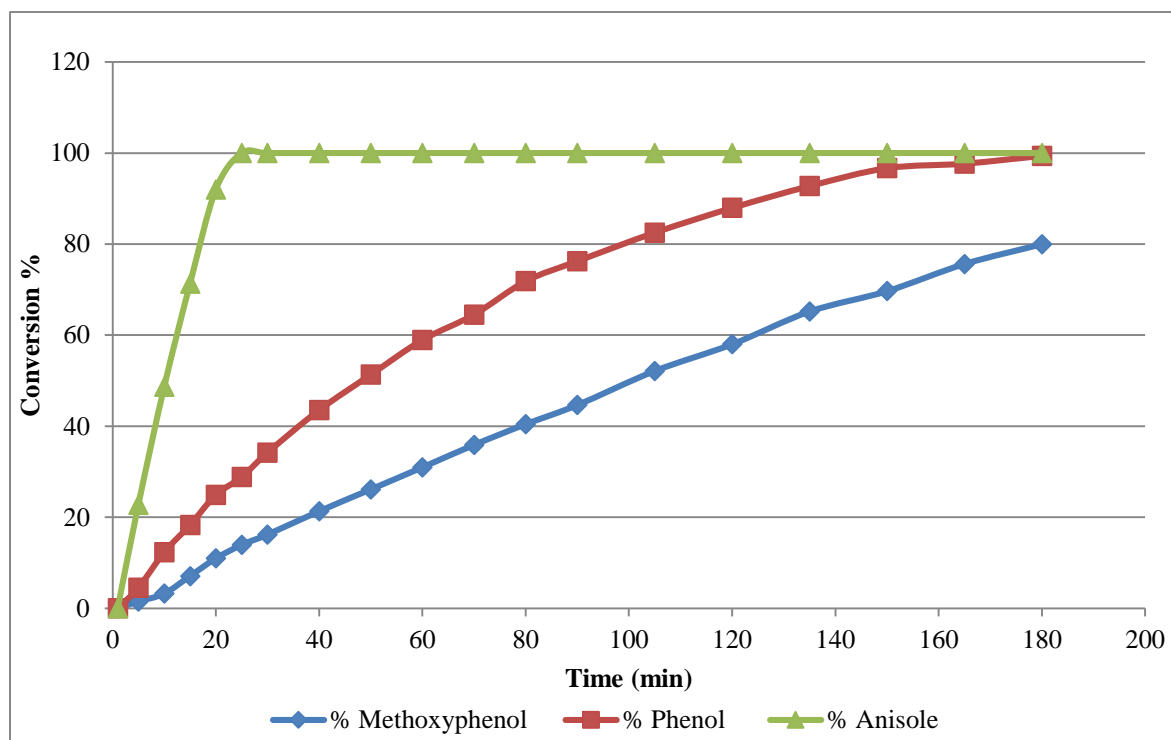


Figure 90. Single substrates conversion

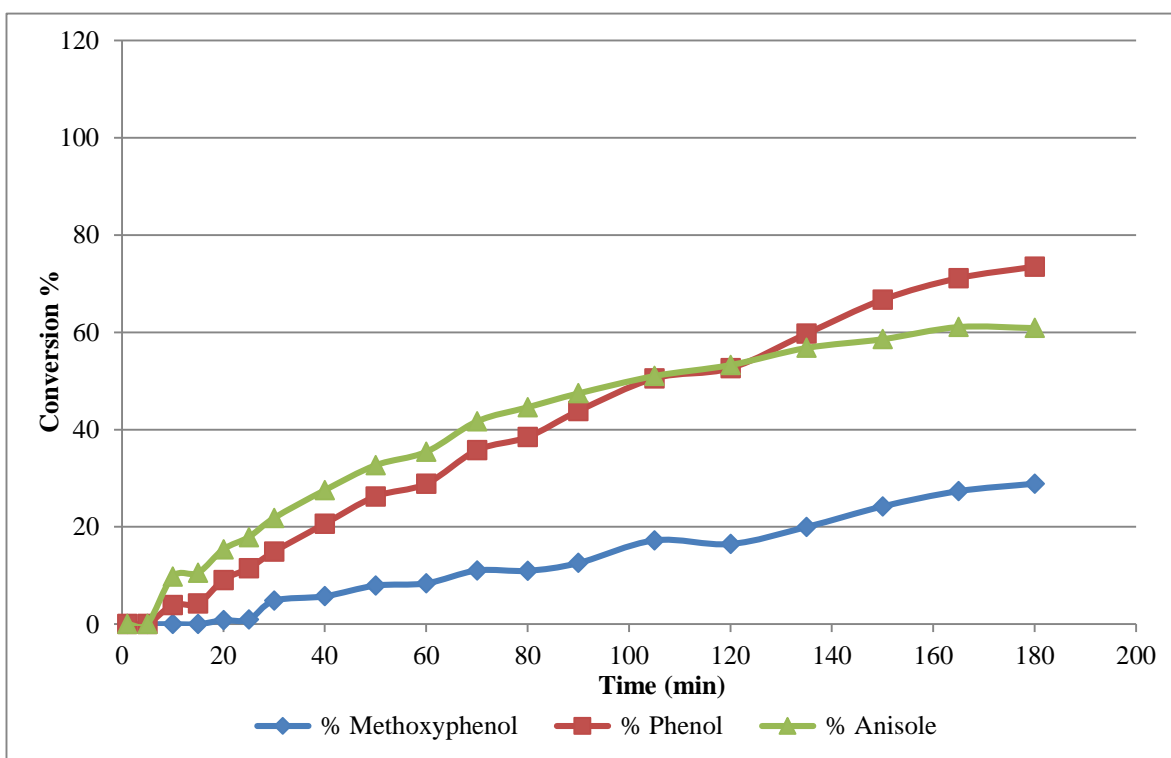


Figure 91. Mixture of three substrates conversion

It is worth mentioning that it was difficult to differentiate between some of the products during the competitive hydrogenations because the three substrates will produce cyclohexanone, cyclohexanol and cyclohexane as common products. However, noticeable observations for each substrate will be described.

4.7.1 Methoxyphenol

As single substrate and as stated earlier, reaction was relatively slow. Conversion was 80%. Five different products were observed (4-methoxycyclohexanone, methoxycyclohexane, cyclohexanone, cyclohexanol and cyclohexane) and concentration of 4-methoxycyclohexanone, which form directly, was about 45% (Figure 89).

In the presence of phenol, methoxycyclohexane and cyclohexane were not observed. As for 4-methoxycyclohexanone, which is formed directly from the hydrogenation of methoxyphenol, it was not observed for the first 10 min which might indicate a slight decrease in the rate.

In the presence of anisole, methoxyphenol was completely consumed after 180 min as shown in Figure 92. Both of substrates produce methoxycyclohexane in addition to cyclohexanone, cyclohexanol and cyclohexane. As for 4-methoxycyclohexanone, it was only observed after 25 min which suggests lower activity in the presence of anisole.

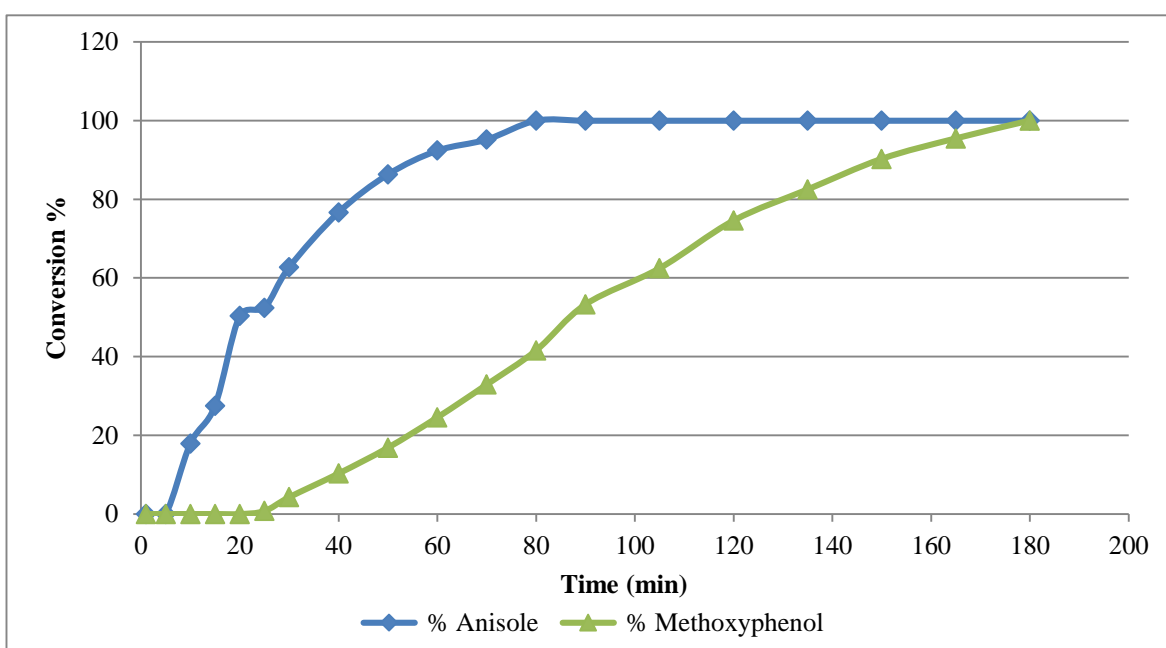


Figure 92. Conversion of anisole and methoxyphenol in the complete hydrogenation

In the mixture of three substrates, methoxyphenol conversion was decreased from 80% to about 30%. In addition, cyclohexanol was not observed and 4-methoxycyclohexanone was detected after 30 min.

4.7.2 Phenol

In the presence of methoxyphenol, cyclohexane was not observed. The rate of phenol hydrogenation and conversion was not affected by the presence of methoxyphenol.

In the presence of anisole and as explained earlier, conversion of phenol decreased to around 75% and cyclohexanol was not observed.

In the mixture with methoxyphenol and anisole, the rate of phenol reaction was slightly decreased and the conversion decreased to about 80%. In the hydrogenation of phenol competitively with methoxyphenol and anisole, cyclohexane was not observed.

4.7.3 Anisole

Anisole was affected slightly by the presence of methoxyphenol. The conversion was 100% after 80 min it was completed after 25 min in the hydrogenation of anisole as a single substrate.

In the presence of phenol, the rate of reaction was slower and the conversion decreased to 70% and cyclohexanol was not observed.

In the mixture with phenol and methoxyphenol, conversion of anisole decreased to about 60% and cyclohexanol was not detected.

Competitive hydrogenation of methoxyphenol, phenol and anisole is shown in Figure 93. In this graph, substrates were divided into three groups each group starts with a red column.

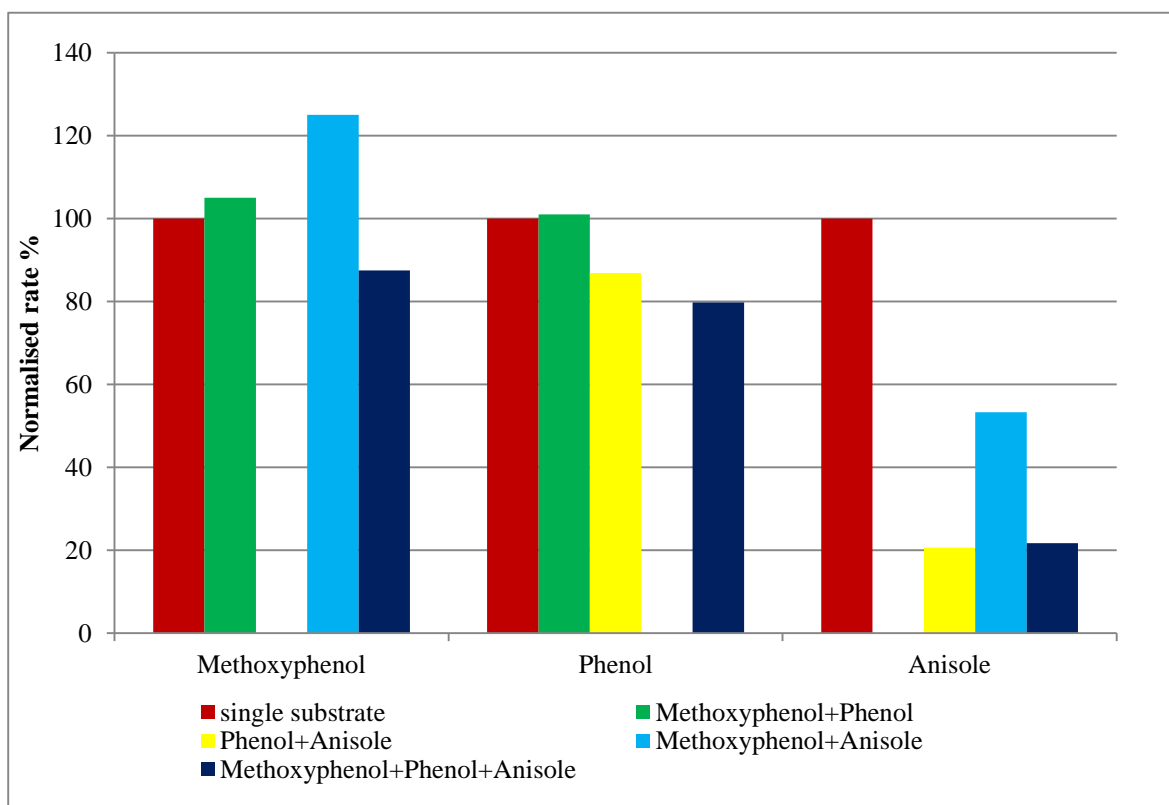


Figure 93. Competitive hydrogenation of methoxyphenol, phenol and anisole

The red columns represent the single substrates which were set to a 100 and the others were normalised against them to allow comparison with other results. Taking into consideration that anisole results were compared after 20 min of reaction. In the first group, the rate of methoxyphenol hydrogenation increased to over 120% in the presence of anisole. On the other hand, it decreased to less than 40% in the mixture of three substrates.

Anisole rate decreased to 50% in the presence of methoxyphenol. Moreover, the anisole rate decreased to 20% in the presence of phenol and in the mixture of three substrates. Phenol was the least affected by the presence of anisole and methoxyphenol. The rate of phenol decreased to about 80% in the presence of anisole and to about 75% in the mixture of the three substrates.

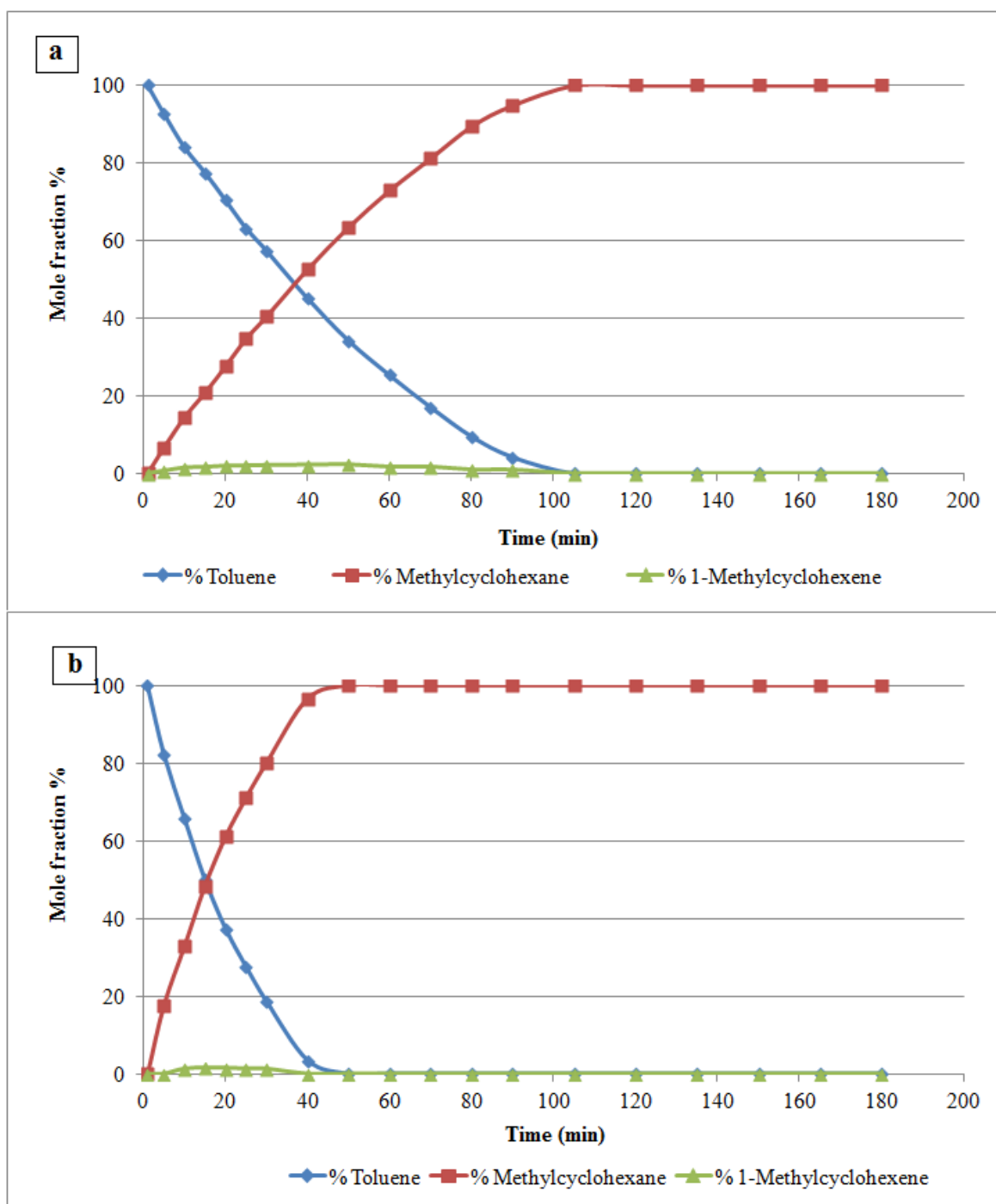
4.8 Hydrogen-deuterium exchange reactions

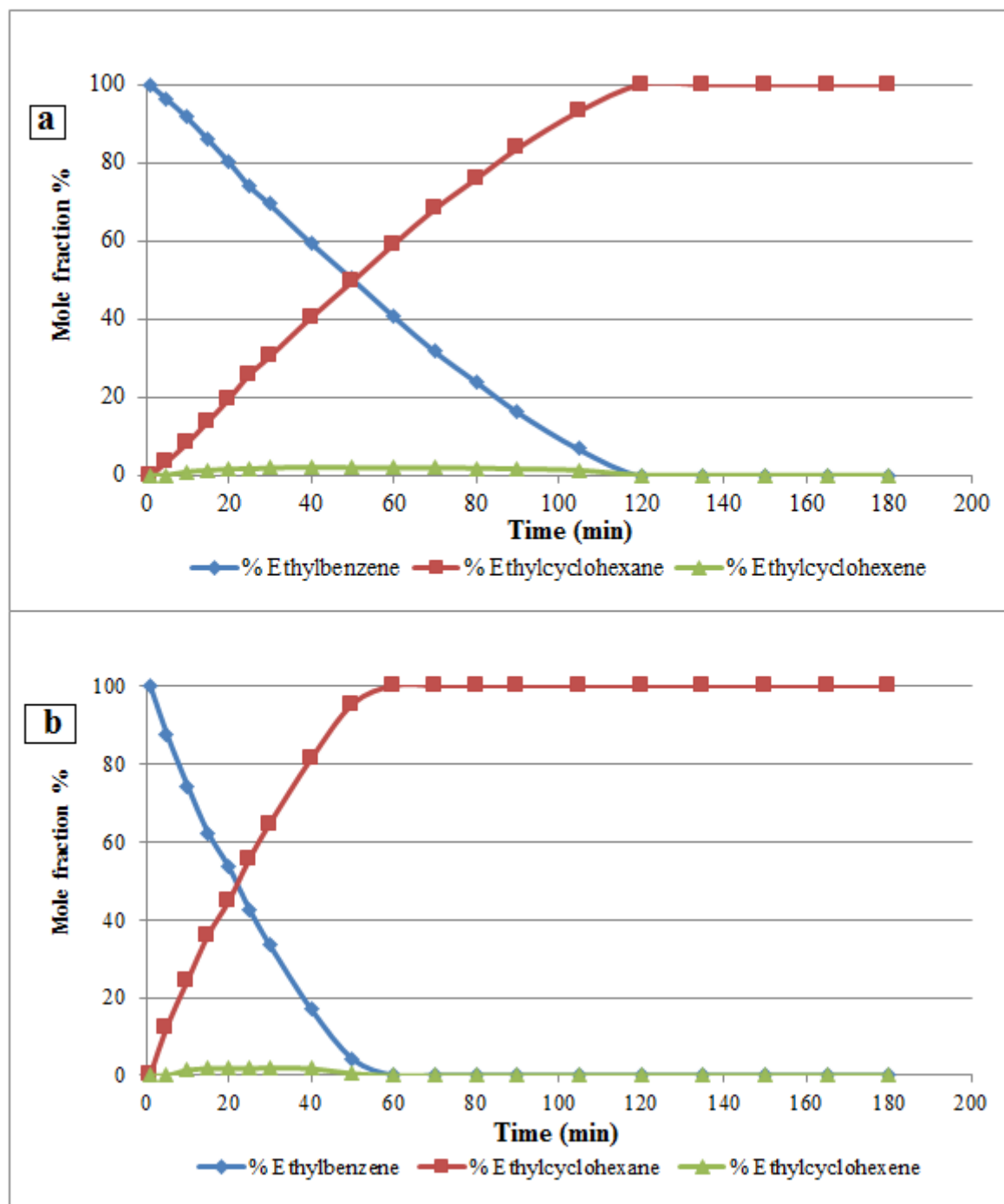
In this set of reactions, deuterium was used instead of hydrogen in the reduction reactions. Rate constant comparison is important in these reactions as this can give mechanistic insight. Comparing the values of rate constants for reaction with deuterium with reactions with hydrogen (k_H/k_D) will give indication of the type and size of KIE on the hydrogenation reaction.

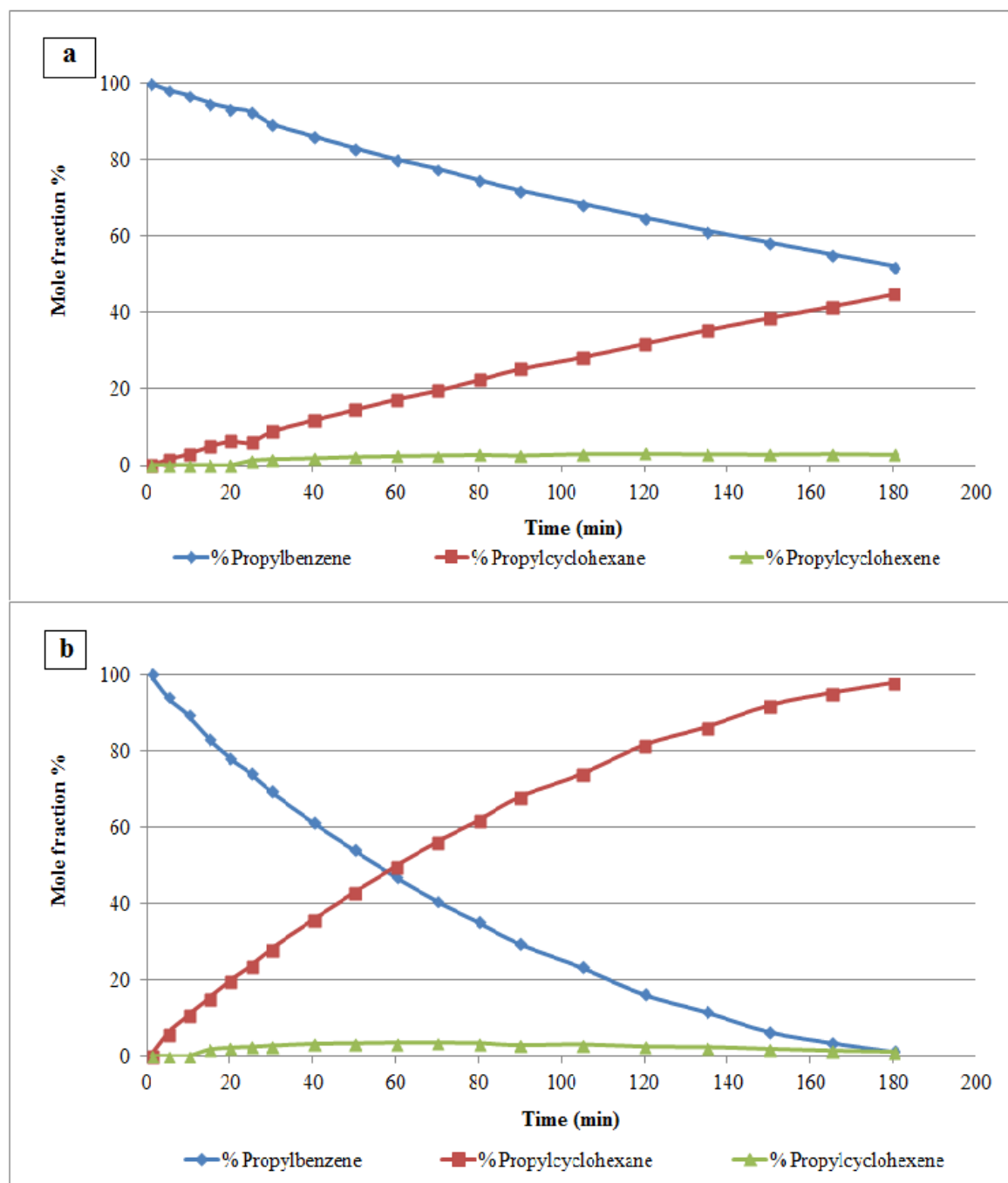
For the three alkylbenzenes (toluene, ethylbenzene and n-propylbenzene) the rate constant of the reaction with hydrogen over the rate constant with deuterium is less than 1, which means that the deuterium reaction is faster than reaction with hydrogen. That indicates an inverse KIE as shown in Figure 94, Figure 95 and Figure 96. The same effect can be seen for deuterium reacting with 4-methoxyphenol, Figure 97. Values of k_H/k_D are presented in Table 33.

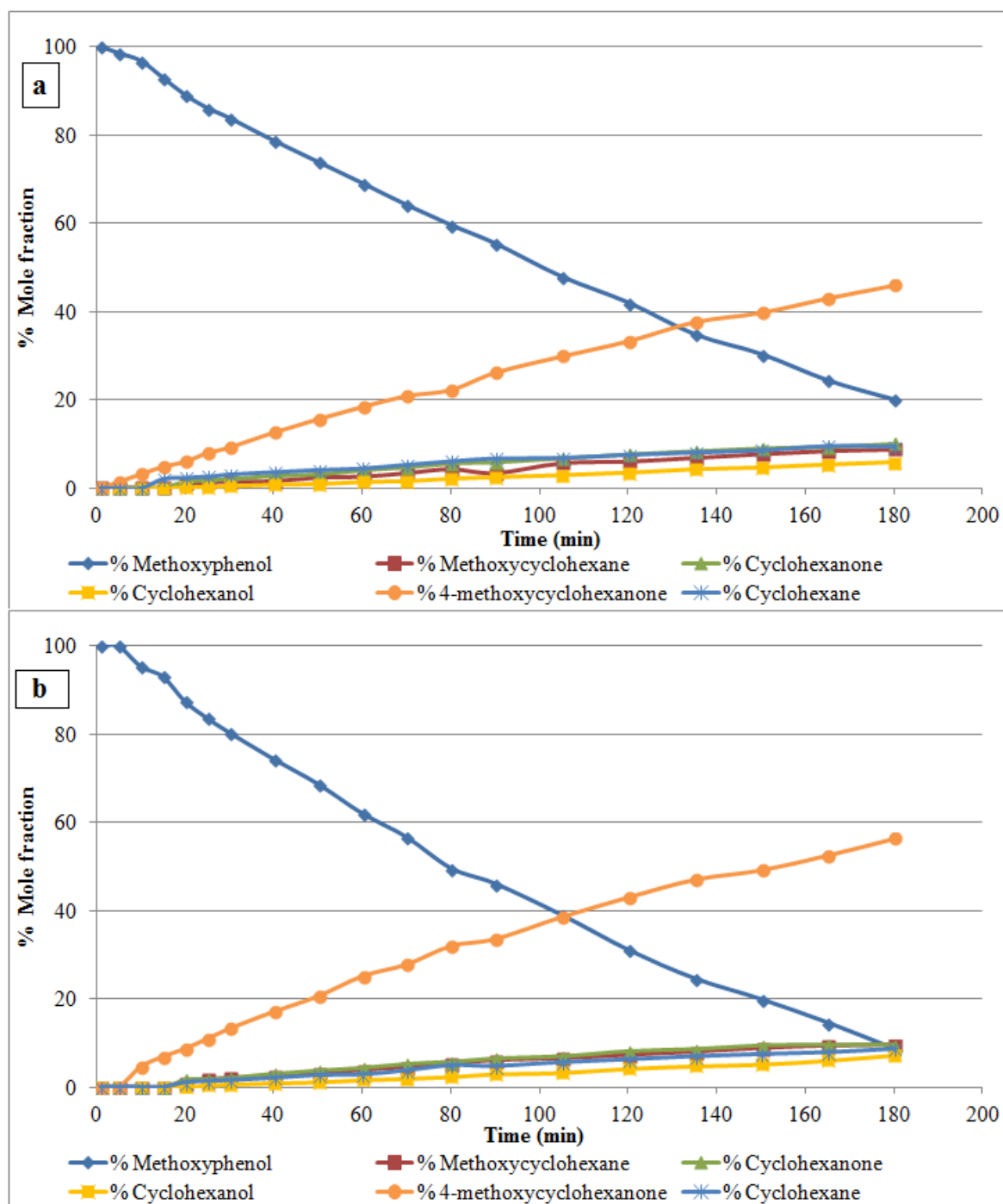
Table 33. KIE for different substrates

Reactant	k_H	k_D	k_H/k_D
Toluene	1.44	2.54	0.57
Ethylbenzene	1.1	2.14	0.51
N-propylbenzene	0.33	0.85	0.39
4-Methoxyphenol	0.38	0.81	0.47
Phenol	1.16	0.76	1.53
Anisole	4.68	3.84	1.22

Figure 94. Toluene hydrogenation with a) H₂ and b) D₂

Figure 95. Ethylbenzene hydrogenation a) H₂ and b) D₂

Figure 96. n-Propylbenzene hydrogenation a) H₂ and b) D₂

Figure 97. 4-Methoxyphenol hydrogenation a) H₂ and b) D₂

In contrast, k_H/k_D for phenol and anisole are greater than 1 which indicates a normal KIE as shown in Figure 98 and Figure 99. Table 33 summarises k_H/k_D values for all substrates that were used in this project.

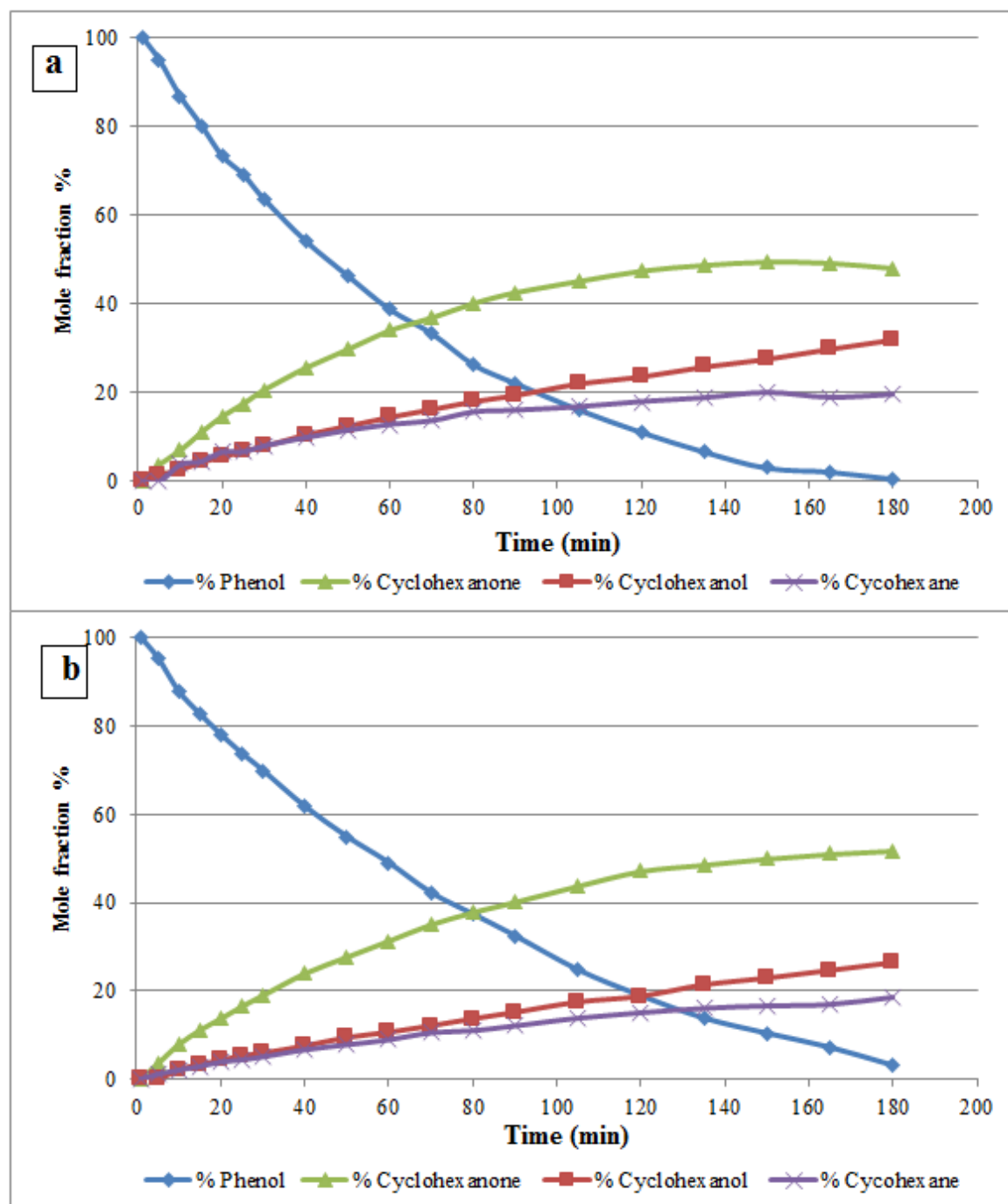


Figure 98. Phenol hydrogenation with a) H₂ and b) D₂

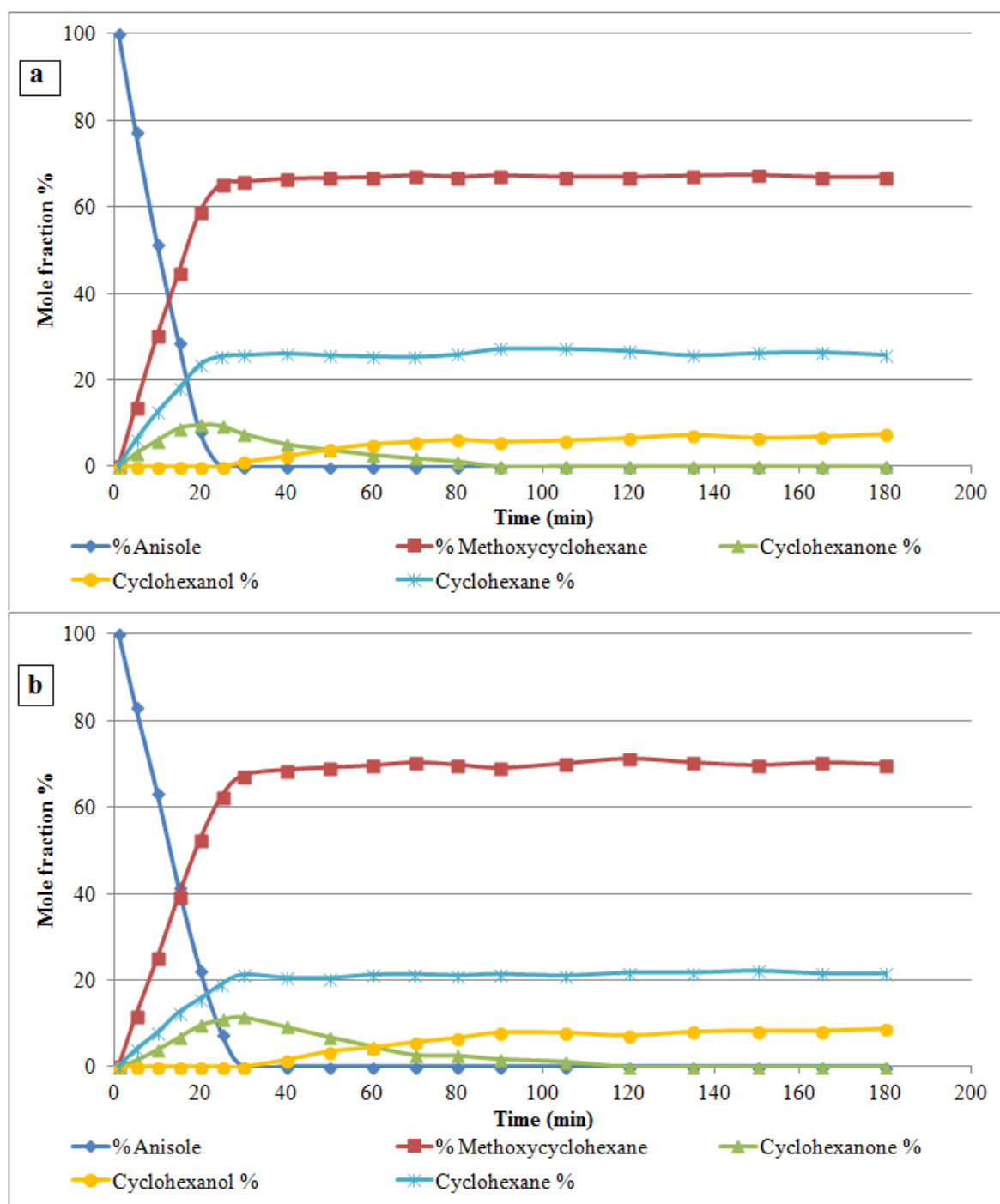
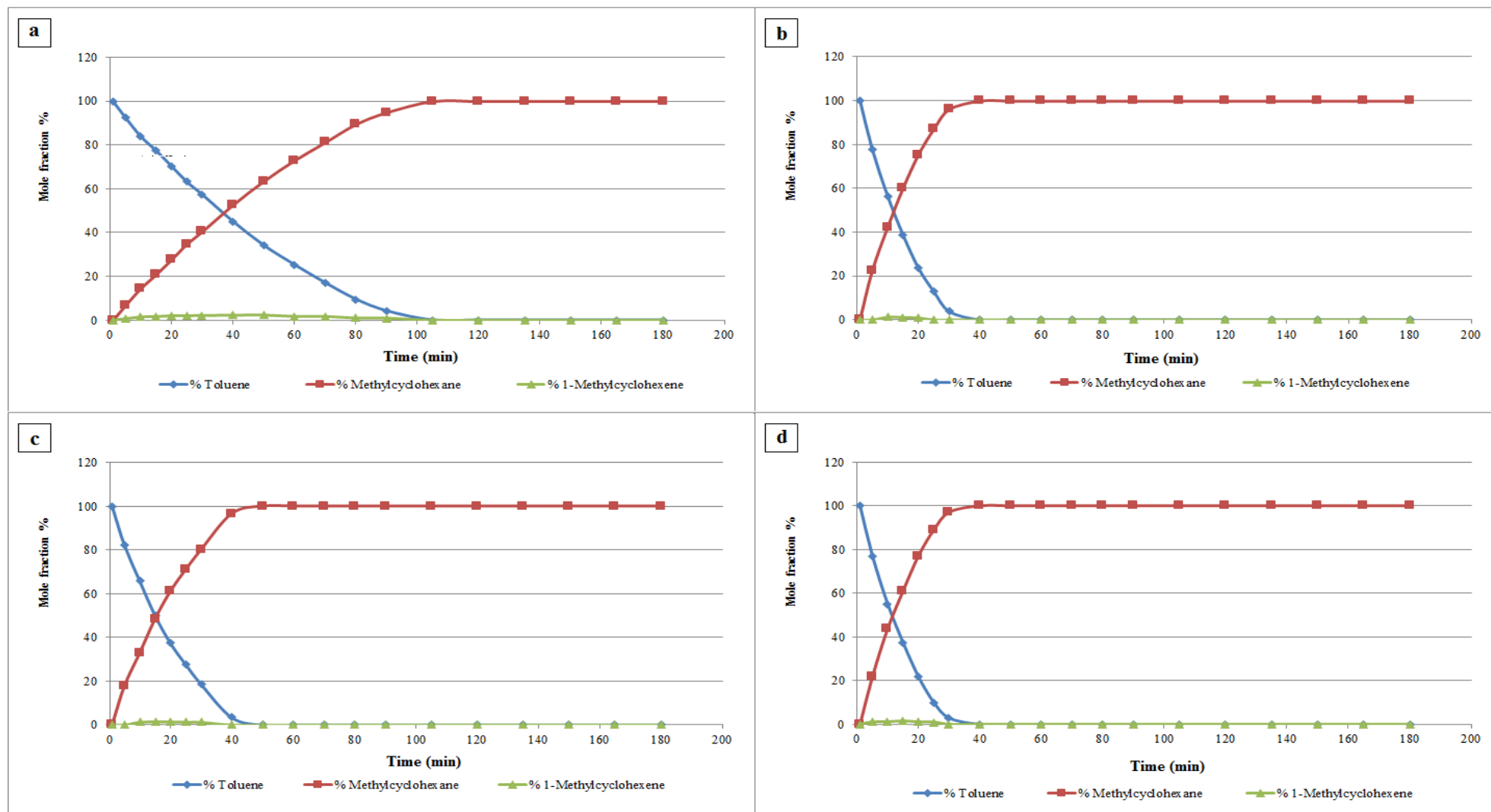


Figure 99. Anisole hydrogenation with a) H₂ and b) D₂

Figure 100 shows four reaction profiles. Reaction a) is toluene hydrogenation under hydrogen pressure. This reaction was compared with b) toluene d₈ + H₂, c) toluene + D₂ and d) toluene d₈ + D₂. Reactions b, c and d were faster than reaction a, which agrees with the suggestion of inverse KIE in all reactions involving deuterium and deuterated toluene.

Figure 100. Reaction profiles for a) toluene + H₂, b) toluene d8 + H₂, c) toluene + D₂ and d) toluene d8+ D₂

4.8.1 NMR results

A number of samples were collected from toluene and deuterated toluene reactions with deuterium and hydrogen to observe and analyse the behaviour of deuterium and hydrogen during reactions. Three samples were taken from toluene and deuterium reaction. The first one was collected at the beginning of the reaction and the others were taken after 60 and 180 min. Another sample was taken from the reaction of deuterated toluene with hydrogen after 10 min. last sample was a reference sample of deuterated toluene. Reactions parameters were set at 50 °C, 1 mL reactant and under 3 barg pressure. The spectra are shown in Figure 101 - Figure 108.

The samples are summarised in the following table:

Table 34 NMR tests on selected samples

Samples	Reaction	Test performed
Sample 1	Toluene + D ₂ at t = 0	¹ H NMR + ² H NMR
Sample 2	Toluene + D ₂ at t = 60	¹ H NMR + ² H NMR
Sample 3	Toluene + D ₂ at t = 180	² H NMR
Sample 4	d ₈ -toluene + H ₂ at t=10	¹ H NMR + ² H NMR
Sample 5	d ₈ -toluene (reference)	² H NMR

A number of points can be concluded from NMR spectra. Figure 101 shows the proton NMR of a sample from the toluene and deuterium reaction at time zero. The main peaks at 1.1 ppm, 3.8 ppm and 5 ppm are due to the solvent (IPA) and are from CH₃, CH, and OH respectively. Figure 102 shows the equivalent ²H NMR, where no solvent peaks can be seen but a spectrum of d₈-toluene can be observed (c.f. Figure 108, CD₃ at 2.7 ppm and aromatic CD at ~ 7.6 ppm). Both aromatic and aliphatic hydrogen atoms have exchanged.

Figure 106 shows the ²H NMR spectrum of the d₈-toluene reaction with hydrogen after 10 min. As well as the d₈-toluene, peaks at 5.8 ppm and 1.3 ppm suggest that the IPA has also exchanged some hydrogen for deuterium. The other bands are likely due to methylcyclohexane.

Figure 107 (sample 4) shows a small peak in the aromatic region in the proton spectra at around 7 ppm, which could be due to protiated toluene but this is unlikely as there is no peak at around 2.3 ppm for the methyl group.

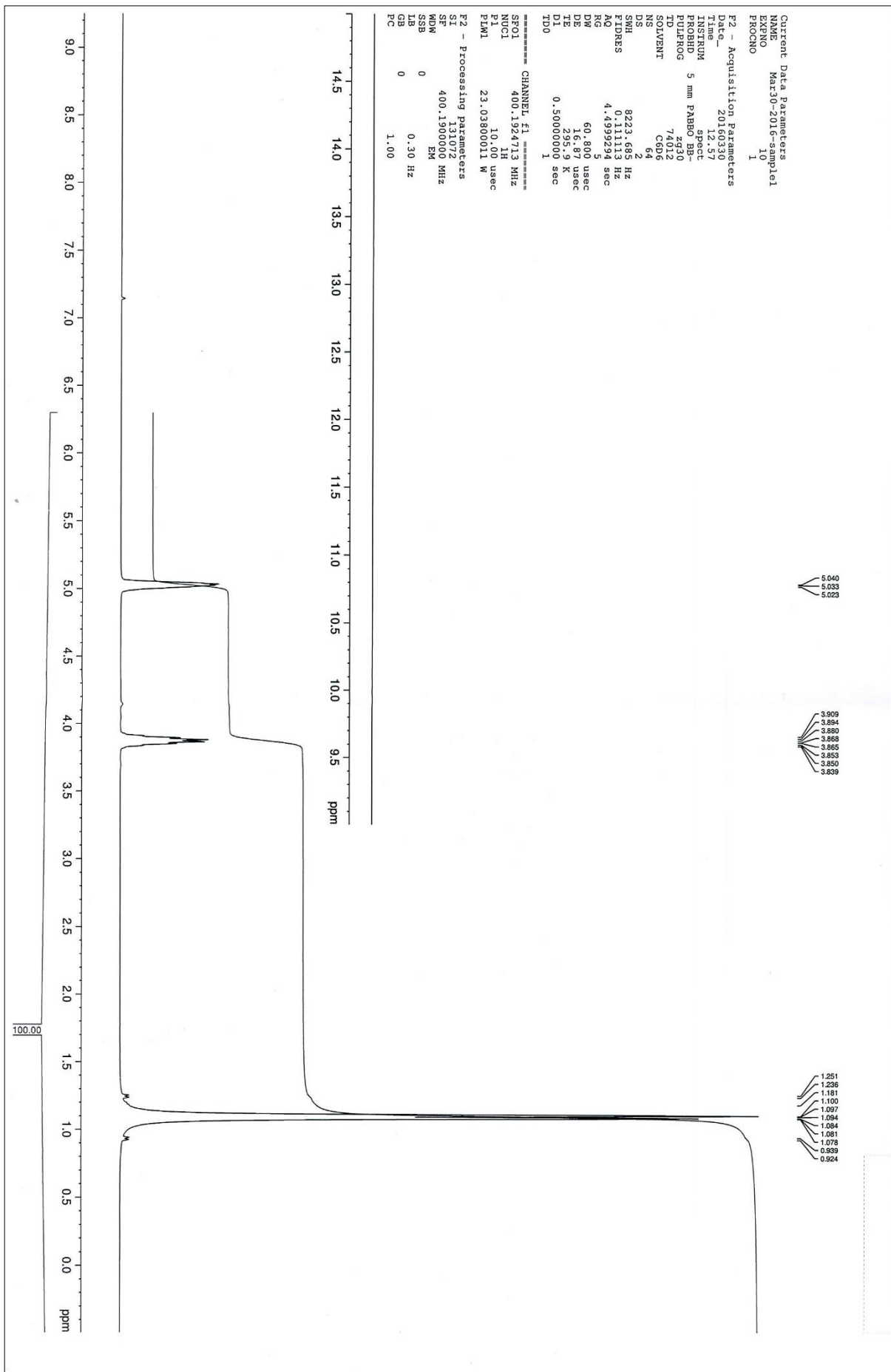
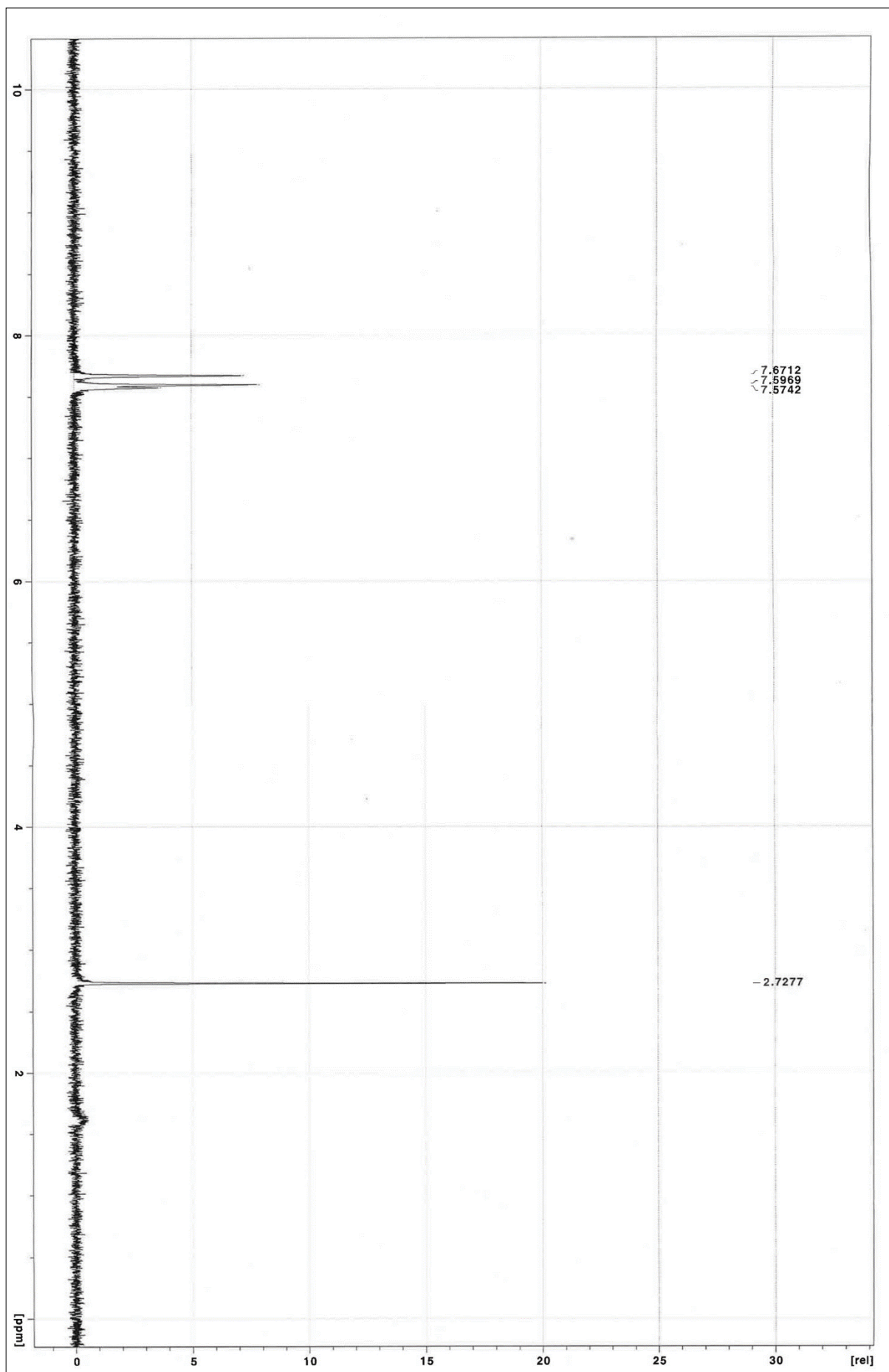
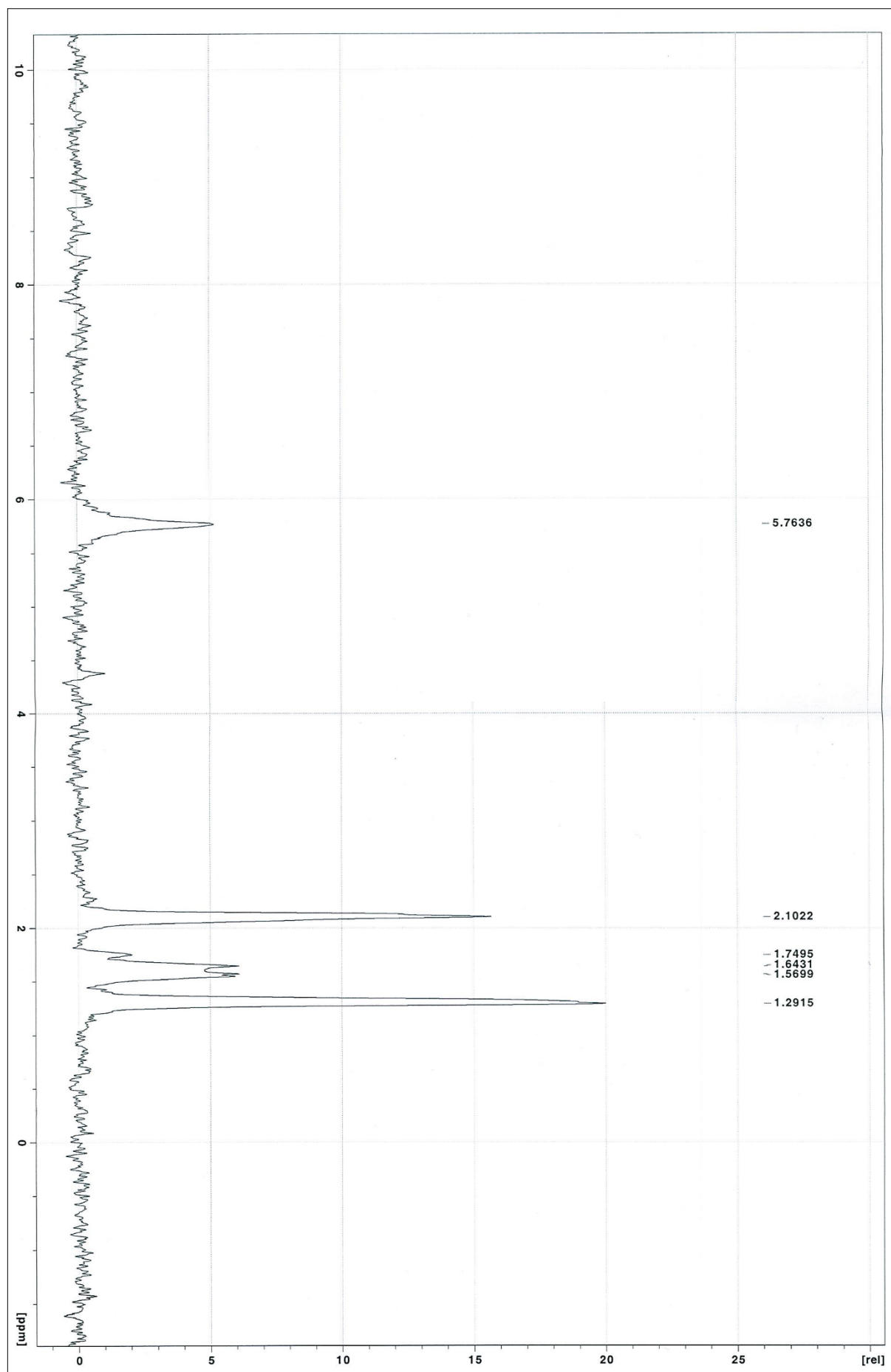


Figure 101. Sample 1, ¹H NMR spectrum

Figure 102. Sample 1, ^2H NMR spectrum

Figure 103. Sample 2, ^2H NMR spectrum

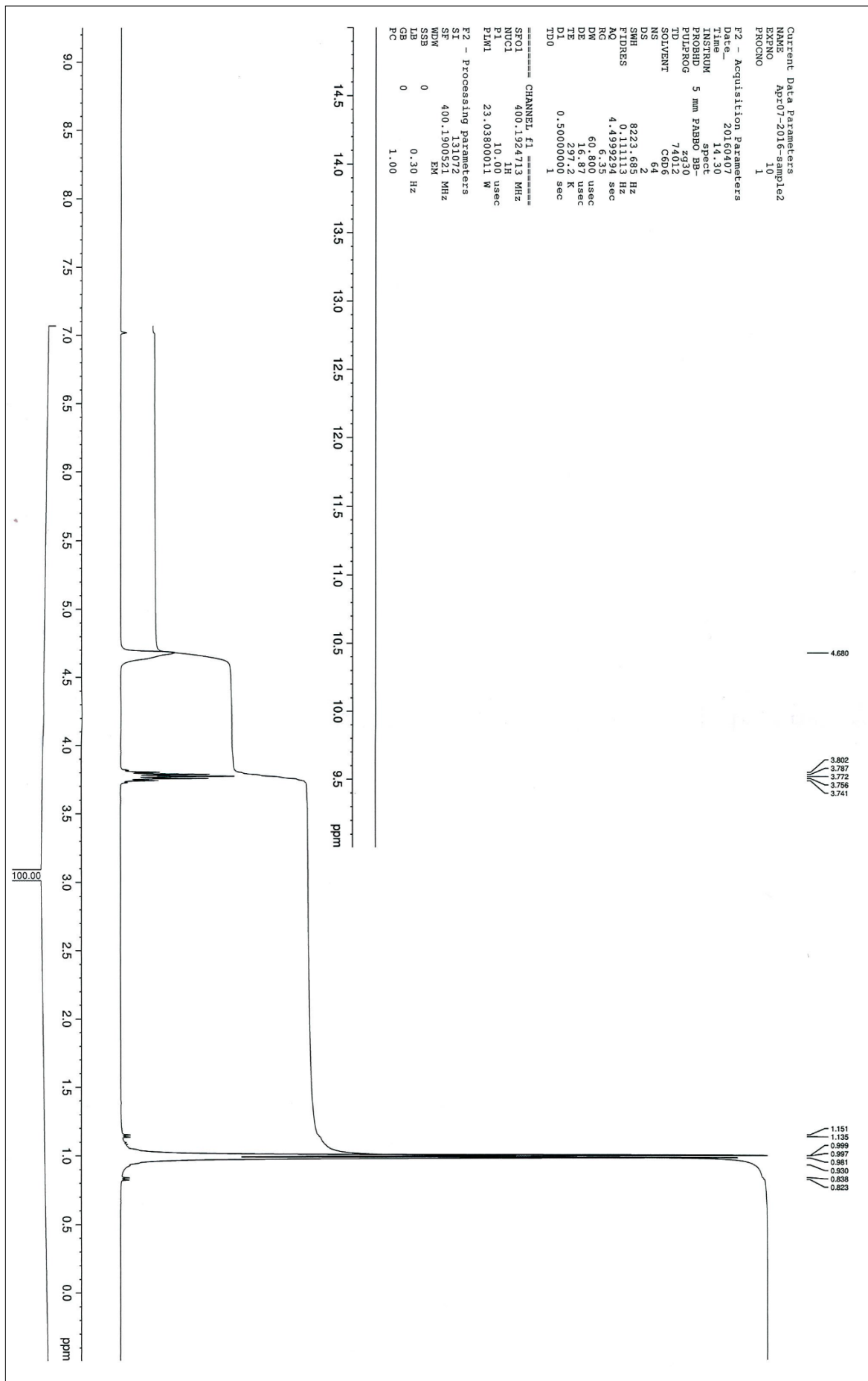
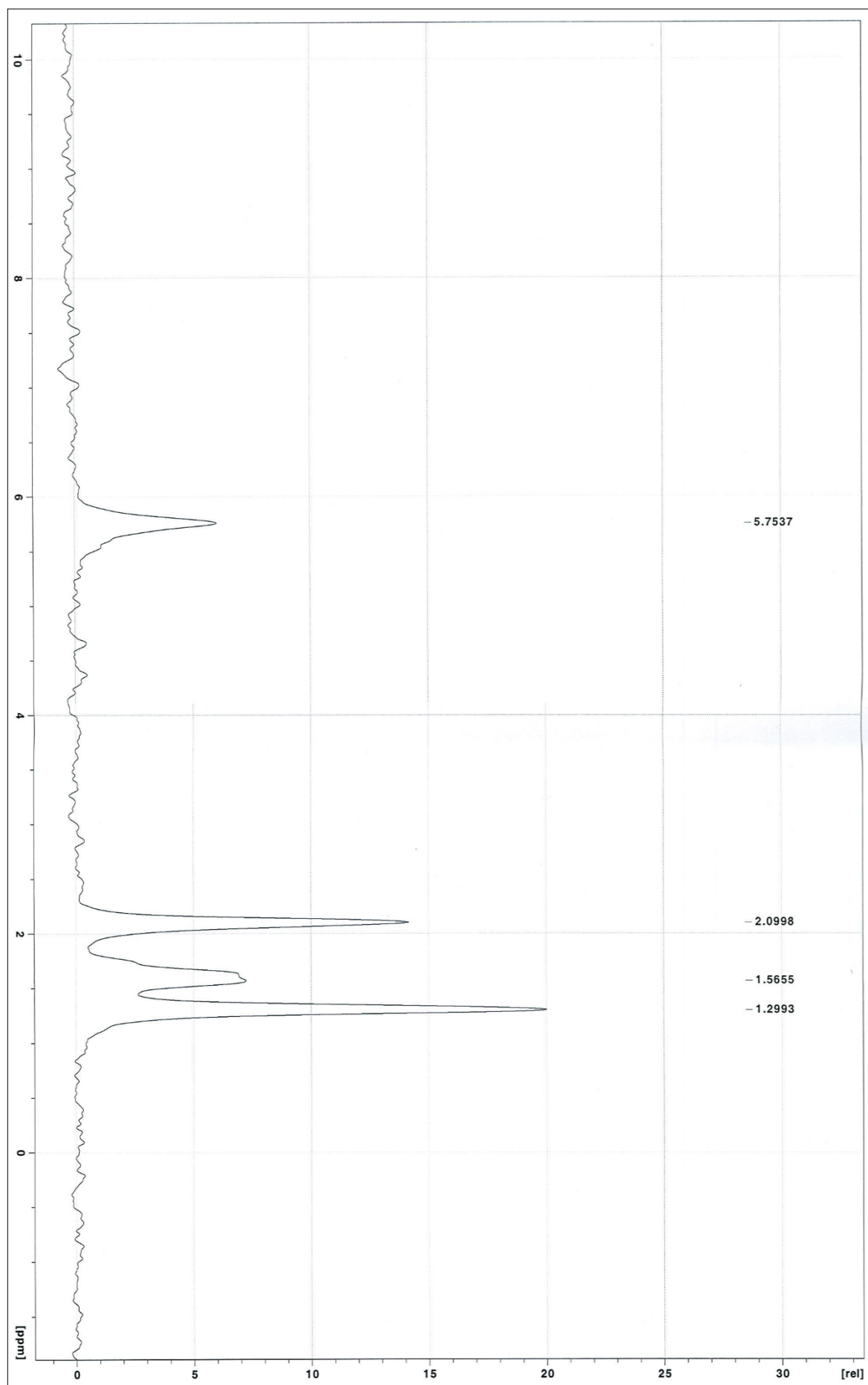
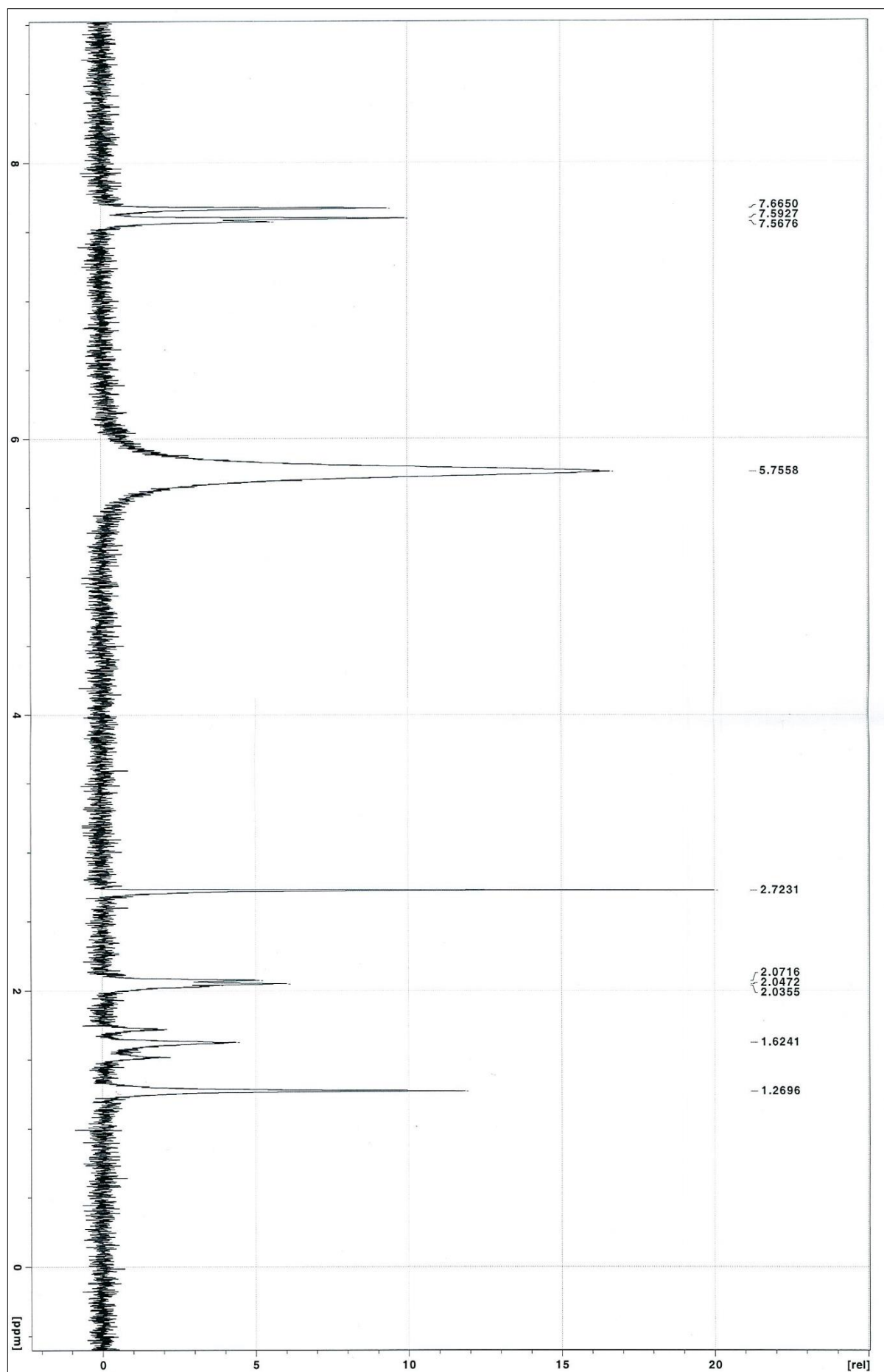


Figure 104. Sample 2, ¹H NMR spectrum

Figure 105. Sample 3, ^2H NMR spectrum

Figure 106. Sample 4, ^2H NMR spectrum

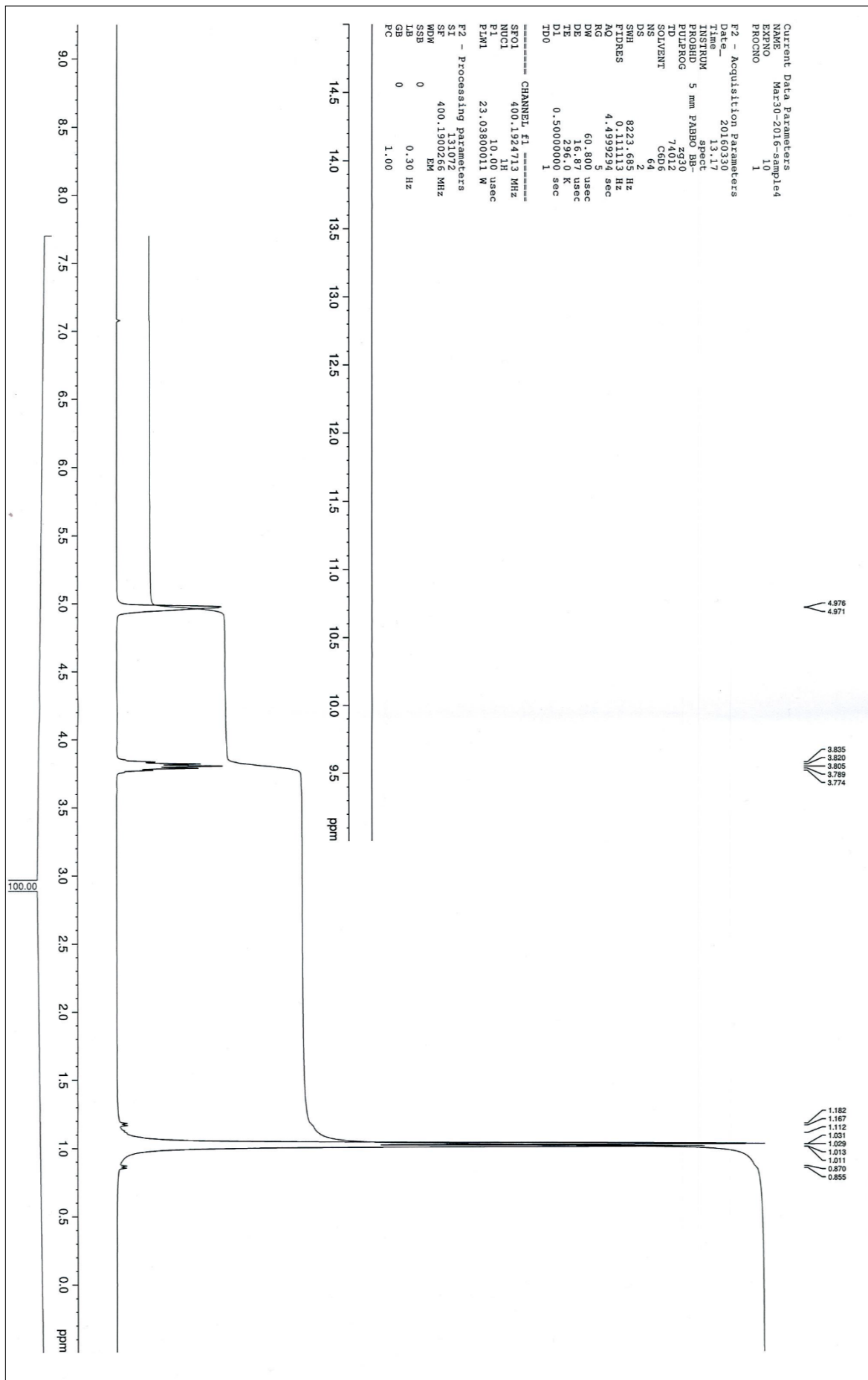
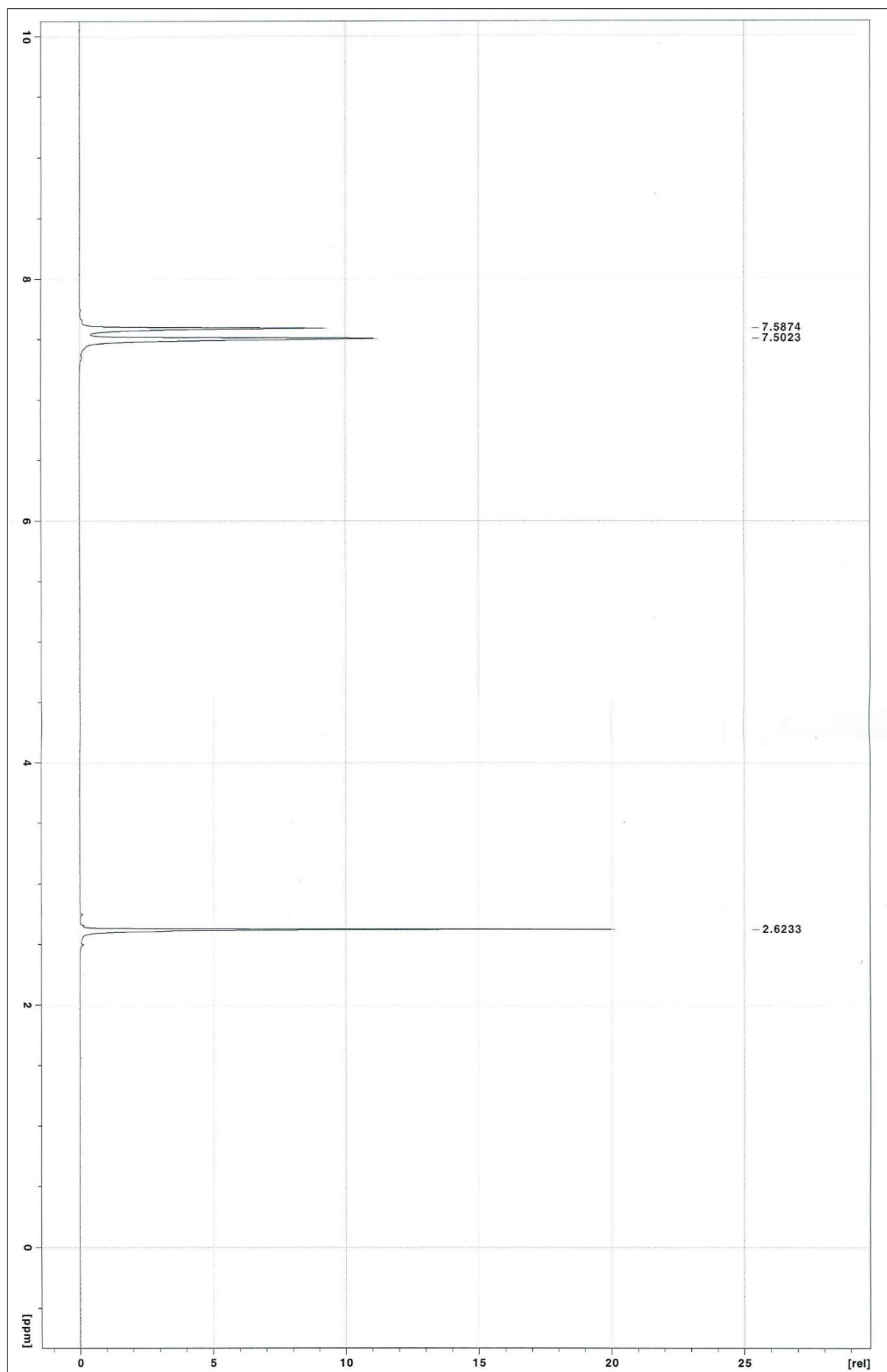


Figure 107. Sample 4, ¹H NMR spectrum

Figure 108. Sample 5, ^2H NMR spectrum

5 Discussion

This chapter will include three main subjects, alkylbenzenes hydrogenation in turn and as mixtures, phenol and anisole hydrogenation as single substrates and as mixtures in addition to toluene and finally, the competitive hydrogenation of phenol, anisole and methoxyphenol.

5.1 Alkyl aromatics hydrogenation

This section will discuss the results obtained from the hydrogenation of toluene, ethylbenzene and n-propylbenzene. This will include the results from varying reaction parameters; temperature, pressure and concentration. It will also discuss the competitive hydrogenation between the three substrates.

5.1.1 Single substrate hydrogenation

Toluene, ethylbenzene and n-propylbenzene were hydrogenated at different reaction conditions; temperature 30 – 70 °C, H₂ pressure 3 – 5 barg and substrate concentration around 8 mmolL⁻¹. All three substrates were hydrogenated to the corresponding alkylcyclohexane. In addition, corresponding alkylcyclohexenes were also detected (yield <3%), especially at higher temperature. The formation of alkylcyclohexenes leads to the suggestion of the stepwise mechanism as suggested by different researchers [5, 12, 21, 37]. It was expected that the concentration of alkylcyclohexenes formed will be low due to their high reactivity when compared with aromatics [99].

Lietz and Völter [100] studied the hydrogenation of toluene, p-xylene and mesitylene over Pt/glass in a vapour phase reaction at temperatures up to 100 °C. They found that hydrogenolysis increased as the number of substituents increased and decreased when temperature was increased. They also concluded that hydrogenolysis, when present, was in parallel process with hydrogenation. Hydrogenolysis was also observed in very low concentrations at high temperatures (over 200 °C) for the hydrogenation of toluene and o-xylene over Ni/SiO₂ [101]. In our tests no hydrogenolysis of the alkylbenzenes was detected, which is in keeping with the literature for alkylbenzenes hydrogenation over Rh catalysts especially at low temperatures [100, 102], where it was stated that hydrogenolysis was not observed.

As the temperature is increased the rate of reaction increases for all substrates and activation energies were obtained. As the alkyl chain is lengthened the activation energy

increases giving an order of n-propylbenzene > ethylbenzene > toluene. At the highest temperature (70 °C) however the reaction rate decreased, for example it can be seen that the reaction rate for ethylbenzene decreased to about the half of the rate of the 60 °C reaction, Table 35. By examining the change of conversion with time it appeared that at 70 °C a first order kinetic analysis was a better fit to the data than a zero order analysis. In other words, the surface coverage changed as the temperature increased. This behaviour is in agreement with some previous work [29, 101, 103]. Keane and Patterson [101] studied the hydrogenation of benzene, toluene and xylene over Ni/SiO₂ catalyst and they observed that reaction order changed from zero to 0.5 as the temperature increased.

Table 35. Reactions rates for alkylbenzenes hydrogenation at different temperatures

Temp. °C	Substrate	Toluene	Ethylbenzene	n-Propylbenzene
	Rate of reaction (mols ⁻¹)			
30		3.3×10^{-6}	1.18×10^{-6}	-
40		6.93×10^{-6}	2.4×10^{-6}	7.7×10^{-7}
50		5.97×10^{-6}	4×10^{-6}	1.3×10^{-6}
60		8.23×10^{-6}	4.8×10^{-6}	1.1×10^{-6}
70		6.9×10^{-6}	2.67×10^{-6}	-

It can be concluded from the rates of hydrogenation at different temperatures for the three alkylbenzenes, shown in Table 35 that the rate decreased as the alkyl chains attached to the ring increased. This behaviour can be explained by the steric effect performed by longer chains [35, 104, 105]. These longer chains may inhibit the adsorption of the ring to the surface or inhibit hydrogen atoms from attacking the ring in the *ortho* positions.

In general from the literature, the order of reaction for the aromatic hydrogenation is zero order in aromatic substrate and first order in hydrogen [35, 38, 45, 46]. The results obtained are in good agreement with this with all the systems showing first order in hydrogen. The order in aromatic substrate was zero for toluene and ethylbenzene, however the order in n-propylbenzene was closer to negative first order suggesting a strong adsorption. This would also agree with the higher activation energy found with n-propylbenzene.

5.1.2 Competitive hydrogenation

These tests were performed at 50 °C, 3 barg H₂ pressure and at 1:1:1 ratios of toluene, ethylbenzene and n-propylbenzene. It is worth remembering that during the hydrogenation

of the three alkylbenzenes individually that they reacted in the following order; toluene > ethylbenzene > n-propylbenzene. This behaviour can be explained by the steric effect of the longer alkyl group attached to the ring in the case of ethylbenzene and n-propylbenzene. However different behaviour was observed during the competitive hydrogenation of the three alkylbenzenes. Surprisingly n-propylbenzene showed higher reactivity during competitive hydrogenations, especially when mixed with toluene where the rate of n-propylbenzene hydrogenation increased to almost double, Figure 109.

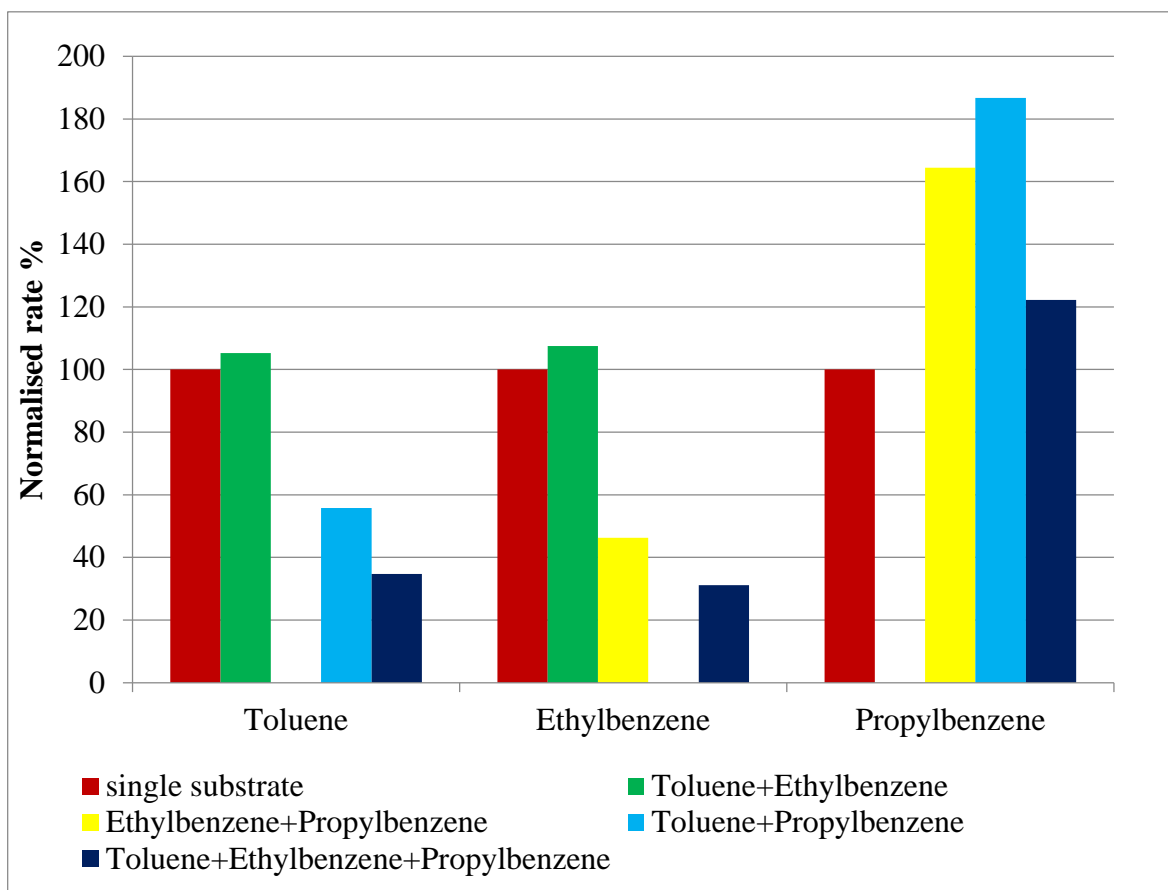


Figure 109. Competitive hydrogenation of alkylbenzenes

The literature on alkylbenzene competitive hydrogenations is rather scarce. Smith [106] studied the competitive hydrogenation on a number of aromatic substrates. He suggested that the rate was affected differently in single and competitive hydrogenations. Although he did consider competitive hydrogenation involving toluene, it was with xylenes and other methyl-substituted benzenes. We could find no literature pertaining to toluene, ethylbenzene, n-propylbenzene competitive hydrogenation. Alkyl groups are categorised as electron donor groups and the electron donation is increased by increasing the length of chain attached to the ring, therefore as the alkyl chain increases the strength of adsorption can increase as the increased electron density in the ring gives stronger π -bonds to the surface [70, 76]. In agreement with this the competitive hydrogenation results suggest that

n-propylbenzene is the most strongly bound of the alkylbenzenes, inhibiting the adsorption of both toluene and ethylbenzene. This is also supported by the kinetic analysis where n-propylbenzene showed a negative reaction order suggesting strong adsorption. Therefore, when hydrogenated in the absence of other components the low reactivity of n-propylbenzene relates to too strong adsorption, not a steric effect of the alkyl chain. However in the competitive situation not only does the n-propylbenzene inhibit hydrogenation of toluene and ethylbenzene but it also increases in rate. For this to occur either the strength of bonding of n-propylbenzene must be reduced and/or the hydrogen concentration on the surface must increase. Given that in a competitive hydrogenation more species are present on the surface, simple Langmuir adsorption theory would suggest that the amount adsorbed of any given species is unlikely to increase, [107] therefore is likely that the strength of adsorption is weakened and so the rate increases. Ethylbenzene shows similar behaviour but much reduced.

5.2 Phenol and anisole hydrogenation

This section will examine the hydrogenation of phenol and anisole as single substrates then it will discuss their competitive hydrogenation with each other and with toluene. Phenol and anisole were tested in the same procedure as the alkylbenzenes.

5.2.1 Phenol hydrogenation

Conversion of phenol hydrogenation increased as the temperature increased. An apparent activation energy was calculated as explained in the results section and was found to be 23 kJmol⁻¹. Although we could find no activation energy data in the literature for rhodium, this value is lower than what has been found in literature for palladium [108-111], where the activation energy varied between 30 kJmol⁻¹ [108] over Pd/Al₂O₃ and 63 kJmol⁻¹ over Pd/MgO [111].

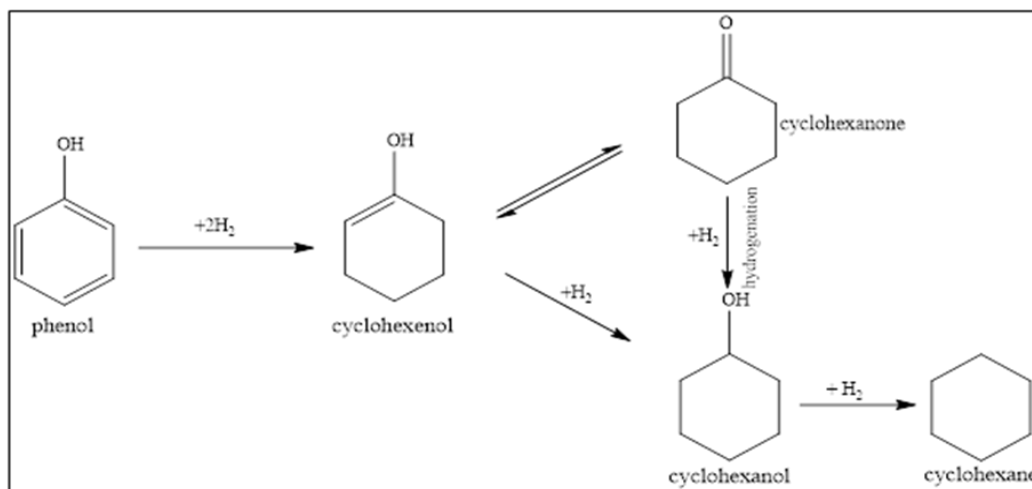


Figure 110. Sequential process of phenol hydrogenation under moderate conditions (Pd/Al₂O₃) [60]

The hydrogenation of phenol resulted in three products, cyclohexanol, cyclohexanone and cyclohexane. Most of the literature cited in the introduction section shows that cyclohexane formation, when observed, was a secondary step in the hydrogenation of phenol as can be seen in Figure 110.

In this mechanism phenol is hydrogenated to 1-hydroxycyclohexene, which isomerises to cyclohexanone. Then cyclohexanone is hydrogenated to form cyclohexanol which will undergo hydrogenolysis to form cyclohexane. Alternatively and as shown in Figure 111, cyclohexane can be formed directly from phenol hydrogenation. This route is possible as outlined by Shin and Keane [13]. However it is not always possible to know from the literature whether or not cyclohexane has been formed during phenol hydrogenation as various researchers used cyclohexane as a solvent during phenol hydrogenation [54, 112, 113] and more recent work by Raut et al. [114] also used cyclohexane as a solvent. In Figure 111 it is clear that the formation of cyclohexane stops when all the phenol is hydrogenated, indicating that in our tests cyclohexane appears to be formed directly from phenol and not via cyclohexanol. However, no benzene was detected under any reaction conditions during the hydrogenation of phenol. Nevertheless, further confirmation of a direct route from phenol to cyclohexane was obtained from the hydrogenation of cyclohexanone, where the formation of cyclohexane was less than 3% even at 70 °C. Therefore, hydrogenolysis of the Ar-OH bond is much more facile than hydrogenolysis of the alkyl-OH bond even though the Ar-OH bond is approximately 100 kJ.mol⁻¹ stronger than the R-OH bond.

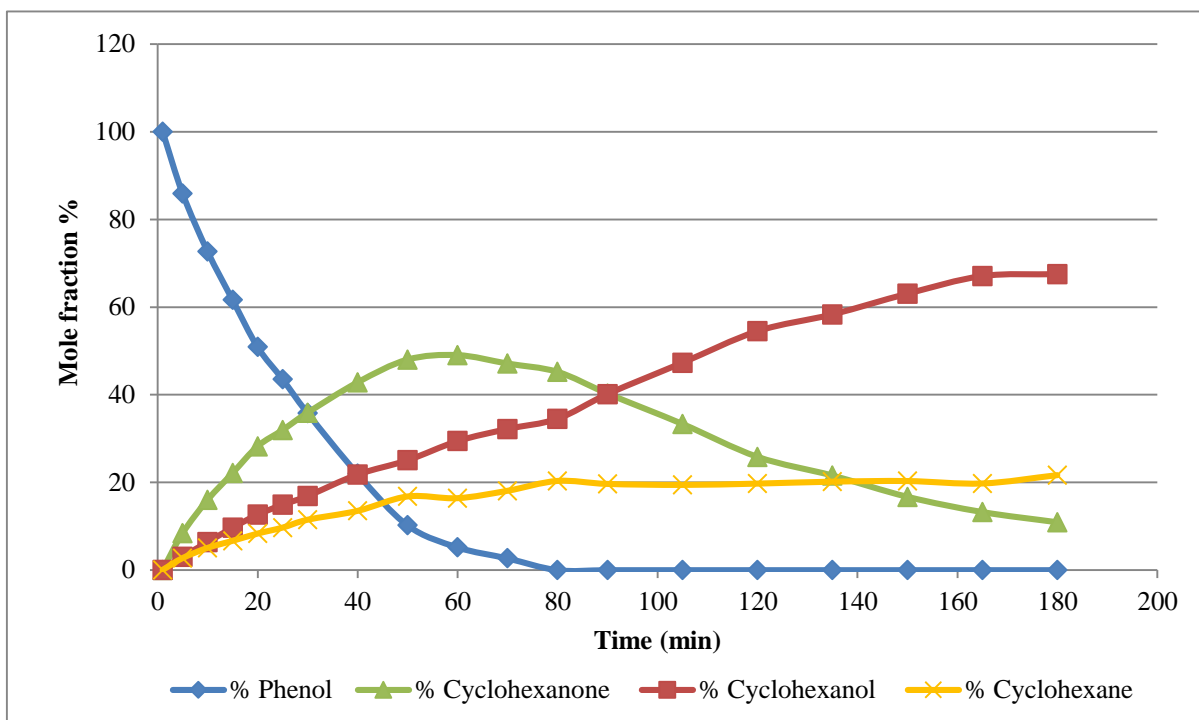


Figure 111. Phenol reaction profile under 5 barg H₂ pressure

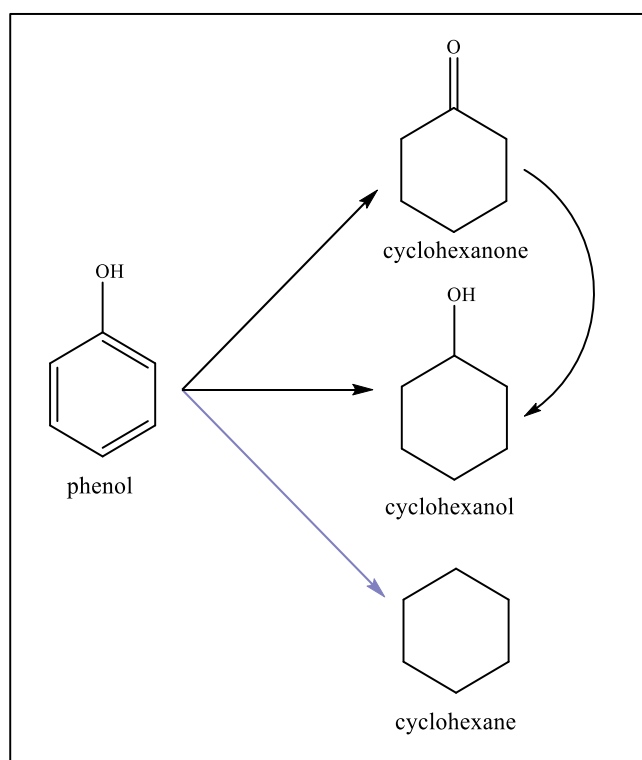


Figure 112. Phenol hydrogenation over Rh/SiO₂

From Figure 111 it can be seen that cyclohexanone is an intermediate product, which can be subsequently hydrogenated to cyclohexanol. This is in keeping with our own testing of cyclohexanone hydrogenation and with the literature, for example, during the vapour phase hydrogenation of phenol over Rh/silica [55], phenol was hydrogenated to three products, cyclohexanone, cyclohexanol and cyclohexane with the cyclohexanol formed from the subsequent hydrogenation of cyclohexanone.

Nevertheless, from Figure 111 it can be seen that all three products appear to be formed directly as the reaction started, which agrees with the suggestion of a direct and independent route for each product. In addition, as temperature was increased, the selectivity to cyclohexanone increased, whereas selectivity to cyclohexanol increased as the concentration or hydrogen pressure increased, it is likely that cyclohexanol has a direct route of formation from phenol as well as indirectly via cyclohexanone. Therefore there is support for two mechanisms occurring simultaneously, one has cyclohexane and cyclohexanone formed directly followed by subsequent hydrogenation of cyclohexanone to cyclohexanol, the other has direct formation of all three products independently. This behaviour (Figure 112) with cyclohexanol and cyclohexanone being formed independently, has also been observed over Pd [63, 115] and over Rh [92]. It was suggested that phenols can be hydrogenated without forming an intermediate over Rh, cyclohexanone in our case, indicating a strong adsorption of the phenol which might reduce the resonance effect [116].

The different product pathways may suggest that phenol can be adsorbed in different ways. If it was adsorbed in a vertical mode, where adsorption was through the hydroxyl group adsorbed to the surface, this behaviour is responsible for the formation of cyclohexanone [117]. The other possible mode is co-planar where the aromatic ring is adsorbed parallel to the surface. This behaviour would lead to the complete hydrogenation of phenol to cyclohexanol [55] and the formation of cyclohexane.

5.2.2 Anisole hydrogenation

As expected the rate of anisole hydrogenation increased as temperature increased, allowing an apparent activation energy for anisole hydrogenation of 25 kJmol^{-1} to be calculated. In addition, the reaction order was zero in substrate and first order in hydrogen. Anisole hydrogenation has not been subject to extensive research and among the few articles related to anisole hydrogenation, no activation energy determination nor reaction order was found. Another interesting point in the hydrogenation of anisole is that the selectivity changed considerably by changing the temperature, whereas pressure and concentration variation had minor effect on the selectivity.

Products obtained from anisole hydrogenation in this work follow three routes, direct hydrogenation to methoxycyclohexane, which is the corresponding saturated form of anisole, hydrogenolysis to cyclohexane and formation of cyclohexanone which is further hydrogenated to form cyclohexanol as shown in Figure 113. It is worth mentioning that cyclohexanol was not observed at 30 °C reaction.

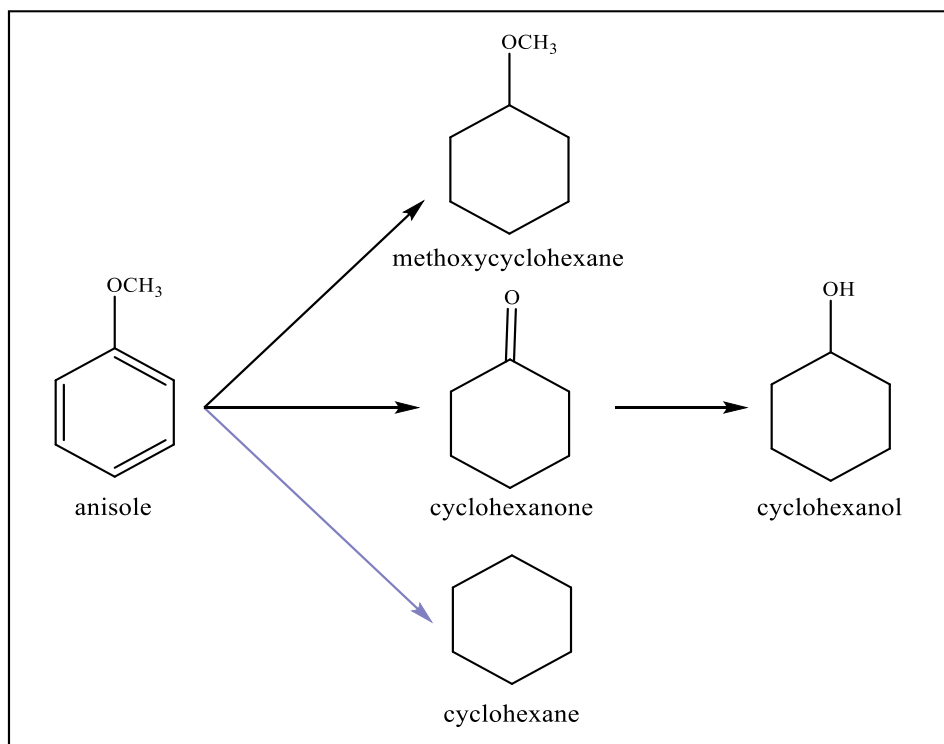


Figure 113. Anisole hydrogenation over Rh/SiO₂ (except for the 30 °C test)

In their paper Kluson and Cerveny concluded that anisole was first hydrogenated to methoxycyclohexane, which was subsequently directly hydrogenated to methoxycyclohexane [59]. In our tests no evidence was found for methoxycyclohexane but the reaction is fast so the concentration may have been below detection limits. In addition, the formation of cyclohexanone was also reported with 23% yield [71]. It was found that cyclohexane was formed independently and not via cyclohexanol, as shown in Figure 113. The breaking of ArO-CH₃ bond (bond dissociation energy ~381 kJmol⁻¹ [118]) leads to the formation of cyclohexanone, which is further hydrogenated to cyclohexanol, whereas it is the breaking of the Ar-OCH₃ bond (bond dissociation energy ~419 kJmol⁻¹, [119]) that leads to the formation of cyclohexane. However it is the cyclohexane that has the highest selectivity at ~25%, while cyclohexanol has a selectivity of ~6% indicating that on the surface it is easier to break the Ar-OCH₃ bond rather than the ArO-CH₃ bond. This may be related to the mode of adsorption, if the anisole is adsorbed

parallel to the surface bonding through the ring and the oxygen then Ar-O bond breaking may be favoured.

During phenol hydrogenation, cyclohexanol was formed independently and directly whereas in anisole hydrogenation it was formed via cyclohexanone and only after the total conversion of anisole, Figure 114. Hence there is no direct route to cyclohexanol from anisole.

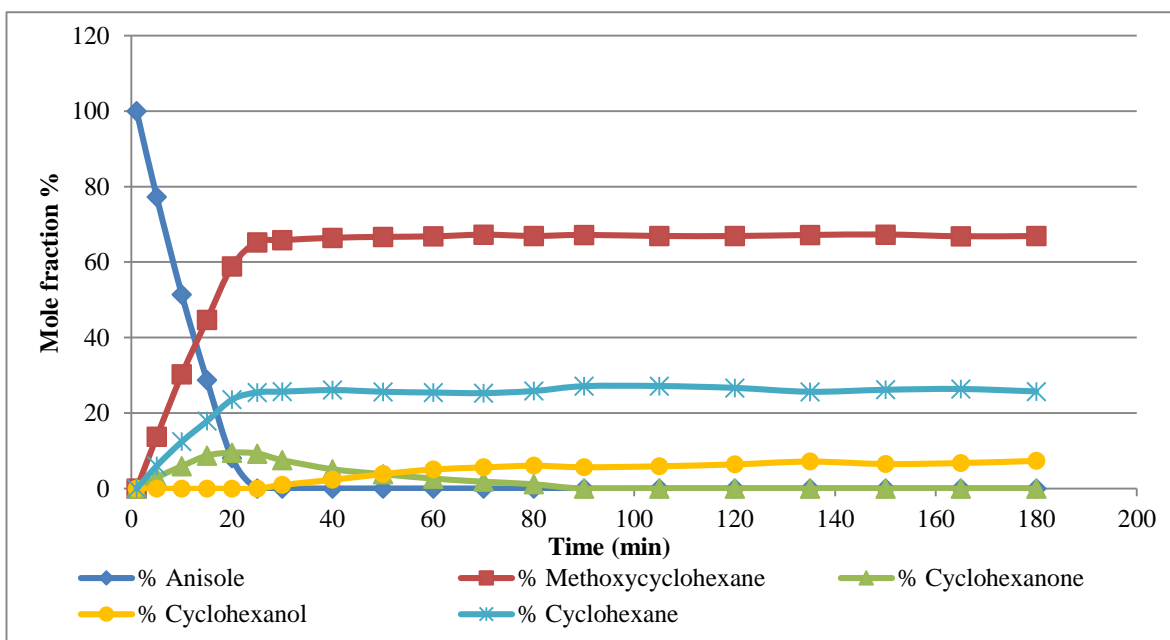


Figure 114. Anisole reaction profile at 50 °C

The formation of cyclohexane is suggested to follow the same route in phenol and anisole reactions. In both cases it was formed directly and independently via hydrogenolysis of functional group attached to the benzene ring. However, the yield of cyclohexane was different for each substrate, Figure 115 summarises these differences. It is clear that for each temperature that anisole forms cyclohexane with higher yields and the yield increased as the temperature increased. It worth mentioning that anisole was found to react with higher rates than phenol [59].

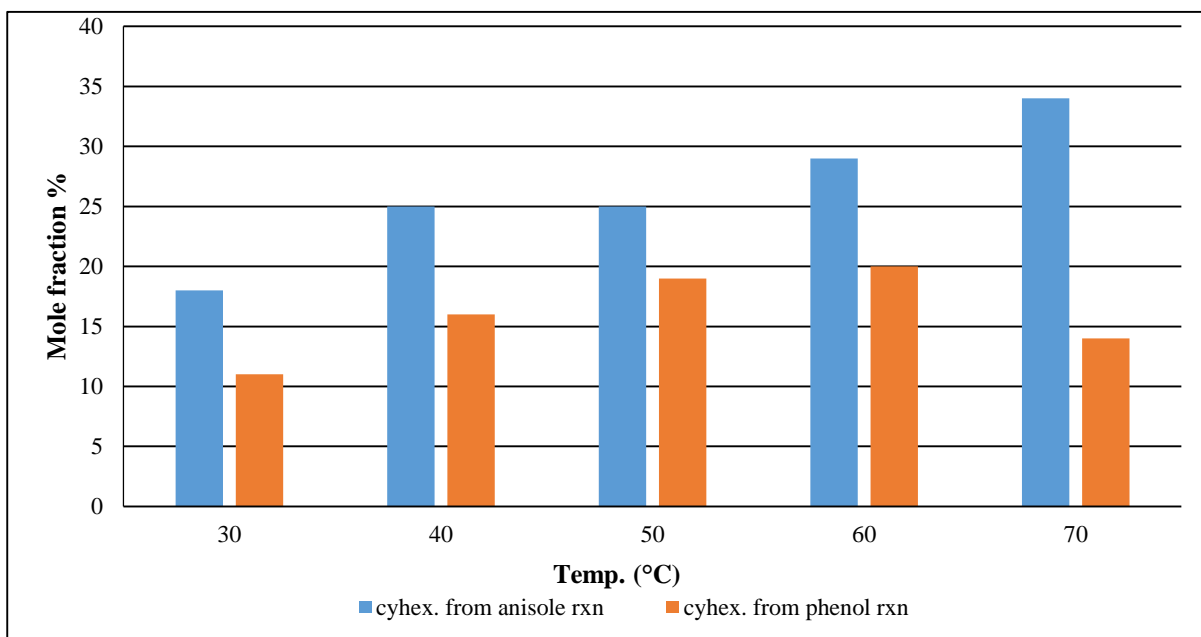


Figure 115. Cyclohexane yield from phenol and anisole hydrogenation

The difference between phenol and anisole hydrogenation might be attributed to the mode of adsorption of each substrate, for example Popov et al. [120] found that anisole formed an hydrogen bond, while phenol formed a phenate species and a hydrogen bond to support surface when using SiO_2 . However the difference in activity may also be related to the electron-donation into the ring by the substituent group.

5.2.3 Phenol, anisole and toluene competitive hydrogenation

Phenol, anisole and toluene were hydrogenated competitively in 1:1:1 ratio to examine their effect on each other. The findings of the competitive hydrogenation are summarised in Figure 116, taking into consideration that toluene and anisole were compared after 90 and 20 min respectively of the reaction which is the time needed to reach 100% conversion of each substrate. It is clear that anisole was affected significantly by the presence of phenol and toluene.

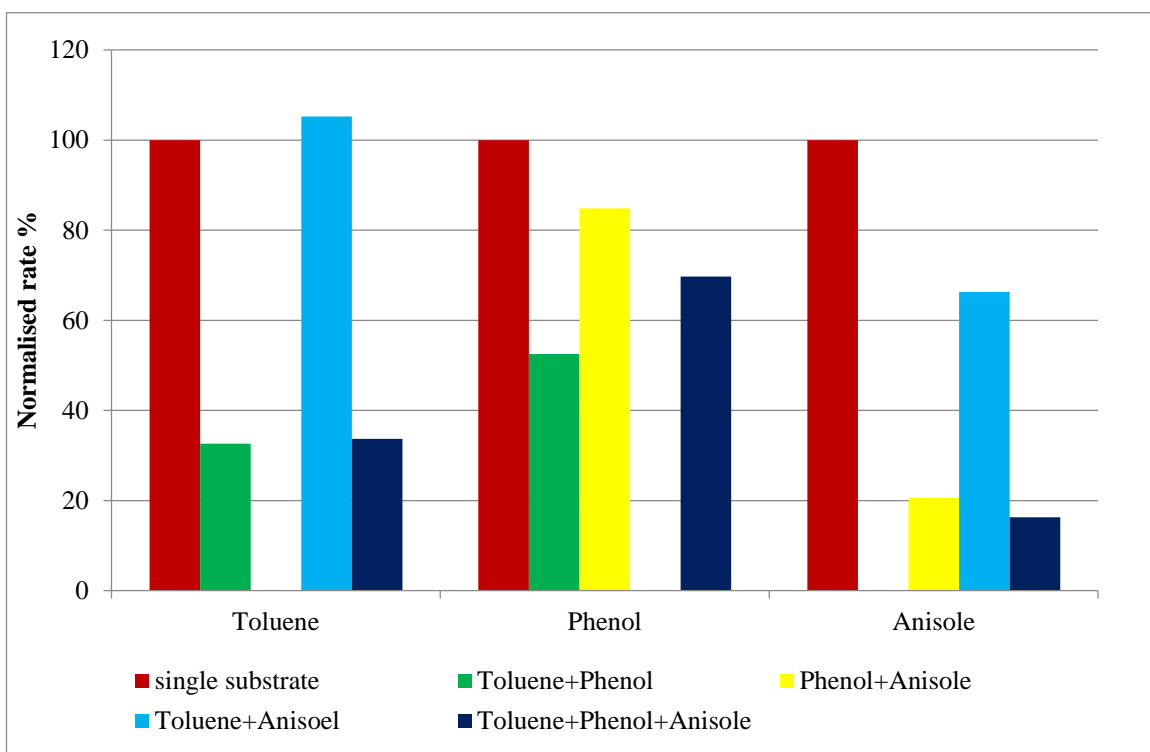


Figure 116 Competitive hydrogenation of toluene, phenol and anisole

The competitive reaction between anisole and phenol has been reported in the literature over a Ru catalyst, where it was found that anisole reacts faster than phenol [59]. In our tests, although the anisole was reduced to only 20% of its rate when hydrogenated in isolation, the actual rate was slightly faster than phenol in agreement with the Ru system. As shown in Figure 117 and Figure 118, in single substrates the conversion order was anisole > toluene > phenol. This order changed in the competitive hydrogenation to anisole \geq phenol > toluene. Clearly there is no one species that is more strongly adsorbed as was the case with the alkylbenzenes. We may view anisole as the weakest adsorber (rate reduced the most in all competitive reactions) and phenol as the strongest but in general the absolute rate observed is often similar.

One reason for the changes in activity may be related to changes in the mode of adsorption, for example, the benzene ring is usually adsorbed parallel to the catalyst surface [81, 82], however when an excess amount of hydrogen or aromatics are covering the surface, an edgewise adsorption was observed [83]. Therefore in the competitive system it is possible that the mode of bonding of the reactants has changed. In addition, the substituent group might have an effect on the aromatic ring activity. As shown in Figure 117 and Figure 118 toluene conversion was lower than the other two phenols. this might be because toluene has an alkyl group which activates aromatic ring only moderately via an inductive effect which is a weaker effect when compared to resonance or conjugation applied by hydroxy or methoxy groups [79]. Indeed the high activity of anisole may be related to the activating aspect of the methoxy group.

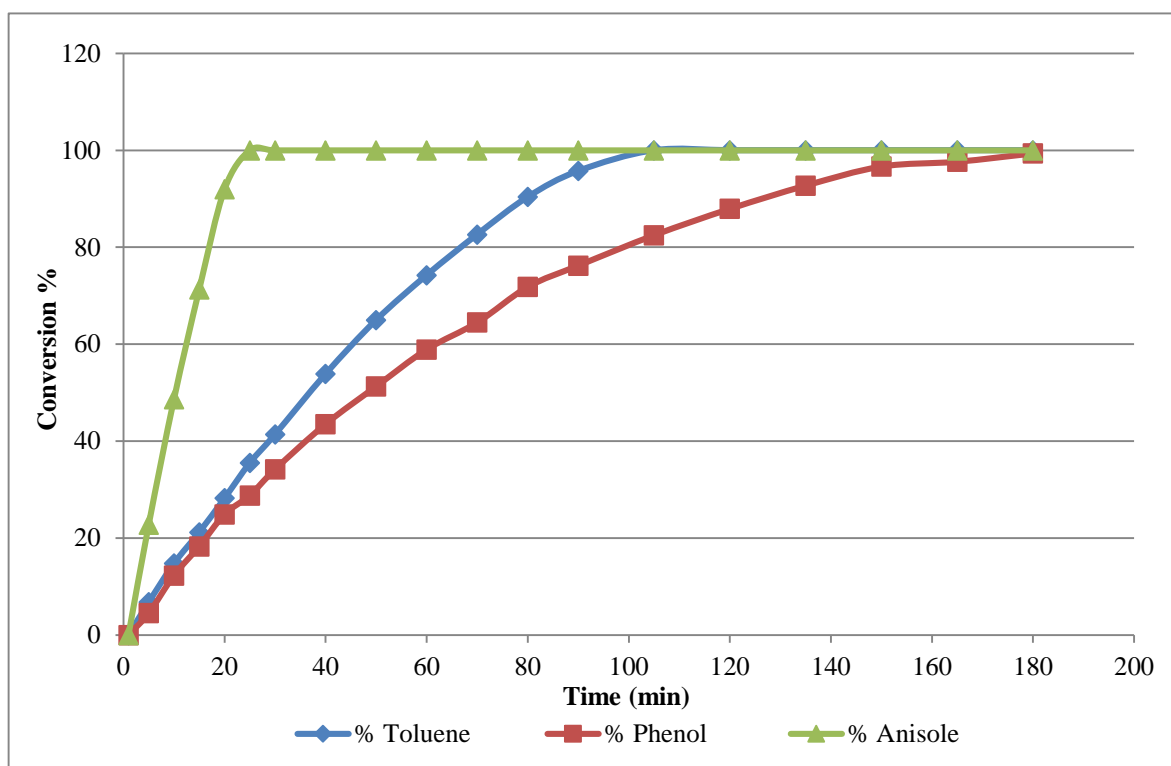


Figure 117. Single substrates conversion

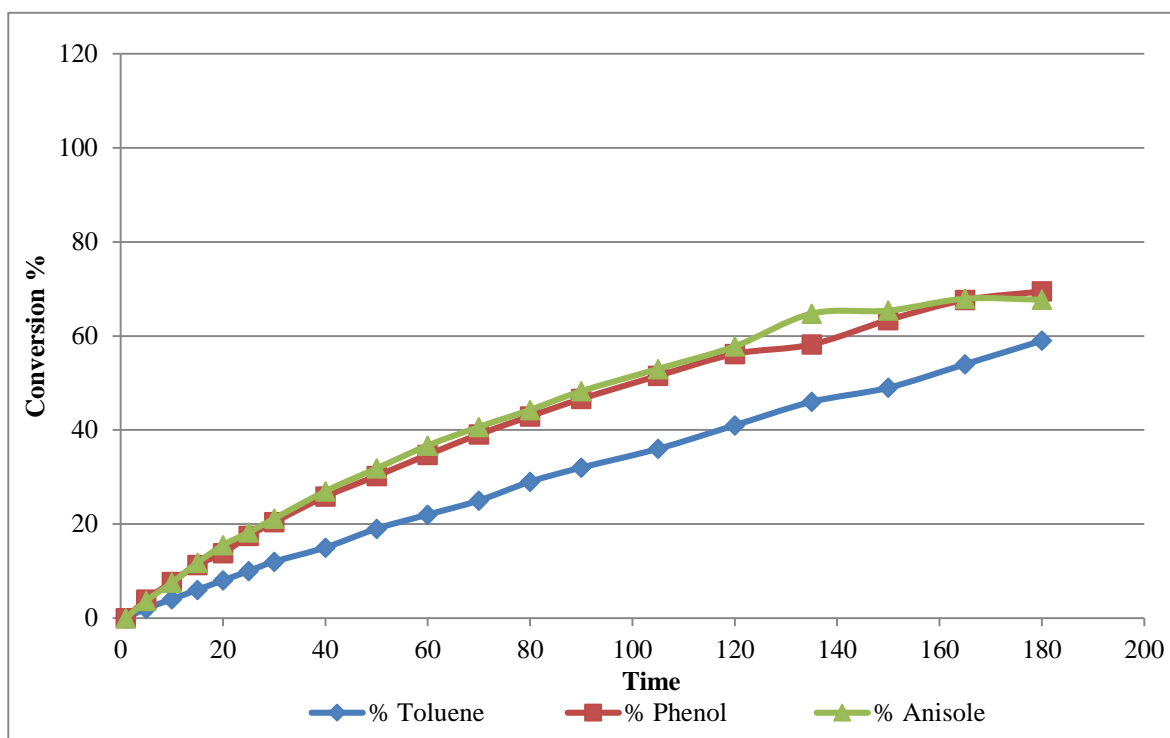


Figure 118. Mixture of three substrates conversion

5.3 Cyclohexanone hydrogenation

It is generally recognised that cyclohexanone follows a stepwise mechanism in which hydrogen atom is added to the carbon and oxygen atoms after the carbonyl group being adsorbed to the surface [121, 122].

A point to be considered from cyclohexanone hydrogenation is that cyclohexane was not formed during the five different reactions carried out at different temperatures (30 – 70 °C) as shown in Figure 119 for example. Cyclohexane was also not observed during cyclohexanone hydrogenation over Pt [123]. This observation confirms the suggestion that cyclohexane was formed independently and directly from the hydrogenation of the three different phenols.

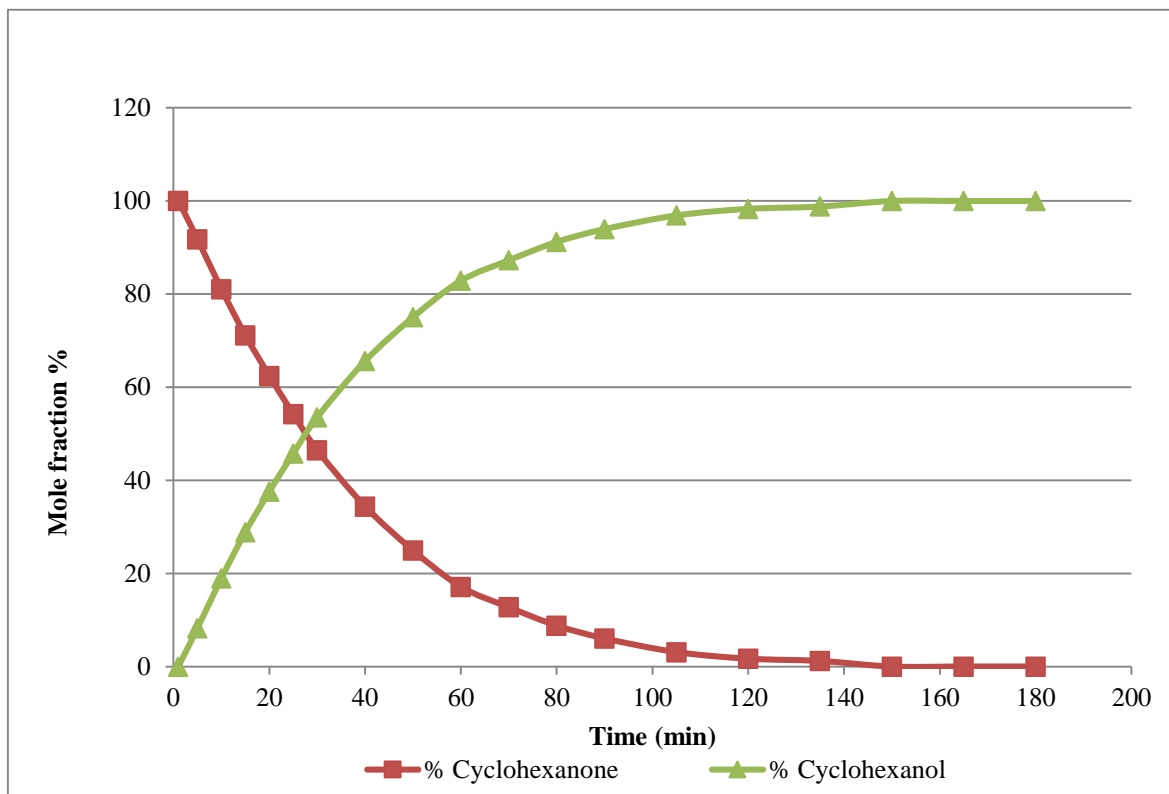


Figure 119. Cyclohexane reaction profile at 70 °C

5.3.1 Cyclohexanone competitive hydrogenation

A number of points can be concluded from the competitive hydrogenation of cyclohexanone with phenol and anisole. Firstly, there was no change in cyclohexane formation in both reactions. This supports the idea that cyclohexane was formed directly and independently from phenol and anisole and it was not produced via an intermediate. In addition, cyclohexanol was increased in both reactions and it was increased significantly in the anisole reaction. It is also noticeable that the production of cyclohexanol did not start until after all the anisole was consumed, indicating that anisole was more strongly adsorbed than cyclohexanone. This was not observed with the phenol/cyclohexanone system confirming that there must be a direct route from phenol to cyclohexanol.

5.3.2 Phenol, anisole and methoxyphenol competitive hydrogenation

In this set of competitive hydrogenation reactions, 4-methoxyphenol was introduced instead of toluene to be hydrogenated competitively with phenol and anisole. The results showed that the mixture of the three substrates affect each other during the competitive hydrogenation. As shown in Figure 121 and Figure 122, anisole was also significantly affected by the presence of the other substrates. In addition to factors such as steric and electronic effects that were mentioned earlier, which might affect the competitive hydrogenation, the adsorption mode of substrate was found to be a possible factor. In a

recent work by Popov et al. [120], they investigated the adsorption modes of phenol, anisole and 2-methoxyphenol over different supports at temperatures that are usually used during hydrodeoxygenation reactions. They used SiO_2 , Al_2O_3 and $\text{SiO}_2\text{-Al}_2\text{O}_3$. They observed a variation on adsorption modes with different supports. Most importantly, when SiO_2 was used, phenol and methoxyphenol formed two modes, a phenate species (Figure 120) and a hydrogen bond attached to the silica for the former and a 4-methoxyphenate (Figure 120) species and a hydrogen bond attached to the silica for the latter. On the other hand, anisole only formed an hydrogen bond when silica was used.

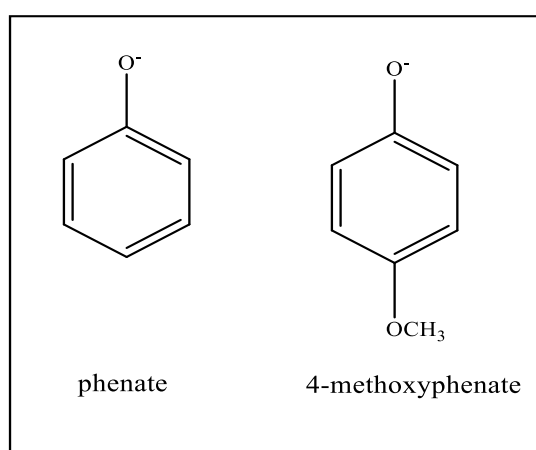


Figure 120. Phenate and 4-methoxyphenate

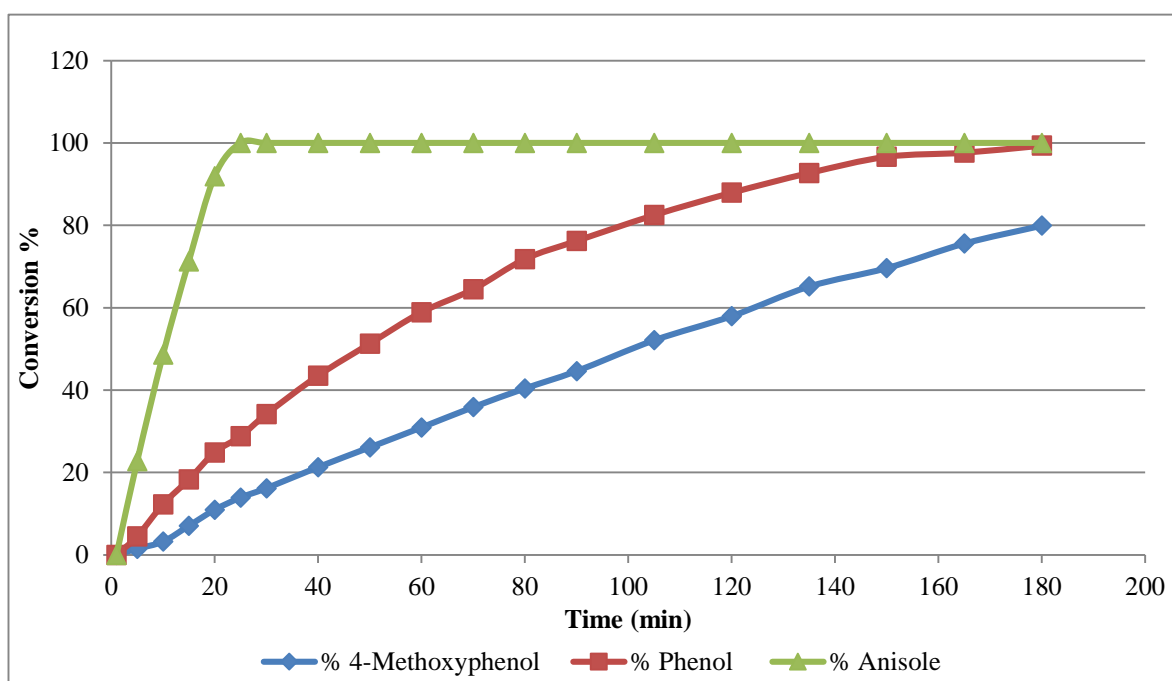


Figure 121. Single substrates conversion

Rochester performed number of studies on the adsorption behaviour of phenols over silica [124, 125]. Rochester and Trebilco [124] tested the adsorption of phenols on silica. They concluded that there were two adsorbate species that were attached to the silica surface.

Both of them involved the formation of hydrogen bonds. One of them was the interaction between the silica surface and the oxygen atom of the hydroxy group and the other was the interaction between the silica surface and the aromatic π -complex (Figure 8).

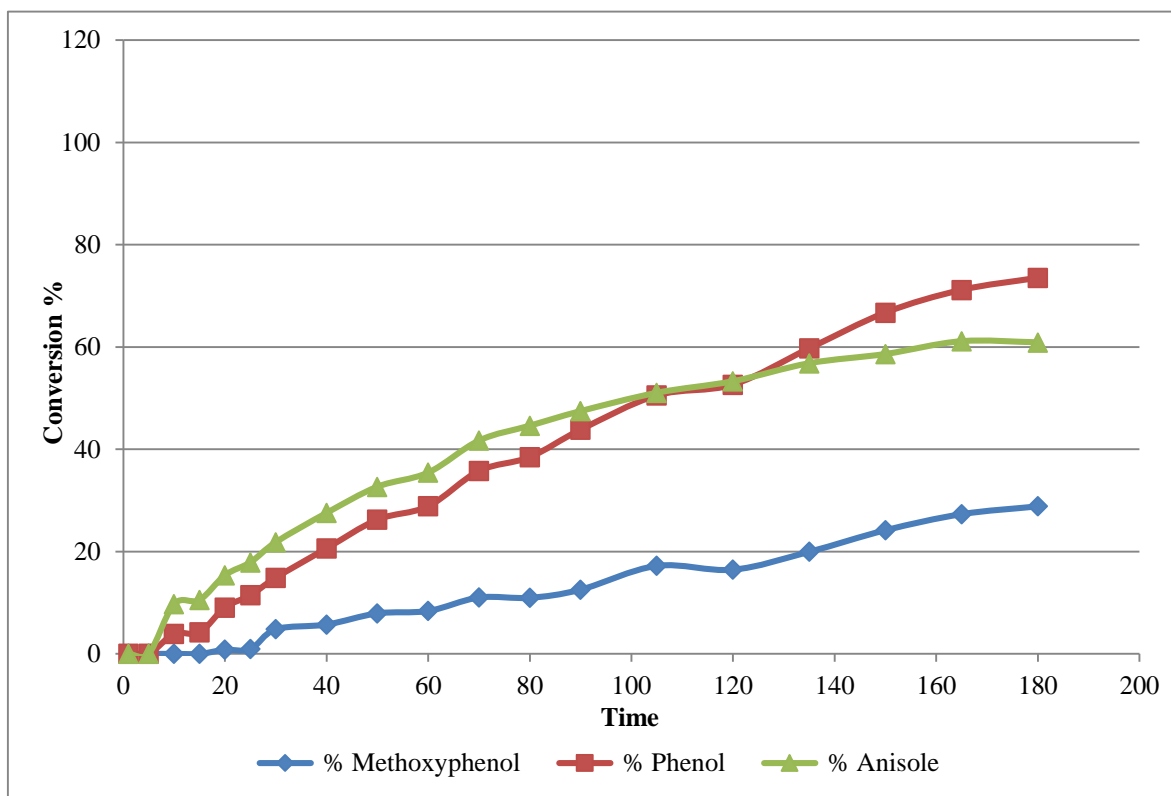


Figure 122. Mixture of three substrates conversion

5.4 Deuterium Isotope studies

As shown in Table 33 the three alkylbenzenes as well as 4-methoxyphenol showed an inverse KIE. The inverse KIE was also found when *ortho*-, *meta*- and *para*-xylenes were hydrogenated with same catalyst under similar reaction parameters [126]. It was only phenol and anisole that showed a normal KIE.

Table 36 Inverse KIE for xylenes [126]

Reactant	k_H	k_D	k_H/k_D
<i>Ortho</i> -Xylene	0.838	1.273	0.71
<i>Meta</i> -Xylene	1.205	1.554	0.92
<i>Para</i> -Xylene	2.0	2.0	1.0

Number of suggestions have been presented to explain the phenomena of inverse kinetic isotope effect [127]. One of these suggestions was that the inverse isotope effect was formed due to a change in carbon hybridisation from sp^2 to sp^3 [128]. Shi and Jin [129] explained that as the difference in energy between the out of plane bending forces of C-H and C-D bonds. An inverse isotope effect was also found in other reactions such as ammonia synthesis [130] and nitrobenzene hydrogenation [131]. The suggestion that was given for these reactions to show an inverse isotope effect is that deuterium has the ability to change the adsorption of reaction intermediates which in turn increases rate of the reaction. Therefore, it was suggested that phenol as well as anisole reacted in a different way from the other alkylbenzenes and 4-methoxyphenol.

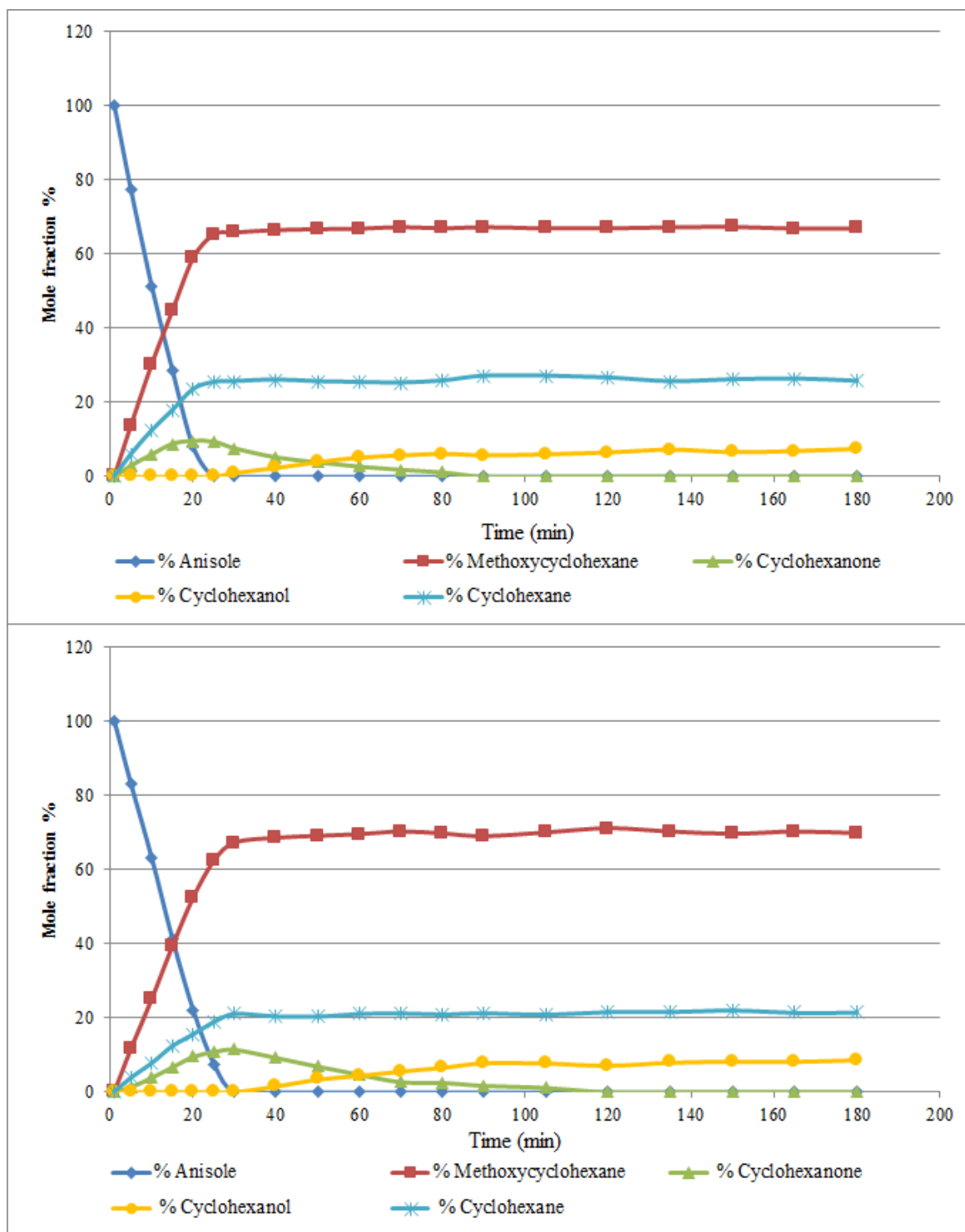


Figure 123. Anisole hydrogenation and deuteration reaction profiles

By examining the hydrogenation and deuteration of anisole shown in Figure 123, it is clear that (see section 4.8) the reaction follows three different routes as shown in Figure 113 but examination of the product distribution for both reactions shows that there have been changes in selectivity.

For the hydrogenation of anisole to methoxycyclohexane, selectivity increased from 65% to 70% when D_2 was used instead of H_2 , whereas with the hydrogenolysis reaction to

cyclohexane, the selectivity decreased from 25% to about 20% when D₂ was used. Similarly, the hydrogenation and deuteration of 4-methoxyphenol gave an increase in selectivity to 4-methoxycyclohexanone, which increased from 45% to 55% using D₂.

These changes in selectivity gives information on the different reactions occurring with some of the reactants. Anisole can be hydrogenated to give methoxycyclohexane but it can also hydrogenolyse breaking either the Ar-OCH₃ bond or the ArO-CH₃ bond giving cyclohexane and cyclohexanol respectively (Figure 113). From the results shown it is clear that the breaking of the Ar-OCH₃ bond is slower with deuterium (reduction in yield of cyclohexane) while the hydrogenation is faster (increased yield of methoxycyclohexane).

For the ring hydrogenation we should not be too surprised at the observation of an inverse KIE. Typically an inverse KIE can be seen when there is a change in hybridisation of a carbon from sp² to sp³; it is a secondary effect rather than a primary and is exactly the process that occurs on hydrogenating the aromatic ring. The maximum value for such a KIE would be 0.7 or lower, especially if related to the transition state, which is in agreement with our values.

5.5 NMR isotope study

NMR results showed an interesting point that in the reaction of toluene with deuterium, both aromatic and aliphatic hydrogen atoms were exchanged with deuterium before any evidence of hydrogenation. This is clear from the deuterium NMR spectra of toluene + deuterium at $t = 0$ (sample 1, Figure 102) and pure deuterated toluene (sample 5, Figure 108). The comparison is shown in Figure 124, the aromatic peaks are at ~ 7.5 ppm while the aliphatic peak is at 2.6 ppm. A rough estimate of the extent of exchange suggests approximately 50 % of the toluene has exchanged.

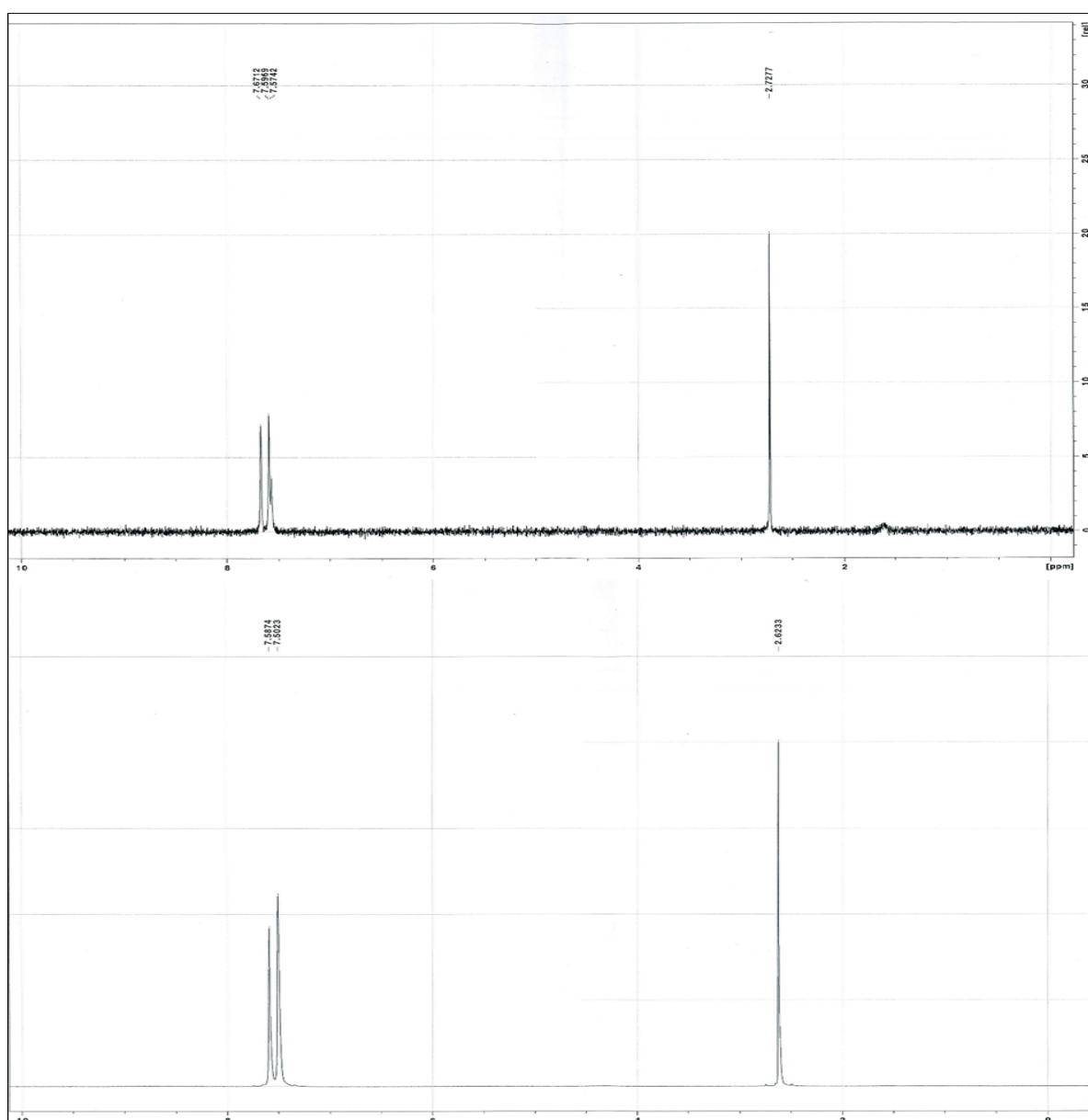


Figure 124. ^2H NMR results for toluene + D_2 (top) and toluene d_8 sample (bottom)

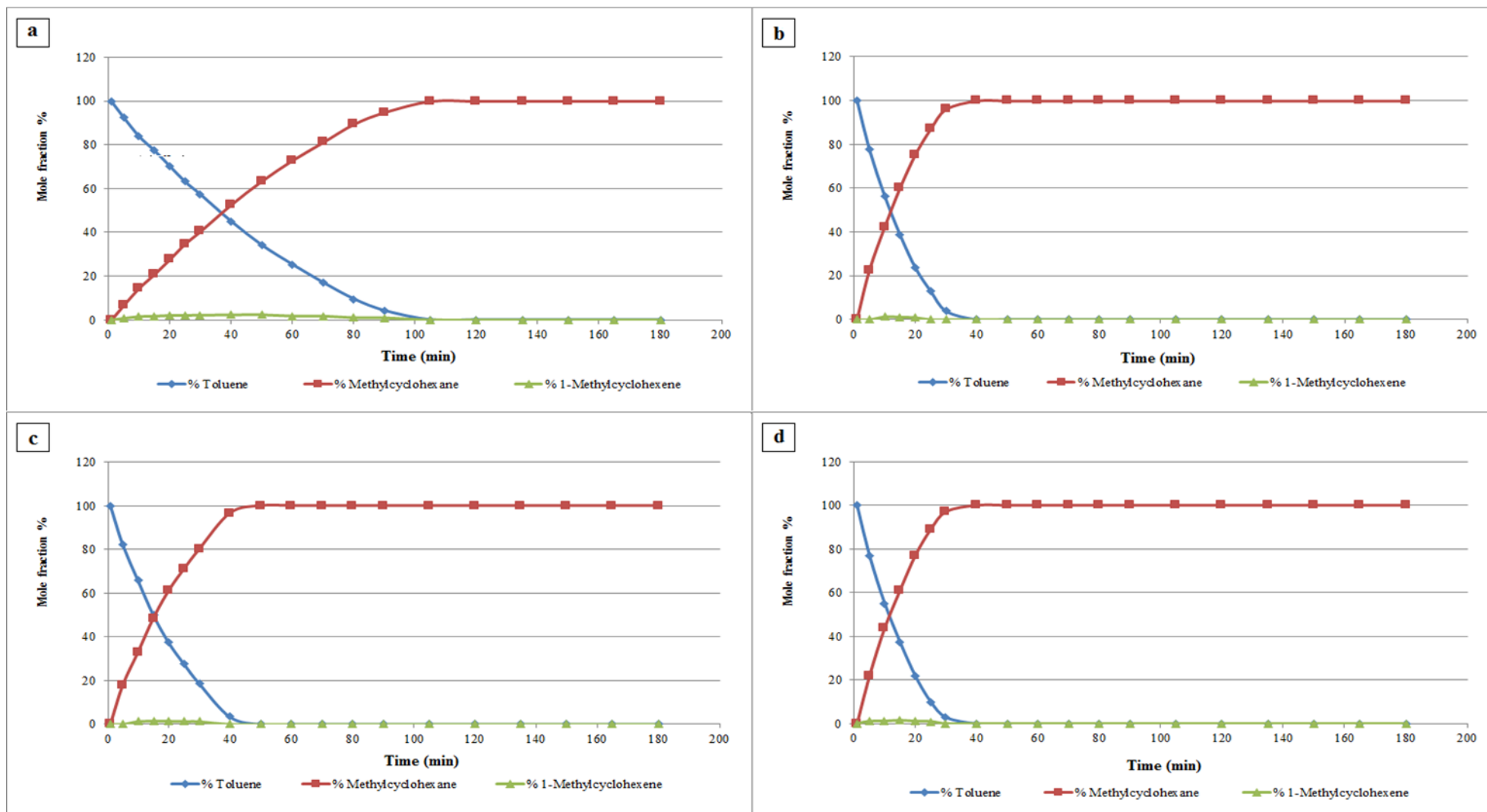


Figure 125. Reaction profiles for a) toluene + H₂, b) toluene d₈ + H₂, c) toluene + D₂ and d) toluene d₈+ D₂

However the ratio of the aliphatic:aromatic peaks in the reaction setting is not the same as in the reference sample. In the reference sample the ratio of peaks is 1.8 whereas in the reaction sample the ratio is 2.5. Therefore the rate of exchange of the protons in the methyl group is faster than that of the aromatic protons, which contrasts with the exchange over palladium [132] where only the methyl groups were exchanged and nickel where both sets of hydrogen exchanged but the rate of methyl group exchange was over an order of magnitude faster [133]. The effect of this rapid exchange is to make reactions c and d, that are shown in Figure 125, to become the same reaction. Moreover, Figure 125 showed that reaction d is faster than reaction a, which confirms the inverse kinetic isotope effect. This clearly shows that H/D exchange is a separate process from hydrogenation. For the exchange process to occur as fast, it is likely that there is no loss of aromatic stability during the exchange suggesting a dissociative mechanism. Another interesting point that was observed from NMR results was the confirmation of that attached CH₃ group was in contact with the catalyst surface. This was clear from the formation of -CD₃ (observed at 2.7 ppm in the ²H NMR, Figure 102) and it confirms the proposal by Webb and Orozco [86] that toluene adsorbed to the surface via the methyl group as well as the aromatic ring.

6 Conclusion

In this study five different substituted benzenes were tested: two with oxygen containing groups in addition to three alkylbenzenes. A number of points can be concluded from the outcome of this project.

Firstly, rhodium was chosen after testing iridium catalyst for the hydrogenation of toluene and ethylbenzene (see appendix). Although the iridium catalyst was active, the activity was low in comparison to the rhodium catalyst even at elevated temperatures. Intermediates were also observed during the hydrogenation of the alkylbenzenes over Rh catalyst, which was not the case for iridium. From this behaviour it was concluded that the stepwise mechanism was active in the formation of these intermediates.

As for the hydrogenation of phenol and anisole, it was concluded that cyclohexane was formed directly and independently even at low temperatures. It was not formed as consequence of hydrogenolysis of the substituted cycloalkanes as the literature suggests, nor were temperatures in excess of 200 °C required. The hydrogenolysis of anisole and 4-methoxyphenol revealed that the Ar-O bond was more favourable to break than the O-H or O-CH₃ bonds.

Products from the hydrogenation of phenol showed that there was a direct route to cyclohexanol as well as one at the expense of cyclohexanone, along with direct HDO to cyclohexane. This has not been proposed previously in the literature.

The competitive reactions were a unique set of experiments that have not been previously attempted. Depending on the specific reaction combination a number of factors were suggested to explain the behaviour of the competitive hydrogenations. These factors include steric effect, electronic effect and the mode of adsorption of each substrate. For example for the toluene/ethylbenzene/propylbenzene competitive reaction the strength of adsorption due to electronic effects was the key factor, whereas with the phenol/anisole/4-methoxyphenol competitive reaction changes in the mode of adsorption was the important parameter.

NMR results revealed that deuterium atoms replaced around 50% of both aromatic and aliphatic hydrogen atoms at the beginning of the reaction of toluene with deuterium before hydrogenation had initiated. The exchange of the methyl protons was observed to be faster

than that of the aromatic protons. These results confirmed that the methyl group must be adsorbed to the surface as well as the aromatic ring.

7 Future work

This project has shown that our understanding of aromatic hydrogenation is less than ideal. It would be useful and complimentary to this study if the xylenes were studied in a similar manner. This would allow a more complete understanding of alkyl aromatic hydrogenation. In the future it would be good to expand this study to cover typical species that are used in hydrodeoxygenation (HDO) studies, such as the intermediates formed from the depolymerisation of lignin to see if they can be deoxygenated at lower temperatures and to consider the relationship between hydrogenolysis and hydrogenation. Molecules such as guaiacol, cresols, and hydroxyphenols are all typical products from lignin degradation and are typically subjected to HDO at high temperatures and pressures. The results in this thesis from the reaction of phenol, anisole and 4-methoxyphenol suggest that HDO could be performed at lower temperatures and pressures.

8 Appendix

8.1 Toluene reaction profiles using iridium catalyst

Reaction parameters were 40, 50, 60 and 70 °C also under 2,3,4 and 5 H₂ pressure in addition to 0.5, 1, 0.75 and 1.5 mL toluene. It is worth mentioning that ethylbenzene was also hydrogenated using Ir at 60 and 70 °C and also under 5 barg H₂. Ethylcyclohexane was not observed, it was less than 3% at 70 °C

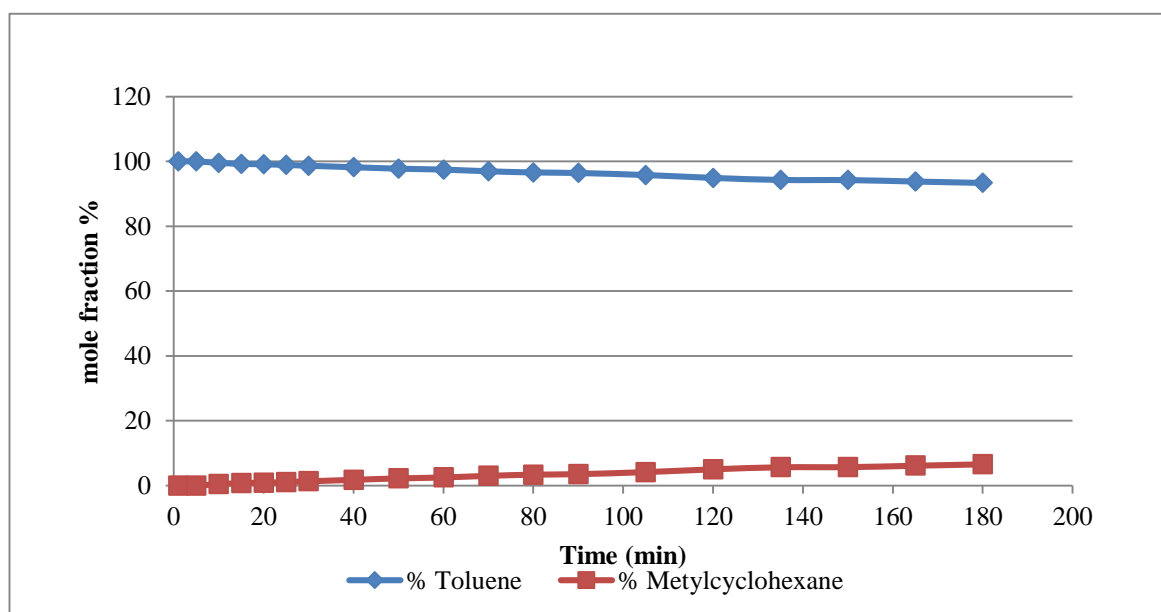


Figure 126. Toluene-40 °C-1mL-3b

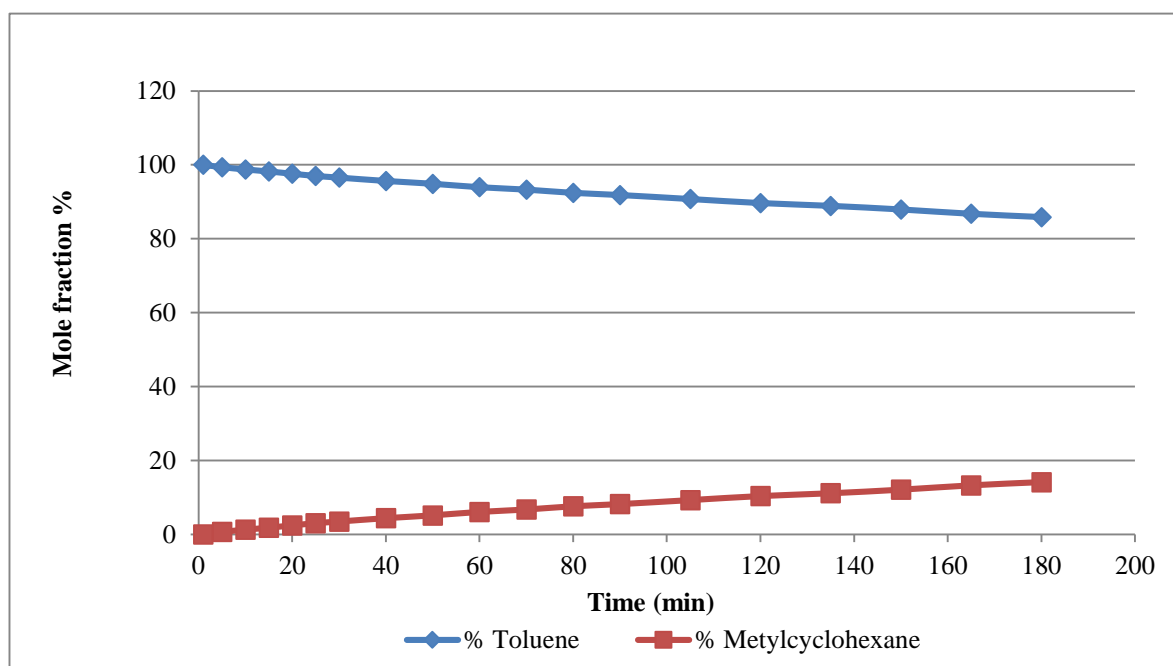


Figure 127. Toluene-50 °C-1mL-3b

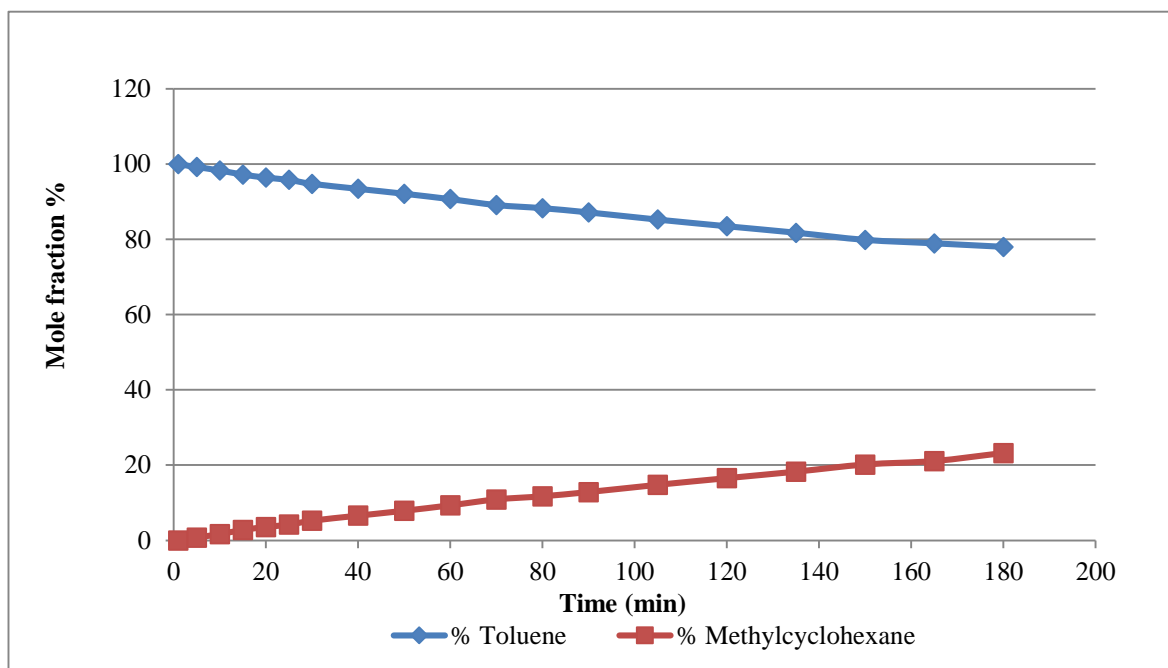


Figure 128. Toluene-60 °C-1mL-3b

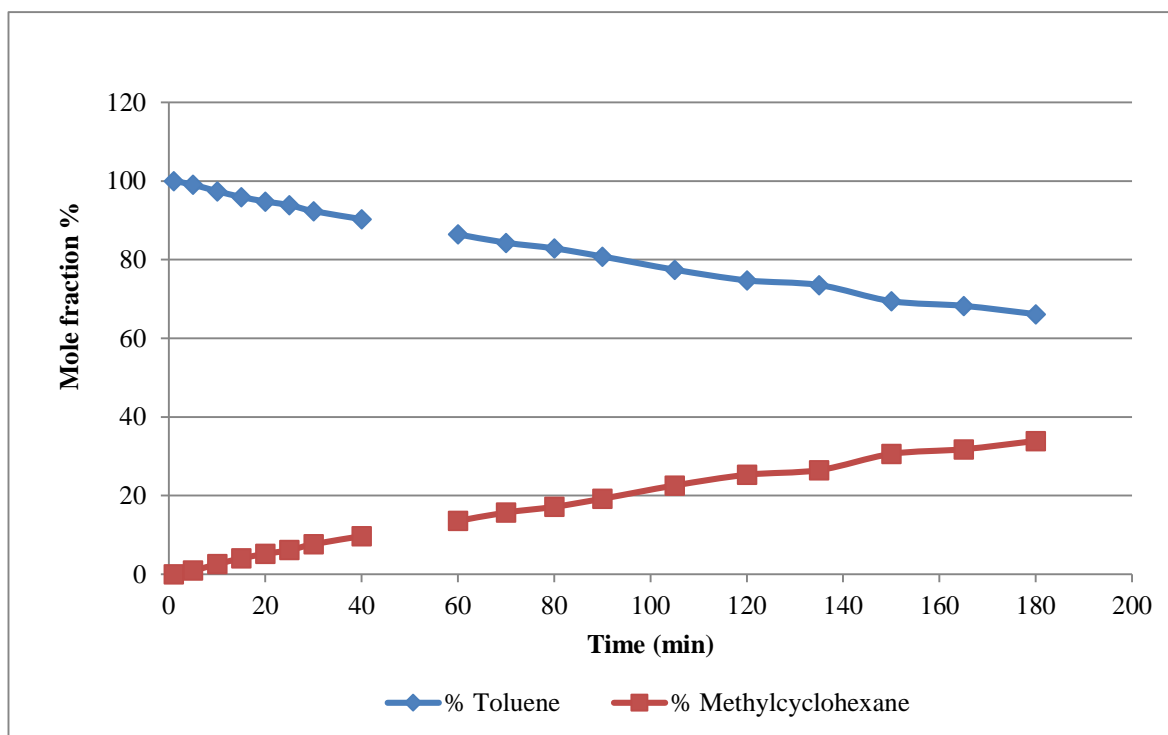


Figure 129. Toluene-70 °C-1mL-3b

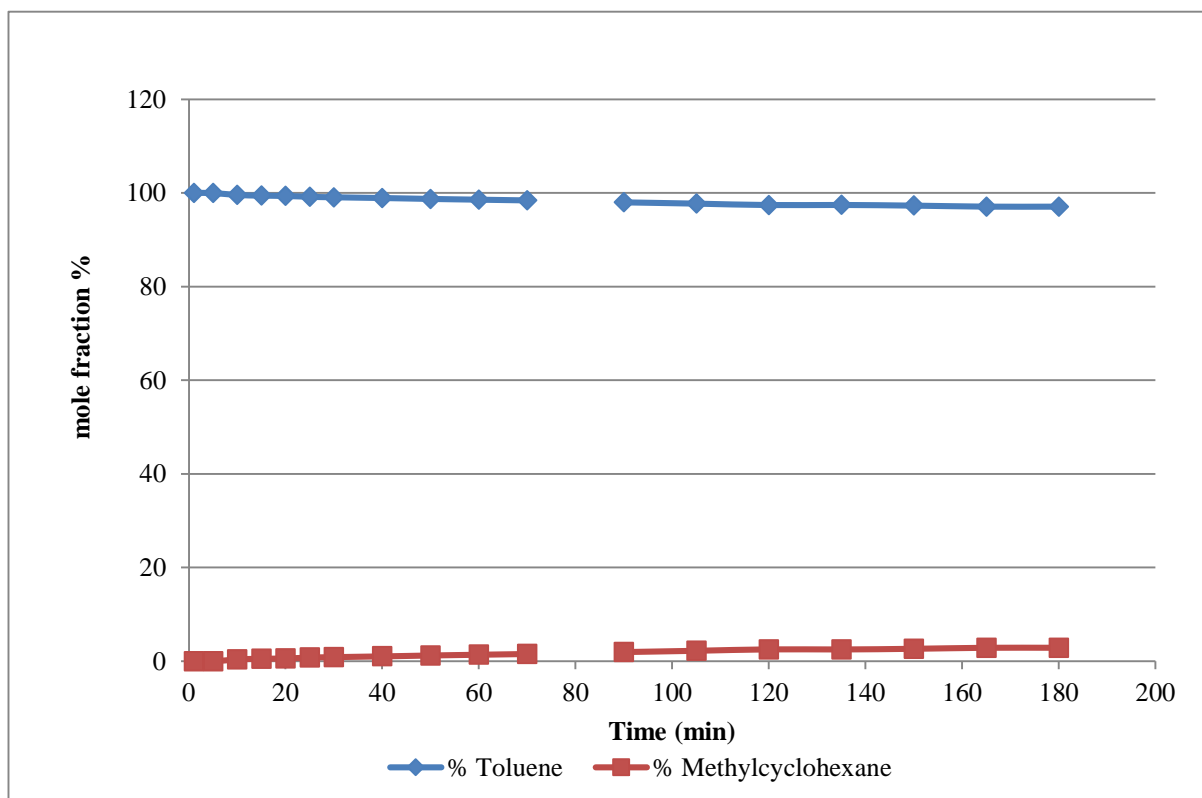


Figure 130. Toluene-60 °C-1mL-2b

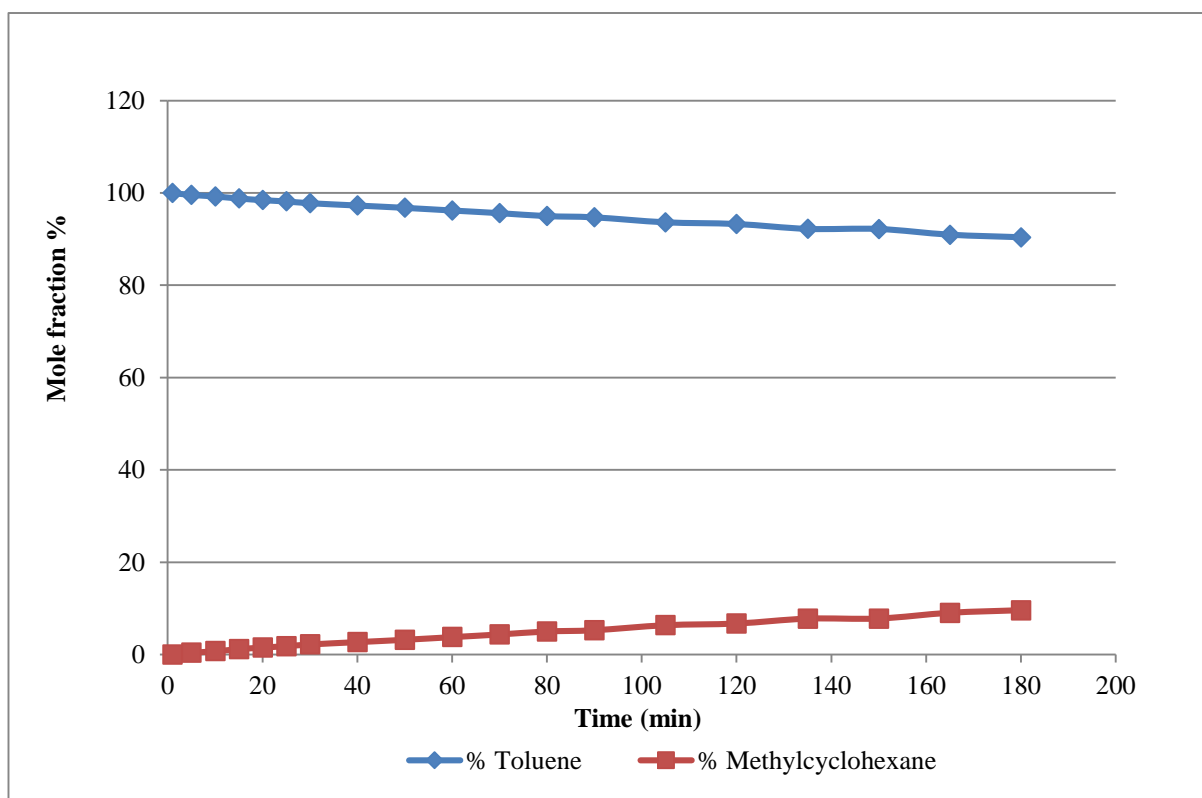


Figure 131. Toluene-60 °C-1mL-4b

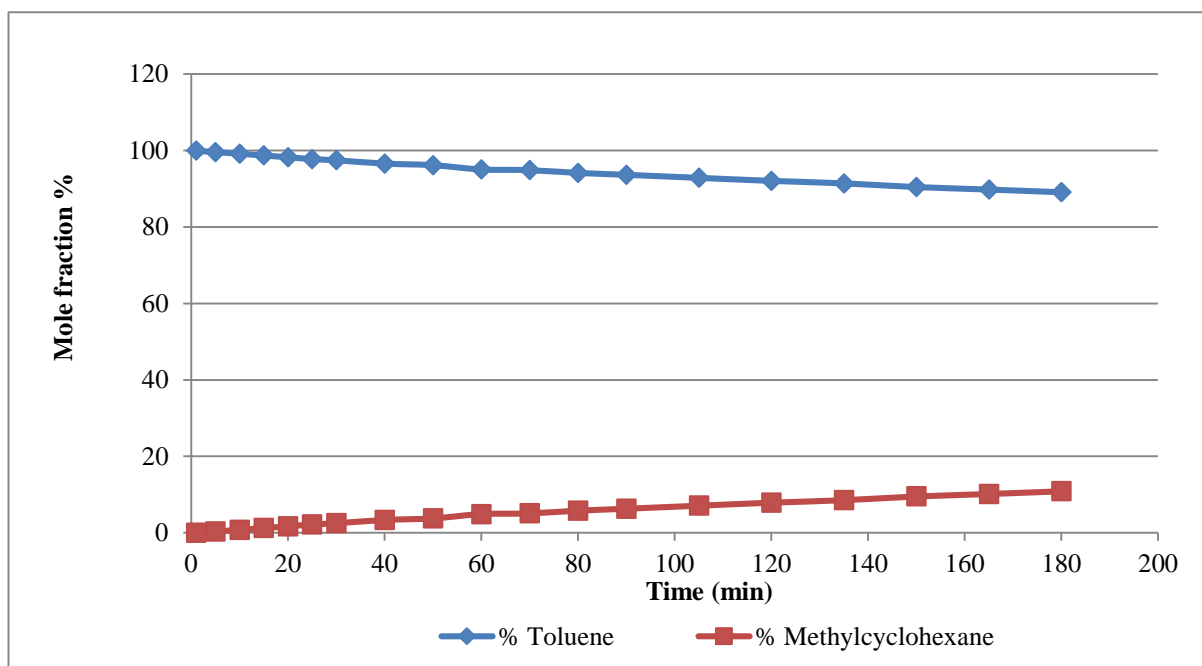


Figure 132. Toluene-60 °C-1mL-5b

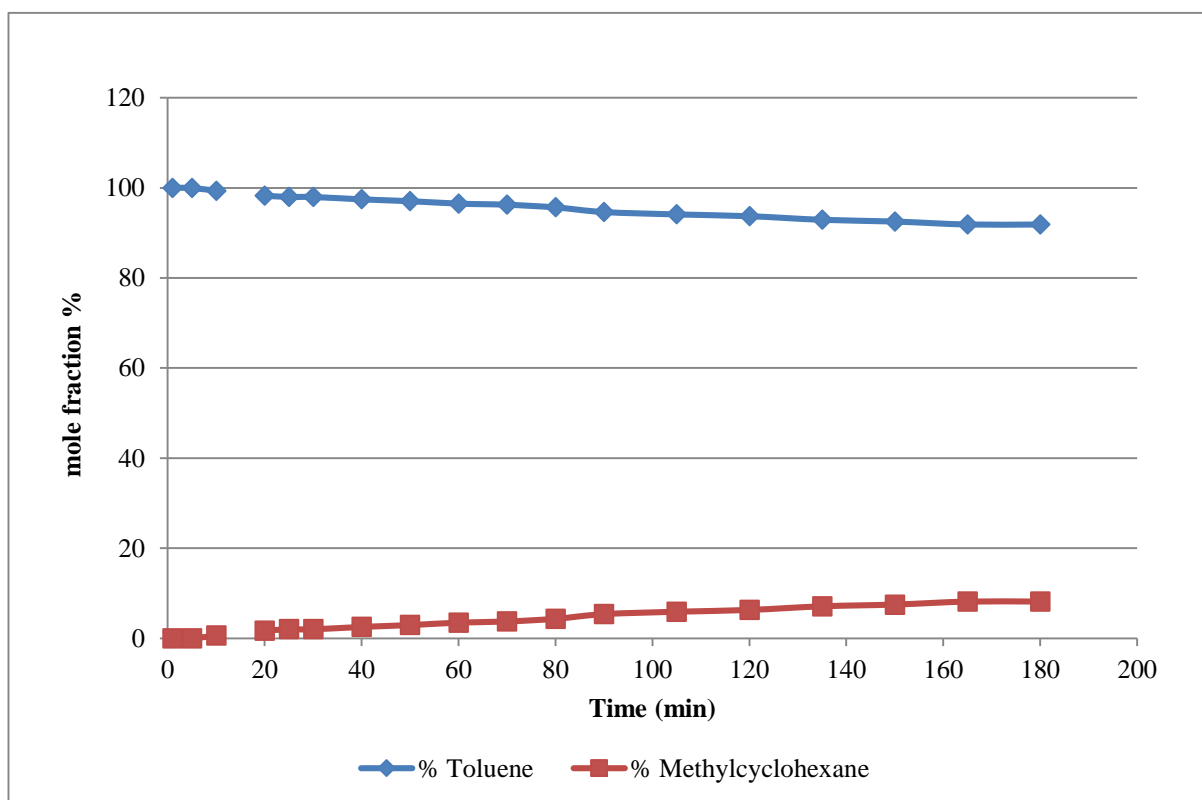


Figure 133. Toluene-60 °C-0.5 mL-3b

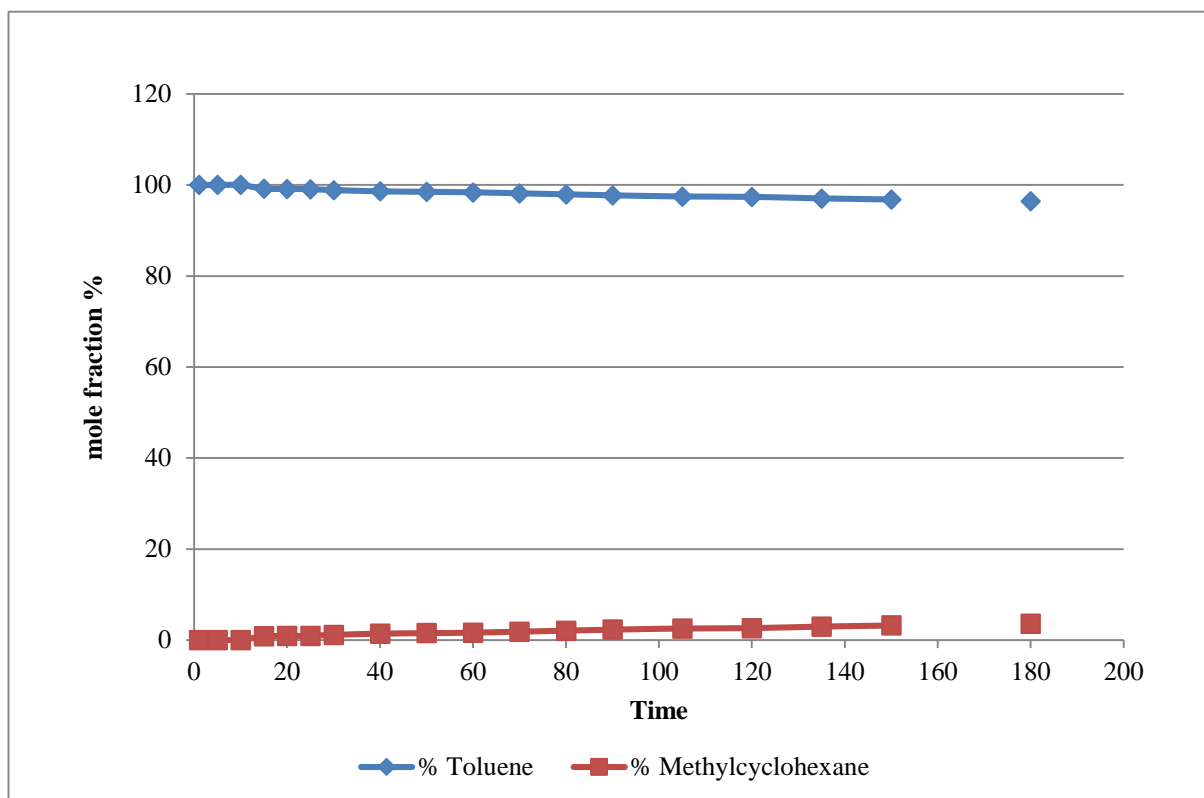


Figure 134. Toluene-60 °C-0.75 mL-3b

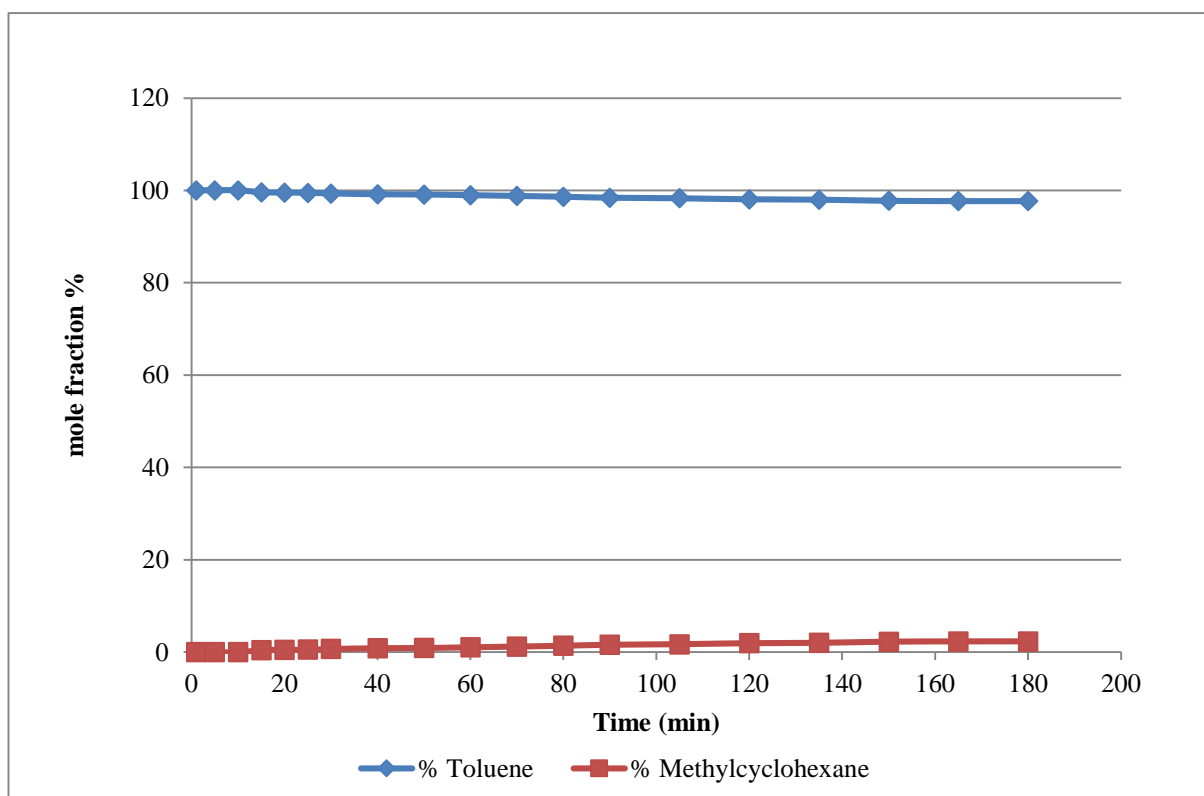


Figure 135. Toluene-60 °C- 1.5 mL-3b

9 List of references

1. S. Nishimura, Handbook of Heterogeneous Catalytic Hydrogenation for Organic Synthesis.: Wiley, 2001.
2. H.-U. Blaser, C. Malan, B. Pugin, F. Spindler, H. Steiner, M. Studer, *Advanced Synthesis & Catalysis*, 2003. 345(1-2) 103-151.
3. P.Sabatier, *Industrial & Engineering Chemistry*, 1926. 18(10) 1005-1008.
4. Z.Wang, *Comprehensive Organic Name Reactions and Reagents*. John Wiley & Sons, Inc., 2010.
5. G.V. Smith, F. Notheisz, *Organic Chemistry*, Academic Press: San Diego, 1999.
6. A. Louloudi, N. Papayannakos, *Applied Catalysis A: General*, 1998. 175(1-2), 21-31.
7. I. P. Rothwell, *Chemical Communications*, 1997(15), 1331-1338.
8. L. Plasseraud, G. Süß-Fink, *Journal of Organometallic Chemistry*, 1997. 539(1-2), 163-170.
9. P.J. Dyson, *Dalton Transactions*, 2003(15), 2964-2974.
10. A.Roucoux, J. Schulz, and H. Patin, *Chemical Reviews*, 2002. 102(10), 3757-3778.
11. M. A. Aramendia, V. Borau, C. Jiminez, J. M. Marinas, F. Rodero and M. E. Sempere, *React. Kinet. Catal. Lett.*, 1992. 46(2), 305-312.
12. P.J., Van Der Steen, J.J.F Scholten, *Applied Catalysis*, 1990, 58(1), 291-304.
13. E.-J Shin, M.A. Keane, *Industrial & Engineering Chemistry Research*, 2000, 39(4), 883-892.
14. M.A. Keane, P.M. Patterson, *Industrial & Engineering Chemistry Research*, 1999, 38(4), 1295-1305.
15. S. Qi, X. Yong Wei, Z. Zong, Y. Wang, *RSC Advances*, 2013, 3(34), 14219-14232.

16. M. Guerrero, N. T. T. Chau, S. Noel, A. Denicourt-Nowicki, F. Hapiot, A. Roucoux, E. Monflier, K. Philippot, *Current Organic Chemistry*, 2013. 17(4), 364-399.
17. J. Struijk, J.J.F. Scholten, *Applied Catalysis A: General*, 1992. 82(2), 277-287.
18. P. Kluson, J. Had, Z. Belohlav, L. Cerveny *Applied Catalysis A: General*, 1997. 149(2), 331-339.
19. J.Q. Wang, Y.Z. Wang, S.H. Xie, M.H. Qiao, H.X. Li, K.N. Fan, *Applied Catalysis A: General*, 2004. 272(1-2), 29-36.
20. H. Nagahara, M. Ono, M. Konishi, Y. Fukuoka, *Applied Surface Science*, 1997. 121: p. 448-451.
21. A. Stanislaus, B.H. Cooper, *Catalysis Reviews*, 1994. 36(1): p. 75-123.
22. J.-M. Bader, G. Rolland, *Hydrocarbon Processing*, 2012. 91(10), 41-45.
23. J. Medeiros, L. de Araújo, O. Q. F. Gaspar, A. B. Silva, M. A. P. Britto, J. M., *Brazilian Journal of Chemical Engineering*, 2007, 24, 119-133.
24. Z.M. Zhou, T.Y. Zeng, Z.M. Cheng, W.K. Yuan, *Industrial & Engineering Chemistry Research*, 2010, 49(21), 11112-11118.
25. T. Maegawa, A. Akashi, K. Yaguchi, Y. Iwasaki, M. Shigetsura, Y. Monguchi, H. Sajiki, *Chemistry – A European Journal*, 2009, 15(28), 6953-6963.
26. Y. Wang, X. Cui, Y. Deng, F. Shi, *RSC Advances*, 2014, 4(6), 2729-2732.
27. M. Che, C.O. Bennett, *Advances in Catalysis*, 1989, 36, 55-172.
28. M.A. Ermakova, D.Y. Ermakov, *Applied Catalysis A: General*, 2003, 245(2), 277-288.
29. G.C. Bond, in *Metal-Catalysed Reactions of Hydrocarbons*. 2005, Springer US, 10, 437-471.
30. A.F.B. Flores, L. Robert Butt, B. John, *Journal of the Chemical Society, Faraday Transactions*, 1992. 88(8), 1191-1196.
31. R. Molina, G. Poncelet, *Journal of Catalysis*, 2001, 199(2), 162-170.

32. W.F. Graydon, M.D. Langan, *Journal of Catalysis*, 1981, 69(1), 180-192.
33. W. Geoff, S.D Jackson, J.H. Kenneth, CRC Press, 2005, 77-84.
34. K. T. Hindle, S. D. Jackson, D. Stirling, G. Webb, *Journal of Catalysis*, 2006, 241(2), 417-425.
35. H. Pines, in *The Chemistry of Catalytic Hydrocarbon Conversions*. 1981, Academic Press, 10, 156-184.
36. P.A. Rautanen, J.R. Aittamaa, A.O.I. Krause, *Industrial & Engineering Chemistry Research*, 2000, 39(11), 4032-4039.
37. L.P. Lindfors, T. Salmi, *Industrial & Engineering Chemistry Research*, 1993, 32(1), 34-42.
38. J. Ali, *The hydrogenation of pyrolysis gasolin (PyGas) over nickel and palladium catalysts*, 2012, PhD thesis <http://theses.gla.ac.uk/3542>.
39. M.C. Schoenmaker-Stolk, J.W. Verwijs, J.A. Don, J.J.F. Scholten, *Applied Catalysis*, 1987, 29(1), 73-90.
40. A. Weilhard, G. Abarca, J. Viscardi, M. H. G. Prechtl, J. D. Scholten, F. Bernardi, D. L. Baptista, J. Dupont, *ChemCatChem*, 2017, 9(1), 204-211.
41. L. Foppa, J. Dupont, *Chemical Society Reviews*, 2015, 44(7), 1886-1897.
42. S. Smeds, D. Murzin, T. Salmi, *Applied Catalysis A: General*, 1995, 125(2), 271-291.
43. S. Toppinen, T. Salmi, T. K. Rantakylä, J. Aittamaa, *Industrial & Engineering Chemistry Research*, 1997, 36(6), 2101-2109.
44. S. Toppinen, T. Salmi, T. K. Rantakylä, J. Aittamaa, *Industrial & Engineering Chemistry Research*, 1996, 35(12), 4424-4433.
45. M. Vasiur Bahaman, M. Albert Vannice, *Journal of Catalysis*, 1991, 127(1), 251-266.
46. M. Vasiur Rahaman, M. Albert Vannice, *Journal of Catalysis*, 1991, 127(1), 267-275.
47. S.D. Lin, M.A. Vannice, *Journal of Catalysis*, 1993, 143(2), 539-553.

48. S.D. Lin, M.A. Vannice, *Journal of Catalysis*, 1993, 143(2), 554-562.
49. S.D. Lin, M.A. Vannice, *Journal of Catalysis*, 1993, 143(2), 563-572.
50. J. Tobicik, L. Cerveny, *Journal of Molecular Catalysis A: Chemical*, 2003, 194(1-2), 249-254.
51. Y. Yoon, R. Rousseau, R.S. Weber, D. Mei, J.A. Lercher, *Journal of the American Chemical Society*, 2014, 136(29), 10287-10298.
52. F. E. Massoth, P. Politzer, M. C. Concha, J. S. Murray, J. Jakowski and J. Simons, *The Journal of Physical Chemistry B*, 2006, 110(29), 14283-14291.
53. C.-J. Lin, S.-H. Huang, N.-C. Lai, C.-M. Yang, *ACS Catalysis*, 2015, 5(7), 4121-4129.
54. S. Velu, M. P. Kapoor, S. Inagaki, K. Suzuki, *Applied Catalysis A: General*, 2003, 245(2), 317-331.
55. L. Giraldo, M. Bastidas-Barranco, J.C. Moreno-Piraján, *Molecules*, 2014, (19), 20594-20612.
56. S. Scire, S. Minico, C. Crisafulli, *Applied Catalysis A: General*, 2002, 235(1-2), 21-31.
56. C. Park, M.A. Keane, *Journal of Colloid and Interface Science*, 2003, 266(1), 183-194.
58. E.J. Shin, M.A. Keane, *Journal of Catalysis*, 1998, 173(2), 450-459.
59. P. Kluson, L. Cerveny, *Journal of Molecular Catalysis A: Chemical*, 1996, 108(2), 107-112.
60. G. Neri, A.M. Visco, A. Donato, C. Milone, M. Malentacchi, G. Gubitosa, *Applied Catalysis A: General*, 1994, 110(1), 49-59.
61. Y. Pérez, M. Fajardo, A. Corma, *Catalysis Communications*, 2011, 12(12), 1071-1074.
62. J. Zhong, J. Chen, L. Chen, *Catalysis Science & Technology*, 2014, 4(10), 3555-3569.
63. K.V.R. Chary, D. Naresh, V. Vishwanathan, M. Sadakane, W. Ueda, *Catalysis Communications*, 2007, 8(3), 471-477.

64. Y. Wang, J. Yao, H. Li, D. Su, M. Antonietti, *Journal of the American Chemical Society*, 2011, 133(8), 2362-2365.
65. M. Zhao, J. Shi, Z. Hou, *Chinese Journal of Catalysis*, 2016, 37(2), 234-239.
66. H. Li, J. Liu, S. Xie, M. Qiao, W. Dai, Y. Lu, H. Li, *Advanced Functional Materials*, 2008, 18(20), 3235-3241.
67. Y.H. Zhu, Y. Karen Tang, S.H. Narayan, in *New Aspects for the Future I, Japan*, ed, J.-I. Kadokawa, 2013, 13, 315–346.
68. G.S. Fonseca, A.P. Umpierre, P.F.P. Fichtner, S.R. Texeira, J. Dupont, *Chemistry – A European Journal*, 2003, 9(14), 3263-3269.
69. V. Mevellec, A. Nowicki, A. Roucoux, C. Dujardin, P. Granger, E. Payen, K. Philippot, *New Journal of Chemistry*, 2006, 30(8), 1214-1219.
70. F. Lu, J. Liu, J. Xu, *Advanced Synthesis & Catalysis*, 2006, 348(7-8), 857-861.
71. A. Denicourt-Nowicki, B. Leger, A. Roucoux, *Physical Chemistry Chemical Physics*, 2011, 13(30), 13510-13517.
72. J. Schulz, A. Roucoux, H. Patin, *Chemical Communications*, 1999, (6), 535-536.
73. J.A. Widegren, R.G. Finke, *Inorganic Chemistry*, 2002, 41(6), 1558-1572.
74. C. Hubert, A. Denicourt-Nowicki, J. P. Guégan, A. Roucoux, *Dalton Transactions*, 2009, (36), 7356-7358.
75. C. Moreau, P. Geneste, in *Theoretical Aspects of Heterogeneous Catalysis*, Springer Netherlands: Dordrecht. 1990, 7, 256-310.
76. F. Lu, J. Liu, J. Xu, *Journal of Molecular Catalysis A: Chemical*, 2007, 271(1–2), 6-13.
77. A. Gual, C. Godard, S. Castillon, C. Claver *Dalton Transactions*, 2010, 39(48), 11499-11512.
78. T.R. Viljava, A.O.I. Krause, *Applied Catalysis A: General*, 1996, 145(1), 237-251.

79. C. Aubert, R. Durand, P. Geneste, C. Moreau, *Journal of Catalysis*, 1988, 112(1), 12-20.
80. V. Vetere, A.B. Merlo, M.L. Casella, *Applied Catalysis A: General*, 2015, 491, 70-77.
81. H. Ihm, J. M. White, *The Journal of Physical Chemistry B*, 2000, 104(26), 6202-6211.
82. Y. Tan, S. Khatua, S. Jenkins, J.-Q. Yu, J. Spencer, D. King, *Surface Science*, 2005, 589(1-3), 173-183.
83. M. Quiroz, F. Córdova, E. Lamy-Pitara, J. Barbier, *Electrochimica Acta*, 2000, 45(25-26), 4291-4298.
84. J. Basset, B. D. Imelik, M. Primet, R. Mutin, *Journal of Catalysis*, 1975, 37(1), 22-36.
85. D. Duprez, *Applied Catalysis A: General*, 1992, 82(2), 111-157.
86. J.M. Orozco, G. Webb, *Applied Catalysis*, 1983, 6(1), 67-84.
87. M.A., Keane, *Journal of Catalysis*, 1997, 166(2), 347-355.
88. S. Mukherjee, M. A. Vannice, *Journal of Catalysis*, 2006, 243(1), 108-130.
89. N. Bertero, A. Trasarti, C. Apesteguia, A. Marchi, *Applied Catalysis A: General*, 2011, 394(1-2), 228-238.
90. S. Siegel, Rhodium on Alumina, in *Encyclopedia of Reagents for Organic Synthesis*, John Wiley & Sons, Ltd, 2001, 11, 8559-8563.
91. L. Barthe, A. Denicourt-Nowicki, A. Roucoux, K. Philippot, B. Chaudret, M. Hemati, *Catalysis Communications*, 2009, 10(8), 1235-1239.
92. M. Chatterjee, H. Kawanami, M. Sato, A. Chatterjee, T. Yokoyama, T. Suzuki, *Advanced Synthesis & Catalysis*, 2009, 351(11-12), 1912-1924.
93. H. Michio, N. Shigeo, *Bulletin of the Chemical Society of Japan*, 1992, 65(11), 2955-2959.
94. T. Junk, W. Catallo, *Chemical Society Reviews*, 1997, 26(5), 401-406.

95. J. Atzrodt, V. Derdau, T. Fey, *Angewandte Chemie International Edition*, 2007, 46(41), 7744-7765.
96. M. Zimmer-De Iuliis, R.H. Morris, *Journal of the American Chemical Society*, 2009, 131(31), 11263-11269.
97. R.Z.C van Meerten, A. Morales, J. Barbier, R. Maurel, *Journal of Catalysis*, 1979, 58(1), 43-51.
98. C. Sprung, P. N. Kechagiopoulos, J.W. Thybaut, B. Arstad, U. Olsbye, G.B. Marin, *Microkinetic Applied Catalysis A: General*, 2015, 492, 231-242.
99. M. S. Lylykangas, 2004, *Kinetic Modelling of liquid phase hydrogenation reactors*, PhD Thesis, Helsinki University of Technology, 2004, 37.
100. G. Lietz, J. Völter, *Journal of Catalysis*, 1976, 45(2), 121-127.
101. M.A. Keane, P. M. Patterson, *Journal of the Chemical Society, Faraday Transactions*, 1996, 92(8), 1413-1421.
- 102 J. Völter, M. Hermann, K. Heise, *Journal of Catalysis*, 1968, 12(3), 307-313.
103. Kalantar Neyestanaki, H. Backman, P. Mäki-Arvela, J. Wärnä, T. Salmi, D.Yu. Murzin, *Chemical Engineering Journal*, 2003, 91(2-3), 271-278.
104. A. G. A. Ali, L. I. Ali, S. M. Aboul-Fotouh, A.K. Aboul-Gheit, *Applied Catalysis A: General*, 1998, 170(2), 285-296.
105. G. S. Fonseca, E. T. Silveira, M. A. Gelesky, J. Dupont, *Advanced Synthesis & Catalysis*, 2005, 347(6), 847-853.
106. H. A. Smith, *Annals of the New York Academy of Sciences*, 1967, 145(1), 72-82.
107. Bolis, V., in *Calorimetry and Thermal Methods in Catalysis*, A. Auroux, Springer Berlin Heidelberg, 2013, 1, 3-50.
108. N. Mahata, V. Vishwanathan, *Catalysis Today*, 1999, 49(1-3), 65-69.
109. Y. Li, X. Xu, P. Zhang, Y. Gong, H. Li, Y. Wang, *RSC Advances*, 2013, 3(27), 10973-10982.

110. N. Mahata, K. Raghavan, V. Vishwanathan, *Indian J. Chem., Sect. A: Inorg., Bio-inorg., Phys., Theor. Anal. Chem*, 2000 (39), 856–858.
111. N. Mahata, K. Raghavan, V. Vishwanathan, C. Park, M. Keane, *Physical Chemistry Chemical Physics*, 2001, 3(13), 2712-2719.
112. A. M. Raspolli Galletti, C. Antonetti, S. Giaiacopi, S., O. Piccolo, A. M. Venezia, *Topics in Catalysis*, 2009, 52(8), 1065-1069.
113. S. Hu, M. Xue, H. Chen, J. Shen, *Chemical Engineering Journal*, 2010, 162(1), 371-379.
114. A. N. Raut, S. U. Nandanwar, Y. R. Suryawanshi, M. Chakraborty, S. Jauhari, S. Mukhopadhyay, K. T. Shenoy, H. C. Bajaj, *Kinetics and Catalysis*, 2016, 57(1), 39-46.
115. N. Mahata, V. Vishwanathan, *Journal of Catalysis*, 2000, 196(2), 262-270.
116. M. Higashijima, S. Nishimura, *Bulletin of the Chemical Society of Japan*, 1992, 65(3), 824-830.
117. Y. Z. Chen, C. W. Liaw, L. I. Lee, *Applied Catalysis A: General*, 1999, 177(1), 1-8.
118. J. A. Dean, *Properties of atoms, radicals, and bonds. Lange's Handbook of Chemistry*, 1990, section 4, p 43.
119. S. J. Blanksby, G.B. Ellison, *Accounts of Chemical Research*, 2003, 36(4), 255-263.
120. A. Popov, E. Kondratieva, J. M. Goupil, L. Mariey, P. Bazin, J. P. Gilso, *The Journal of Physical Chemistry C*, 2010, 114(37), 15661-15670.
121. P. Geneste, M. Bonnet, M. Rodriguez, *Catalytic Journal of Catalysis*, 1979, 57(1), 147-152.
122. E. Laurent, B. Delmon, *Applied Catalysis A: General*, 1994, 109(1), 97-115.
123. A. Olivas, D. I. Jerdev, B. E. Koel, *Journal of Catalysis*, 2004, 222(2), 285-292.
124. C. H. Rochester, D.-A. Trebilco, *Journal of the Chemical Society, Faraday Transactions 1: Physical Chemistry in Condensed Phases*, 1978, 74(0), 1137-1145.

125. A. Saracual, C. H. Rochester, *Journal of the Chemical Society, Faraday Transactions 1: Physical Chemistry in Condensed Phases*, 1982, 78(9), 2787-2791.
126. H.M. Weinert, S. D. Jackson, Unpublished raw data. 2017.
127. C. Sprung, B. Arstad, U. Olsbye, *ChemCatChem*, 2014, 6(7), 1969-1982.
128. B. Shi, Y. Liao, J. L. Naumovitz, *Applied Catalysis A: General*, 2015, 490, 201-206.
129. B. Shi, C. Jin, *Applied Catalysis A: General*, 2011, 393(1–2), 178-183.
130. K.-I. Aika, A. Ozaki, *Journal of Catalysis*, 1970, 19(3), 350-352.
131. E. A. Gelder, S. D. Jackson, C.M. Lok, *Chemical Communications*, 2005, (4), 522-524.
132. P. G. Williams, C. Than, S. Rabbani, M. A. Long, J. L. Garnett, *Journal of Labelled Compounds and Radiopharmaceuticals*, 1995, 36(1), 1-14.
133. E. Crawford, C. Kemball, *Transactions of the Faraday Society*, 1962, 58(0), 2452-2467.